LOS ANGELES PUBLIC LIBRARY

MAY 19 1959

ARS JOURNAL

A PUBLICATION OF THE AMERICAN ROCKET SOCIETY

FORMERLY JET PROPULSION

BIND

SURVEY ARTICLE

Recent Developments in Convective Heat Transfer . . . . . Rolf H. Sabersky 325

CONTRIBUTED ARTICLES

Hypersonic Shock Tunnel . H. T. Nagamatsu, R. E. Geiger and R. E. Sheer Jr. 332

Thrust Optimization of a Nuclear Rocket of Variable Specific Impulse . . . . . C. J. Wang, G. W. Anthony and H. R. Lawrence 341

Similarity Parameters for Surface Melting of a Blunt Nosed Body in a High Velocity Gas Stream . . . . . Lester Lees 345

Some Physical Properties for the System Nitrogen Tetroxide–Nitric Oxide . . . . . Donat B. Brice and Norman Fishman 354

TECHNICAL NOTES

Thermostatic Temperature Control of Satellites and Space Vehicles . . . . . R. A. Hanel 358

Use of a Catalytic Probe for Detection of Dissociated Nonequilibrium States in Hypersonic Flow . . . . . Stuart A. Hoenig 361

Velocity of Tank Fragments . . . . . Saunders B. Kramer 363

Burning Rate of an H-Atom Propellant . . . . . Howard B. Palmer 365

Generalized Solution for the Problem of Pipe Flow With Friction and Heat Addition . . . . . R. W. McJones and M. L. Caplan 366

On Satellite Librations . . . . . G. M. Schindler 368

Time for Escape Using a Succession of Small Impulses . . . . . Robert E. Roberson 370

Attitude Stabilization by Means of Solar Radiation Pressure . . . . . Robert L. Sohn 371

DEPARTMENTS

Technical Comments 374 . . . . . New Patents 382

Book Reviews 376 . . . . . Technical Literature Digest 384

May 1959 Volume 29 Number 5

all you need

to store **NITROGEN TETROXIDE**

is a rocket

This liquid-fuel oxidizer needs no refrigeration, causes no freeze-ups

As an oxidizer for liquid fuels, Nitrogen Tetroxide has even more to recommend it than its high performance (99% of theoretical I_{sp}, hypergolic at low altitude). The ease with which it can be stored and handled offers another major advantage.

N_2O_4 requires no refrigeration, no high-pressure vessels. It is noncorrosive, can be stored indefinitely in plain carbon steel tanks at the launching site or right in the rocket itself. And it's ready when it's needed—there are no freeze-ups in valves and motors with N_2O_4.

Availability: excellent. Allied is a major producer of Nitrogen Tetroxide, can ship immediately in cylinders or tank car lots. Allied also produces ammonia, ethylene oxide and methanol for the rocket industry. Write for technical or other information you desire on any of these products.

For specifications and local offices, see our insert in Chemical Materials Catalog, pages 435-442 and in Chemical Week Buyers Guide, pages 35-42.

BASIC TO AMERICA'S PROGRESS

Allied Chemical

NITROGEN DIVISION
Dept. NT 5-12-1, 40 Rector Street, New York 6, N.Y.

LARGE flow rate controlled

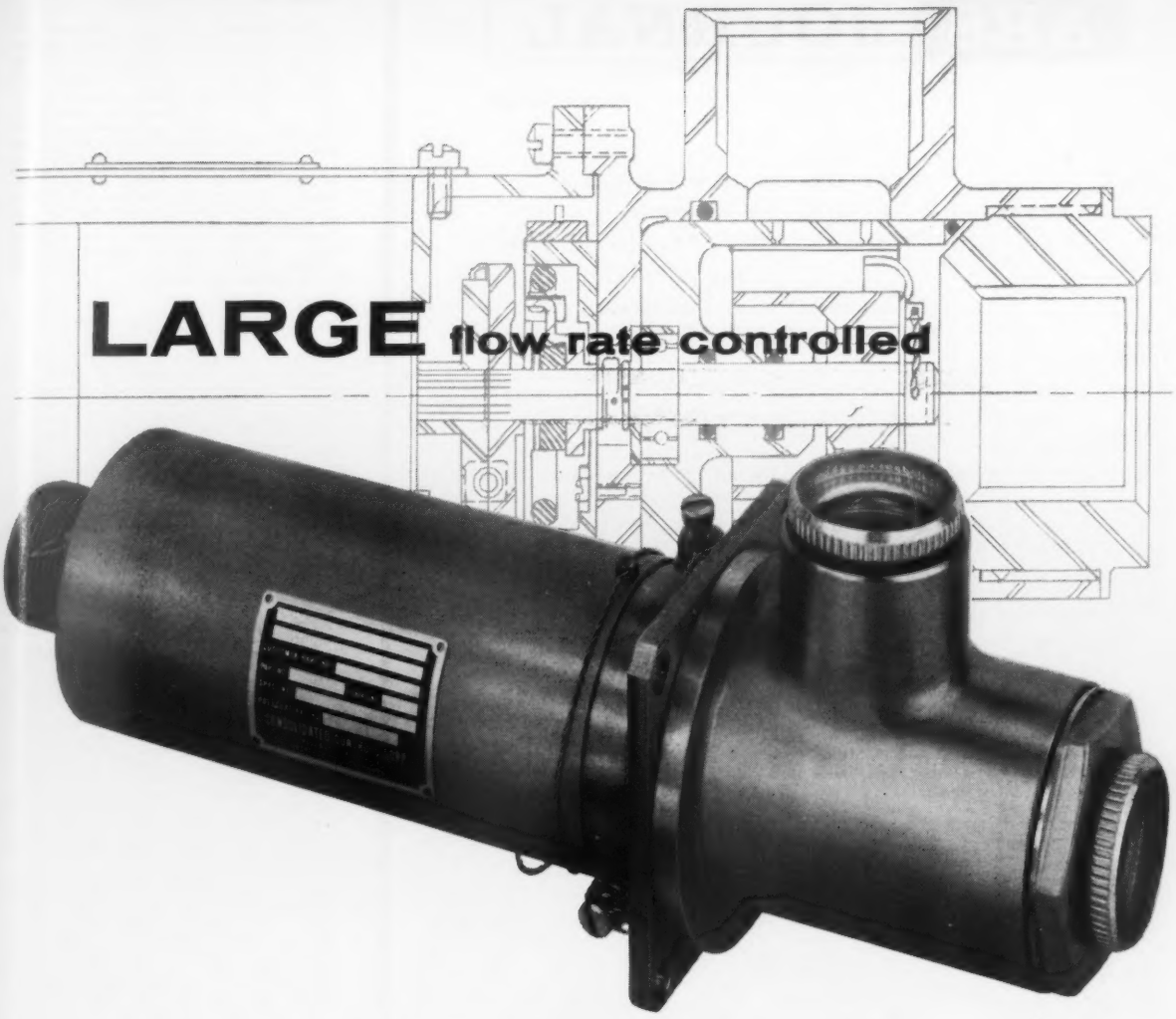

by small electric motor

The new modulating fuel valve offers flow rates up to 200 GPM with low power input. This redesigned version of Consolidated Controls very successful FLEXBELT® valve may be used in control of a wide range of fluids and fuels . . . the latest being hydrogen peroxide.

The flexbelt valve can be provided with linear, square, logarithmic or other unusual flow contours to match control systems requirements. The complete unit which contains a two-phase servo motor, gear train, adjustable stops, feedback, potentiometer, flow control belt and drum, and seat, weighs just over four pounds. The valve is constructed of stainless steel and the belt material for most applications is Teflon impregnated glass fibre. Because the belt is self-seating as it rolls off the drum, operation is insensitive to contamination. This offers users a high degree of reliability in conjunction with versatility.

The unique FLEXBELT® principle enables the valve to handle a wide variety of flow characteristics with a minimum of input power. **Write for complete specifications to Manager—Sales: Consolidated Controls Corporation, 750 So. Isis Avenue, Inglewood, California.**

CONSOLIDATED CONTROLS CORPORATION

BETHEL, CONN., INGLEWOOD, CALIF.

A SUBSIDIARY OF CONSOLIDATED DIESEL ELECTRIC CORPORATION

STAMFORD, CONNECTICUT

ARS JOURNAL

A PUBLICATION OF THE AMERICAN ROCKET SOCIETY

FORMERLY JET PROPULSION

EDITOR **Martin Summerfield**

ASSISTANT EDITOR **Barbara Nowak**

ART EDITOR **John Culin**

ASSOCIATE EDITORS

Ali Bulent Cambel *Northwestern University*
Irvin Glassman *Princeton University*
M. H. Smith *Princeton University*

CONTRIBUTORS

Marshall Fisher *Princeton University*
George F. McLaughlin

ADVERTISING AND PROMOTION MANAGER

William Chenoweth

ADVERTISING PRODUCTION MANAGER

Walter Brunke

ADVERTISING REPRESENTATIVES

D. C. Emery and Associates
155 East 42 St., New York, N. Y.
Telephone: Yukon 6-6855

James C. Galloway and Co.
6535 Wilshire Blvd., Los Angeles, Calif.
Telephone: Olive 3-3223

Jim Summers and Associates
35 E. Wacker Dr., Chicago, Ill.
Telephone: Andover 3-1154

R. F. Pickrell and Associates
318 Stephenson Bldg., Detroit, Mich.
Telephone: Trinity 1-0790

Louis J. Bresnick
304 Washington Ave., Chelsea 50, Mass.
Telephone: Chelsea 3-3335

John W. Foster
239 4th Ave., Pittsburgh, Pa.
Telephone: Atlantic 1-2977

American Rocket Society

500 Fifth Avenue, New York 36, N. Y.

Founded 1930

OFFICERS

President	John P. Stapp
Vice-President	Howard S. Seifert
Executive Secretary	James J. Harford
Treasurer	Robert M. Lawrence
Secretary and Asst. Treasurer	A. C. Slade
General Counsel	Andrew G. Haley
Director of Publications	Irwin Hersey

BOARD OF DIRECTORS

Terms expiring on dates indicated

James R. Dempsey	1961	Simon Ramo	1960
Alfred J. Eggers Jr.	1959	H. W. Ritchey	1959
Krafft Ehricke	1959	William L. Rogers	1959
Samuel K. Hoffman	1960	David G. Simons	1961
J. Preston Layton	1960	John L. Sloop	1961
A. K. Oppenheim	1961	Martin Summerfield	1959
William H. Pickering	1961	Wernher von Braun	1960
Maurice J. Zucrow	1960		

TECHNICAL COMMITTEE CHAIRMEN

Lawrence S. Brown, Guidance and Navigation
Milton U. Clauser, Hydromagnetics
Kurt H. Debus, Logistics and Operations
William H. Dorrance, Hypersonics
Herbert Friedman, Instrumentation and Control
George Gerard, Structures and Materials
Milton Greenberg, Physics of the Atmosphere and Space
Stanley V. Gunn, Nuclear Propulsion
Andrew G. Haley, Space Law and Sociology
Samuel Herrick, Flight Mechanics
Max Hunter, Missiles and Space Vehicles
David B. Langmuir, Ion and Plasma Propulsion
Y. C. Lee, Liquid Rockets
Max Lowy, Communications
Harold W. Norton, Test Facilities and Support Equipment
Paul E. Sandorff, Education
William Shippen, Ramjets
John L. Sloop, Propellants and Combustion
Ivan E. Tuhy, Solid Rockets
Stanley White, Human Factors
George F. Wislicenus, Underwater Propulsion
Abe Zarem, Non-Propulsive Power

Scope of ARS JOURNAL

This Journal is devoted to the advancement of astronautics through the dissemination of original papers disclosing new scientific knowledge and basic applications of such knowledge. The sciences of astronautics are understood here to embrace selected aspects of jet and rocket propulsion, space flight mechanics, high-speed aerodynamics, flight guidance, space communications, atmospheric and outer space physics, materials and structures, human engineering, overall system analysis, and possibly certain other scientific areas. The selection of papers to be printed will be governed by the pertinence of the topic to the field of astronautics, by the current or probable future significance of the research, and by the importance of distributing the information to the members of the Society and to the profession at large.

Information for Authors

Manuscripts must be as brief as the proper presentation of the ideas will allow. Exclusion of dispensable material and conciseness of expression will influence the Editors' acceptance of a manuscript. In terms of standard-size double-spaced typed pages, a typical maximum length is 22 pages of text (including equations), 1 page of references, 1 page of abstract and 12 illustrations. Fewer illustrations permit more text, and vice versa. Greater length will be acceptable only in exceptional cases.

Short manuscripts, not more than one quarter of the maximum length stated for full articles, may qualify for publication as Technical Notes or Technical Comments. They may be devoted to new developments requiring prompt disclosure or to comments on previously published papers. Such manuscripts are usually published within two months of the date of receipt.

Sponsored manuscripts are published occasionally as an ARS service to the industry. A manuscript that does not qualify for publication, according to the above-stated requirements as to subject, scope or length, but which nevertheless deserves widespread distribution among jet propulsion engineers, may be printed as an extra part of the Journal or as a special supplement, if the author or his sponsor will reimburse the Society for actual publication costs. Estimates are available on request. Acknowledgment of such financial sponsorship appears as a footnote on the first page of the article. Publication is prompt since such papers are not in the ordinary backlog.

Manuscripts must be double spaced on one side of paper only with wide margins to allow for instructions to printer. Include a 100 to 200 word abstract. State the authors' positions and affiliations in a footnote on the first page. Equations and symbols may be handwritten or typewritten; clarity for the printer is essential. Greek letters and unusual symbols should be identified in the margin. If handwritten, distinguish between capital and lower case letters, and indicate subscripts and superscripts. References are to be grouped at the end of the manuscript and are to be given as follows: For journal articles: authors first, then title, journal, volume, year, page numbers for books: authors first, then title, publisher, city, edition and page or chapter numbers. Line drawings must be clear and sharp to make clear engravings. Use black ink on white paper or tracing cloth. Lettering should be large enough to be legible after reduction. Photographs should be glossy prints, not matte or semi-matte. Each illustration must have a legend; legends should be listed in order on a separate sheet.

Manuscripts must be accompanied by written assurance as to security clearance in the event the subject matter lies in a classified area or if the paper originates under government sponsorship. Full responsibility rests with the author.

Submit manuscripts in duplicate (original plus first carbon, with two sets of illustrations) to the Editor, Martin Summerfield, Professor of Aeronautical Engineering, Princeton University, Princeton, N. J. Preprints of papers presented at ARS national meetings are automatically considered for publication.

ARS JOURNAL is published monthly by the American Rocket Society, Inc. and the American Interplanetary Society at 20th & Northampton Sts., Easton, Pa., U. S. A. Editorial offices: 500 Fifth Ave., New York 36, N. Y. Price: $12.50 per year, $2.00 per single copy. Second-class mail privileges authorized at Easton, Pa. This Publication is authorized to be mailed at the special rates of postage prescribed by Section 132.122. Notice of change of address should be sent to the Secretary, ARS, at least 30 days prior to publication. Opinions expressed herein are the authors and do not necessarily reflect the views of the Editors or of the Society.

© Copyright 1959 by the American Rocket Society, Inc.

no. 8 OF A SERIES

THE SOUND . . . AND THE JURY

The quiet, solid feeling inside the 1959 Oldsmobile results from patient testing by a highly specialized "jury"—experts in the field of sound analysis.

Unlike most other phases of automotive engineering, there are no instruments which measure the "annoyance" factor of sounds inside an automobile. Subjective, personal evaluation known as the "jury system" is the most important means of determining how quiet it is inside an Oldsmobile.

With the "jury system", several experienced engineers assemble in an acoustically treated room and listen to binaural tape recordings made inside a test car. Careful editing of the tape recording allows rapid side-by-side comparison between two different test conditions and eliminates reliance on memory since considerable time may elapse between actual tests. By pushing a button, each engineer casts a secret "vote" and then the tabulation of the results determines which test condition is superior.

For the greatest possible accuracy, considerable care is taken making the recordings. Special microphones are placed at points corresponding to the passengers' ears. The recording equipment is in a specially equipped vehicle which follows the test car over a "ride road" that is carefully constructed to excite the vibrations and sounds that occur under normal driving conditions.

Quality, like quietness, is not accidental. It is the deliberate effort by Oldsmobile engineers to *design* quality into every automobile they produce. You'll like the 1959 Oldsmobile—with its solid Body by Fisher—it's the quietest car built! Experience this quality for yourself by visiting your local Authorized Oldsmobile Quality Dealer as soon as possible.

OLDSMOBILE DIVISION
GENERAL MOTORS CORPORATION

OLDSMOBILE **Where Quality is Standard Equipment!**

COMMAND DESTRUCT

The flight testing of second generation missiles—more versatile and powerful than their predecessors—requires a device for sure termination of any missile flight that might endanger the test range or surrounding area.

Ramo-Wooldridge engineers, under a United States Army Signal Corps contract, have successfully developed and delivered the first sub-miniature, completely transistorized radio "command destruct" receivers.

Specifically designed for missile flight safety operations, the receiver (AN/DRW-11) can actuate safety mechanisms or destruct devices. It has three command channels, each of which actuates a control relay.

The "command destruct" receiver accepts frequency modulated signals in the UHF radio command control band. It is designed to operate with closer radio frequency and command frequency channel spacing than has been used to date, thus making possible more efficient use of the available radio spectrum.

Compact and rugged, the radio receiver's modular construction permits rapid and complete accessibility to all components. One module houses the basic receiver. The second module contains the three command channels and relays. This integrated package occupies 115 cubic inches, and weighs 4 pounds. The receiver requires no pressurization and operates reliably under the adverse environmental conditions encountered in missile flight testing.

Engineers and scientists interested in being associated with some of the nation's most advanced research and development programs are invited to acquaint themselves with current opportunities at Ramo-Wooldridge. The areas of activity listed below are those in which R-W is now engaged and in which openings exist.

Missile electronics systems
Advanced radio and wireline communications
Information processing systems
Electronic language translation
Anti-submarine warfare
Air navigation and traffic control
Analog and digital computers
Infrared systems
Electronic reconnaissance and countermeasures
Basic and applied physical research

For a copy of our brochure, *An Introduction to Ramo-Wooldridge*, or other additional information write to Mr. Donald L. Pyke.

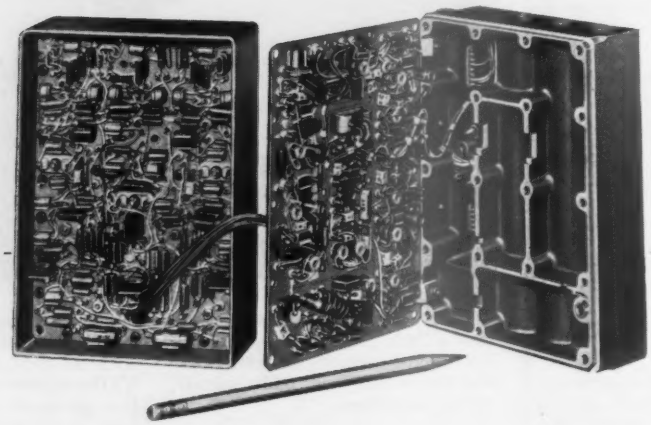

RAMO-WOOLDRIDGE

P. O. BOX 90534, AIRPORT STATION • LOS ANGELES 45, CALIFORNIA

a division of *Thompson Ramo Wooldridge Inc.*

Recent Developments in Convective Heat Transfer

ROLF H. SABERSKY

California Institute of Technology
Pasadena, Calif.

After receiving his Ph.D. degree in 1949, the author joined the staff of the California Institute of Technology, where he is now an Associate Professor of Mechanical Engineering. He has been active in teaching and research in the field of heat transfer and thermodynamics, and has written a textbook on this latter subject. Rocket propulsion has been one of the author's special interests. He has been associated with the Aerojet-General Corp. since 1943 and is now a consultant for that company. Dr. Sabersky is a member of the American Rocket Society.

IN WRITING about recent developments in convective heat transfer, it must first be admitted that the word "recent" has not been interpreted very literally. The developments discussed have been selected largely because they are of current interest, and the exact time at which they were achieved has been considered of secondary importance. An attempt has also been made to include enough of the background of each topic so that the account may be of use to the reader whose main interest lies outside the field of heat transfer. Furthermore, there is no pretense that this short paper should give a comprehensive survey of the extensive field of convective heat transfer. On the contrary, only a few specialized subjects have been selected, and in making this selection the writer's own interests and prejudices could not, of course, be fully suppressed. Heat transfer involving high speed flow has been left out completely, as it has been taken up in other articles of this series. The topics which are discussed in this review are transpiration and film cooling, heat transfer in rough tubes, nucleate boiling, heat transfer to fluids near the critical point, and flow with internal heat generation. Reference has been made to some of the principal sources of information. Although the given bibliography is relatively extensive, it cannot be considered complete, and the interested reader may wish to use the cited references as a further guide to the literature.

Film and Transpiration Cooling

Let us consider a surface being heated on one side by a stream of hot gases. The principle of transpiration cooling consists of cooling such a surface by injecting the coolant directly through the surface and into the hot stream. The coolant is to form a protective layer on the hot side. The injected fluid acts not only by absorbing heat but also by altering the flow pattern so as to reduce the heat transfer rate. In order to be able to cool by transpiration, the wall has to be porous. Attempts were made originally to produce porous walls by sintering powdered metals (1).[1] This method proved to be feasible, and even such complicated shapes as rocket nozzles could be made. The porosity was controlled by mixing the metal powder with a filler of a definite grain size. The filler would then evaporate during sintering, leaving the metal with the desired porosity. One of the major difficulties was probably that related to the clogging of the pores. More recently, the manufacture of porous surfaces has been advanced considerably by the invention of a new technique (2) in which a metal wire is taken as the basic component, and the wire is wound to yield a sheet of the desired porosity. The sheet is then sintered. The final product is generally stronger than the structure obtainable from powdered metals. It is relatively easy to produce shapes of various kinds, and by using different winding patterns variations in porosity and other special properties can be obtained. Early experiments on transpiration cooling have demonstrated the feasibility of the method (1). These experiments showed that relatively small rates of transpiration cooling would protect a surface requiring high heat transfer rates when cooled convectively.

Film cooling differs from transpiration cooling in that the coolant is injected through individual orifices spaced relatively far apart. The coolant is injected in such a way that a protective film is formed adjacent to the wall. Film cooling has the advantage of not requiring any special porous materials. On the other hand, the distribution of the protective film may be less effective. One should actually divide film cooling into two separate types, depending on whether the coolant is an evaporating liquid or a gas. If the coolant is a liquid, the evaporating vapor leaves essentially in a direction normal to the surface, and the mass addition is therefore quite similar to that in transpiration cooling. If a gaseous film is injected tangentially to the wall, the influence on the boundary layer formation is different. Film cooling with a liquid coolant is very advantageous because of the benefit which is derived from the latent heat. When reference is made to film cooling, it is often this type of cooling which is being considered.

One of the best known applications of film cooling has been in the thrust chamber of the V-2 missile (3). Several sets of film cooling holes were provided in the thrust chamber of this unit for the protection of critical areas, such as the throat. In film cooling with a liquid coolant, at least two problems in addition to those occurring in transpiration cooling have to be considered. The first of these is the problem of injecting the coolant in such a way that it attaches to the surface in order to form a film. The second is that of determining the area which can be covered from a single injection station.

Extensive experiments have been conducted regarding this latter aspect (4). In a particular set of experiments, the main flow consisted of heated air flowing through a duct. The walls of the duct were protected by film cooling with water. The film cooling rate was varied, and the corresponding change in the protected area was observed. The tests were repeated for several air flow rates. In each case it was seen that for low film cooling rates the protected area was directly propor-

Received Feb. 1958.

[1] Numbers in parentheses indicate References at end of paper.

tional to the flow rate. Beyond a certain critical value, a progressively more rapid increase in flow rate was required in order to extend the protected area. Visual observation showed that the initial thickness of the film increased as the flow rate was increased. At a flow rate close to the critical one, the film thickness seemed to reach a value at which the surface became unstable. Waves appeared on the surface, and fluid particles seemed to be torn from the crest of the waves and carried into the main stream. Such particles do not contribute to the cooling, and it is because of their breaking away that an ever-increasing flow rate per unit of protected area is required beyond the critical point. In general, therefore, it will be desirable to cool in such a way that the film remains stable. This will mean that from each injection point a relatively small area only can be covered, and in order to protect an extended surface several injection stations may be required.

Attempts have been made to analyze the unstable behavior of the liquid film (5). In this connection, it was noted that the critical thickness y_1 for all of the above mentioned experiments corresponded to a value of 25 for the dimensionless thickness y_1^*, where

$$y_1^* = \frac{y_1\sqrt{\tau_0/\rho}}{\nu}$$

and where

τ_0 = wall shear
ρ = the density of the film
ν = kinematic viscosity of the film

These data led to the hypothesis that the value $y_1^* = 25$ represented a universal constant for the stability of the film. This belief was strengthened by the fact that in the flow of a fluid in a pipe, the edge of the turbulent boundary layer also occurs for a value of y_1^* equal to about 25. It appeared, therefore, that the generation of turbulent motion in the flow of a single fluid and the onset of instability in a film might both be based on the same mechanism. Further experiments (6), however, showed a dependence of the dimensionless critical thickness on the ratio of the viscosity of the film to that of the main stream. It must, therefore, be concluded that the critical film thickness cannot be given by a single value of y_1^*. Nevertheless, it may be useful, in the further development of the theory of film stability, to consider possible connections between the factors limiting the thickness of a stable film and those determining the distance to the turbulent core in normal pipe flow.

The problem of attachment of a liquid film has also been studied experimentally. In addition to the properties and velocities of the fluids, the size as well as the direction of the injection orifices must be counted as variables. For injection normal to the direction of flow of the main stream, it was found that the Reynolds number of the gas and the ratio of the specific kinetic energy of the main stream to that of the injected fluid were important parameters (6, 7). In addition, the experiments of one author show that the Reynolds number of the liquid as well as a cavitation parameter (6) are also quantities affecting the attachment of a film. The cavitation parameter is defined as

$$\rho_l V^2/(p - p_v)$$

where

ρ_l = density of the liquid
V = average liquid velocity
p = prevailing pressure
p_v = vapor pressure of the liquid at the given temperature

The occurrence of such a parameter is certainly plausible and is explained by the following reasoning. The cooling fluid in order to form a surface film has to turn sharply immediately upon leaving the injection orifice. The pressure at the orifice edge must, therefore, be very low. When this pressure reaches the vapor pressure, detachment of the jet is likely. Experiments were also conducted in which the injection orifices were inclined at various angles towards the direction of the main flow (7). It was shown that the condition for attachment became considerably more favorable as the centerline of the orifice was inclined toward the direction of the main flow. In fact, in the set of experiments under discussion, no detachment could be observed when the angle between the centerline of the orifice and the surface was less than 45 deg.

The problem of heat transfer from a stable evaporating film is essentially the same as that from a fluid layer injected through a porous wall. The most important applications probably involve turbulent flow of the main stream. Several theoretical treatments of this problem have been offered (see, e.g., (8, 9)). In one of the earliest, the velocity and temperature profiles were determined for the injection of a gaseous coolant into a stream in turbulent motion (8). In this analysis the flow was divided into a laminar sublayer and a turbulent core. The temperature and velocity profiles in the laminar layer were calculated taking into account the rate of injection of fluid through the wall. In the turbulent core the Reynolds analogy was assumed to be applicable. Furthermore, the flow was considered to remain unaffected by the mass injection, and the usual relations for the friction coefficient, the velocity profile, and the thickness of the laminar layer were assumed to hold. These assumptions were made in order to obtain a first approximation, and they will be modified as additional information becomes available. Nevertheless, the predicted profiles were in relatively good agreement with measured values (10). The theory was next extended so as to be applicable to an evaporating coolant as well as to a coolant which might undergo chemical reaction in the boundary layer (11). In a subsequent analysis for evaporating coolants (12), the Reynolds analogy was used in a somewhat different form in an attempt to take into account the effects of mass addition on the flow in the turbulent core. In addition, the surface temperature of the liquid was made to correspond to the local vapor pressure. The results of this analysis have been compared with experimental data and encouraging agreement has been found to exist.

Further studies of film cooling with both laminar and turbulent flow have been made (see, e.g., (13, 14, 15 and 16)). Many of these also include the effects of compressibility. In (15 and 16), which are concerned with turbulent flow, particular care has been taken to account for the effect of mass injection on the flow in the turbulent core. In the development, assumptions are made regarding the dependence of the turbulent exchange coefficients on the velocity profile and the distance from the wall. Most of the earlier work was limited to the injection of a gas with properties identical to those of the main flow. Several sets of experimental data (see, e.g., (17, 18, 19 and 20)) have also been obtained for this case, and they are in fair agreement with the predicted values. Recently, emphasis has been given to the problem in which the coolant gas differs from that of the main flow (21, 22). The computations show the advantages that can be gained from the injection of a gas of low molecular weight.

One other paper should be mentioned here in which an analysis is given of the heat transfer in laminar flow to a nonporous surface, just downstream of a transpiration-cooled section (23). Such a combination of porous and nonporous regions may be desirable for structural reasons, and the analysis was performed in order to investigate the effectiveness of such an arrangement. In the limit, as the porous regions are reduced, the conditions for gaseous film cooling are approached in which the coolant is injected through individual slots. A special analysis for this type of film cooling has also been performed (24). This analysis is based on an ingenious simplification by which the injection slots are regarded as heat

sinks. The effect of injection on the hydrodynamic boundary layer is neglected. The results of the analysis have been compared (25) to a set of older experimental data (26), and satisfactory agreement is shown to exist. Additional experimental results have become available in recent years (see, e.g., (28, 29)).

The several analyses mentioned are believed to show fruitful approaches to the problem of transpiration and film cooling. They are, however, based on many assumptions which have not yet been sufficiently verified in detail. Special experiments with the purpose of investigating these assumptions will probably be required before any significant further advances may be made.

Before concluding this subject, the unique character of film and transpiration cooling should be emphasized. It is the only method by which a wall can be kept at very low surface temperatures, independent of the heating rate or the temperature of the hot gas. This is quite different from ordinary convective cooling, in which the surface temperature is a function of the hot gas temperature, and depends on the relative magnitude of the heat transfer coefficients of the hot gas and the coolant, and on the heat transfer resistance of the wall. Film or transpiration cooling does, of course, require the expenditure of mass. From the investigations completed so far, however, it can already be shown that this expenditure is feasible for many applications (see, e.g., (30)). For large rocket motors, for example, the amount of coolant required can be calculated to be of the order of 1 per cent of the propellant flow, assuming that the coolant does not benefit the thrust. Actually, however, the coolant does add to the thrust, particularly if the coolant is one of the propellants. In that case, film cooling with unstable films may also be indicated. The fluid particles which are torn off by the main stream can no longer be counted as lost, since they will probably react just as the remainder of the propellant. Film cooling with a small number of injection stations then becomes possible, which is most desirable from the point of view of design and control. It may well be that film cooling will become an essential factor in the design of rocket motors using high energy propellants. Further study of this method of cooling should be of considerable interest.

Heat Transfer in Rough Tubes

Friction in rough tubes has been considered to be one of the fundamental problems in fluid mechanics, and the problem has been investigated thoroughly. The most extensive experimental results are probably those due to Nikuradse (31). One would think that heat transfer in rough tubes should be considered an equally basic problem. Nevertheless, it is apparent that heat transfer in rough tubes has not received the same attention as the corresponding friction problem. Some studies have, of course, been devoted to this subject in the past, and recently it has received somewhat more emphasis. The studies in which friction and heat transfer are treated jointly are of particular interest, as these two phenomena are in general intimately connected.

In one of the earliest studies (32), experimental data were obtained for water flowing in tubes which had been roughened by knurling. These data indicated that there was some increase in the heat transfer coefficient with roughness. The friction coefficient, however, showed a much larger increase than the heat transfer coefficient. As a consequence, the ratio of the heat transfer coefficient to the friction coefficient decreased with increased roughness. Although there has been some question regarding the accuracy of these data, the general results have been reproduced by subsequent investigators.

In one of the important recent studies (33), a set of experiments with rough tubes has been performed, using air as the working fluid. The roughness in these tubes was produced by inserting specially shaped piston rings as roughness elements. These results confirmed that there is a tendency for the friction coefficient to increase more rapidly than the heat transfer coefficient. In addition, it was shown that a fairly unique relationship seemed to exist between the two coefficients, and that this relationship was essentially independent of the type of roughness element. A few tests were also conducted with a naturally rough tube, and the behavior of this tube did not seem to differ materially from that of an artificially roughened tube. In particular, the results of the tests on the naturally rough tube were compared to those of an artificially roughened tube having the same friction factor. It was shown that both tubes also yielded the same heat transfer coefficient.

There are, however, other experiments which may have an important bearing on the above results (34, 35). In these experiments, flow in annular ducts was studied. The inner surfaces of the ducts were provided with transverse fins in the form of annular disks oriented normal to the flow direction. Various fin sizes and spacings were examined, the fins in some cases extending into the duct for about 40 per cent of the width of the annulus. Heat was transferred from the inner surface to the fluid, and the heat transfer rate and friction drop were measured. It was found that the presence of the disks would increase the heat transfer coefficient as well as the friction coefficient. In (34), it was shown that for most spacings the ratio of heat transfer to the friction coefficient would decrease below the value corresponding to a smooth wall, but that for certain particular spacings, equally high or even higher ratios seemed obtainable. The exact numerical values in this comparison are somewhat in question, because the values for the coefficients for smooth walls were estimated rather than measured. There is also some difficulty in making analytical comparisons between heat transfer and the friction coefficient. The latter has to be derived from pressure drop measurements, and it therefore constitutes an average between the friction coefficient of the smooth outer wall and that of the rough inner surface. Nevertheless, for engineering purposes the above result is most significant; it indicates that by using a properly roughened surface a given amount of heat may be transferred from a smaller length of duct with a possible decrease in pumping power. The aim of the experiments in (34) was actually to produce such an effective surface for the heat transfer ducts of the nuclear reactors in Calder Hall. Experiments were also performed in order to visually examine the flow pattern for the various disk arrangements (34, 35). For the spacing most favorable to heat transfer, a set of stable vortices would develop between adjacent disks. The velocities due to these vortices were apparently responsible for providing good heat transfer conditions along all exposed surfaces. For less favorable spacings, one might expect relatively quiescent wake regions behind each disk. In this case, the heat transfer from the surface bounding these regions might be poor, but the friction effect might remain high because of the drag forces caused by the disks.

It must be admitted, of course, that the surface with annular disks as described above differs from the usual concept of a rough surface. Nevertheless, for the present purpose one may well think of it as an artificially roughened surface, and one may suspect that ordinary rough surfaces might show a similar behavior. It seems, therefore, justified to question if the shape and distribution of roughness elements will influence the ratio of the heat transfer to the friction coefficient. The set of experiments previously cited (33) may possibly not have covered a sufficient range of surface arrangements to indicate such an effect. Further work on this aspect promises to be most interesting as well as of practical importance.

Three additional papers should be mentioned as they also contain results of experiments which may be helpful in formalizing a theory for the heat transfer in rough tubes. The first contains data for the flow of air through artificially roughened tubes (37). The second presents information for

the flow of air through a large number of different, naturally rough tubes (38). In the third, a set of experiments is reported concerning the flow of water through a knurled tube (39). In these tests the effect of Prandtl number was studied. The change in Prandtl number was obtained by varying the water temperature. The Prandtl number is one of the essential parameters in heat transfer, and theories can often be tested by comparing their predictions as to the effect of Prandtl number with corresponding experimental results.

Attempts to analyze the effect of roughness on heat transfer have also been made. In an appendix to his well-known paper on heat transfer and fluid friction, Martinelli (40) suggests a simple extension to the relationship which applies to smooth tubes. The modified equation fits some of the experimental data surprisingly well. In a more recent study, an interesting model for analyzing the effect of roughness was proposed (33). In this proposal, the drag force offered by the rough wall is divided into surface drag and form drag. A wire grid is then imagined to be suspended in the fluid at the edge of the laminar boundary layer. The drag of the grid represents the additional shear caused by the roughness. The flow is then analyzed on this basis, and the results compare favorably with the experimental data obtained with air (see, e.g., (33, 41)). The model is an interesting one and certainly deserves further study. Some of the assumptions, such as the one that the thickness of the laminar boundary layer is unaffected by roughness, will have to be checked. Further modification of the model may be required if the roughness type should prove to have an effect on the relationship between friction and heat transfer.

Nucleate Boiling[2]

Boiling heat transfer occurs when heat is transferred from a surface to an adjacent liquid under such conditions that the vapor phase is formed in the neighborhood of the surface. Boiling heat transfer occurs in many applications, such as the cooling of rocket motors and the transfer of heat from the core of a nuclear reactor. The phenomena occurring in boiling heat transfer have been subject to intensive study. Qualitatively, the process is now rather well understood, and the typical experimental results have become quite familiar. These results are usually presented in the form of a graph of the heat transfer rate vs. the temperature of the heating surface at constant fluid temperatures. As the surface temperature is increased above that of the liquid, heat transfer will take place by the usual convection process. When the temperature reaches a value approximately equal to the boiling point of the liquid at the prevailing pressure, bubbles appear in the liquid. If the liquid is near its saturation temperature, the bubbles will detach. If the liquid is at a temperature well below its boiling point, most bubbles will grow to a certain size and then collapse again at the surface. As the bubbles appear, a very marked increase in the heat transfer coefficient is observed, so that a minor increase in temperature brings about a very large increase in the heat transfer rate. As the surface temperature is raised further, the bubbles become more numerous and the strong effect of temperature on heat transfer continues. A maximum heat transfer rate is reached just before the bubbles become so numerous that they coalesce periodically, forming an unstable and intermittent vapor blanket over the surface. An additional increase in surface temperature leads to more vapor formation and to a decrease in the heat transfer coefficient. As a consequence, the heat transfer rate now decreases with increasing temperature. Finally, sufficient vapor is generated so that a rather stable vapor film forms over the surface. Further increase in surface temperature will now again lead to an increased heat transfer rate. The region from the initiation of the first vapor bubbles to the point of maximum heat transfer rate is known as the *nucleate boiling region*. The region in which the heat transfer rate decreases with surface temperature is called the *partial film boiling region*, and the region beyond has been named the *stable film boiling region*. The fact that a maximum occurs at the end of the nucleate boiling region is a characteristic of boiling heat transfer. In order to exceed this maximum, the surface has to pass into film boiling. The corresponding surface temperature may, however, have to be very high, the exact magnitude depending on the properties of the fluid involved. In many instances this temperature would have to be so high that the surface material would melt if attempts were made to exceed the maximum heat transfer rate of the nucleate boiling region. This maximum is, therefore, often called the *burnout point*. This general description of boiling heat transfer applies regardless of whether the fluid is at its saturation temperature or below, and it also applies to free convection as well as to forced convection. However, the existence of a maximum and the transition from nucleate boiling to film boiling becomes, of course, less pronounced as the pressure approaches the critical pressure of the fluid. A large amount of data for various liquids under a variety of conditions has been obtained (see, e.g., (43 to 48)). A very complete list of information available on rocket propellants is contained in (49).

The nucleate boiling region is of special importance in engineering, since it affords a possibility of obtaining very high heat transfer rates without necessitating excessive wall temperatures. The burnout point takes on a special significance since it presents a limit which in many designs should not be exceeded. In analyzing nucleate boiling it is convenient to divide the problem into three parts: The generation of the bubbles, the growth and collapse of the bubbles, and the interaction between bubble motion and heat transfer. As to the generation of bubbles, most investigators believe at present that bubbles form from pre-existing nuclei (see, e.g., (50, 51, 52)). These nuclei probably consist of gas or vapor pockets which are stabilized either in cavities on the surface or on solid impurities contained in the liquid itself. As the temperature of the surrounding fluid increases, vapor will evaporate into these nuclei. If the inside pressure becomes sufficiently large to overcome the effects of surface tension, the nucleus will grow into a bubble. The next phase, i.e., the growth and subsequent detachment or collapse, is governed largely by the heat transfer between the bubble and the surrounding fluid. Finally, the improvement in the heat transfer coefficient is believed to be due in part to the agitation caused by the bubbles, and in part to the vapor transport. In the case where bubbles are actually leaving the surface, the effect of vapor transport is a most important one. If the bubbles collapse on the surface, most investigators believe the effect of agitation to be the essential one, although some feel that the rate of evaporation across the bubble makes a significant contribution to the total heat transfer.

This general description of nucleate boiling probably still applies if the fluid flowing along a pipe is made to spiral. Quantitatively, however, the results have been shown to differ. Experiments have recently been carried out in which water was ducted through a heated tube in such a manner that it had a tangential velocity component in addition to the usual axial one (53). In this way, a very significant increase in the burnout point was achieved. The increase was larger than that corresponding to an axial velocity equal to the total velocity along the spiral path, and the change could not be explained by the increase in surface velocity. The spiral motion does, however, give rise to a strong radial pressure gradient, and it is believed that the influence of this gradient on bubble motion is responsible for the observed increase in the burnout heat flux. The fact that spiral motion may lead

[2] For an account of work in boiling heat transfer in Russia, the reader is referred to a book by S. S. Kutadeladze which has been translated into English (42).

to an increase in the burnout point may be of great value to the designer of heat transfer equipment.

It is, of course, the purpose of a heat transfer investigation to arrive at a sufficient understanding of the phenomenon so that the heat transfer rate can be predicted quantitatively as a function of the fluid properties and the wall temperature. In working towards this goal, several of the individual steps in the process of nucleate boiling have been studied in detail. The bubble growth has, for example, been analyzed quite extensively (see, e.g., (54,55,56)). Most of these analyses have been based on a spherical bubble and spherically symmetrical conditions. The results are in satisfactory agreement with experiments which were devised to fulfill the assumptions of the analyses (57). In recent years, an interesting new approach has also been pursued which is aimed particularly at determining the maximum heat transfer rate which can be achieved in nucleate boiling. In this approach, attention is focused on the vapor in the region of partial film boiling. The stability criteria of this film are studied, and the maximum of the nucleate region is regarded as the limit of the partial film boiling region (58,59). The concept of film stability in connection with the boiling heat transfer may prove to be very fruitful.

A complete solution of a problem as complicated as nucleate boiling heat transfer will be very difficult to obtain. As in many other problems in fluid mechanics or heat transfer, however, the determination and experimental correlation of the significant dimensionless parameters would in itself be of great usefulness. Considerable attention has been devoted to this approach. The problem is, however, so complicated that even this approach proved to be by no means easy. The reader who is interested in educational problems might use this fact as an example to illustrate that the application of dimensionless analysis and the Pi-theorem does not lead to the solution of a problem quite as readily as some textbooks would have one believe.

Two principal types of correlations have been developed: Correlations for the nucleate boiling region and correlations for the point of maximum heat transfer in nucleate boiling. For many engineering applications, the latter are of particular importance. In selecting the significant parameters, careful attention was paid to the theoretical analyses described previously. In developing appropriate expressions, many investigators followed the concept that the heat transfer is due to vapor transport and added agitation. In order to express the effect of agitation, appropriate Reynolds numbers were selected (see, e.g., (51, 60, 61)). In forming these Reynolds numbers, the bubble diameter and bubble growth velocities (change of radius with time) have often been used as the significant quantities. A great simplification was introduced when it was shown that for a bubble growing in a fluid of uniform temperature, the product of growth velocity and diameter was a constant (61). Although the temperature field is not generally uniform, a correlation for the nucleate boiling region based on this simplification (61) has shown promising agreement with experiments. It has been shown to cover the results of fluids with such wide variations in properties as water and liquid metals (62).

A comprehensive equation for the determination of the point of maximum heat transfer has also been published recently (60). The equation is intended to be applicable when the motion of the liquid is forced as well as when it is free, and it is applicable to any fluid at all temperatures including the saturation temperature. Correlations based on the concept of film stability have also been developed. It is interesting and encouraging to see that one of these is quite similar in form to the correlation based on the concept of a Reynolds number (59).

It appears, therefore, that the attempts to develop suitable correlations for nucleate boiling are becoming more successful, and there is some hope that further experimentation will prove some of the proposed relationships to be adequate for many engineering applications.

There is, however, at least one phase which will need further intensive study before the present correlations can be used with confidence and that is the nucleation process which was briefly described previously. It was stated that the initial appearance of bubbles was believed to depend on the size and number of pre-existing gas or vapor cavities. This number will depend on the condition of the surface, the surface tension and contact angle between the fluid and the surface, and on the amount of dissolved gas and impurities contained in the liquid. The fact that these various characteristics can have an influence on nucleate boiling has been demonstrated experimentally (see, e.g., (51, 52, 63, 64)). In particular, these factors may influence the temperature at which bubbles will first form, the slope of the curve of heat transfer vs. wall temperature, as well as the wall temperature at which burnout occurs.

There is some indication, however, that nucleation is sufficiently insensitive to the above mentioned surface factors, so that variations in these factors can be ignored for "normal" conditions and when extreme accuracy is not required. There is also some indication, based on the reasoning presented in (59) and on the form of the correlations in (59 and 60), that the burnout heat flux is relatively independent of surface conditions. If these indications can be verified in general, correlations for nucleate boiling may prove successful.

In discussing nucleate boiling, it has so far been assumed that the main body of the fluid was in liquid form. The case in which the main body itself is a mixture of liquid and vapor is becoming of increasing importance. Heat transfer to such a two-phase mixture is actually not a new problem. On the contrary, it occurs in the boiler of every conventional steam powerplant. In boilers, however, the heat transfer from the combustion gases to the steam is largely controlled by the gas film resistance which is usually the highest resistance in this process. The exact magnitude of the heat transfer coefficient between the pipe wall and the steam is, therefore, often of secondary importance, and the heat transfer rates are generally sufficiently low so that there is no danger of "burnout." In water-boiling nuclear reactors, however, the gas film resistance is absent, and the transfer process between wall and steam becomes of major significance. It is largely because of this application that the heat transfer to vapor-liquid mixtures is being studied extensively.

Studies of the flow of two-phase mixtures have been undertaken previously (see, e.g., (65, 66)). In some of these it was shown that different types of flow are possible, each type corresponding to a certain distribution of vapor and liquid. In the region of most interest in heat transfer, the distribution is probably such that there exists a vapor core surrounded by a liquid film. It is quite possible, therefore, that the heat transfer between the wall and the film is similar to that previously described for nucleate boiling.

Several correlations have been proposed based on experimental data. In particular, one of the correlations for the burnout point, previously mentioned in connection with nucleate boiling in a liquid (60), has also been suitable in correlating some of the data for liquid-vapor mixtures. This fact, as well as the occurrence of a burnout point in itself, may indicate that the process of heat transfer consists of nucleate boiling in a liquid film as proposed above. Other correlations, limited to water-steam mixtures, have also been suggested. In one of these, the thickness of the assumed liquid film appears as a factor (67). The thickness is calculated on the basis of the quality of the flowing mixture. Another correlation involves the total enthalpy (68) of the mixture as a significant quantity, which again is a function of the quality.

From the foregoing account on boiling heat transfer, it may be concluded that significant progress has been made in this field. The phenomenon is, however, a very intricate one, and many properties of the fluid as well as of the heating surface seem to exert an important influence. It therefore

must be expected that a considerable amount of time will pass before the engineer will have available a reliable general correlation suitable for all fluids. Until then, he will have to base his design largely on direct experimental data obtained for the particular fluid of interest and under conditions simulating those of the prototype as closely as possible.

Heat Transfer to Fluids Near the Critical Point

In several modern applications, heat transfer takes place to fluids which are near their critical state. Steam powerplants, for example, are now being designed for pressures of 5000 psi and higher, and in the process of heating, the steam passes through states which are relatively close to the critical point (p_{cr} = 3206.2 psia, T_{cr} = 705.4 F). As a second example, the cooling of rocket motors may be cited. Fuels based on hydrocarbons have critical pressures of the order of 500 to 600 psia, and liquid oxygen has a critical pressure of 730 psia. When these fluids are used as coolants, they will in many designs reach pressures and temperatures close to the critical values.

Some experimental work on the heat transfer to fluids near their critical point is available. The volume of existing data is, however, not yet very extensive. Experiments which have been performed include work with water (69), oxygen (70), nitrogen (71) and carbon dioxide (72).

From one point of view, heat transfer to fluids near the critical point may not require a special classification. The principal characteristic of fluids in this region is that their properties are strongly affected by pressure and temperature. It may, therefore, be that the heat transfer to these fluids may be regarded as normal convection to a fluid under conditions for which the variations of properties through the boundary layer are of essential importance. From another point of view, however, heat transfer near the critical point may be regarded as the limit of boiling heat transfer, and one might suggest that some of the characteristics of this type of heat transfer may still prevail.

To study these aspects of the problem, heat transfer coefficients were calculated on the basis of analyses in which the change in fluid properties throughout the boundary layer was taken into account. The analytical results were compared to the experimental data in question, and it was seen that the trends were in general well predicted by the theory (69, 72). However, there was at least one exception, in that the heat transfer coefficient for water in the immediate neighborhood of the critical temperature showed a very marked increase not predicted by the theory (69). On the basis of this result, it was suggested that the fluid in this region still might behave similarly to a fluid in nucleate boiling (see, e.g., (69, 73)). Since the pressure is above the critical value, one can not, of course, expect the appearance of a second phase. If the decrease in density with temperature is very pronounced, one may, however, imagine that regions of relatively low density form near the heating surface. These regions might become unstable and grow and collapse or detach from the surface. In other words, they may possibly behave in a manner very similar to bubbles in nucleate boiling. If so, the activity of these low density regions may provide the explanation for the improved heat transfer observed for water near the critical temperature. Whether or not such bubble-like activity will occur may well depend on the variation of density with temperature of the particular fluid as well as on the temperature gradients existing near the surface. It may be quite possible, therefore, that such a phenomenon might occur near the critical point in some fluids but not in others. Further work to clarify the mechanism of heat transfer near the critical point should be most interesting and timely.

Flow With Heat Generation

One of the special problems which has arisen out of the nuclear reactor field is that involving heat transfer in a fluid with internal heat generation. This problem occurs principally in reactors in which the fuel is in liquid form and where this fluid itself is circulated. This problem has been analyzed for turbulent flow in a circular pipe (74) assuming a fully developed velocity profile and a constant axial temperature gradient across the pipe. In the analysis, the turbulent exchange coefficient for heat transfer was set equal to that for friction. The latter was derived from the known velocity profile. With these assumptions, the differential equation for heat transfer could be solved. The solution was given in terms of the temperature distribution which prevails when the pipe walls are insulated. It was furthermore shown that solutions for other wall conditions could be obtained easily by superimposing these temperature profiles on the normal profiles which exist in the absence of internal heat generation.

In order to check the analyses, an ingenious experiment was devised (74). An electrolytic solution was used in the test fluid so that the internal heat generation could be obtained by conducting electric current directly through the fluid. Temperature and heat flow rate measurements were made, and the results were in satisfactory agreement with the predicted values. The analysis, although involving certain simplifying assumptions, is certainly accurate enough to be of great value in guiding the designer faced with problems involving internal heat generation.

Closing Remarks

As stated earlier, an attempt has been made in this paper to briefly review some of the problems in low velocity convective heat transfer. Most of the subjects discussed are directly related to design applications of current interest, and, in fact, the problems usually have arisen from such applications. A full understanding of the various heat transfer mechanisms would be most beneficial in further advancing the designs in question.

The subjects reviewed are all quite complicated and most difficult to approach analytically. As a consequence, the designer as well as the research engineer has to rely heavily on experimental information. Most of the problems mentioned are in the stage in which such experimental work is being pursued actively and in which initial steps toward an analytical solution have been taken. Few of the problems, however, can be said to have been fully solved or to be completely understood. It should be a genuine challenge to the research engineer to pursue these problems to a satisfactory conclusion.

References

1 Duwez, Pol and Martens, H., "The Powder Metallurgy of Porous Metals and Alloys Having a Controlled Porosity," Amer. Inst. of Mining and Metallurgical Engng., Pub. no. 2343, 1948.

2 Wheeler, H. L., Jr. and Duwez, Pol, "Wire Wound Porous Metals," Calif. Inst. of Tech., Jet Prop. Lab., Report no. PR-20-198, Sept. 1953.

3 Sutton, G. P., "Rocket Propulsion Elements," Wiley and Sons, New York, 1956, 2nd ed., chap. 7.

4 Kinney, R. G. and Sloop, J. L., "Internal Film Cooling Experiments in 4″ Duct with Gas Temperatures to 2000°F," NACA, RM E 50 F 19, Cleveland, Sept. 1950.

5 Kinney, R. G. and Abramson, A. E., "Investigation of Annular Liquid Flow with Cocurrent Air Flow in Horizontal Tubes," NACA, RM E 51 C 13, Cleveland, May 1951.

6 Knuth, E. L., "The Mechanics of Film Cooling, Part I," Jet Propulsion, vol. 24, Nov.-Dec. 1954, p. 359.

7 Warner, C. F. and Reese, B. A., "Investigation of the Factors Affecting the Attachment of a Liquid Film to a Solid Surface," Jet Propulsion, vol. 27, Aug. 1957, p. 877.

8 Rannie, W. D., "A Simplified Theory of Porous Wall Cooling," Calif. Inst. of Tech., Jet Prop. Lab., Progress Rep. no. 4-50, Pasadena, Nov. 1947. Abstracted in "Heat Transfer," University of Michigan Press, Ann Arbor, 1953, chap. 7.

9 Friedmann, J., "A Theoretical and Experimental Investigation of Rocket-Motor Sweat Cooling," Journal of the American Rocket Society, Dec. 1949, p. 174.

10 Duwez, Pol and Wheeler, H. L., Jr., "Heat Transfer Through Sweat Cooled Porous Tubes," Jet Propulsion, vol. 25, Oct. 1955, p. 519.

11 Crocco, L., "An Approximate Theory of Porous Sweat and Film Cooling with Reactive Fluids," Journal of the American Rocket Society, vol. 22, Nov.-Dec. 1952, p. 331.

12 Knuth, E. L., "The Mechanics of Film Cooling, Part II," JET PROPULSION, vol. 25, Jan. 1955, p. 16.

13 Yuan, S. W., "Cooling by Protective Fluid Films," in "High Speed Aerodynamics & Jet Propulsion," vol. V, sec. G, Princeton University Press (to be published).

14 Low, G. M., "The Compressible Laminar Boundary Layer with Fluid Injection," NACA TN 3404, March 1955.

15 Rubesin, M. W., "An Analytical Estimation of the Effect of Transpiration Cooling on the Heat Transfer and Skin Friction Characteristics of a Compressible Turbulent Boundary Layer," NACA TN 3341, Dec. 1954.

16 Dorrance, W. H. and Dore, F. J., "The Effect of Mass Transfer on the Compressible Turbulent Boundary-Layer Skin Friction and Heat Transfer," *J. Aeron. Sci.*, vol. 21, 1954, p. 404.

17 Brunk, W. E., "Experimental Investigation of Transpiration Cooling for a Turbulent Boundary Layer in Subsonic Flow Using Air as a Coolant," NACA TN 4091, Oct. 1957.

18 Rubesin, M. W., "The Influence of Surface Injection on Heat Transfer and Skin Friction Associated with the High Speed Turbulent Boundary Layer," NACA RM A 55 L 13, Feb. 1956.

19 Mickley, H. S., Ross, R. C. Squyres, A. L. and Stewart, W. E., "Heat, Mass and Momentum Transfer for Flow over a Flat Plate with Blowing or Suction," NACA TN 3208, July 1954.

20 Green, L. and Nall, K. L., "Experiments on Porous Wall Cooling and Flow Separation Control in a Supersonic Nozzle," IAS annual meeting, Jan. 1959; *see also* Aerojet-General Rep. no. 1381, available through ASTIA.

21 Rubesin, M. W. and Pappas, C. C., "An Analysis of the Turbulent Boundary Layer Characteristics on a Flat Plate with Distributed Light-Gas Injection," NACA TN 4149, Feb. 1958.

22 Eckert, E. R. G., Schneider, P. J., Hayday, A. A. and Larson, R. M., "Mass-Transfer Cooling of a Laminar Boundary Layer by Injection of a Light-Weight Foreign Gas," JET PROPULSION, vol. 28, Jan. 1958, pp. 34–39.

23 Rubesin, M. W. and Inouye, M., "A Theoretical Study of the Effect of Upstream Transpiration Cooling on the Heat Transfer and Skin Friction Characteristics of a Compressible Laminar Boundary Layer," NACA TN 3969, May 1957.

24 Univ. of Michigan, "Heat Transfer," Univ. of Michigan Press, Ann Arbor, 1953, chap. 8.

25 Eckert, E. R. G. and Drake, R. M., "Heat and Mass Transfer," 2nd ed., McGraw-Hill Book Co., N. Y., 1959, chap. 10.

26 Wieghardt, K., "Hot Air Discharge for De-Icing," AAF Translation no. F-TS-919, RE, Air Materiel Command, Dec. 1946. See also Ref. 27.

27 Eckert, E. R. G. and Livingood, J. N. B., "Comparison of Effectiveness of Convection, Transpiration, and Film Cooling Methods with Air as Coolant," NACA Report no. 1182, 1954.

28 Seban, R. A., Chan, H. W. and Scesa, S., "Heat Transfer to a Turbulent Boundary Layer Downstream of an Injection Slot," ASME Paper no. 57-A-36.

29 Chin, J. H., Skirvin, S. C., Hayes, L. E. and Silver, A. H., "Adiabatic Wall Temperature Downstream of a Single, Tangential Injection Slot," ASME Paper no. 58-A-107.

30 Zucrow, M. J. and Graham, R. R., "Film Cooling for Rocket Motors," JET PROPULSION, vol. 27, June 1957, p. 650.

31 Schlichting, H., "Boundary Layer Theory," McGraw-Hill Book Co., N. Y. 1953, p. 418.

32 Cope, W. F., "The Friction and Heat Transmission Coefficients in Rough Pipes," Proc. Inst. Mech. Engrs., London, vol. 145, 1941, p. 99.

33 Nunner, W., "Warmeubergang und Druckabfall in rauhen Rohren," *VDI, Forschungsheft*, Ausgabe B, vol. 22, 1956.

34 Fortescue, P. and Hall, W. B., "Heat Transfer Experiments in the Fuel Elements—Calder Hall Reactor," *J. British Nuclear Energy Conf. 2*, April 1957; *see also* "Nucleonics," McGraw-Hill Book Co., vol. 14, Dec. 1956, p. 8-16.

35 Knudsen, J. G. and Katz, D. L., "Heat Transfer and Pressure Drop in Annuli," *Chem. Engng. Progr.*, vol. 46, 1950, p. 490. See also Ref. 36.

36 Knudsen, J. G. and Katz, D. L., "Fluid Dynamics and Heat Transfer," McGraw-Hill Book Co., N. Y., 1958, p. 196.

37 Sams, E. W., "Experimental Investigation of Average Heat Transfer and Friction Coefficients for Air Flowing in Circular Tubes having Screw-Type Roughness," NACA RM E 52 D 17, 1952.

38 Smith, J. W. and Epstein, N., "Effect of Wall Roughness on Convection Heat Transfer in Commercial Pipes," *J. AIChE*, vol. 3, 1957, p. 242.

39 Hastrup, R. C., Sabersky, R. H., Bartz, D. R. and Noel, M. B., "Friction and Heat Transfer in a Rough Tube at Varying Prandtl Numbers," JET PROPULSION, vol. 28, April 1958, pp. 259–263.

40 Martinelli, R. C., "Heat Transfer to Molten Metals." *Trans. ASME*, vol. 69, 1947. p. 947.

41 Lancet, R. T., "The Effect of Surface Roughness on the Convection Heat Transfer Coefficient for Fully Developed Turbulent Flow in Ducts with Uniform Heat Flux," ASME Paper no. 58-A-122, 1958.

42 Kutadeladze, S. S., "Problems of Heat Transfer During a Change of State," AEC Translation no. 3405, AEC Tech. Inf. Service, Oakridge, Tenn.

43 Gunther, F. C., "Photographic Study of Surface Boiling Heat Transfer Data to Water with Forced Convection," *Trans. ASME*, vol. 73, Feb. 1951, p. 115.

44 McAdams, W. H., Kennel, C. S., Minden, R. C., Picornell, P. M. and Dew, J. E., "Heat Transfer at High Rates to Water with Surface Boiling," *Ind. and Engng. Chem.*, vol. 41, 1949, p. 1945.

45 Farber, E. A., "Free Convection Heat Transfer from Electrically Heated Wires," *J. Appl. Phys.*, vol. 22, Dec. 1951, p. 1437.

46 Buchberg, H., Romie, F., Lipkis, R. and Greenfield, M., "Heat Transfer, Pressure Drop, and Burnout Studies with and without Surface Boiling for Deaerated and Gassed Water at Elevated Pressures in a Forced Flow System," Heat Transfer and Fluid Mech. Inst., Stanford University Press, 1951.

47 Rohsenow, W. M. and Clark, J. A., "Heat Transfer and Pressure Drop Data for High Heat Flux Densities to Water at High Subcritical Pressures," Heat Transfer and Fluid Mech. Inst., Stanford University Press, 1951.

48 Cichelli, M. T. and Bonilla, Ch. F., "Heat Transfer to Liquids Boiling under Pressure," *Trans. AIChE*, vol. 42, 1946, p. 411.

49 Bartz, D., "Factors Which Influence the Suitability of Liquid Propellants as Rocket Motor Regenerative Coolants," JET PROPULSION, vol. 28, Jan. 1958, pp. 46–53.

50 Bankoff, S. G., "Ebullition from Solid Surfaces in the Absence of a Pre-existing Gaseous Phase," *Trans. ASME*, vol. 79, May 1957, p. 735.

51 Ellion, M. E., "A Study of the Mechanism of Boiling Heat Transfer," Calif. Inst. of Tech., Jet Prop Lab., Memo no. 20-88, March 1954.

52 Sabersky, R. H. and Gates, C. W., Jr., "On the Start of Nucleation in Boiling Heat Transfer," JET PROPULSION, vol. 25, Feb. 1955, p. 67.

53 Gamhill, W. R. and Greene, N. D., "Boiling Burnout with Water in Vortex Flow," *Chem. Engng. Progr.*, vol. 54, Oct. 1958, p. 68.

54 Plesset, M. S. and Zwick, S. A., "The Growth of Vapor Bubbles in Super-Heated Liquids," *J. Appl. Phys.*, vol. 25, April 1954, p. 493.

55 Forster, H. K. and Zuber, N., "Growth of a Vapor Bubble in a Super-Heated Liquid," *J. Appl. Phys.*, vol. 25, April 1954, p. 474.

56 Bankoff, S. G. and Mikesell, R. D., "Growth of Bubbles in a Liquid of Initially Non-Uniform Temperature," ASME Paper no. 58-A105, Dec. 1958.

57 Dergarabedian, P., "The Rate of Growth of Vapor Bubbles in Superheated Water," *Trans. ASME*, vol. 75, 1953, p. 537.

58 Chang, Y. P., "A Theoretical Analysis of Heat Transfer in Natural Convection and in Boiling," *Trans. ASME*, vol. 79, Oct. 1957, p. 1501.

59 Zuber, N. and Tribus, M., "Further Remarks on the Stability of Boiling Heat Transfer," Univ. of California, Los Angeles, Dept. of Engineering Rep. no. 58-5, Jan. 1958.

60 Griffith, P., "The Correlation of Nucleate Boiling Burnout Data," ASME Paper no. 57 HT 21, Sept. 1957.

61 Forster, H. K. and Zuber, N., "Dynamics of Vapor Bubbles and Boiling Heat Transfer," *J. AIChE*, vol. 1, 1955, p. 531.

62 Camack, W. G. and Forster, H. K., "Test of a Heat Transfer Correlation for Boiling Liquid Metals," JET PROPULSION, vol. 27, Oct. 1957, pp. 1104–1106.

63 Corty, C. and Foust, A., "Surface Variables in Nucleate Boiling," AIChE-Chem. Eng. Progress Symposium Series, no. 17, 1955.

64 Jens, W. H. and Leppert, G., "Recent Developments in Boiling Research," *J. Amer. Soc. Naval Engrs.*, vol. 67, Feb. 1955.

65 Bergelin, O. P. and Gazley, C., "Co-current Gas Liquid Flow in Horizontal Tubes," Heat Transfer and Fluid Mech. Inst., Berkeley, 1949.

66 Reid, R. C. Reynolds, A. B., Diglio, A. J. Spiewak, I. and Klipstein, D. H., "Two Phase Pressure Drops in Large Diameter Pipes," *J. AIChE*, vol. 3, 1957, p. 321.

67 Reynolds, J. M., "Burnout in Forced Convection Nucleate Boiling of Water," MIT Rep. no. 10, Nonr-1848 (39), July 1957.

68 DeBortoli, R. A., Green, S. J., LeTourneau, B. W., Troy, M. and Weiss, A., "Forced Convection Heat Transfer Burnout Studies for Water in Rectangular Channels and Round Tubes at Pressures above 500 psia," Westinghouse Electric Corp., Rep. no. WAPD-188, available through Tech. Services, U. S. Dept. of Commerce, Washington, D. C., Oct. 1958.

69 Dickinson, N. L. and Welch, C. P., "Heat Transfer to Supercritical Water," *Trans. ASME*, vol. 80, April 1958, p. 746.

70 Powell, W., "Heat Transfer to Fluids in the Region of the Critical Temperature," JET PROPULSION, vol. 27, July 1957, pp. 776–783.

71 Dean, L. E. and Thompson, L. M., "Study of Heat Transfer to Liquid Nitrogen," ASME Paper no. 56 SA4, June 1956.

72 Bringer, R. P. and Smith, J. M., "Heat Transfer in the Critical Region," *J. AIChE*, vol. 3, 1957, p. 149.

73 Goldmann, K., "Heat Transfer to Supercritical Water and Other Fluids with Temperature Dependent Properties," AIChE-Chem. Eng. Progress Symposium Series, no. 11, 1954.

74 Poppendick, H. F., "Forced Convection Heat Transfer in Pipes with Volume Heat Sources within the Fluids," AIChE-Chem. Eng. Progress Symposium Series, no. 11, 1954.

ARS—NORTHWESTERN UNIVERSITY GAS DYNAMICS SYMPOSIUM

"Dynamics of Conducting Fluids"

August 24–26, 1959, Northwestern University, Evanston, Illinois

Hypersonic Shock Tunnel[1]

H. T. NAGAMATSU,[2]
R. E. GEIGER[3] and
R. E. SHEER Jr.[4]

General Electric Research
Laboratory
Schenectady, N. Y.

A hypersonic shock tunnel has been developed for obtaining fluid mechanic information at the high Mach numbers and corresponding stagnation temperatures encountered in flight by long range ballistic vehicles and satellites. This report describes the hypersonic shock tunnel and presents some of the results obtained in the driven tube and in the nozzle. A stoichiometric mixture of oxygen and hydrogen with an excess of helium is ignited in the driver to produce strong shock waves in air. A shock velocity in air as high as 55,000 fps with a calculated equilibrium temperature of 16,000 K has been produced in the driven tube. The effects of high stagnation temperatures upon the detached shock wave and the pressure distribution for blunt bodies have been observed in the nozzle test section. The detachment distance decreased greatly at high temperatures. The pressure distribution for the hemisphere was found to be less than that predicted by the modified Newtonian theory. Shock wave boundary layer interaction at the leading edge of a flat plate was observed, and the results agreed with the analytical prediction. A detached shock wave was observed for a blunt two-dimensional body at very low densities in the test section with a flow Mach number of 19.6.

THE PRIMARY purpose of the hypersonic shock tunnel is the investigation of high temperature gas effects on the flow around bodies traveling at hypersonic Mach numbers encountered by intercontinental ballistic missiles and satellites re-entering the Earth's atmosphere. Representative Mach numbers and corresponding equilibrium stagnation temperatures encountered by such vehicles at an altitude of 100,000 ft are Mach number 20 at 6500 K and Mach number 26 at 8000 K, respectively. At such temperatures, the air may no longer be considered an ideally behaving mixture of diatomic oxygen and nitrogen; the gas molecules will dissociate, ionize, and chemical reactions will occur. These microscopic phenomena are usually referred to as "real gas effects."

At the present time very little information is available concerning the effects of these phenomena upon the inviscid and viscous flow fields of hypersonic bodies. The hypersonic shock tunnel, a limited number of which have been developed in recent years (1 to 4),[5] is a facility which can simulate simultaneously both the flight Mach numbers and stagnation temperatures associated with practical hypersonic vehicles. This is in contrast to the constant area shock tube (5 to 8) in which only high stagnation temperatures can be achieved. For example, with air as the working gas, the flow Mach number behind a reasonably strong shock wave is only about 3. Therefore, only problems where Mach number is unimportant, such as blunt body stagnation point heating, can be investigated.

This paper will present a description of the hypersonic shock tunnel and its operating characteristics. Some of the instrumentation that has been developed for the shock tube and the shock tunnel will be described. The combustion technique used in the driver for consistent results will be discussed in conjunction with the safety precautions for the operation. Extremely strong shock waves produced in the driven section of the shock tube will be discussed. Some preliminary results obtained in the test section and the flow over blunt bodies will be presented. The latter include surface pressure measurements as well as Schlieren and luminosity photographs of different bodies showing high temperature effects. Shock wave boundary layer interaction at the leading edge of a flat plate has been observed and is compared with the analytical prediction.

Description of the Hypersonic Shock Tunnel

Driver and Diaphragm Section

The hypersonic shock tunnel consists of a driver, a diaphragm section, a shock tube of constant area and a nozzle partly installed in a dump tank, as shown in Figs. 1 and 2. The driver section is 20-ft long with an ID of 6 in. and a wall thickness of 4 in. Maximum design driver operating pressure after combustion is 10,000 psi with an adequate margin of safety. To prevent corrosion, the inside surface of the driver was plated with a 0.005-in. layer of hard chromium. The driver length was determined so that the reflected driver expansion would not be the limiting factor in nozzle testing times.

To produce uniform combustion and to minimize the possibility of detonation in the driver using a stoichiometric mixture of hydrogen and oxygen with helium as a diluent, 18 modified automotive-type spark plugs are mounted flush with the inner surface in a spiral arrangement along the tube. Capacitors, charged to 450 v, are discharged through an automotive-type coil to each spark plug. All the capacitors are discharged by a single solenoid switch to simultaneously ignite the mixture at all 18 locations.

Besides having ignition take place simultaneously at a number of locations, the gases must be well-mixed before combustion. Therefore, the gases are injected at six locations, each inlet having an orifice of four 0.018-in. diam holes

Received Feb. 2, 1959.

[1] This work was sponsored jointly by General Electric and Ballistic Missile Division, ARDC, U. S. Air Force under contract AF 04(645)-24.

[2] Research Associate; also Adjunct Professor, Rensselaer Polytechnic Institute, Troy, N. Y.

[3] Aeronautical Engineer. Present address: General Electric Co., Missile & Space Vehicles Dept., Philadelphia, Pa.

[4] Designer, Gas Dynamics

[5] Numbers in parentheses indicate References at end of paper.

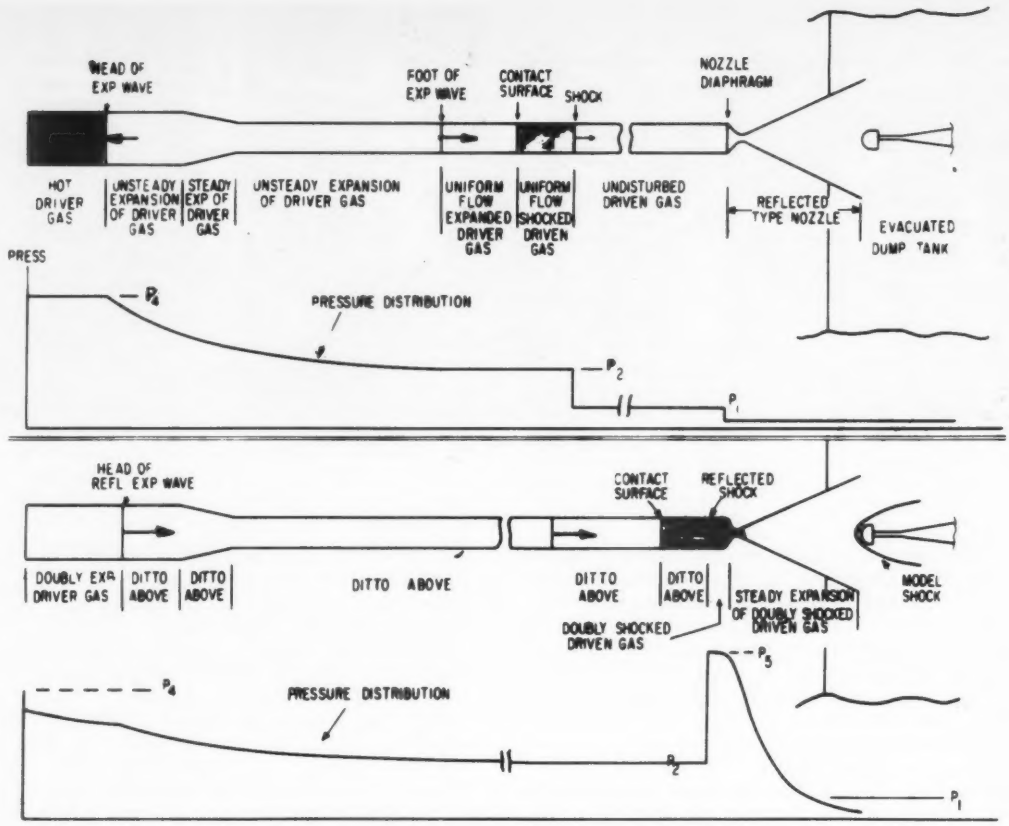

Fig. 1 Idealized picture of shock tunnel phenomena

drilled at an angle of 45 deg, to produce spiral motion. The driver is evacuated to a low pressure before the oxygen is injected. Then about 50 per cent of the total helium charge is injected. Next, the hydrogen is added at high pressure in stoichiometric proportions with oxygen. Finally, the remainder of helium is injected at high pressures to produce a swirling motion in the mixture and to clear the charging lines of combustible gases. With this loading procedure, the oxygen and hydrogen mixture is always diluted by a considerable amount of helium during the loading process. This is important, since normal detonation pressures as high as 50 times the initial pressure (9) or, in certain cases, as high as 150 times (10) have been observed. After the gases have been injected into the driver there is a waiting period of about 5 min before the mixture is ignited by the multiple sparks. With this method of loading and igniting the gases, extremely reliable and reproducible driver combustion results have been attained.

The driver section is connected to the driven tube by a 4-ft conical transition piece. At the entrance of the transition section, there is a section which holds the diaphragm. Three hydraulic pistons operating at 3000 psi pressure are used to move the clamping unit of the diaphragm section. Check valves and mechanical locks prevent the opening of the clamping section during the combustion process.

Stainless steel, copper, monel and aluminum have been used as diaphragm material. For most operations, stainless steel has been utilized, since it has reasonably high yield strength. The stainless steel diaphragms open uniformly and do not shatter as they are slapped against the inside wall of the transition piece. To permit the diaphragm to open into petals, two grooves are cut at right angles to each other to a depth of one-third to one-half the material thickness. A cutter radius of 0.020 in. is maintained in order to keep the stress concentration consistent. The pressure at which the diaphragm

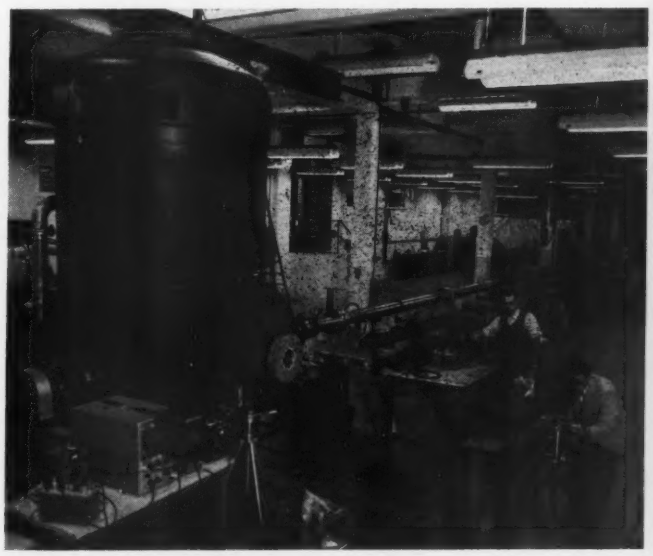

Fig. 2a General Electric Research Laboratory hypersonic shock tunnel

Fig. 2b Combustion driver and diaphgram section

bursts is controlled by varying the material thickness and the depth of the cuts. Consistent bursting pressures have been achieved by this method of fabricating the diaphragms.

To permit longitudinal recoil of the driver section when strong shocks are produced, the driver is anchored to the floor, as shown in Fig. 2b, by a large channel section which is bolted through rubber inserts to a steel beam embedded in the floor. The transition piece at the clamping section is designed to permit movement of the driver relative to the driven tube. Since the diaphragm is stainless steel with a maximum thickness of $\frac{3}{8}$ in., the diaphragm will always be much weaker than the end flange of the driver and will therefore act as a safety valve.

The use of hydrogen and the possibility of detonation with its extremely high peak pressures require precaution to protect the operating personnel and the equipment. During the charging of the driver, the area housing the driver is ventilated by four exhaust fans on the blowoff roof of the building. This eliminates the possibility of hydrogen accumulating in the driver room. All lines bringing the gases to the driver are designed for an operating pressure of 30,000 psi. A blast mat was installed between the driver and the driven tube, as shown in Fig. 2b, to contain any fragments within the driver area. The back wall of the driver room was constructed of material that will blow out under a small pressure differential.

The gases are stored in standard high pressure bottles which stand along the outside wall of the driver room. All lines coming from these bottles to the loading panel are designed for an operating pressure of 6000 psi. The loading panel is located on the opposite side of the blast mat from the driver room. The entire hypersonic shock tunnel facility is located in a reinforced concrete building with steel doors. The control room, to which all personnel are evacuated for high pressure tests, is adjacent to the shock tunnel room and is separated from it by a 12-in. thick reinforced concrete wall with two high strength shatterproof observation windows.

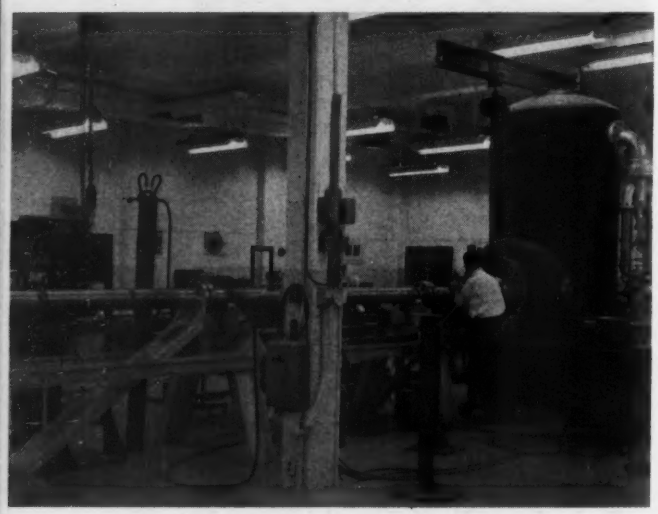

Fig. 3 Shock tunnel nozzle and dump tank

Driven Section of Shock Tube

The constant area or driven section of the shock tube consists of stainless steel tubing with a wall thickness of 1 in. and an ID of 4 in. In order to minimize the wall viscous effects, the inside surface was bored and honed to obtain an extremely smooth finish. This section was designed for a maximum operating pressure of 10,000 psi. Adjacent sections of the tube are joined with a tapered fit and sealed by two O-rings. This arrangement eliminates both inner surface discontinuities at the joints and misalignments that might otherwise result from the impact loadings experienced when the shock tunnel is fired. A total driven section length of 103 ft is attained with ten 10-ft sections and one 3-ft section which is connected to the conical nozzle. These sections have varying numbers of holes in their walls for installation of pressure pickups, heat gages and other instrumentation.

The entire shock tube is supported on a welded rail and I-beam structure which is anchored to the steel beam imbedded in the floor as shown in Fig. 3. At the downstream end, the tube is anchored to the floor with large steel channel members (Fig. 3). A thick rubber slab is used between the channel member and the steel beam imbedded in the floor to absorb some of the impact produced when the shock wave reflects from the nozzle entrance at the end of the tube.

The end of the shock tube is fitted with a threaded collar for clamping the second diaphragm at the entrance to the conical nozzle. O-ring seals permit the tube to move relative to the nozzle in order to accommodate thermal expansion as well as the recoil caused by the reflected shock wave.

It is important for shock tube operation to know the pressure in the driven tube accurately before firing. To

measure the initial pressure in the driven tube, McCloud gages are used for the pressure range of 1 μ to 2 mm of mercury. For intermediate pressure to atmospheric, both Bourdon-type and mercury manometers are utilized. For low pressure operations, provisions are made for evacuating the driven section by means of a large vacuum pump. For operations where pressures above atmosphere are required, clean dry air is led into the tube from the building air supply.

Nozzle, Test Section, Dump Tank and Sting Support

A conical nozzle of the reflected type with a total expansion angle of 30 deg and an exit diameter of 24 in. is connected to the end of the shock tube and is partly housed inside a dump tank as shown in Fig. 3. The area ratio for the conical nozzle is varied by changing a short throat section. The throat diameter can be varied from 4 to 0.05 in. Throat diameters of 1, 0.33, 0.19 and 0.10 have been tested to produce flow Mach numbers in the test section of approximately 10, 16, 20 and 26 for nearly perfect gas conditions.

At the entrance to the nozzle an aluminum diaphragm, cross cut in the same manner as the driver diaphragm, is used to permit the shock tube and the dump tank to be evacuated to different pressures. Usually the dump tank and the nozzle are evacuated to low pressures in order to facilitate flow establishment in the test section. For very high flow Mach numbers, 20 and 26, the dump tank is evacuated to about 7 μ of mercury. At lower Mach numbers, it is only necessary to evacuate to pressures below about 100 μ of mercury. The second diaphragm opens upon the arrival of the incident shock wave. The bursting pressure is controlled again by using different material thicknesses and cut depths.

The shock tunnel was designed for three possible nozzle arrangements: (a) straight-through configuration with the throat diameter equal to the shock tube diameter of 4 in., (b) converging-diverging or reflected shock wave configurations, and (c) a straight-through double nozzle arrangement (4) which removes the boundary layer. The reflected nozzle arrangement was selected for initial operation because the shock tube boundary layer effects are minimized and higher nozzle stagnation temperatures may be attained for a given driver pressure. Moreover, the large area ratios required for high flow Mach numbers can be achieved without a prohibitively large nozzle exit diameter or the complications of the double nozzle arrangement.

A 200-ft^3 dump tank houses the test section of the conical nozzle as shown in Fig. 3. The large dump tank insures moderate steady-state pressure in the facility even for maximum driver charges. Observation windows are located at the exit of the nozzle to permit optical investigations of the flow field around models. The windows are optically selected plate glass. The dump tank was designed for operation with the long side either horizontal or vertical. A vertical arrangement for the dump tank was selected initially to permit the shortest length for the model sting. Even in this position, the unsupported sting length is 5 ft.

The sting is a 6-in. OD hollow cylinder which tapers to a 1-in. OD tube behind the model. The sting support structure is separate from the dump tank and the sting rides on Teflon bushings so that a considerable degree of vibration isolation is achieved. The sting is actuated by a lead screw which is driven by a reversible d-c motor.

Instrumentation

Pressure Gages

Piezoelectric pressure gages (11) have been used to measure pressures in the shock tube and on the models in the nozzle test section. The standard Kistler SLM quartz pressure pickups have been successfully used in some applications, but for many model investigations their large size and small output make them unsatisfactory. Consequently, small barium-titanate pressure pickups have been developed to meet these needs. This type of pressure gage, while much smaller than the Kistler, nevertheless has considerably greater output. These pickups are more sensitive to vibration than the Kistler and must be shock mounted in rubber. The response time of the barium-titanate gages is about 10 microsec as compared to 50 microsec for the Kistler gages. Barium-titanate crystals are more sensitive to heat than quartz crystals; hence, the pickup is designed with a certain amount of heat insulation depending on the installation for which the gage is intended.

For pressures above 5 psia, the Kistler gages have very linear and consistent calibrations. Below 5 psia, both the Kistler and the barium-titanate are sensitive to the installation in models. For model pressure measurements, a dynamic calibration of the gages in their actual installations is made. This is accomplished by mounting the model at the end of the constant area driven section in place of the nozzle and subjecting it to the pressure behind reflected shocks obtained with weak incident shock Mach numbers (about 1.5).

For higher pressures, the Kistler and barium-titanate gages are fitted with adapters which decrease the effective area on which the pressure acts. With these adapters, it is possible to calibrate and use the gages above 10,000 psi.

Ionization Gages

A simple air gap with 300 v d-c between the center electrode and the outer wall is used as an ionization pickup. The ionization of the air due to strong shocks breaks down the resistance across the gap, and the resultant voltage change is used as a time of arrival signal for shock velocity measurements. For a gap of 0.03 in., the response time of the gage is of the order of 1 microsec.

Heat Gages

A thin platinum film, sputtered or painted, on a quartz or glass piece acts as a resistance thermometer, and the output of such a device, when a current is passed through it, is related to the surface heat transfer rate. This type of gage has been developed at various laboratories in recent years (12 to 15). The resistance of the platinum film is usually about 40 ohms. A current of 50 milliamp is used to detect a voltage variation produced by the change of film resistance. The thin sputtered heat gages have a response of about 1 microsec, but are not as durable as the painted ones. For shock waves too weak to ionize the gas in the shock tube, the platinum film heat gages have been used to detect the arrival of the shock wave at stations along the shock tube. Similar heat gages can be used on models in the test section to measure the heat transfer rate at various stagnation temperatures. At very high temperatures for which air becomes ionized, the heat gage must be coated with a very thin electrically insulating coating, such as silicon dioxide as described in (15). This coating prevents the ionized gas from short circuiting the platinum film at a small loss in response time.

Determination of Shock Velocity

The instrumentation used to determine the shock wave position as a function of time in the 100-ft long driven tube consists of heat or ionization gages which serve as time of arrival pickups, a modified Tektronix 535 oscilloscope, a crystal controlled raster generator, and a display chassis. The raster generator produces up to 500-cm sweep length with a nearly vertical sawtooth or raster arrangement in which each vertical line represents a given time. The output of 12 sensing elements in the shock tube wall is fed into the display chassis which produces signals that are displayed as horizontal markers on the vertical sawtooth pattern. In normal operation of the shock tunnel, the shock velocity

measurements are supplemented by a Berkeley counter which measures the shock wave traversal time over the last $6\frac{1}{4}$ ft of the tube with 1 microsec accuracy.

Optical Methods

A single pass Schlieren system with 6-ft focal length parabolic mirrors is used to obtain photographic records of the model flow fields. A spark of about 0.2 microsec duration, produced by the discharge of a capacitor, is used as the light source. For high temperature conditions with a large amount of luminosity from the hot gas, an optical shield is placed at the knife edge to permit only small amounts of luminosity to reach the film. It is thus possible to photograph the shock wave with the luminous gas region.

Direct luminosity or "flash" photographs have been taken by leaving the camera open at the test section window during the entire test. In this manner, both color and black and white photographs of the luminous region around blunt bodies have been obtained. For investigations of the flow phenomena as a function of time, direct photographs have been taken with a Fastax camera operating at 8000 frames per sec.

For spectroscopic investigations of the heated gas after a shock wave, quartz windows may be inserted in the instrumentation holes in the shock tube walls. Some preliminary results have been obtained in the shock tube and in the test section.

Preliminary Results From the Shock Tunnel

Combustion Driver

Initial combustion investigations (9) were made in a 10-ft section of the driver in order to determine combustion performance using gas mixtures of helium and stoichiometric hydrogen-oxygen. The driver "loading" pressure was varied from 25 to 500 psia, and the mixture ratio from 45 to 80 per cent helium. Tests were performed with one to nine spark plugs igniting the combustible mixtures. Two Kistler pressure pickups were installed to obtain the pressure time history during the constant volume combustion tests.

The observed peak pressures for smooth burning were close to the theoretical values calculated by assuming no dissociation (Fig. 4). Richer mixtures and higher loading pressures tended to produce detonation in the driver. At 25 psia loading pressure, detonation occurred in mixtures with 45 per cent or less helium, whereas at 300 psia loading, detonation occurred with a 65 per cent helium mixture. With detonation, peak pressure to loading pressure ratios as high as 50 were measured at the higher driver loadings; ratios as high as 150 have been observed in a long tube (10). It was determined during these studies that a 70 to 75 per cent helium mixture with a balance of stoichiometric hydrogen and oxygen was lean enough to prevent detonation within the range of driver loading pressures investigated.

It was observed that the time to reach peak pressure increases with the amount of helium in the mixture and with increased loading pressures as indicated in Fig. 5. With nine sparks, the time to peak for 70 per cent helium is 10 to 15 millisec. As the detonation mixture ratio at a given loading pressure is approached, the time to reach peak pressure drops rapidly to about 5 millisec, and the amplitude of the pressure oscillations increases greatly.

These combustion results indicate that great flexibility can be obtained in the driver characteristics by varying the percentage of helium and the number of ignition sparks.

Following the assembly of the complete 20-ft driver section, another series of combustion investigations were conducted. The results of these tests were quite similar to those in the 10-ft section except for the longer period of pressure oscillations when the mixture approached the detonation limits. Thus, with the technique currently in use in the Research Laboratory shock tunnel, it has been possible to obtain consistent repeatable combustion driver performance.

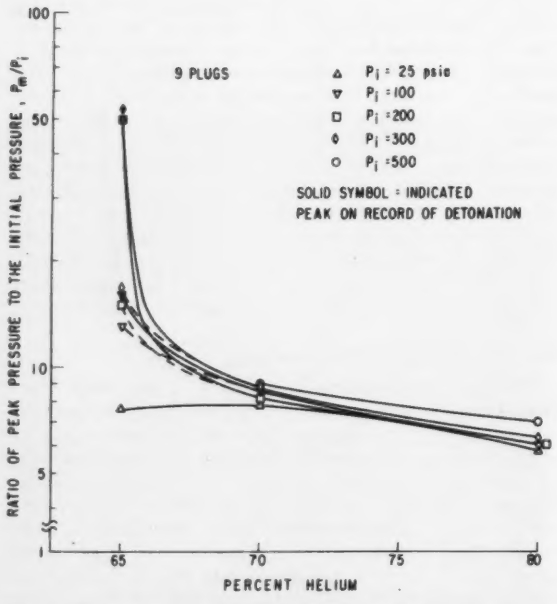

Fig. 4 Ratio of peak pressure to the initial pressure vs. per cent helium

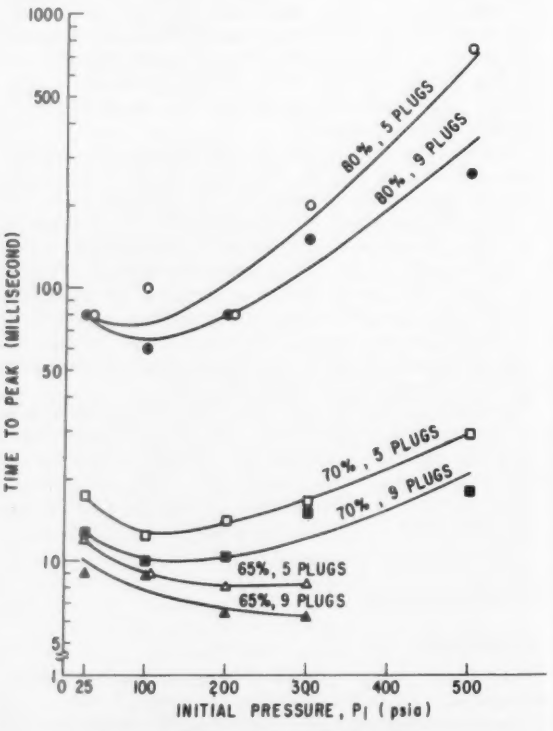

Fig. 5 Time to peak vs. initial pressure

Results in the Shock Tube

At low shock Mach numbers, the agreement between the observed shock velocity at the 40-ft station and the predictions of the idealized shock tube theory (16, 17) was reasonable, allowing for shock wave attenuation (Fig. 6). However, as the shock Mach number is increased, the trend of the experimental results for the pressure ratio across the driver diaphragm vs. the shock Mach number varies from that of the theory (Fig. 7). For shock Mach numbers above 25, the observed velocities were much greater than one would predict from the simplified theory. Similar results with a cold driver were observed and investigated in more detail (18). The results of the investigation indicated that better agreement between theory and experiment could be obtained by taking into account the finite opening time of the diaphragms and the mixing of the driver and driven gases at the contact surface. In addition, with the present case where combustion driving is utilized, it is possible to produce shocks greater than predicted by theory by letting the diaphragm burst well before the combustion is completed, so that an approximately constant pressure combustion situation exists during the remainder of the burning of the gases (19). This last effect was appreciable in producing the hypervelocity shock wave. A typical variation of the shock Mach number with distance is shown in Fig. 6.

To date, a maximum shock velocity of 55,000 fps has been produced with combustion driving and air as the driven gas. The calculated gas velocity after the shock wave was approximately 52,000 fps, and the equilibrium temperature was 16,000 K. Thus, it may be possible to investigate the stagnation heat transfer for a blunt body at a flight Mach number of about 50.

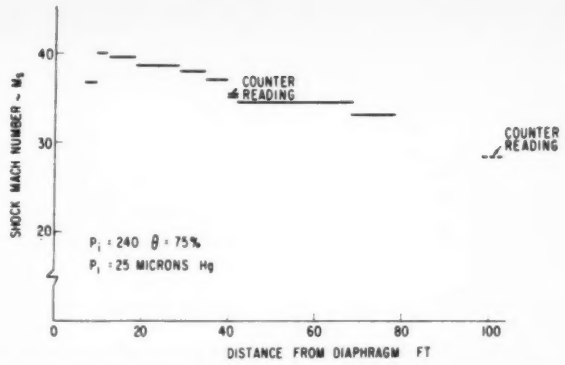

Fig. 6 Shock Mach number vs. distance for very strong shock

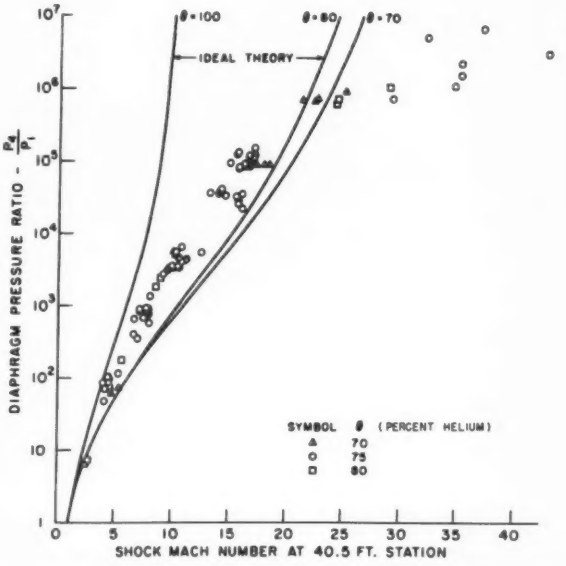

Fig. 7 Diaphragm pressure ratio vs. shock Mach number at 40.5-ft station

Determination of Flow Conditions in the Nozzle

All tests so far have been conducted with the reflected-type nozzle, and thus the conditions behind the reflected shock wave were the nozzle stagnation conditions. Both the incident shock velocity just before the end of the tube and the pressure behind the reflected shock wave are measured for each test. The gas behind the reflected shock is assumed to be in thermodynamic equilibrium so the temperature can readily be computed by numerically solving the normal shock equations for both the incident and reflected shocks, based upon the thermodynamic properties for air (20 to 22).

Test section conditions can be estimated from one-dimensional isentropic nozzle calculations and measurements of reflected pressure and test section static or impact pressure. For low temperatures where air is nearly an ideal gas, the standard $\gamma = 1.4$ results are applicable. For higher temperatures, a series of calculations based upon equilibrium assumptions and carried out for a range of stagnation conditions are utilized.

Preliminary Nozzle Flow Results

The hypersonic shock tunnel may be operated at different nozzle flow stagnation temperatures by varying the strength of the incident shock at the end of the constant area section. The strength of the incident shock is a function of the shock tube initial conditions. Initial shock tunnel investigations were conducted in the nominal Mach 10 nozzle having a throat diameter of 1 in. and an exit diameter of 24 in. The reflected stagnation temperature was high enough, about 1100 K, to avoid condensation in the nozzle, yet low enough so that the air may be considered a perfect gas with constant ratio of specific heats of 1.4. Thus, the ideal gas calculations for air were applicable. These nearly ideal gas results served as the reference for the investigations at higher temperatures for a given nozzle area ratio.

Reflected equilibrium temperatures, at the entrance to the nozzle, as high as 12,000 K have been produced. For stagnation temperatures greater than about 2000 K, the real gas effects must be considered during the expansion process in the nozzle. The flow Mach number in the test section decreases as the stagnation temperature is increased, provided the flow during expansion in the nozzle is in thermodynamic equilibrium. Results of a one-dimensional isentropic nozzle calculation for an equilibrium nozzle expansion show a decrease in flow Mach number with stagnation temperature. Some preliminary investigations into the question of whether an "equilibrium" or "frozen" nozzle expansion takes place seem to indicate that if the nozzle stagnation pressure is high enough the gas will be nearly in thermodynamic equilibrium. At low pressures, the indications are that the expansion is nearly a frozen one. As used in this paper, a completely "frozen" expansion is one in which only the translational and rotational energies of the gas change from their stagnation value, while all the others remain at their stagnation limits as the gas expands in the nozzle. Further research is being conducted to obtain more information regarding the state of the air during the expansion process.

Flow establishment times are determined by measurement of the impact pressure at the exit of the nozzle as a function

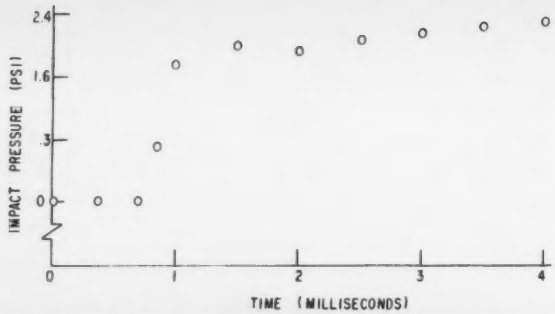

Fig. 8 Impact pressure vs. time for Mach 10 nozzle with T_5 = 3000 K

Fig. 9 Five-in. span 40-deg wedge in Mach 10 nozzle with T_5 = 1300 K

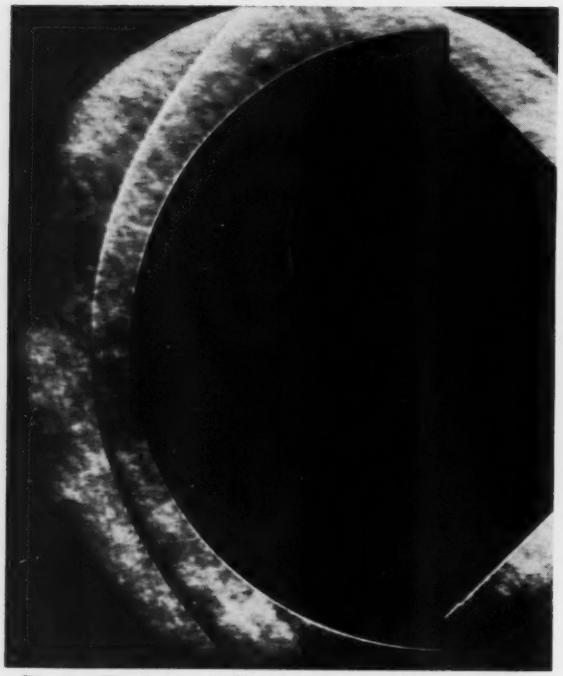

Fig. 10 Hemisphere in Mach 10 nozzle with T_5 = 1050 K

of time. A representative impact pressure time history for the nominal Mach 10 nozzle is shown in Fig. 8. For this particular test at 3000 K reflected stagnation temperature, the starting time of the flow was about 0.7 millisec, and the flow duration was about 2.5 millisec. In general, the flow starting times were found to vary between 0.6 and 1 millisec.

To check the flow uniformity in the test section, an impact rake with five pressure gages was tested at the usual model location in the nominal Mach 10 nozzle. The results obtained at 1100 K reflected stagnation temperature have indicated that, within the accuracy of the measurements, the transverse impact pressure distribution is uniform at the model location. A 40-deg wedge with a 5-in. span was also used to detect any large disturbances in the test section, such as might be caused by separation of the flow from the nozzle wall. The Schlieren photograph taken at a reflected stagnation temperature of 1300 K in the Mach 10 nozzle is shown in Fig. 9. For the 40-deg wedge, the shock wave was approximately straight up to the point where the expansion from the shoulder starts interacting with the shock wave.

Flow over a hemisphere was investigated at different stagnation temperatures in the nominal Mach 10 nozzle. At an equilibrium reflected temperature of 1050 K, the impact Mach number was 10.1, and the ratio of the bow shock detachment distance to the hemisphere radius δ/R was 0.13, as indicated in Fig. 10. At the stagnation temperatures of approximately 10,000 K, the detached shock wave moved closer to the hemisphere and the δ/R ratio decreased to approximately 0.09. The calculated normal shock density ratio for this test condition, assuming the flow to be in thermodynamic equilibrium, is approximately 15. These results indicate that the detachment distance decreases with the increase in the shock density ratio caused by the real gas effects at high temperatures, as discussed in (26).

A luminosity photograph of a 5-in. diam hemisphere at a reflected stagnation temperature of 5800 K in the nominal Mach 10 nozzle is shown in Fig. 11. At this temperature the region of luminosity was very sharply defined at the front, indicating that the relaxation time after the shock wave was very short. The luminosity disappears as the flow expands around the hemisphere and the temperature decreases. Similar results for the luminosity for a 50-deg cone-hemisphere were obtained for an equilibrium reflected stagnation temperature of 5800 K as shown in Fig. 12.

Fig. 11 Luminosity photograph of hemisphere in Mach 10 nozzle with T_5 = 5800 K

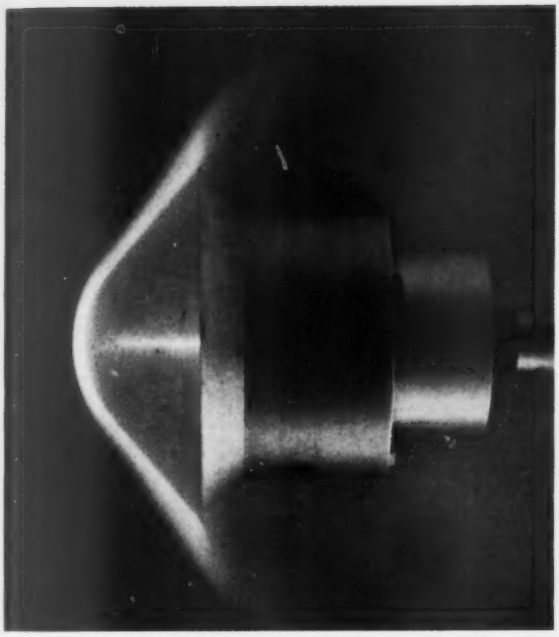

Fig. 12 Luminosity photograph of 50-deg cone-hemisphere in Mach 10 nozzle with T_0 = 5800 K

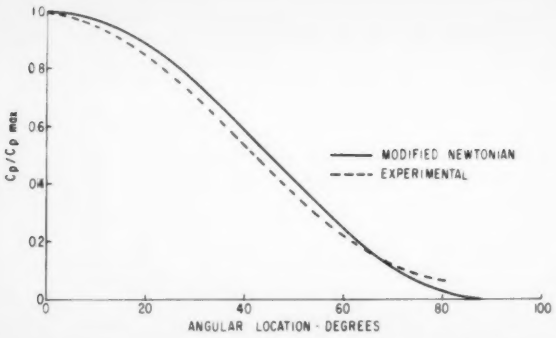

Fig. 13 Pressure distribution for hemisphere in Mach 10 nozzle with T_0 = 1300 K

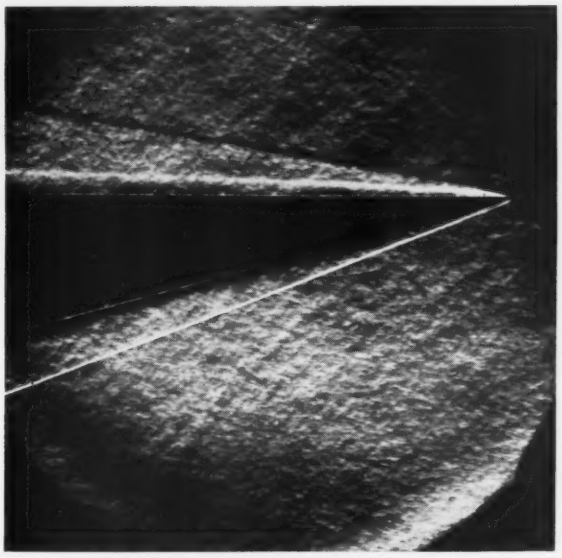

Fig. 14 Flat plate in Mach 10 nozzle with T_0 = 1560 K

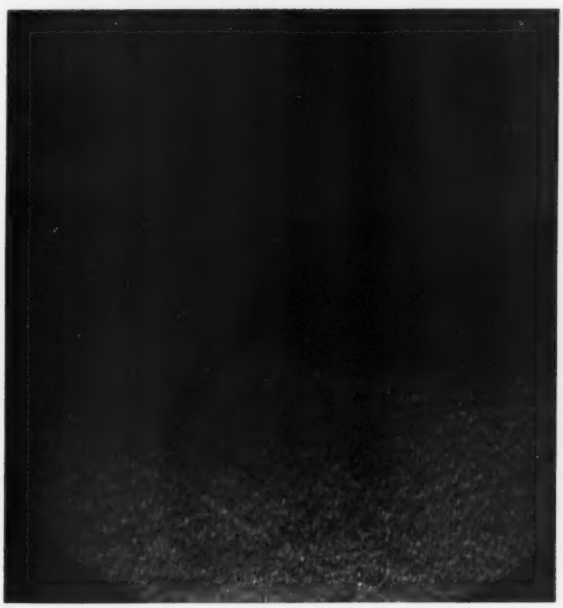

Fig. 15 Two-dimensional impact rake in Mach 20 nozzle with T_0 = 2140 K

Preliminary pressure distributions for a hemisphere and a 50-deg cone-hemisphere have been obtained in the Mach 10 nozzle. The pressure distribution for the hemisphere at a stagnation temperature of 1300 K is shown in Fig. 13. Over most of the hemisphere the pressure was lower than that predicted by the modified Newtonian theory.[6] Recent analytical results (23 to 25) have indicated lower pressures than the modified Newtonian at hypersonic Mach numbers. At higher temperatures, the real gas effects cause the shock wave to move closer to the body without affecting the pressure distribution to any extent. A more detailed discussion of the high temperature effects upon the pressure distribution and the shock wave shape is presented in (26).

Flow over a 5-in. wide flat plate was investigated in the Mach 10 nozzle at a stagnation temperature of 1560 K. For this condition the flow Mach number was approximately 10, and the Reynolds number per inch was 60,000. A Schlieren picture of the flat plate showing the shock wave and the boundary layer is presented in Fig. 14. At the leading edge, the shock wave and the boundary layer are merged together, and they both vary with distance along the plate as $X^{0.74}$. In (27), the analytical prediction was $X^{0.75}$, so that the agreement with the experiment is quite good. As the distance from the leading edge increases, the shock wave and the viscous boundary layer separate. This has been observed by others (28 to 30).

It has been possible to establish flow in the test section for the nominal Mach 16 and 20 nozzles. In the latter case, with a throat diameter of 0.19 in., the impact flow Mach number in the test section was 19.6 for a stagnation temperature of 2140 K. The corresponding calculated static pressure in the test section for adiabatic flow conditions was about 15 μ of mercury.

It is seen in Fig. 15 that this relatively rarefied Mach 19.6 flow produced a sharp detached shock ahead of a two-

[6] Private communications from Dr. Eva Winkler of the Naval Ordnance Laboratory at White Oak, Maryland, have indicated similar results in the hypersonic wind tunnel for the hemisphere.

dimensional blunt body. Rarefied flow phenomena have been investigated (31) at lower Mach numbers in ideal gas flows where rarefied conditions exist before and after a weak shock wave. At higher Mach numbers and stagnation temperatures, the change in mean free path across the shock should be quite large due to the larger shock density ratio caused by the real gas effects. Thus, it seems possible to have a rarefied flow ahead of a detached shock and continuum flow behind.

Conclusions

The combustion driver technique, using a mixture of stoichiometric hydrogen and oxygen with an excess of helium, is a reliable and useful method for producing strong shock waves in air.

At high pressure ratios across the diaphragm separating the driver and the driven tube, it is possible to produce shock wave velocities in the shock tube in excess of those predicted by the simple shock tube theory.

A shock velocity of 55,000 fps has been produced in the shock tube. The calculated equilibrium temperature behind the shock wave was 16,000 K with the air after the shock moving at a velocity of 52,000 fps and with a Mach number of approximately 7.

Hypersonic flows in the conical nozzle have been established with durations of 1 to 4 millisec of fairly uniform flow in the test section. A flow Mach number of about 20 has been obtained in the test section, and with further investigations it will be possible to produce even higher Mach numbers.

Pressure distribution, shock wave shape, luminosity regions and heat transfer rates can be obtained for models in the test section at hypersonic flow Mach numbers and the temperatures corresponding to those encountered in flight.

Flows over blunt bodies at high stagnation temperatures have been investigated in the shock tunnel. The shock wave detachment distance decreases significantly with increasing stagnation temperature.

At very high flow Mach numbers and low densities, rarefied flow conditions, it has been possible to observe a detached shock wave for a blunt two-dimensional body using a conventional Schlieren system.

The hypersonic shock tunnel is a useful research tool for investigating the flow phenomena associated with the high flow Mach numbers and high stagnation temperatures in air under continuum and rarefied flow conditions.

References

1 Pomerans, J., Winkler, E. H. and Siegel, A. E., "Thermodynamic Properties of One-Dimensional Flow of a Partially Ionized Monatomic Gas," U. S. Nav. Ord. Lab., NAVORD Rep. 4222, Feb. 1958.

2 Warren, W. R., "The Design and Performance of the General Electric Six Inch Shock Tunnel Facility," AFSWC Shock Tube Symposium, SWR-TM-57-2, Feb. 1957.

3 Hertzberg, A., Smith, W. E., Glick, H. S. and Squire, W., "Modifications of the Shock Tube for the Generation of Hypersonic Flow," Cornell Aero. Lab. Rep. AD-789-A-2, AEDC TN-55-15, March 1955.

4 Yoler, Y. A., "Hypersonic Shock Tube," Calif. Inst. of Tech., GALCIT Memo no. 18, July 1954.

5 Rose, P. H., "Physical Gas Dynamic Research at the AVCO Research Laboratory," AVCO Research Lab. Res. Note 37, May 1957.

6 Bleakney, W. and Taub, A. H., "Interaction of Shock Waves," *Rev. Modern Phys.*, vol. 21, 1949, p. 584.

7 Glass, I. I. and Patterson, G. N., "A Theoretical and Experimental Study of Shock Tube Flow," *J. Aeron. Sci.*, vol. 22, no. 2, 1955, pp. 73–100.

8 Kemp, N. H., Rose, P. H. and Detra, R. W., "Laminar Heat Transfer Around Blunt Bodies in Dissociated Air," AVCO Research Lab. Res. Rep. 15, May 1958.

9 Nagamatsu, H. T. and Martin, E. D., "Combustion Investigation in the Hypersonic Shock Tunnel Driver," G.E. Research Lab Rep. 58-RL-2092, Aug. 1958.

10 White, D. R., "On the Existence of Higher Than Normal Detonation Pressures," *J. Fluid Mech.*, vol. 2, July 1957, p. 513.

11 Yoler, Y. A. and Nagamatsu, H. T., "A Study of Piezoelectric Elements for the Measurements of Transient Forces," Calif. Inst. of Tech. GALCIT Hypersonic Wind Tunnel Memo 13, Dec. 1954.

12 Vidal, R. J., "Model Instrumentation Techniques for Heat Transfer and Force Measurements in a Hypersonic Shock Tunnel," Cornell Aero. Lab. Rep. AD-917-A-1, WADC TN-56-315, Feb. 1956.

13 Rabinowitz, J., Jessey, M. E. and Dortsch, C. A., "Resistance Thermometer for Transient High Temperature Studies," *J. Appl. Phys.*, vol. 27, 1956, p. 97.

14 Rose, P. H., "Development of the Calorimeter Heat Transfer Gage for Use in Shock Tubes," AVCO Research Lab. Rep. 17, 1958.

15 Nagamatsu, H. T. and Geiger, R. E., "A Fast Response Device for Measuring Heat Transfer," Turbine Machinery Instrumentation Seminar, General Electric Co., May 1957

16 Resler, E. L., Lin, S. C. and Kantrowitz, A., "The Production of High Temperature Gases in Shock Tubes," *J. Appl. Phys.*, vol. 23, 1952, p. 1390.

17 Alpher, R. A. and White, D. R., "Ideal Theory of Shock Tubes With Area Change Near Diaphragm," G. E. Research Lab. Rep. 57-RL-1664, 1957.

18 White, D. R., "Influence of Diaphragm Opening Time on Shock Tube Flows," G.E. Research Lab. Rep. 58-RL-1999, 1958.

19 Hertzberg, A. and Smith, W. E., "Methods for Generating Strong Shock Waves, *J. Appl. Phys.*, vol. 25, 1954, p. 130.

20 Hilsenrath, J. and Beckett, C. W., "Tables of Thermodynamic Properties of Argon-Free Air to 15,000°K," TN-56-12, Arnold Engng. Dev. Ctr., Sept. 1956.

21 Treanor, C. E. and Logan, J. C., Jr., "Tables of Thermodynamic Properties of Air from 3000°K to 10,000°K," Cornell Aero. Lab. Rep. AD-1052-A-2, June 1956.

22 Gilmore, F. R., "Equilibrium Composition and Thermodynamic Properties of Air to 24,000°K," Rand Rep. RM-1542, Aug. 1955.

23 Van Dyke, M. D., "The Supersonic Blunt Body Problem—Review and Extension," *J. Aeron. Sci.*, vol. 25, Aug. 1958.

24 Gravalos, F. G., Edelfelt, I. H. and Emmons, H., "The Supersonic Flow About a Blunt Body of Revolution for Gases in Chemical Equilibrium," 9th Annual Congress, IAF, Amsterdam, Aug. 1958.

25 Gorabedian, P. R. and Lieberstein, H. M., "On the Numerical Calculation of Detached Bow Shock Waves in Hypersonic Flow," *J. Aeron. Sci.*, vol. 25, Feb. 1958.

26 Nagamatsu, H. T., Geiger, R. E. and Sheer, R. E., Jr., "Real Gas Effects in Flow Over Blunt Bodies at Hypersonic Speeds," presented at summer meeting, IAS, Los Angeles, July 1958; *also* G.E. Research Lab. Rep. 59-RL-2177.

27 Nagamatsu, H. T. and Li, T. Y., "Shock Wave Effects on the Laminar Skin Friction of an Insulated Flat Plate at Hypersonic Speeds," *J. Aeron. Sci.*, vol. 20, 1953.

28 Betram, M. H., "Boundary-Layer Displacement Effects in Air at Mach Numbers of 6.8 and 9.6," NACA TN 4133, Feb. 1958.

29 Kendall, J. M., Jr., "An Experimental Investigation of Leading-Edge Shock-Wave-Boundary-Layer Interaction," *J. Aeron. Sci.*, vol. 24, Jan. 1957.

30 Hammitt, A. G., Vas, I. E. and Bogdonoff, S. M., "Leading Edge Effects on the Flow Over a Flat Plate at Hypersonic Speeds," Princeton Univ., Aero. Eng. Lab. Rep. 326, Sept. 1955.

31 Schaaf, S. A., Hurlbut, F. C. and Talbot, L., "Induced Pressures on Flat Plate in Hypersonic Low Density Flow," Univ. of Calif., Berkeley, Jan. 1957.

ARS ANNUAL MEETING

November 16–20, Sheraton-Park Hotel, Washington, D.C.

PROPELLANTS AND COMBUSTION
LONG RANGE MISSILE TELEMETRY
HUMAN FACTORS
GUIDANCE AND NAVIGATION
ION AND PLASMA PROPULSION
INSTRUMENTATION AND CONTROL
SOLID ROCKETS
FLIGHT MECHANICS
TEST FACILITIES AND SUPPORT EQUIPMENT
HYDROMAGNETICS
COMMUNICATIONS IN SPACE
STRUCTURES AND MATERIALS
NON-PROPULSIVE POWER
NUCLEAR PROPULSION

Abstracts should be submitted to Meetings Manager, American Rocket Society, 500 Fifth Avenue, New York 36, N.Y. They will be forwarded to the appropriate Technical Committee. Deadline date for reviewed and approved manuscripts is August 17.

Thrust Optimization of a Nuclear Rocket of Variable Specific Impulse

C. J. WANG,[1]
G. W. ANTHONY[2]
and H. R. LAWRENCE[3]

Space Technology Laboratories, Inc.
Los Angeles, Calif.

A simple relation is derived between the specific impulse and the flow rate of a propellant gas under nuclear reactor operating conditions which allow molecular dissociation of the gas. Utilizing this relationship, the optimum variable thrust program maximizing the kinetic energy of a vertically ascending vehicle is obtained under the assumptions of constant gravity and zero aerodynamic drag. The advantage of this program is demonstrated by comparison with the usual constant thrust program.

SINCE a nuclear rocket is a source of practically unlimited energy, the problem of a nuclear rocket is to maximize the energy absorbed by the thrust producing working medium during its passage through the reactor. The amount of energy which a working medium could absorb depends, of course, on the temperature in the reactor core, which in turn is a property of the reactor materials used. Once, however, the best high temperature materials are developed and incorporated into the reactor, there remains the problem of insuring that the energy communicated to the rocket at burnout of the total energy injected into the rocket system be a maximum. The present paper is mainly concerned with the latter problem.

At temperatures attainable by some possible reactor core materials, certain propellant gases will dissociate to a significant degree. With dissociation, the gas will have drastically increased specific heats. The enhanced specific heats will then yield specific impulse values greater than expected by the usual square-root-of-temperature law. Thus, molecular dissociation is an important property of a gas as a nuclear rocket propellant (1).[4]

The amount of dissociation products present depends on the temperature and pressure of the gases. Although the temperature is limited by the materials available, the pressure is strictly a design parameter, subject to the designer's selection. However, for a fixed size of engine and a given temperature, the operating pressure would determine the thrust level. Therefore, the thrust level determines the degree of dissociation and hence the value of specific impulse which a particular gas is able to produce. In general, since high thrust requires high operating pressure which tends to suppress gas dissociation, a high thrust operation will result in low specific impulse, whereas a low thrust operation will result in high specific impulse. These facts lead to the problem of determining the optimum thrust level for a nuclear rocket.

It is well understood that when the specific impulse is a constant, efficient use of a rocket powered vehicle requires full thrust operation of the rocket, or, if aerodynamic drag is a factor, the use of an optimum thrust program which would accelerate the vehicle to the maximum before the drag becomes limiting. This is because low acceleration will waste energy by unnecessarily lifting the propellants to high altitudes. Thus, in the ideal case of limitless engine capacity and zero drag, the most efficient operation would mean an impulsive thrust. However, for engines of practical size and when the specific impulse is not a constant, and specifically if it increases with the decrease of thrust, there will exist an optimum thrust program which represents the most efficient operation under the conflicting requirements of high thrust to avoid working against gravity and low thrust to realize the advantage of increased specific impulse.

In this paper, a mathematical representation is developed for the specific impulse of nuclear rockets in terms of the propellant flow rate (and consequently engine thrust) on the basis of dissociation considerations. To a first approximation, it is found that the specific impulse can be represented by a simple power of the propellant flow rate multiplied by a constant. The exponent and the constant multiplier depend upon the particular engine and its operating conditions. Using the power law, an analysis is carried out to determine the optimum thrust program which will maximize the kinetic energy of a vertically ascending nuclear rocket vehicle. To simplify the analysis, air drag is neglected, and constant gravity is assumed. This approach leads to the very simple conclusion that for optimum operation the propellant flow rate must be reduced with time in such a way that the acceleration is maintained constant. The performance of a vehicle utilizing the constant acceleration program is then compared with that expected from a constant thrust rocket. The advantage of the optimum program is clearly demonstrated.

It should be noted that problems of thrust programming have been studied by other investigators, see for example (2 to 4). These investigations, however, are dealing exclusively with rockets of constant specific impulse. The problem in this paper is new, and the thrust program derived is quite different from those derived for constant specific impulse rockets.

Specific Impulse

Basically the specific impulse (I_{sp}) is obtained by combining the propellant discharge momentum and the force resulting from the pressure at the nozzle exit in excess of the ambient pressure. It can be shown that the following formula yields I_{sp} for given gas conditions at the reactor discharge, an isentropic expansion ratio ϵ and the ambient pressure p_a.

$$I_{sp} = a\sqrt{H_c - H_e} + \epsilon \frac{C^*}{g}\left(\frac{p_e}{p_c} - \frac{p_a}{p_c}\right) \qquad [1]$$

Presented at the ARS 13th Annual Meeting, New York, N.Y., Nov. 17–21, 1958.

[1] Associate Manager, Aerophysics Department. Member ARS.
[2] Member, Technical Staff.
[3] Associate Director, Astrovehicles Laboratory. Member ARS.
[4] Numbers in parentheses indicate References at end of paper

The first term represents the momentum relative to the vehicle per unit mass flow rate. The second term represents the force per unit mass flow rate due to the static pressure at the exit plane.

To evaluate Equation [1], it is necessary to determine the shifting equilibrium composition of the gas during its expansion through the thrust chamber. The computation required is, in general, very complex, and a high speed machine computing program would be desirable. Such a program has been employed at the Space Technology Laboratories, Inc., to calculate the I_{sp} for H_2 as a nuclear rocket propellant. For example, in Fig. 1 are shown the results of shifting equilibrium calculations as compared with frozen equilibrium values of the specific impulse for a nozzle expansion ratio of 40 and zero ambient pressure.

In order to facilitate analytical investigations, some simplifications will now be considered in the calculation of I_{sp}. Since rockets of high performance operate most of the time at high altitudes, the ambient pressure p_a may be taken as zero. Furthermore, these rockets usually employ high expansion nozzles so that p_e/p_c is very small, and the whole pressure term in Equation [1] can be neglected. This leaves the first term which will enable one to compute I_{sp} from the enthalpy differential $(H_c - H_e)$, namely

$$I_{sp} \backsimeq a\sqrt{H_c - H_e} \qquad [2]$$

We shall now investigate this term for a diatomic gas, for example, H_2.

The enthalpy per unit mass of the heated working fluid may be expressed as

$$H = \frac{f_1}{M_1}\left(\frac{D_0}{2RT} + \frac{5}{2}\right)RT + \frac{f_2}{M_2}\int_0^T C_p dT \qquad [3]$$

The first term represents the contribution of the atoms to the total enthalpy, and consists of the energy of their translational motion and the energy of molecular dissociation. The second term represents the molecular contribution to the enthalpy due to the translational, rotational and vibrational energies of the molecules. At the temperature of the reactor discharge, $T = T_c$, the gas molecules may dissociate to a significant degree, resulting in the first term being the most important. At the nozzle exit, $T = T_e$, the recombination of the atoms is usually complete, and the enthalpy expression will consist of the second term only.

Reference to Fig. 2 illustrating the enthalpy value of hydrogen, shows that the monatomic contribution can indeed be dominant at a high temperature such as may exist at the reactor discharge. Assuming this to be the case and neglecting the molecular contribution, the change in enthalpy per unit mass becomes

$$H_c - H_e \backsimeq \frac{f_1}{M_1}\left(\frac{D_0}{2RT_c} + \frac{5}{2}\right)RT_c = f_1 h(T_c) \qquad [4]$$

where $h(T_c)$ is a function of T_c only.

The weight fraction f_1 of the atoms is dependent upon pressure as well as temperature. By definition, the pressure equilibrium constant K_p is given by

$$K_p = \left(\frac{2f_1}{f_2 + 2f_1}\,p_c\right)^2 \Big/ \left(\frac{f_2}{f_2 + 2f_1}\,p_c\right) \qquad [5]$$

where p_c is in atm, and K_p is a function of T_c only. Utilizing the relation $f_1 + f_2 = 1$, and assuming that $K_p \ll p_c$ (which is generally true in the temperature range of interest), one may readily derive the following relation for the weight fraction f_1

$$f_1 \backsimeq \sqrt{K_p/4p_c} \qquad [6]$$

Considering Equations [4 and 6] together, we see that the enthalpy differential $(H_c - H_e)$ for a given temperature T_c is inversely proportional to the square root of the reactor discharge pressure.

We further note that the weight flow rate $\dot{G}$ through a unit area of the nozzle throat is given by

$$\dot{G} = p_c g/C^* \qquad [7]$$

Calculations show the characteristic velocity C^* to change by only a few per cent at temperatures of interest as the pressure p_c varies from 2 to 20 atm. Thus we may consider $\dot{G}$ to be proportional to p_c and, therefore, conclude that for a given temperature T_c, the enthalpy differential $(H_c - H_e)$ is inversely proportional to the square root of $\dot{G}$. Since I_{sp} is related to $(H_c - H_e)$ by Equation [2], if we use the total flow $\dot{w}$ instead of $\dot{G}$, we obtain

$$I_{sp} \backsimeq \alpha(-\dot{w})^{-\beta}, \qquad \alpha, \beta, -\dot{w} > 0 \qquad [8]$$

where α is a constant, $\beta \backsimeq 1/4$.

It should be pointed out that Equation [8] is valid neither for an undissociated gas nor for a completely dissociated gas.

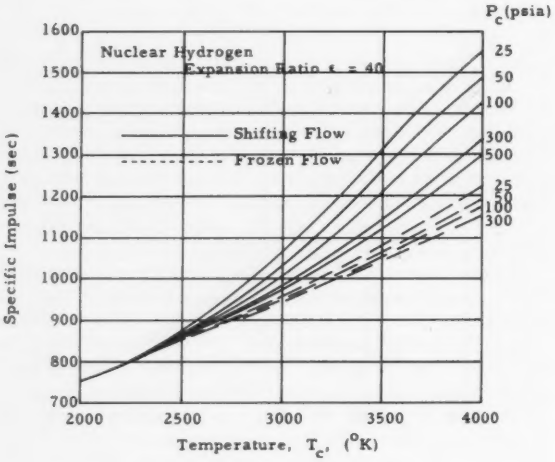

Fig. 1 Vacuum specific impulse

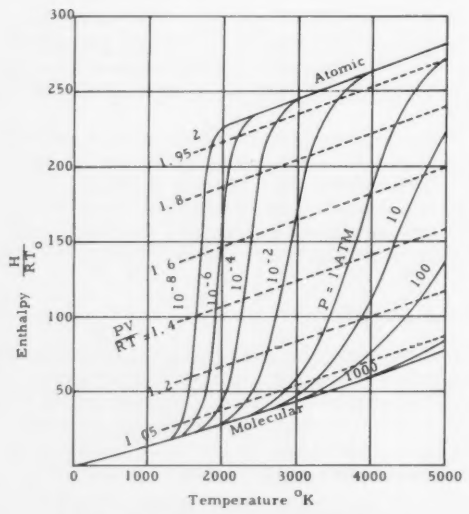

Fig. 2 Enthalpy of dissociating hydrogen

Thrust Program

The problem here is to determine an optimum thrust program for a nuclear rocket of variable I_{sp}. The I_{sp} is assumed to vary according to Equation [8]. Although there are many trajectories of interest, we shall confine the following discussion to the trajectory offering simplicity of result and presenting a clear demonstration of the effect of dissociation on nuclear rocket propulsion. Thus the vehicle is assumed to ascend vertically under constant gravity and with zero drag. The thrust program is to be such that for a given take-off weight and a given amount of propellant, the velocity gained shall be a maximum. The first step of the analysis will be to establish the optimization equation. The second step is to derive the optimum program for the type of reactor under consideration by applying the optimization equation. The third step is to compare the performance of such a programmed rocket with that of the more conventional constant thrust program.

Optimization Equation

Under the above conditions, the equation of motion of the rocket is

$$w \frac{dv}{dt} = -g \left(I_{sp} \frac{dw}{dt} + w \right) \qquad [9]$$

since

$$\frac{dv}{dt} = \frac{dv}{dw} \frac{dw}{dt} = \frac{dv}{dw} \dot{w} \qquad [10]$$

Equation [9] reduces to

$$dv = -g \left(\frac{I_{sp}}{w} + \frac{1}{\dot{w}} \right) dw \qquad [11]$$

which by integration gives the velocity

$$v = -g \int_{w_0}^{w_b} \left(\frac{I_{sp}}{w} + \frac{1}{\dot{w}} \right) dw \qquad [12]$$

In order for the velocity to have a stationary value, it is necessary that its variation δv be zero; thus we obtain the optimization equation

$$\dot{w}^2 \frac{\partial I_{sp}}{\partial \dot{w}} = w \qquad [13]$$

Optimum Program

We shall now determine the optimum thrust program for a nuclear rocket governed by Equation [8]. To do this, one can solve Equation [13 and 8] simultaneously as follows:

Differentiating Equation [8] yields

$$\frac{\partial I_{sp}}{\partial \dot{w}} = \alpha\beta(-\dot{w})^{-(1+\beta)} \qquad [14]$$

Substituting Equation [14] into Equation [13] results in the following equation

$$\alpha\beta(-\dot{w})^{1-\beta} = w$$

or

$$\dot{w} = \frac{dw}{dt} = -\left(\frac{w}{\alpha\beta} \right)^{1/1-\beta} \qquad [15]$$

Integrating Equation [15], the "burnout" time is obtained

$$t_b = (\alpha\beta)^{1/1-\beta} \left(\frac{1-\beta}{\beta} \right) \left(w_b^{-\beta/1-\beta} - w_0^{-\beta/1-\beta} \right) \qquad [16]$$

Since the vehicle acceleration is given by

$$\frac{dv}{dt} = -g \left(\frac{I_{sp}\dot{w}}{w} + 1 \right) \qquad [17]$$

substituting Equations [8 and 15] into [17] and then integrating will give the velocity

$$v(t) = g \left(\frac{1-\beta}{\beta} \right) t \qquad [18]$$

The altitude at time t can be obtained by integrating Equation [18], thus

$$y(t) = \frac{1}{2} g \left(\frac{1-\beta}{\beta} \right) t^2 \qquad [19]$$

To obtain the "burnout" velocity and altitude as a function of the launch weight and "burnout" weight, one can simply substitute Equation [16] into Equations [18 and 19].

To determine how the specific impulse varies with time, it is most convenient to examine Equation [13] which may be written

$$\dot{w}^2 \frac{\partial I_{sp}}{\partial \dot{w}} = \dot{w}^2 \frac{dI_{sp}}{dt} \frac{dt}{d\dot{w}} = w \qquad [20]$$

or

$$\frac{dI_{sp}}{dt} = w \frac{(d^2w/dt^2)}{(dw/dt)^2} \qquad [21]$$

Upon noting the identity

$$\frac{d}{dt} \left(\frac{w}{\dot{w}} \right) = 1 - w \frac{(d^2w/dt^2)}{(dw/dt)^2} \qquad [22]$$

Equation [21] may be expressed as

$$\frac{dI_{sp}}{dt} = 1 - \frac{d}{dt} \left(\frac{w}{\dot{w}} \right) \qquad [23]$$

Hence

$$I_{sp} = t - (w/\dot{w}) + \text{constant} \qquad [24]$$

Referring to Equation [20] again, [24] becomes

$$I_{sp} + \dot{w} \frac{\partial I_{sp}}{\partial \dot{w}} = t + \text{constant} \qquad [25]$$

This is a general result whatever the dependence of specific impulse on mass flow rate. From relation [8]

$$\frac{\partial I_{sp}}{\partial \dot{w}} = -\frac{\beta I_{sp}}{\dot{w}} \qquad [26]$$

so that

$$I_{sp} = t/(1-\beta) + \text{constant} \qquad [27]$$

the constant being determined from satisfaction of Equation [13] at time of launch.

Rocket Performance

Equations [16, 18 and 19] give the performance of the nuclear rocket when operated under the thrust program which gives the maximum burnout velocity. Utilizing the following parameters, the rocket's performance was calculated and the results are presented in Figs. 3, 4 and 5.

$$\alpha = 4500 \qquad [28]$$

$$\beta = +1/4 \qquad [29]$$

$$w_0 = 200{,}000 \text{ lb} \qquad [30]$$

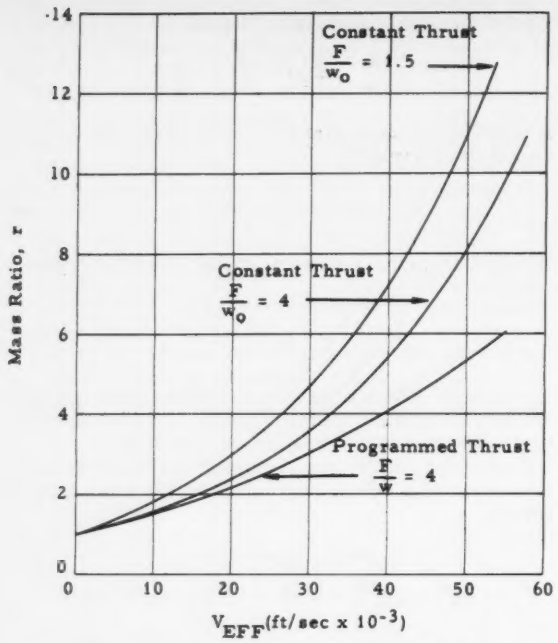

Fig. 3 Mass ratio vs. effective launch velocity

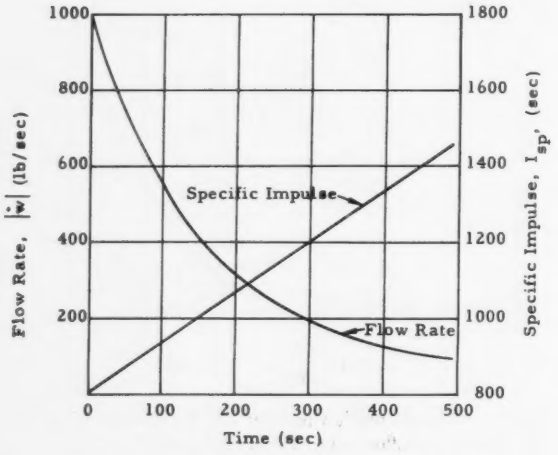

Fig. 4 Specific impulse and flow rate vs. time

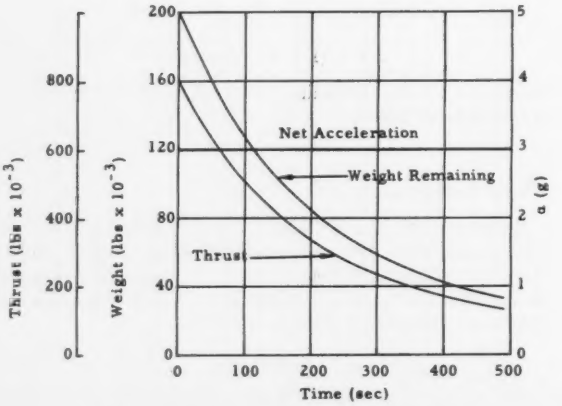

Fig. 5 Weight, thrust and acceleration vs. time

In Fig. 3, the effective launch velocity v_{eff} is a measure of the total energy per unit mass being defined as

$$v_{eff} = \sqrt{v^2 + 2gy} \qquad [31]$$

For comparison, the performance of two constant thrust vehicles is also presented. For one, the initial thrust to weight ratio and initial specific impulse were assumed to be the same as for the programmed rocket, while for the other, the same initial specific impulse was assumed but with a reduced initial thrust to weight ratio of 1.5. It is apparent that the programmed thrust rocket greatly outperforms the constant thrust vehicles even at moderate mass ratios. Moreover, at the higher velocities the constant thrust vehicles are undergoing an acceleration an order of magnitude greater than the constant acceleration rocket.

In Fig. 4 the variation of specific impulse and propellant flow rate with time is shown for the programmed vehicle, while Fig. 5 presents the variation of the thrust and remaining weight with time. The last two quantities vary in such a way that the vehicle acceleration remains constant.

Conclusion

The present analysis has shown that, for a nuclear rocket of variable specific impulse, there is definitely an optimum way of programming the thrust to fulfill a particular mission. This is because the dissociation characteristics of gases are such that, for a given temperature, a decrease in the operating pressure (and thereby the thrust) is accompanied by an increase in the specific impulse. In the case considered, the optimum thrust program results in a much better performance than the usual constant thrust operation.

Nomenclature

a = constant $\sqrt{2/g}$
A^* = throat area, ft²
C^* = characteristic velocity, fps
C_p = specific heat at constant pressure, ft lbf/R lbm-mole
D_0 = dissociation energy, ft lbf/lbm-mole of diatomic gas
f = weight fraction
g = conversion factor, lb/slug; gravitational acceleration, fps²
$\dot{G}$ = weight flow rate per unit throat area, lbf/ft² sec
H = enthalpy, ft lbf/lbm
I_{sp} = specific impulse, lbf/(lbm/sec)
K_p = pressure equilibrium constant
m = mass of vehicle, slug
M = molecular (atomic) weight
p = pressure, lbf/ft²
R = universal gas constant, ft lbf/R lbm-mole
t = time, sec
v = velocity
w = mg, weight of vehicle, lbf
y = altitude, ft
α, β = constants
ϵ = area ratio of nozzle, A_e/A^*

Subscripts

a = ambient condition
b = burnout
c = reactor discharge or stagnation condition
e = exit condition
0 = take-off
1, 2 = monatomic and diatomic, respectively

References

1 Logan, J. G., and Colichman, E. L., "The Effect of Dissociation on the Performance of Working Fluids for Nuclear Propulsion," in publication.

2 Tsien, H. S. and Evans, R. C., "Optimum Thrust Programming for a Sounding Rocket," Journal of the American Rocket Society, vol. 21, 1951, p. 99.

3 Lawden, D. F., "Stationary Rocket Trajectories," *Quart. J. Mech. and Appl. Math.*, vol. 7, 1954, p. 487.

4 Leitman, G., "Stationary Trajectories for a High Altitude Rocket with Drop Away Booster," *Astronautica Acta*, vol. 2, 1956, p. 119.

Similarity Parameters for Surface Melting of a Blunt Nosed Body in a High Velocity Gas Stream[1]

LESTER LEES[2]

Space Technology Laboratories, Inc.
Los Angeles, Calif.

By employing a simple model for the two-phase boundary layer produced by surface melting, "scaling laws" are obtained for the regime in which vaporization does not occur at the gas-liquid interface. When the liquid is fairly viscous, the gas boundary layer is virtually independent of the liquid film. The temperature rise across this film depends not only on the local heat transfer rate, but also on the difference in total enthalpy across the gas boundary layer. Thus, tests in rocket exhaust jets may not simulate vaporization or film instability phenomena that could occur in flight. Calculations of the behavior of Corning glass No. 7740 are carried out for some typical flight conditions. One interesting result is the low value of the liquid film Reynolds number, which indicates that the liquid film is almost certainly laminar. This liquid-solid system absorbs about 1125 Btu/lb, or about six times the heat capacity of a nonmelting copper heat sink. A study of the effect of mass addition to the gas phase shows that the amount of heat "blocked" by this process is sensitive to the total enthalpy difference across the gas boundary layer. The possible increase in effective heat capacity with vaporization at the gas-liquid interface is quite substantial at hypersonic flight velocity. This phenomenon can also be analyzed along the lines of the present paper.

THE PRESENT paper contains a simplified analysis for the two-phase boundary layer formed when a solid surface melts and the molten material flows around the body under the influence of the aerodynamic forces exerted by the gas. When the heat transfer rate to the liquid film is below a certain critical value, no appreciable vaporization takes place at the gas-liquid interface, and the flow in the gas phase is virtually unaffected by the presence of the extremely thin liquid film. The present study is limited to this regime, but one of the objectives is to bring out the parameters that govern the temperature rise across the liquid film, and thereby determine the critical conditions for vaporization. The effects of vaporization are discussed later.[3]

Sutton (1)[4] and Roberts (2) have analyzed the differential equations governing the motion of the gas boundary layer and the molten liquid film at the forward stagnation point of a blunt body, in the absence of vaporization. The results of their calculations bring out the importance of the liquid viscosity in determining the interfacial temperature and the shielding effect of the liquid film. Roberts (2) in particular obtained simple approximate expressions for the melting rate and other quantities of interest in terms of a parameter containing the ratio of the driving enthalpy difference for heat transfer to the sum of the heat of fusion and the heat capacity of the solid up to the melting point. More recently, Bethe and Adams (3) gave an approximate treatment of this problem for highly viscous, glassy materials in which the viscosity is strongly temperature dependent. Their approximation depends upon the fact that the liquid layer is thin in comparison with the "thermal thickness" in the material. Therefore, the temperature gradient rapidly approaches the exponential variation associated with a material countercurrent of uniform velocity toward the interface. By utilizing this exponential variation as a first approximation in the continuity and momentum equations, Bethe and Adams obtain a relation between the melting rate and the interfacial temperature. Sutton's (4) comparison of their approximate results for pyrex glass with numerical integrations of the same differential equations shows that the melting rate is underestimated by about 30 per cent for a given heat transfer rate at the interface. The equilibrium vapor pressure corresponding to the interfacial temperature is too low by about the same amount. Similar conclusions can be drawn by inserting numerical values into the "second order" approximations derived in the Appendix to reference (3). In other words, the variation in countercurrent velocity across the liquid layer plays a significant role. Nevertheless, the Bethe-Adams analysis is very useful in estimating the effective heat capacity of the material; it is also worked out for the case where vaporization occurs (3), and it can be extended around the body.

In an unpublished report Carrier (5) developed an integral method for this problem, which also starts with an exponential temperature variation, but regards the logarithmic decrement as an unknown quantity to be determined by satisfying an integral of the heat conduction equation multiplied by a judiciously chosen weighing function. No numerical results utilizing this promising method are available at present.

The conservation laws should furnish a relation between the interfacial temperature and the liquid viscosity that is relatively insensitive to the details of the velocity and temperature distributions across the liquid film. We require a simple, approximate relation that is applicable not only at the stagnation point, but also around the body, including regions

Received Dec. 1, 1958.

[1] This paper is a revised version of a report with the same title dated July 29, 1957, issued originally by Space Technology Laboratories for limited distribution.

[2] Consultant; also Professor of Aeronautics, Guggenheim Aeronautical Laboratory. Member ARS.

[3] In certain cases a portion of the heated solid material near the surface may be pyrolyzed into a gas. Sutton (1) suggested that the aerodynamic effect of this process can be roughly simulated by assuming that a fixed fraction of the melted material enters the gaseous boundary layer as a gas. Then, this case also can be included in the present study without much additional work. (See section titled Effect of Mass Addition to Gas Boundary Layer.)

[4] Numbers in parentheses indicate References at end of paper.

of turbulent flow in the gas phase. The liquid film itself is laminar, provided the Reynolds number based on film thickness and liquid properties evaluated at the interface does not exceed a certain critical value of about 150. Above this value the film is almost certainly unstable[5] when the gas phase is turbulent. Thus it is essential to be able to estimate this Reynolds number in terms of the parameters of the problem (see next section). Although detailed calculations are probably required for precise numerical values, the approximate relations for interfacial temperature and melting rate obtained here may serve as a useful guide.

Similarity Parameters for the Liquid Film

In order to fix our ideas, consider the flow over an unyawed blunt nosed body of revolution (or a cylindrical body). In this case, the properties of the single-phase boundary layer at ambient density levels corresponding to flight altitudes below about 200,000 ft are now fairly well established. In a coordinate system fixed in the gas-liquid interface, the problem is quasi-steady (Fig. 1). Suppose we start out with the assumption that u_i/u_e is so small that the gaseous phase behaves as if u_i were zero. (The correctness of this statement will be tested later.) Then the shear stress at the gas-liquid interface is equal to the value it would have at a solid boundary at the enthalpy level $h_{s_i} = h_i(T_i)$

$$(\tau_g)_i = (\rho_e u_e^2/2)c_f = (\tau_L)_i \qquad [1]$$

where c_f is known for $u_i = 0$. Also

$$(\dot{q}_g)_i = \rho_e u_e c_H (h_{s_e} - h_{s_i}) \qquad [2]$$

and in the absence of vaporization or chemical reaction at the interface

$$(\dot{q}_L)_i = (\dot{q}_g)_i = \dot{q}_i \qquad [2a]$$

For simplicity, take $Le = 1$ and $c_H = c_f/2(\overline{Pr_g})^{-2/3}$ with $\overline{Pr_g} = 0.71$.

To an observer fixed in the gas-liquid interface the molten material appears to be flowing toward him, as well as along the body surface (Fig. 1), and this countercurrent of material against the direction of heat flux absorbs heat energy at a rate given by

$$\int_0^{\delta_L} \rho v c_{p_L} (\partial T/\partial y) dy$$

Based on the simplest assumption that (ρv) varies linearly with distance across the film, and that $(\partial T/\partial y)$ is constant, this quantity has the value $0.50\dot{m}_L c_{p_L}(T_i - T_m)$. A more careful calculation (Appendix A) shows that the numerical factor is actually approximated very closely by the value 0.60 over the whole body surface. Thus the heat flux at the surface $\dot{q}_s$ is given by

$$\dot{q}_s = \dot{q}_i - 0.60\dot{m}_L c_{p_L}(T_i - T_m) \qquad [3]$$

When the heat of fusion is small compared to the heat capacity of the solid up to the melting temperature, or $L_m \ll \bar{c}_s (T_m - T_0)$, the melting rate approaches its steady-state value for a semi-infinite slab very soon after melting begins (Fig. 2 of (7)). Therefore

$$\dot{m}_L \cong \frac{\dot{q}_s}{L_m + \bar{c}_s(T_m - T_0)} \qquad [4]$$

and by Equation [3]

$$\dot{m}_L \cong \dot{q}_i/\mathcal{H} \qquad [5]$$

where $\mathcal{H} = L_m + \bar{c}_s (T_m - T_0) + 0.60 c_{p_L} (T_i - T_m)$.

In spite of the change in heat flux $\dot{q}$ across the liquid film, the temperature rise across this layer is given by the "thin film" relation with a maximum error of about 20 per cent (Appendix A), i.e.

$$\dot{q}_i = [\bar{k}_L(T_i - T_m)]/\delta_L \qquad [6]$$

Since the thermal conductivity of the liquid varies relatively slowly with temperature compared to the viscosity, it is sufficient at this stage to take $\bar{k}_L = (k_L)_i$.

As expected, the inertia forces in the liquid film are negligibly small (Appendix A), so that $\partial\tau/\partial y = dp_e/ds$, and the shear stress varies linearly with distance across the film when $dp_e/ds \neq 0$. Although it is certainly possible to account for this variation, let us avoid this added complication for the present by taking

$$(\tau_L)_i = (\tau_g)_i = (\mu_L)_i(u_i/\delta_L) \qquad [7]$$

The final relation connecting the four unknowns, $\dot{m}_L$, u_i, T_i and δ_L, is provided by the mass balance for the liquid film

$$2\pi r_0{}^k \dot{m}_L = (d/ds)\left(2\pi r_0{}^k \int_0^{\delta_L} \rho_L u_L dy\right) \qquad [8]$$

Let

$$\int_0^{\delta_L} \rho_L u_L dy = \alpha \rho_L u_i \delta_L$$

where $\alpha = 1/2$ for a linear velocity profile (for example). Then

$$r_0{}^k \dot{m}_L = \alpha(d/ds)[r_0{}^k \rho_L u_i \delta_L] \qquad [9]$$

where $k = 0$ for two-dimensional flow, and $k = 1$ for axially symmetric flow.

By utilizing Equation [7] together with Equations [1 and 2], the film thickness δ_L is expressed in terms of u_i, so that Equation [9] furnishes a simple relation for the velocity ratio u_i/u_e. Thus

$$\delta_L = (\mu_L)_i u_i/(\tau_g)_i \qquad [10]$$

but

$$\frac{(\dot{q}_g)_i}{(\dot{\tau}_g)_i} \cong \frac{h_{s_e} - h_{s_i}}{u_e}(\overline{Pr_g})^{-2/3} \qquad [11]$$

from which

$$\delta_L = \left[\frac{(\mu_L)_i u_i}{u_e}\right]\left(\frac{h_{s_e} - h_{s_i}}{\dot{q}_i}\right)(\overline{Pr_g})^{-2/3} \qquad [12]$$

By substituting this last result into Equation [9] and employing Equation [5], one obtains

$$\frac{u_i^2}{u_e^2} = \frac{(1/\alpha)(\overline{Pr_g})^{2/3}}{\rho_L(\mu_L)_i}\left[\frac{\dot{q}_i \int_0^s (\dot{q}_i/\mathcal{H})\, r_0{}^k ds}{r_0{}^k u_e (h_{s_e} - h_{s_i})}\right] \qquad [13]$$

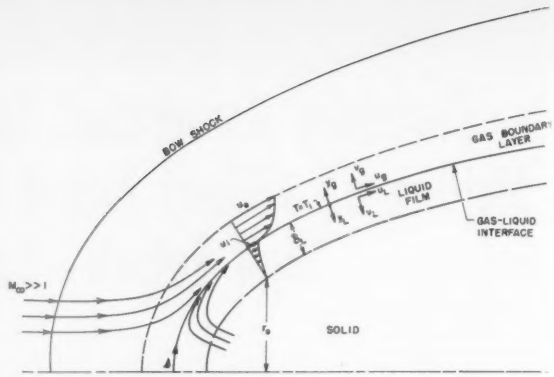

Fig. 1 Schematic diagram of two-phase boundary layer over melting blunt nosed body at high velocity

[5] The dynamical stability of the liquid film on a body decelerating through the Earth's atmosphere is analyzed by Feldman (6).

Now define

$$\dot{Q} = \dot{q}_i/(\dot{q}_i)_0$$

where $(\dot{q}_i)_0$ is the stagnation point heat transfer rate. Regardless of conditions over the rest of the body, the gas boundary layer at the forward stagnation point is almost certainly laminar, so that (8)[6]

$$(\dot{q}_i)_0 \cong (0.50)2^{k/2}\,(\overline{Pr_g})^{-2/3}\sqrt{(\rho_e\mu_e)_{g,0}}\,(h_{s_e} - h_{s_{i_0}})\sqrt{(du_e/ds)_0}$$

and[7]

$$\frac{u_i^2}{u_e^2} \cong \frac{(\overline{Pr_g})^{-2/3}}{(2)^{2-k}\alpha}\left[\frac{(\rho_e\mu_e)_{g,0}}{\rho_L(\mu_L)_i}\right]\left(\frac{h_{s_e} - h_{s_{i_0}}}{\mathcal{K}_0}\right)\cdot N \qquad [14]$$

Here

$$N = \left(\frac{s}{u_e}\right)\left(\frac{du_e}{ds}\right)_0 \dot{Q}\cdot\overline{\mathfrak{IR}}$$

and

$$\overline{\mathfrak{IR}} = \frac{\mathcal{K}_0}{r_0{}^k s}\int_0^s \left(\frac{\dot{Q}}{\mathcal{K}}\right)_{,0}{}^k\, ds$$

According to Equation [14], u_i/u_e depends mainly on the driving potential $(h_{s_e} - h_{s_{i_0}})$ and on the ratio of the $\rho\mu$ product in the liquid and the gas. Numerical calculations of u_i/u_e for both laminar and turbulent flow are presented in the next section. However, a rough estimate of u_i/u_e for a highly viscous glass-like material can be given here. For laminar gas flow at the forward stagnation point, $N = 2^{-k}$.

Suppose

h_{s_e}	=	8000 Btu/lb (u_∞ = 20,000 fps)
T_i	=	4500 R
$h_{s_{i_0}}$	$\cong h_{s_i}$ =	1500 Btu/lb
$\mathcal{K}_0$	=	750 Btu/lb
$(\rho_e)_{g,0}$	=	ρ_0 = 0.074 lb/ft³ (altitude = 60,000 ft)
ρ_L	=	131 lb/ft³
$(\mu_e)_{g,0}$	$\cong$	7×10^{-5} lb/ft sec
$(\mu_L)_i$	$\cong$	1 lb/ft-sec
α	=	1/2

Then Equation [14] yields $u_i/u_e \cong 5 \times 10^{-4}$, i.e., the velocity ratio is negligibly small even under these rather extreme conditions, and our original assumption that the flow in the gas phase is virtually independent of the presence of the liquid film is justified.

By employing Equations [6 and 12], one obtains

$$\frac{T_i - T_m}{T_m} = c_{p_L}\frac{(\mu_L)_i}{(k_L)_i}\left(\frac{h_{s_e} - h_{s_i}}{c_{p_L}T_m}\right)\left(\frac{u_i}{u_e}\right)(\overline{Pr_g})^{-2/3} \qquad [15]$$

and this relation is combined with Equation [14] to give the following expression for the temperature rise across the liquid film

$$\frac{T_i - T_m}{T_m} = \frac{1}{2^{1-(k/2)}\sqrt{\alpha}}\frac{(c_{p_L})/(k_L)_i\sqrt{(\mu_L)_i(\mu_e)_{g,0}}}{\overline{Pr_g}}\times$$

$$\left(\frac{h_{s_e} - h_{s_i}}{c_{p_L}T_m}\right)\sqrt{\frac{h_{s_e} - h_{s_i}{}^0}{\mathcal{K}_0}}\sqrt{\frac{(\rho_e)_{g,0}}{\rho_L}}\,N^{1/2} \qquad [16]$$

According to Equation [16], the temperature rise across the film depends not only on the heat transfer rate, which is contained in the factor

$$\sqrt{(\rho_e\mu_e)_{g,0}}\,(h_{s_e} - h_{s_i})$$

but also of course on the film thickness, which is proportional to the factor

$$\sqrt{(h_{s_e} - h_{s_{i_0}})/\mathcal{K}_0}\,\sqrt{(\nu_L)_i}$$

(The importance of the "driving potential" is discussed in the conclusions.) Once the interfacial temperature is calculated from Equation [16], the melting rate is obtained from the expression

$$\frac{\dot{m}_L}{\rho_\infty u_\infty} = (0.50)2^{k/2}\times$$

$$\frac{\sqrt{(\rho_e\mu_e)_{g,0}/\rho_\infty\mu_\infty}\,[(h_{s_e} - h_{s_i})/\mathcal{K}]\sqrt{(1/\mu_\infty)(du_e/d\theta)_{\theta=0}}\cdot\dot{Q}}{\sqrt{Re_\infty}} \qquad [17]$$

where

$$Re_\infty = \rho_\infty u_\infty R_0/\mu_\infty$$

When the gaseous portion of the boundary layer is turbulent, the most important parameter for the stability of the liquid film is the liquid flow Reynolds number based on quantities evaluated at the liquid-gas interface. By utilizing Equations [12 and 13], we obtain

$$(Re_L)_i = \frac{\rho_L u_i\delta_L}{(\mu_L)_i} = \frac{1}{\alpha}\frac{1}{(\mu_L)_i}\frac{1}{r_0{}^k}\int_0^s\left(\frac{\dot{q}_i}{\mathcal{K}}\right)r_0{}^k\, ds \qquad [18]$$

or

$$(Re_L)_i = \frac{(\overline{Pr_g})^{-2/3}}{2^{1-(k/2)}\alpha}\left[\frac{(\mu_e)_{g,0}}{(\mu_L)_i}\right]\left(\frac{h_{s_e} - h_{s_i}}{\mathcal{K}_0}\right)\times$$

$$\sqrt{\left(\frac{1}{\mu_\infty}\frac{du_e}{d\theta}\right)_{\theta=0}}\frac{s}{R_0}(\overline{\mathfrak{IR}})\sqrt{Re_0} \qquad [18a]$$

where

$$Re_0 = \frac{u_\infty R_0}{(\nu_e)_{g,0}} \cong 2Re_\infty$$

For some purposes, the liquid film thickness may also be of interest; its value is given by the expression

$$\frac{\delta_L}{R_0} = \frac{(\overline{Pr_g})^{-1/3}}{\sqrt{\alpha}}\sqrt{\frac{(\nu_L)_i}{(\nu_e)_{g,0}}}\sqrt{\frac{h_{s_e} - h_{s_{i_0}}}{\mathcal{K}_0}}\left[\frac{(s/R_0)(u_\infty/u_e)}{Re_0}\frac{\overline{\mathfrak{IR}}}{\dot{Q}}\right]^{1/2} \qquad [19]$$

For laminar flow at the forward stagnation point, the quantity in brackets in Equation [19] becomes

$$\frac{1}{\sqrt{(1/u_\infty)(du_e/d\theta)_{\theta=0}}}\frac{2^{-k/2}}{\sqrt{Re_0}}$$

If the region of laminar gas flow persists for an appreciable distance downstream of the forward stagnation point, the expressions for u_i/u_e and $(T_i - T_m)/T_m$ given by Equations [14 and 16] can be considerably simplified. According to (8)

$$\dot{Q} \cong \frac{1}{2^{k+1/2}}\frac{Pr_0{}^k}{\left(\int_0^s Pr_0{}^{2k}ds\right)^{1/2}}\frac{1}{(1/u_\infty)(du_e/ds)_0} \qquad [20]$$

where $P = (p/p_0{}')(u_e/u_\infty)$. Now, by squaring both sides of Equation [20] and differentiating with respect to s, we obtain a first order equation for P, as follows (10)

$$\left(\frac{d}{ds}\right)\left(\frac{P}{\dot{Q}}r_0{}^k\right) = 2^k r_0{}^k\dot{Q}\left(\frac{1}{u_\infty}\frac{du_e}{ds}\right)_0 \qquad [21]$$

[6] Relatively small corrections to this expression are introduced when $Le \neq 1$ (8, 9). In (9), it is also shown that $\dot{q}_i$ depends weakly on the value of $(\rho\mu)_g$ at the solid surface, or in this case, on $(\rho_0\mu_0)_i$.

[7] The factor $(h_{s_e} - h_{s_{i_0}}/h_{s_e} - h_{s_i})$ is replaced by unity in this approximation.

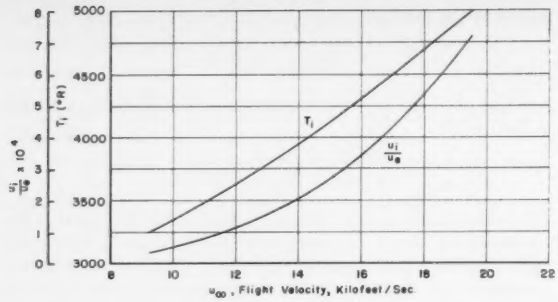

Fig. 2 Velocity ratio and temperature at gas-liquid interface with laminar boundary layer at stagnation point; altitude = 60,000 ft; Corning Glass No. 7740; melting temperature = 3000 R

By integration

$$P = \frac{2^k}{u_\infty}\left(\frac{du_e}{ds}\right)_0 \frac{\dot{Q}}{r_0^k}\int_0^s r_0^k \dot{Q}\, ds \qquad [22]$$

Therefore, the quantity

$$N = \frac{s}{u_e}\left(\frac{du_e}{ds}\right)_0 \dot{Q}\,(\overline{\mathfrak{M}})$$

appearing in Equations [14 and 16] is approximately $2^{-k} \times (p/p_0')$, for laminar gas flow. In this case we see that u_i/u_e and $(T_i - T_m)/T_m$ actually *decrease* with distance around a convex blunt nosed body, while the liquid film *thickness* increases.

Numerical Calculations of Flow Quantities at the Gas-Liquid Interface

In order to determine the orders of magnitude of u_i/u_e, $(T_i - T_m)/T_m$ and $(Re_L)_i$, numerical calculations are carried out for the following cases: (a) laminar flow at the forward stagnation point (from which values in the rest of the laminar flow region can be quickly estimated); (b) turbulent gas flow at the sonic point on a blunt nosed body.

Laminar Flow at the Forward Stagnation Point

In this case the values of u_i/u_e and $(T_i - T_m)/T_m$ are given by Equations [14 and 16], respectively, with $N = 2^{-k}$. Of course $(Re_L)_i = 0$ here. The calculation procedure, which is utilized also in the turbulent case to be discussed in the next section, consists in multiplying Equation [16] by

$$\sqrt{\frac{1}{(\mu_L)_i}}\sqrt{\frac{\mathcal{K}_0}{L_m + \bar{c}_s(T_m - T_0)}}$$

and computing the new left-hand side for various values of T_i; inserting a value of h_{s_i} corresponding to one of these values of T_i on the new right-hand side of the modified Equation [16], and calculating this right-hand side for a series of values of h_{s_e}, or flight velocity u_∞ at a given altitude. The correct value of u_∞ is readily obtained by graphical interpolation. Calculated values of u_i/u_e and $(T_i - T_m)/T_m$ are plotted against flight velocity in Fig. 2. These numerical results agree well with those obtained by more elaborate methods (1 to 4). The basic data utilized in the calculation are as follows:

1 Flight altitude = 60,000 ft, or $\rho_\infty/\rho_0 = 9.084 \times 10^{-2}$; $T_\infty = 218$ K, and $p_\infty = 7.232 \times 10^{-2}$ atm.

2 Melting temperature of the surface material (T_m) is 3000 R; $c_{p_L} = 0.33$ Btu/lb/F, and $L_m + \bar{c}_s(T_m - T_0) = 750$ Btu/lb. Also, $\rho_L = 131$ lb/ft^3; $(k_L)_i = 1.71 \times 10^{-3}$ Btu/ft-R-sec, and $(\mu_L)_i = 0.0672 \exp\,[(8720/T_i)^{1.612}]$, where T is in deg R. (These data for Corning No. 7740 glass (1).)

3 $(h_{s_i})_g = 0.33\,T_i$, in Btu/lb. Values of $(\rho_e)_{g,0}$ and $(T_e)_{g,0}$ are obtained from the charts in (11), and values of $(\mu_e)_{g,0}$ are computed by the Sutherland formula. (See also Fig. 21 of (10).)

Turbulent Gas Boundary Layer at Sonic Point on Body Surface

So far as the temperature rise across the liquid film is concerned, the most severe conditions are encountered at or near the sonic point on the body surface when laminar-turbulent transition occurs in the gas boundary layer near the forward stagnation point. Because the viscosity of the liquid is strongly temperature dependent, the highest film Reynolds numbers are also attained near the sonic point, unless the afterbody is unusually long. In order to predict the turbulent heat transfer rate to the liquid film in this region, we must resort to semi-empirical methods, supported wherever possible by qualitative physical reasoning. If the mechanism of turbulent shear flow is not much affected by enthalpy level, then the turbulent heat transfer rate is expected to depend mainly on the total enthalpy difference across the boundary layer and only weakly on the mode of heat transfer (12, 13). In fact, the principal effect of the high temperatures appears in the physical properties. In the present paper we regard the values of these properties at the outer edge of the gas boundary layer as the most significant for the heat transfer problem.

If this reasoning is correct, supersonic wind tunnel measurements of turbulent heat transfer rates on blunt nosed bodies at low to moderate enthalpy levels can probably be extrapolated to hypersonic flight conditions with some confidence. Such measurements have been made by Libby and Cresci (14) at the Polytechnic Institute of Brooklyn Aeronautical Laboratory by means of a new "shroud" technique (15) which produces very high pressures and Reynolds numbers around the model. Their experiments on a spherically blunted cone show that the curve of heat transfer rate vs. distance along the body is "flat" near the forward stagnation point, and then rises rapidly to a peak somewhat upstream of the sonic point. Of course, the location and height of this peak is strongly influenced by the location of laminar-turbulent transition. The fully turbulent heat transfer rates correlate best with the local low-speed, nearly isothermal, flat-plate empirical relation $c_H = 0.030\,Re^{-0.2}\,Pr^{-2/3}$, over a range of ratios of stagnation enthalpy to surface enthalpy of about 1.3 to 2.0.

Recently Beckwith and Gallagher (16) measured turbulent heat transfer rates on a hemispherical nose at Mach numbers of 2.0 and 4.15 in the blowdown jet at NASA Langley Aeronautical Laboratory. At a Reynolds number based on nose diameter of 3.4×10^6, the peak turbulent heat rate is about 2.5 times $\dot{q}_0$, and this peak value is very close to the local flat-plate prediction. Again, $\dot{q}$ is within 20 per cent of $\dot{q}_0$ so long as $\theta < 20$ deg.

Shock tube data obtained by Rabinowicz (17) over a range $3 < (h_{s_e}/h_w) < 8$ and by Rose, Probstein and Adams (13) at enthalpy ratios equivalent to satellite velocity, support the conclusion that for subsonic and low supersonic Mach numbers, turbulent heat transfer rates are to a remarkable degree independent of falling pressure gradients and the ratio of stagnation to surface enthalpy. This conclusion suggests the following procedure for the present problem of the two-phase boundary layer:

1 For a spherically blunt nose, let us suppose that $\dot{q}$ rises linearly with distance along the body surface from the value $\dot{q}_0$ at $s = 0$ to $\dot{q}_i{}^*$ at the sonic point, which we take at $\theta = 45$ deg, i.e.

$$\dot{Q} = \frac{\dot{q}}{\dot{q}_0} = 1 + (\dot{Q}_i{}^* - 1)\,\frac{\theta}{(\pi/4)}$$

See Sketch A.

2 Suppose that the turbulent heat transfer rate at the sonic point is given by the usual (local) flat-plate value, i.e.

$$\dot{q}_t^* = \rho_e u_e c_H (h_{s_e} - h_{s_i})$$

where

$$c_H = \frac{0.037}{[(\rho_e^* u_e^* s^*)/\mu_e^*]^{0.2}} \, (\bar{Pr}_0)^{-2/3}$$

Because of the rather conservative first assumption, no correction factor for $\mathfrak{Le} \neq 1$ or $h_{s_e}/h_{s_i} \gg 1$ is applied here.

3 Take $\mathfrak{C} = \mathfrak{C}_0$ in the entire subsonic region up to the sonic point.

With the aid of these three working assumptions, one obtains the following expressions for the quantities required in evaluating u_i/u_e, $(T_i - T_m)/T_m$, and $(Re_L)_i$ (Eqs. [14, 16 and 18a])

$$\bar{\mathfrak{N}}^* = \bar{Q}^* = 0.18 + 0.35\dot{Q}_t^* \qquad [23]$$

$$N^* = \left[\frac{s}{u_e}\left(\frac{du_e}{ds}\right)_0 \dot{Q}\bar{Q}\right]^* = \frac{\pi/4}{(a^*/u_\infty)}\left(\frac{1}{u_\infty}\frac{du_e}{d\theta}\right)_{\theta=0} \times [\dot{Q}_t^*(0.18 + 0.35\dot{Q}_t^*)] \qquad [24]$$

where

$$\dot{Q}_t^* = \frac{0.091}{2^{k/2}}\left(\frac{\rho^* a^*}{(\rho_e)_{0,0} u_\infty}\right)^{0.8} \times \frac{1}{\sqrt{(1/u_\infty)(du_e/d\theta)_{\theta=0}}} \frac{1}{(\pi/4)^{0.2}} (Re_\infty)^{0.3} \qquad [25]$$

But $\rho^*/\rho_{s_{g,0}} = 0.620 \pm 0.007$ over the range $8 \leqq M_\infty \leqq 25$, while

$$\frac{a^*}{u_\infty} \cong \sqrt{\frac{\rho_\infty}{\rho_{s_{g,0}}}}$$

and

$$\left(\frac{1}{u_\infty}\frac{du_e}{d\theta}\right)_{\theta=0} \cong \sqrt{2\frac{\rho_\infty u_\infty^2}{\rho_{s_{g,0}}}}$$

so that

$$N^* = 1.11\,\dot{Q}_t^*(0.18 + 0.35\,\dot{Q}_t^*) \qquad [26]$$

and

$$Q_t^* \cong \frac{0.050}{2^{k/2}}\left(\frac{\rho_\infty}{\rho_{s_{g,0}}}\right)^{0.15}(Re_\infty)^{0.30} \qquad [27]$$

In particular, for a nose radius of 2 ft and a flight altitude of 60,000 ft

$$Q_t^* = 5.01\left(\frac{\rho_\infty}{\rho_{s_{g,0}}}\right)^{0.15}\left(\frac{u_\infty}{10^4}\right)^{0.30} \qquad [27a]$$

(Over the range $8 \times 10^3 < u_\infty < 22 \times 10^3$, Q_t^* increases slowly from 3.50 to 4.31.)

The calculation procedure is very much the same as that employed in the discussion of laminar flow at the forward stagnation point, except of course that the value of N on the right-hand side of Equation [16], is given by Equations [26 and 27], or [27a]. Values of u_i/u_e, $(T_i - T_m)/T_m$, $(R_L)_i$ and surface melting rate at the sonic point are plotted against flight velocity in Fig. 3. Evidently the temperature rise across the film is much larger than in the laminar case (Fig. 2), but u_i/u_e is still negligibly small. A somewhat surprising result is the relatively low value of $(Re_L)_i$. These results are discussed later.

Effect of Mass Addition to Gas Boundary Layer—Preliminary Study

So far in this paper, it has been assumed that no transfer of mass occurs at the gas-liquid interface. General Electric experiments on glass-impregnated materials suggested to

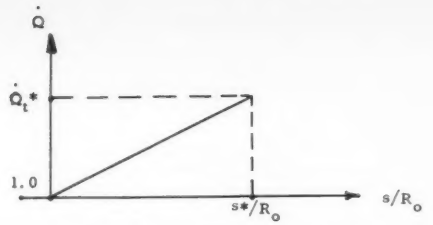

Sketch A Turbulent heat transfer rate distribution over blunt nose

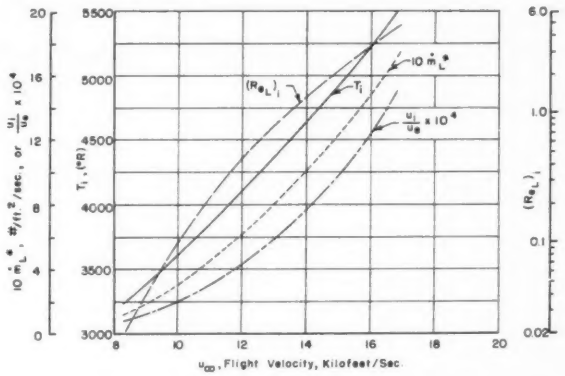

Fig. 3 Liquid film properties at gas-liquid interface and peak surface melting rate—turbulent gas boundary layer at sonic point; altitude = 60,000 ft; R_0 = 2 ft; Corning Glass No. 7740; T_m = 3000 R

Sutton (1) that a certain fraction of the melted substance is pyrolyzed into a gas that diffuses across the liquid film and enters the gas boundary layer. Presumably no additional heat transfer is required. The details of this process are probably quite complicated, and no way is known at present to determine the fraction f that is gasified, except by experiment. This phenomenon is quite different physically from the process of vaporization at the gas-liquid interface, which is uniquely determined by mass diffusion and energy transfer at the interface, in conjunction with the curve of equilibrium vapor pressure vs. temperature for the liquid.

Actually this "floating parameter" f is quite useful, because it furnishes a simple method of illustrating the effect of mass addition to the gas phase. Since $u_i/u_e \ll 1$, the gaseous portion of the boundary layer behaves as if the mass addition occurred at a permeable solid surface at the enthalpy level $h_{s_i}(T)_i$. In Fig. 4 the ratio c_H/c_{H_0} of the Stanton number with mass addition to the value with no mass addition is plotted against the injection parameter $B = \dot{m}_i/\rho_e u_e c_{H_0}$ for two important cases: (a) laminar flow at the stagnation point of a blunt body, as calculated by Reshotko and Cohen (18)[8]; (b) turbulent flow over a flat plate at $M_e = 2.7$, as obtained experimentally by Rubesin et al. (19, 20). (Both cases apply to air injection into an air boundary layer; the reduction in c_H is greater for injected gases of higher specific heat than air, e.g., lighter molecular weight.) Now in the present problem the rate of mass addition $\dot{m}_i$ is given by

$$\dot{m}_i = f\dot{m}_L = f(\dot{q}_i/\mathfrak{C}_0)$$

[8] Reshotko and Cohen (18) utilized the injection parameter $v_w/\sqrt{\nu_w c} = \tilde{B}$, but $\tilde{B} = [(Pr)_w/(Nu/\sqrt{Re})_0]\tilde{B}$, or $B = 1.165\,\tilde{B}$. (See Fig. 2 of (18).)

according to Equation [5], so that

$$\frac{\dot{m}_i}{\rho_e u_e c_{H_0}} = B = f \cdot \frac{h_{s_e} - h_{s_i}}{\mathcal{H}_0} \cdot \frac{c_H}{c_{H_0}} \qquad [28]$$

or

$$c_H/c_{H_0} = g^{-1}B \qquad [28a]$$

where

$$g = f \cdot \frac{h_{s_e} - h_{s_i}}{\mathcal{H}_0}$$

The intersections of the straight lines represented by Equation [28a] with the curves of c_H/c_{H_0} vs. B in Fig. 4 give the only possible solutions.

The reduction in heat transfer rate, or the "heat blockage," can be regarded as an increase in effective heat sink capacity. Suppose

$$\dot{m}_L = (\dot{q}_i)_0/\mathcal{H}_{eff}$$

Then the effective heat sink capacity $\mathcal{H}_{eff}$ is defined by the relation

$$\frac{\mathcal{H}_{eff}}{\mathcal{H}_0} = \frac{c_{H_0}}{c_H} = \frac{(\dot{m}_L)_{B=0}}{(\dot{m}_L)_{B\neq 0}}$$

and $\mathcal{H}_{eff}/\mathcal{H}_0$ depends only on the parameter

$$g = f \cdot \frac{(h_{s_e} - h_{s_i})}{\mathcal{H}_0}$$

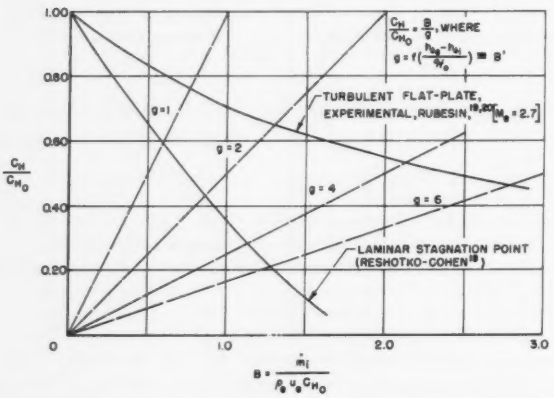

Fig. 4 Effect of mass injection on heat transfer rate (air-air)

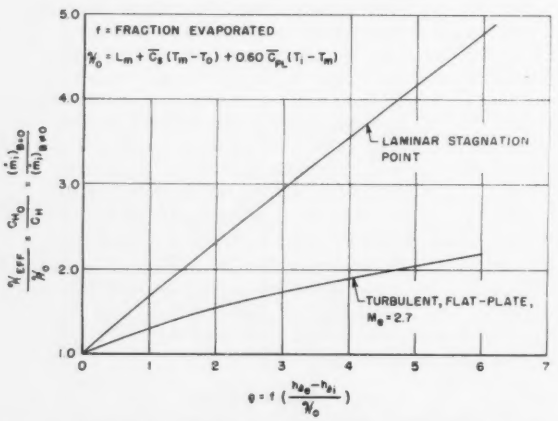

Fig. 5 Effective heat sink capacity with mass addition, as a function of driving enthalpy potential and fraction of melted material evaporated

Once again we see the importance of the ratio of the driving enthalpy potential to the original heat capacity (Fig. 5).

Although it does not seem worthwhile to go into the details here, the present scheme is easily modified to take account of the fraction of melted material that enters the gas boundary layer as a gas. For example, in the relation expressing the mass balance for the liquid film (Eq. [9]) the quantity $\dot{m}_L$ is replaced by $\dot{m}_L(1-f)$, and $(1-f)$ appears on the right-hand side of Equation [13] for u_i^2/u_e^2. What is more important, Equation [16] for the temperature rise across the liquid film now contains the mutliplier $(c_H/c_{H_0})_{LAM}\sqrt{1-f}$ on the right-hand side. In both Equations [17 and 18a], the simple factor $(c_H/c_{H_0})_{LAM}$ appears, so that $\mathcal{H}_0$ is replaced by $\mathcal{H}_{eff}$. For a given arbitrary value of f, the calculations proceed much as described in the discussion of the numerical calculations, except that for every value of h_{s_e} (with a fixed T_i) the value of $(c_H/c_{H_0})_{LAM}$ is obtained from Fig. 5. When laminar-turbulent transition occurs near the forward stagnation point the value of Q_i^* (Eq. [25]) is increased by the factor

$$\frac{(c_H/c_{H_0})_t^*}{(c_H/c_{H_0})_{LAM}}$$

Evidently mass addition by this process can have an important effect in reducing $(T_i - T_m)/T_m$ and $(Re_L)_i$.

When true vaporization takes place at the gas-liquid interface, the situation is somewhat more complicated in general (3, 5). However, when T_i is close to the local boiling temperature, $f \to 1$, i.e., practically all of the molten liquid vaporizes. In this limiting case the problem is again considerably simplified, and the main features can be distinguished without considering all the details. When $L_{vap} \gg \mathcal{H}_0$, a similar simplification occurs even for relatively small values of f, as in the case of H_2O; here L_{vap} is the heat of vaporization. In both cases $\dot{q}_i \cong \dot{m}_i(L_{vap} + \mathcal{H}_0)$, so that

$$B' \cong \frac{\dot{m}_i}{\rho_e u_e c_H} = \frac{(h_{s_e} - h_{s_i})}{(L_{vap} + \mathcal{H}_0)}$$

also

$$\frac{c_H}{c_{H_0}} = \frac{B}{B'}$$

Now at hypersonic flight velocity, h_{s_e} is 3 to 10 times larger than h_{s_i}, and both $(h_{s_e} - h_{s_i})$ and $(\mathcal{H}_0 + L_{vap})$ are relatively insensitive to the value of the interfacial temperature T_i, which is unknown initially. Therefore B' can be determined rather accurately by inserting a reasonable first estimate for T_i, and the values of B and $\dot{m}_i$ are then obtained as before from the curves of c_H/c_{H_0} vs. B in Fig. 4. For $Le = 1$, the analysis of (12) shows that

$$(\tilde{K}_E)_i = \frac{B'}{B'+1}$$

where $(K_E)_i$ is the element mass fraction of the vaporizing material at the gas-liquid interface. In the absence of chemical reactions involving the vaporizing material, the species mass fraction $K_E = \tilde{K}_E$, and

$$\frac{p_E}{p} = \left[1 + \left(\frac{1}{K_E} - 1\right)\frac{\mathfrak{M}_E}{\mathfrak{M}_{air}}\right]^{-1}$$

where p_E is the partial pressure of the vapor, and $\mathfrak{M}_E$ and $\mathfrak{M}_{air}$ are the molecular weights of vapor and air, respectively. Thus a better approximation to the interfacial temperature is determined by means of these last two relations, and a second iteration usually suffices.

These simple relations furnish a rapid estimate of the flow regime for any particular problem; in the "boiling" regime they show that T_i "adjusts itself" to a value determined mainly by the energy balance and the "blockage" effect of mass addition on heat transfer. Chemical reactions can also be included in this scheme in the manner described in (12).

Discussion and Conclusions

1 By employing a simple "model" for the two-phase boundary layer produced by surface melting, simple algebraic expressions are obtained for the velocity ratio u_i/u_e at the interface, the temperature rise across the liquid film, and the film thickness and Reynolds number. These relations contain the "scaling laws" for the regime in which no vaporization takes place at the gas-liquid interface.

Even under the most extreme conditions, one finds that $u_i/u_e \ll 1$ for fairly viscous liquids, so that the original assumption that the gas boundary layer is virtually independent of the liquid film is justified.

2 Because the liquid viscosity is strongly temperature dependent, the temperature rise across the liquid film is an important indicator not only for the onset of vaporization, but also for the film Reynolds number, or liquid film stability when the gas boundary layer is turbulent. This temperature rise $(T_i - T_m)/T_m$ depends on the product of the local heat transfer rate and the factor

$$\sqrt{(h_{s_e} - h_{s_i})/\mathcal{H}_0}\ \sqrt{(\nu_L)_i}$$

where $(h_{s_e} - h_{s_i})$ is the driving enthalpy potential, and $\mathcal{H}_0$ is the heat capacity of the melting substance up to the interfacial temperature. Thus, it is not sufficient to duplicate the local heat transfer rate alone in model experiments. For example, in tests made in rocket exhaust jets the ratio

$$(h_{s_e} - h_{s_i})/\mathcal{H}_0$$

is generally of the order of unity, as compared with a value of 6 to 8 at a flight velocity 20,000 fps. $(T_i - T_m)/T_m$, in other words, might not be high enough in such experiments to produce vaporization at the gas-liquid interface, or the liquid film Reynolds number might be too low to bring out film instability that could occur under flight conditions.

3 In free flight, the temperature rise across the liquid film is proportional to $\sqrt{\rho_\infty}\ u_\infty{}^4$ at the forward stagnation point, and to $\rho_\infty{}^{0.8}\ u_\infty{}^{4.3}$ (approximately) at the sonic point on the body surface when laminar-turbulent transition occurs near the stagnation point. Thus, the critical conditions for the liquid film can be determined for any given flight trajectory. For ballistic missile re-entry, for example, the well-known Allen-Eggers analysis could be applied to this problem.

In order to illustrate the properties of the liquid film for typical flight conditions, calculations were made for a flight altitude of 60,000 ft. The material selected is Corning glass No. 7740, which melts at 3000 R. As expected, the value of $(T_i - T_m)/T_m$ is much smaller at the forward stagnation point with a laminar gas boundary layer than it is at the sonic point on the body surface when laminar-turbulent transition occurs near the nose (Figs. 2 and 3). For example, the interfacial temperature T_i is 5000 R at the sonic point when the flight velocity u_∞ is 15,350 fps, but T_i does not reach this value at the forward stagnation point until u_∞ = 19,600 fps. To put it another way, when u_∞ = 15,350 fps, the value of T_i at the stagnation point is 4100 R, or $(T_i - T_m)$ is about one-half the value at the sonic point. Vaporization is unlikely at the forward stagnation point, but quite possible at the sonic point when transition occurs near the nose.

4 A somewhat surprising result is the low value of the liquid film Reynolds number (Fig. 3). At a flight velocity of 15,350 fps, $(Re_L)_i \cong 2.5$ at the sonic point. In other words, the liquid film is quite stable; in fact, vaporization would take place before instability could occur, and this mass loss should hold the film thickness and Reynolds number to low values.

5 About 750 Btu/lb is absorbed by this material up to the melting temperature. But the countercurrent of molten material toward the interface (and against the direction of heat flux) absorbs an additional amount of energy equivalent to that required to heat about 60 per cent of the melt from the melting temperature up to the interfacial temperature. At a flight velocity of 15,350 fps, this energy increment amounts to about 375 Btu/lb, and the total $\mathcal{H}$ = 1125 Btu lb. The melting rate at the sonic station is 1.30 lb/ft²/sec. This material has about six times the heat capacity of a nonmelting copper heat sink.

6 A study of the effect of mass addition to the gas phase shows that the amount of heat "blocked" by this process is sensitive to the ratio

$$(h_{s_e} - h_{s_i})/\mathcal{H}_0$$

to the state of the gas boundary layer, and, of course, to the fraction of melted material that is gasified or evaporated. For example, in the process considered by Sutton (1), a certain fraction (f) of the melted pyrex glass is pyrolyzed into a gas and enters the gas boundary layer. With f = 0.08, the increase in "effective" heat capacity at a flight Mach number of 18 is about 30 per cent at the forward stagnation point, but only about 10 per cent for a turbulent gas boundary layer at the sonic point. On the other hand, in experiments in a typical rocket exhaust the effect at the forward stagnation point is reduced to 10 per cent, while at the sonic point it is negligible for turbulent flow.

More spectacular results are expected when true vaporization occurs at the gas-liquid interface. When T_i approaches the local "boiling temperature," $f \to 1$, and the problem is considerably simplified. For the same flight conditions considered by Sutton (1), the effective heat capacity of the pyrex material is about doubled to a value of 2500 Btu/lb in the turbulent case, while at the forward stagnation point $\mathcal{H}_{eff} \cong$ 5000 Btu/lb (Fig. 5). It would seem desirable to search for (or invent) a material that is fairly viscous in the liquid state, with a boiling temperature not too far above the melting temperature.

Appendix A

Estimate of Magnitude of Inertia Forces in Liquid Film

The change in shear stress across the liquid film required to provide the molten material with its momentum parallel to the surface is given by the expression

$$\Delta\tau = \int_0^{\delta_L} \rho_L v(\partial u/\partial y)dy \cong (\rho_L v)u_i$$

so that

$$\frac{\Delta\tau}{\tau_i} \cong \frac{\rho_L v u_i}{\tau_i} = \frac{(\rho_L v)u_i}{\dot{q}_i u_e}(h_{s_e} - h_{s_i})(\overline{Pr_e}^{-2/3})$$

by Equation [11] of the text.

But $(\rho_L v) \cong m_L = \dot{q}_i/\mathcal{H}$, so that

$$\left(\frac{\Delta\tau}{\tau_i}\right) \cong \left(\frac{u_i}{u_e}\right)\left(\frac{h_{s_e} - h_{s_i}}{\mathcal{H}}\right)$$

Now u_i/u_e is about 5 to 7 $\times 10^{-4}$ at most, while

$$\frac{h_{s_e} - h_{s_i}}{\mathcal{H}}$$

is 7 to 8 at most; therefore, $\Delta\tau/\tau_i \leqq 6 \times 10^{-3}$, and the correction to τ_i from this source is less than 1 per cent. A similar calculation shows that the term $\delta_L \rho_L u(\partial u/\partial s)$ is also of this order of magnitude compared with τ_i near the forward stagnation point, but is generally much smaller on a conical afterbody.

Energy Balance for the Liquid Film

Because the thermal diffusivity of the liquid is small compared to its kinematic viscosity, the "thermal inertia" terms like $\rho_L v c_{p_L}(\partial T/\partial y)$ must be taken into account. In fact the

contribution of this term to the relative change in heat flux $\Delta\dot{q}/\dot{q}$ across the film is larger than the corresponding contribution of $\rho_L v(\partial u/\partial y)$ to $\Delta\tau/\tau$ by a factor of the order of the Prandtl number. At a temperature of 4000 R, $Pr_L = 445$, for a typical highly viscous glass; therefore, a more detailed calculation is required. On the other hand, the contribution of the viscous dissipation to $\Delta\dot{q}/\dot{q}$ is of order u_i/u_e, and the contribution of the term $u(dp/ds)$ is also of this order.

In a region where the gas phase boundary layer is either wholly laminar or wholly turbulent, and the pressure is nearly constant over the body, the variation in the interfacial temperature T_i along the surface is negligibly small. However, when the pressure is dropping rapidly, as on a blunt nose, or in a region of laminar-turbulent transition in the gas phase, the term $\rho_L u c_{p_L}(\partial T/\partial s)$ cannot be ignored. Roughly, the contribution of this term to $\Delta\dot{q}/\dot{q}$ is proportional to the quantity

$$c_{p_L}(T_i - T_{i_0})/\mathcal{H}_0$$

where T_{i_0} is the interfacial temperature at the forward stagnation point. This term therefore *opposes* the main contribution from $\rho_L v c_L(\partial T/\partial y)$ over a blunt nose, except in the region of laminar-turbulent transition in the gas phase, where T_i increases with distance along the surface. It appears that the contribution made by this term is about 5 to 20 per cent of the main effect, at most. Therefore, it seems justified to retain only the principal term in the heat conduction equation in order to obtain a useful estimate of the change in heat flux across the liquid film. Thus

$$\rho_L v c_{p_L}\left(\frac{\partial T}{\partial y}\right) = k_L\left(\frac{\partial^2 T}{\partial y^2}\right) \qquad [A\text{-}1]$$

By integration, one obtains

$$\log_e\left(\frac{\dot{q}}{\dot{q}_i}\right) = \frac{c_{p_L}}{k_L}\int_0^y (\rho_L v)dy \qquad [A\text{-}2]$$

and some estimate of the lateral velocity is required.

According to the equation of continuity

$$\partial/\partial y(\rho_L v) = -\left(\frac{1}{r_0}\right)\left(\frac{\partial}{\partial s}\right)(\rho_L u_L r_0) \qquad [A\text{-}3]$$

Suppose that $u/u_i = 1 - (y/\delta_L)$. Then

$$(\rho_L v) = Ay^2 - By \qquad [A\text{-}4]$$

where

$$A = \frac{1}{2}\left(\frac{1}{r_0}\right)\left(\frac{\partial}{\partial s}\right)\left(\frac{\rho_L u_i r_0}{\delta_L}\right)$$

and

$$B = \left(\frac{1}{r_0}\right)\left(\frac{\partial}{\partial s}\right)(\rho_L u_i r_0)$$

By substituting this last result into Equation [A-2], we obtain

$$\log_e\left(\frac{\dot{q}}{\dot{q}_i}\right) = \frac{c_{p_L}}{k_L}\left(\frac{Ay^3}{3} - \frac{By^2}{2}\right) \qquad [A\text{-}5]$$

or

$$\frac{\dot{q}}{\dot{q}_i} = 1 + \frac{c_{p_L}}{k_L}\left(\frac{Ay^3}{3} - \frac{By^2}{2}\right) + \frac{1}{2}\left[\frac{c_{p_L}}{k_L}\left(\frac{Ay^3}{3} - \frac{By^2}{2}\right)\right]^2 + \ldots \qquad [A\text{-}6]$$

The value of $\dot{q}_s/q_i$ is obtained by substituting $y = \delta_L$ into Equation [A-6]. By integrating Equation [A-6] once more, we obtain

$$(T_i - T_m) = \frac{\dot{q}_i\delta_L}{k_L}\left[1 + \frac{c_{p_L}}{k_L}\left(\frac{A\delta_L^3}{12} - \frac{B\delta_L^2}{6}\right) + \ldots\right] \qquad [A\text{-}7]$$

The coefficients A and B are readily evaluated in two important special cases: (a) near the forward stagnation point; (b) in a region of constant pressure on a conical afterbody. In the first case, δ_L is constant, and

$$A = \frac{1}{2}\left(\frac{1}{\delta_L^2}\right)\left(\frac{1}{r_0}\right)\left(\frac{\partial}{\partial s}\right)(\rho_L u_i r_0 \delta_L) = \left(\frac{\dot{m}_L}{\delta_L^2}\right)$$

by Equation [9] of the text, with $\alpha = 1/2$. Similarly, $B = 2\dot{m}_L/\delta_L$. Therefore,

$$\frac{\dot{q}_s}{\dot{q}_i} = 1 - \frac{2c_{p_L}}{3k_L}\delta_L\dot{m}_L + \left(\frac{2}{9}\right)\left(\frac{c_{p_L}}{k_L}\delta_L\dot{m}_L\right)^2 + \ldots \qquad [A\text{-}8]$$

and

$$(T_i - T_m) = \frac{\dot{q}_i\delta_L}{k_L}\left[1 - \left(\frac{1}{4}\right)\left(\frac{c_{p_L}}{k_L}\delta_L\dot{m}_L\right) + \ldots\right] \qquad [A\text{-}9]$$

By Equation [A-9]

$$\delta_L = \frac{k_L(T_i - T_m)}{\dot{q}_i}\left[1 - \frac{1}{4}\left(\frac{c_{p_L}}{k_L}\delta_L\dot{m}_L\right) + \ldots\right]^{-1} \qquad [A\text{-}10]$$

For our purposes, one cycle of this recursion formula is sufficient, so that

$$\delta_L \cong \frac{k_L(T_i - T_m)}{\dot{q}_i}\left[1 - \frac{1}{4}\frac{c_{p_L}(T_i - T_m)}{\mathcal{H}}\right]^{-1} \qquad [A\text{-}11]$$

Thus in the most extreme case (Figs. 2 and 3), where

$$c_{p_L}(T_i - T_m)/\mathcal{H} \cong 0.8$$

the simple "thin-film" relation

$$\dot{q}_i = [k_L(T_i - T_m)]/\delta_L$$

is accurate to within 20 per cent; in most cases the error is much smaller.

From Equation [A-8], one finds that

$$\dot{q}_s \cong q_i - \frac{2}{3}[c_{p_L}\dot{m}_L(T_i - T_m)] + \frac{1}{18}\left[\frac{c_{p_L}(T_i - T_m)}{\mathcal{H}}\right][c_{p_L}\dot{m}_L(T_i - T_m)] \qquad [A\text{-}12]$$

so that the relation

$$\dot{q}_s = \dot{q}_i - 0.60c_{p_L}\dot{m}_L(T_i - T_m) \qquad [A\text{-}13]$$

is sufficiently accurate for the present analysis. In other words, the energy absorbed across the film is equivalent to that required to heat about 60 per cent of the melted material up to the interfacial temperature.

A similar calculation can be carried out for a region of constant pressure over a conical afterbody. In this case the constant 1/4 appearing in Equation [A-11] is replaced by 7/36, while the coefficients 2/3 and 1/18 in Equation [A-12] are replaced by 5/9 and 5/108, respectively. In the computations, the relation given by Equation [A-13] is used both at the forward stagnation point and at the sonic point on the body surface.

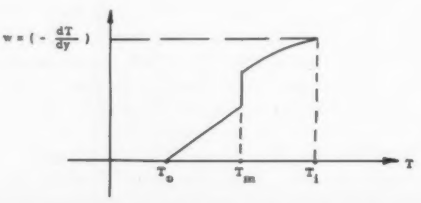

Sketch B Temperature gradient as a function of temperature across liquid film

Appendix B

The approximate expressions obtained for the velocity at the gas-liquid interface and the temperature rise across the liquid film (Eqs. [14 and 16]) can be given a simple interpretation by means of a polynomial representation of the temperature gradient $(-dT/dy) = w$ as a function of temperature (see Sketch B).

For $T_0 \leqq T \leqq T_m$

$$w(T) = b(T - T_0)$$

while for $T_m \leqq T \leqq T_i$

$$w(T) = \sum_{n=0}^{3} a_n (T - T_i)^n$$

where

$$a_n = \frac{1}{n!}\left(\frac{d^n w}{dT^n}\right) T_i$$

and

$$a_0 = w_i$$

At the junction point of these two regions, we require that dw/dT and d^2w/dT^2 are continuous, or that T, v and u are all continuous, and that

$$\Delta \dot{q} = -\rho_L v_\infty L_m = k_L \, \Delta w$$

Now from Equation [A-1]

$$\frac{dw}{dT} = -\frac{\rho_L c_{p_L} v}{k_L} \qquad \text{[B-1]}$$

while the equation of continuity yields the following relation at the forward stagnation point

$$\frac{d}{dy}(\rho_L v) = +\frac{k_L w}{c_{p_L}}\frac{d^2w}{dT^2} = -2^k \rho_L \left(\frac{du_e}{ds}\right)_0 \left(\frac{u}{u_e}\right) \qquad \text{[B-2]}$$

Also the relation $\tau = \mu(\partial u/\partial y)$ yields

$$w\frac{d}{dT}\left(w\frac{d^2w}{dT^2}\right) = +\frac{2^k \rho_L}{u_e}\left(\frac{du_e}{ds}\right)_0 \frac{c_{p_L}}{k_L}\frac{\tau}{\mu_L} \qquad \text{[B-3]}$$

We recognize that at $T = T_i$ the value of τ in Equation [B-3] is equal to

$$-\tau_g = -\frac{u_e \dot{q}_i (\overline{Pr_g})^{2/3}}{(h_{s_e} - h_{s_i})}$$

In the absence of vaporization

$$(dw/dT)_{T_i} = 0$$

and the left-hand side of Equation [B-3] at $T = T_i$ is simply

$$w_i^2 \, (d^3w/dT^3)_i$$

By evaluating w_i, $(d^2w/dT^2)_{T_i}$ and $(d^3w/dT^3)_{T_i}$, recognizing that $b = -(c_{p_L}/k_L)\rho_L v_\infty$, and utilizing the three conditions that dw/dT and d^2w/dT^2 are continuous, and that

$$\Delta w = -(\rho_L v_\infty L_m/k_L)$$

at $T = T_m$, we are able to solve for the three unknowns $T_i - T_m$, u_i/u_e, $\rho_L v_\infty$; the results are identical with the expressions given in Equations [15 and 16], with $\alpha = 1/2$, except that

$$\mathfrak{IC}_0 = L_m + c_{p_L}(T_m - T_0) + (2/3)c_{p_L}(T_i - T_m)$$

Nomenclature

a = local sound speed
B = $\dot{m}_i/\rho_e u_e c_{H_0})$, mass addition parameter
B' = $\dot{m}_i/\rho_e u_e c_H$, mass addition parameter
c_f = local skin friction coefficient, $(\tau_g)/(\frac{1}{2}\rho_e u_e^2)$
c_H = local Stanton number, $\dot{q}_g/\rho_e u_e(h_{s_e} - h_{s_i})$
c_p = specific heat at constant pressure
$\bar{c}_s$ = average value of specific heat of solid material up to melting point
f = fraction of melted material gasified or evaporated
g = $f\cdot(h_{s_e} - h_{s_i})/(\mathfrak{IC}_0)$
h_s = stagnation enthalpy
$\mathfrak{IC}$ = heat capacity of liquid-solid system, $L_m + \bar{c}_s(T_m - T_0) + 0.60c_{p_L}(T_i - T_m)$
$\mathfrak{IC}_{eff}$ = effective heat capacity
k = thermal conductivity, also geometric index
L_m = heat of fusion
$\dot{m}_i$ = rate of mass addition to gas phase
$\dot{m}_L$ = melting rate
M = Mach number, $\sqrt{u^2 + v^2}/a$
$\bar{\mathfrak{M}}$ = average value of normalized melting rate (Eq. [14])
N = $s/u_e(du_e/ds)_0 \dot{Q}\bar{\mathfrak{M}}$. (See Eq. [14].)
p = pressure
p_0' = stagnation pressure behind a normal shock
Pr = Prandtl number, $c_p\mu/k$
$\dot{q}$ = local heat transfer rate
$\dot{Q}$ = $\dot{q}/\dot{q}_0$
$\bar{\dot{Q}}$ = average value of $\dot{Q}$, $(1/r_0{}^k s)\int_0^s \dot{Q}\, r_0{}^k ds$
r_0 = radius of cross section of body of revolution
R_0 = nose radius
$(Re_L)_i$ = liquid film Reynolds number, $\rho_L u_i \delta_L/(\mu_L)_i$
Re_0 = $u_\infty R_0/(\nu_e)_{g,0}$
Re_∞ = $u_\infty R_0/\nu_\infty$
s = distance along gas-liquid interface, measured from forward stagnation point (Fig. 1)
T = absolute temperature
T_m = melting temperature
T_0 = "internal" solid temperature
u, v = components of velocity parallel and normal to gas-liquid interface (Fig. 1)
y = distance normal to interface (Fig. 1)
α = velocity profile parameter for liquid film, $\int_0^{\delta_L} \rho_L u_L dy = \alpha \rho_L u_i \delta_L$
δ = boundary layer thickness
μ = viscosity
ν = kinematic viscosity, μ/ρ
ρ = density
θ = angle between flight direction and radius vector from center of curvature of nose
τ = shear stress

Subscripts

e = flow quantities evaluated at outer edge of gas boundary layer
g = gas
i = gas-liquid interface
L = liquid
0 = stagnation point (except T_0), also zero mass addition rate
s = body surface
t = turbulent flow
∞ = free stream ahead of bow shock wave

Superscript

$(^4)$ denotes physical quantities evaluated at sonic point on body surface

References

1 Sutton, G., "The Hydrodynamics and Heat Conduction of a Melting Surface," *J. Aeron. Sci.*, vol. 25, no. 1, Jan. 1958, pp. 29–32, 36; *see also*, Scala, S. M. and Sutton, G. W., "The Two-Phase Laminar Boundary Layer—A Study of Surface Melting," Aerophysics Laboratory, Missile and Ordnance Systems Dept., General Electric Co., Technical Memorandum no. 23, Feb. 14, 1958.

2 Roberts, L., "On the Melting of a Semi-Infinite Body of Ice Placed in a Hot Stream," Department of Mathematics, MIT, June 1957, ONR Contract no. Nonr-1841(12); *see also*, *J. Fluid Mech.*, vol. 4, Part 5, Sept. 1958, pp. 505–528.

3 Bethe, H. A. and Adams, Mac C., "A Theory for the Ablation of Glassy Materials," Avco Research Laboratory, Research Rep. no. 38, Nov. 1958.

4 Sutton, G. W., "On an Approximate Solution to the Problem of Aero-

dynamic Surface Melting of a Material of Large Prandtl Number," General Electric Co., Aerophysics Operation Research Memorandum no. 17, Aug. 8, 1958.

5 Carrier, G., "Aerodynamic Heat Transfer to a Melting Body," Space Technology Laboratories, Rep. no. GM-TM-0165-00268, Aug. 8, 1958.

6 Feldman, S., "On the Instability Theory of the Soft or Melted Surface of an Ablating Body when Entering the Atmosphere," Avco Research Laboratory, Research Rep. no. 34, Aug. 1958.

7 Landau, H. G., "Heat Conduction in a Melting Solid," *Quart. Appl. Math.*, vol. 8, no. 1, 1950, pp. 81–94.

8 Lees, L., "Laminar Heat Transfer over Blunt-Nosed Bodies at Hypersonic Flight Speeds," JET PROPULSION, vol. 26, no. 4, April 1956, pp. 259–269.

9 Fay, J. A. and Riddell, F. R., "Theory of Stagnation Point Heat Transfer in Dissociated Air," *J. Aeron. Sci.*, vol. 25, no. 2, Feb. 1958, pp. 73–85, 121.

10 Rabinowicz, J., "Aerodynamic Studies in the Shock Tube," GALCIT Hypersonic Research Project, Memorandum no. 38, June 10, 1957.

11 Feldman, S., "Hypersonic Gas Dynamic Charts for Equilibrium Air," Avco Research Laboratory, Jan. 1957.

12 Lees, L., "Convective Heat Transfer with Mass Addition and Chemical Reactions," paper presented at Third AGARD Combustion and Propulsion Panel Colloquium, Palermo, Italy, March 17–21, 1958.

13 Rose, P., Probstein, R. F. and Adams, Mac C., "Turbulent Heat Transfer through a Highly Cooled Partially Dissociated Turbulent Boundary Layer," Avco Research Report no. 14, Jan., 1958 .

14 Libby, P. A. and Cresci, R. J., "Evaluation of Several Hypersonic Turbulent Heat Transfer Analyses by Comparison with Experimental Data," Wright Air Development Center, ARDC, USAF, Technical Note 57-72; ASTIA no. AD 118093, July 1957.

15 Ferri, A. and Libby, P. A., "A New Technique for Investigating Heat Transfer and Surface Phenomena under Hypersonic Flow Conditions," *J. Aeron. Sci.*, vol. 24, no. 6, June 1957, pp. 464–465.

16 Beckwith, I. E. and Gallagher, J. J., "Heat Transfer and Recovery Temperatures on a Sphere with Laminar, Transitional and Turbulent Boundary Layers at Mach Numbers of 2.00 and 4.15," NACA Technical Note no. 4125, Dec. 1957.

17 Rabinowicz, J., "Measurement of Turbulent Heat Transfer Rates on the Aft Portion and Blunt Base of a Hemisphere Cylinder in the Shock Tube," JET PROPULSION, vol. 28, no. 9, Sept. 1958, pp. 615–620.

18 Reshotko, E. and Cohen, C. B., "Heat Transfer at the Forward Stagnation Point of Blunt Bodies," NACA TN 3513, July 1955.

19 Rubesin, M. W., Pappas, C. C. and Okuno, A. F., "The Effect of Fluid Injection on the Compressible Turbulent Boundary Layer—Preliminary Tests on Transpiration Cooling of a Flat Plate at M = 2.7 with Air as the Injected Gas," NACA Research Memorandum no. A55I19, Dec. 21, 1955.

20 Rubesin, M. W., "The Influence of Surface Injection on Heat Transfer and Skin Friction Associated with the High-Speed Turbulent Boundary Layer," NACA Research Memorandum no. A55L13, Feb. 20, 1956.

Some Physical Properties for the System Nitrogen Tetroxide-Nitric Oxide[1]

DONAT B. BRICE[2] and NORMAN FISHMAN[3]

Food Machinery and Chemical Corp. San Jose, Calif.

Mixed oxides of nitrogen may become an important oxidizer with the advent of storable, prepackaged, liquid propellant rocket engines. This paper presents some physical property data for the liquid system nitrogen tetroxide–nitric oxide at temperatures between zero and minus 100 F. Properties included are vapor pressure, density, viscosity and surface tension.

RAPID progress in the development of solid propellants has threatened to force into obsolescence liquid fueled systems with their notorious complex arrays of hardware and their unreliability. However, recent advances in the prepackaging of liquid propellants, with the resulting effect of instant readiness previously reserved for solids, have brought about a resurgence of interest in liquids, with particular emphasis on storable systems. It is thought to be timely, therefore, to present physical property data for MON (mixed oxides of nitrogen) obtained in 1953 during the course of studies concerned with the production of this potential liquid oxidant.

No experimental physical property data for vapor pressure, density, viscosity and surface tension were found in the literature for mixtures of nitrogen tetroxide-nitric oxide (mixed oxides) containing 20 to 30 weight per cent nitric oxide at temperatures between 0 and −100 F. Such information is desirable in the design of propulsion systems utilizing mixed oxides as the oxidizer. The information is also necessary in the design of equipment for the manufacture of mixed oxides.

Whittaker et al. (1)[4] have determined the vapor pressure of mixed oxides for mixtures containing a maximum of 16.85 weight per cent nitric oxide at temperatures as low as −40 F. Sage and co-workers have determined vapor pressure (2) and viscosity (3) of mixtures of nitrogen tetroxide and nitric oxide. Most of these latter data were measured at temperatures above 40 F and in the range of 5 to 25 weight per cent nitric oxide. Results of investigations presented in this paper appear to be in substantial agreement with extrapolated values of the referenced data.

Equipment and Results

Materials

The mixtures of nitrogen tetroxide-nitric oxide used for these determinations were prepared by condensing gaseous mixtures of commercial grade nitric oxide and nitrogen tetroxide, distilled from commercial grade liquid. The gases were flowed in the required proportions to obtain the desired compositions of the mixed oxides. The exact percentages of nitric oxide in the mixtures were determined by freezing point techniques, using the data of Fig. 1.

Received Dec. 5, 1958.

[1] This paper is a presentation of data obtained during one phase of research carried out by Food Machinery and Chemical Corp., for the U. S. Air Force under Contract no. AF 18(600)-34. This experimental program was supported by Wright Air Development Center, United States Air Force. Permission to publish these results are gratefully acknowledged.

[2] Present address, The Fluor Corp., Whittier, Calif.

[3] Present address, Stanford Research Institute, Menlo Park, Calif. Member ARS.

[4] Numbers in parentheses indicate References at end of paper.

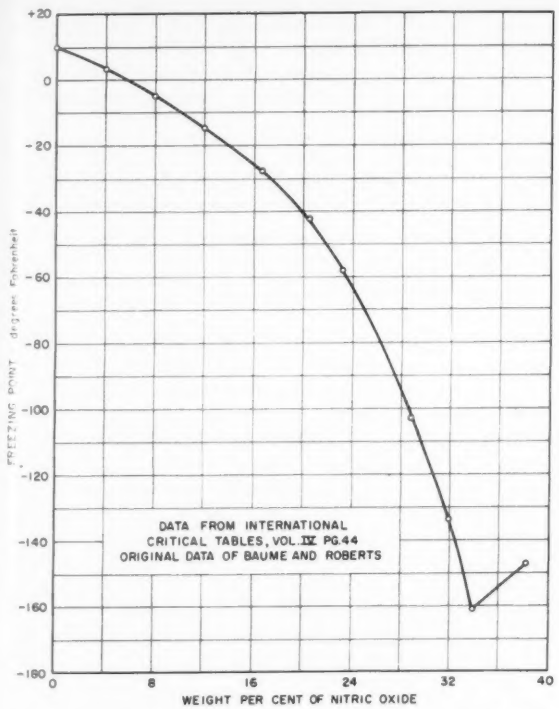

Fig. 1 Freezing point curve of nitric oxide-nitrogen dioxide mixture vs. weight per cent of nitric oxide

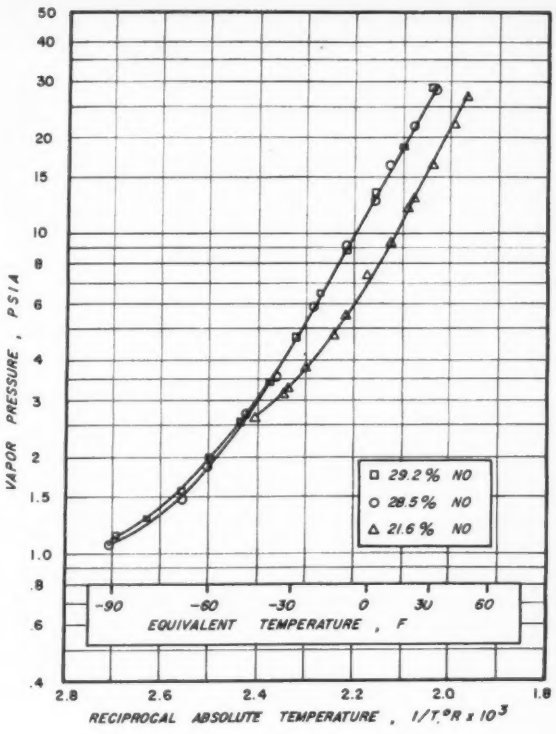

Fig. 3 Vapor pressure of mixed oxides

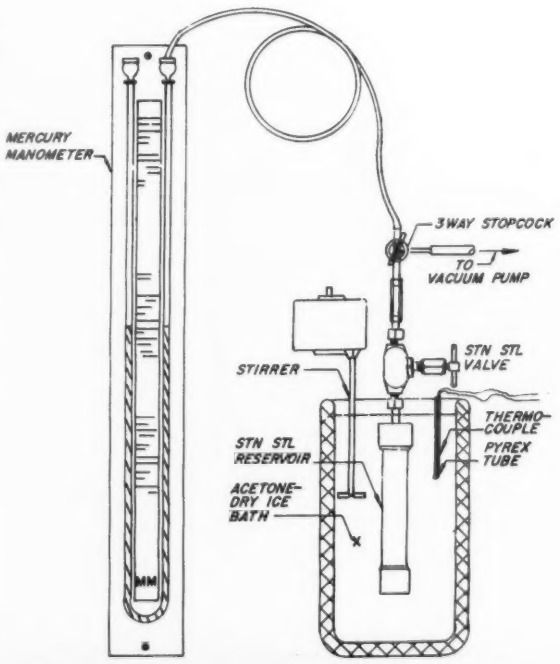

Fig. 2 Apparatus for measurement of vapor pressure

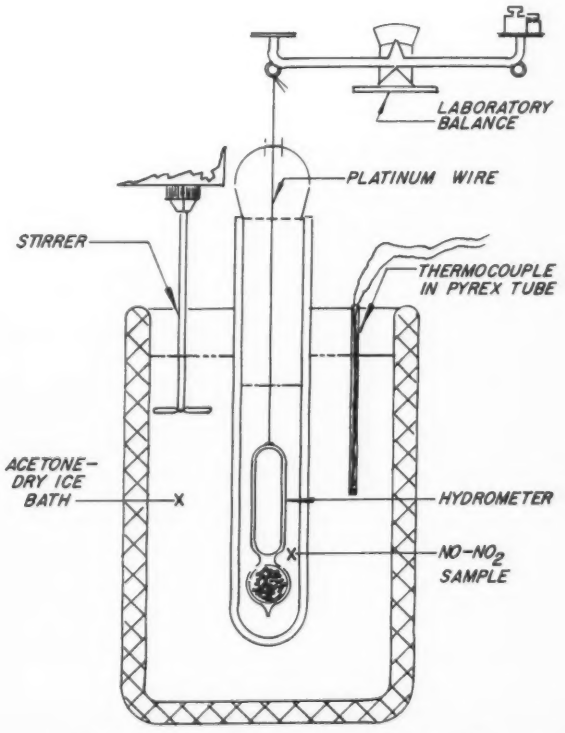

Fig. 4 Apparatus for measurement of density

Vapor Pressure

For the vapor pressure measurement, the sample was contained in a stainless steel cylinder. As can be seen from Fig. 2, a manometer was connected to the cylinder through a suitable valving arrangement. After the lines were evacuated, the cylinder was transferred from storage under liquid nitrogen to an acetone-dry ice bath and thawed at the lowest temperature at which vapor pressure was to be measured. The liquid material was allowed to come to thermal equilibrium at each successively higher temperature prior to reading the vapor pressure indicated by the manometer. The data are presented in Fig. 3 as a plot of the log of the vapor pressure vs. the reciprocal of the absolute temperature.

It can be seen from the shape of the curves of Fig. 3 that the log of the vapor pressure deviates from the straight line relationship with reciprocal temperature as the liquid temperature approaches the freezing point. This is explained by the possibility that at temperatures near freezing, nitrogen trioxide (N_2O_3) is more stable as a compound, and therefore less pressure is exerted. As the temperature is raised, the

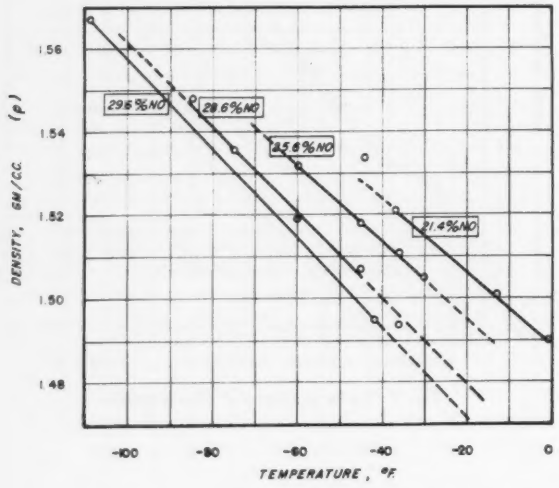

Fig. 5 Density of mixed oxides

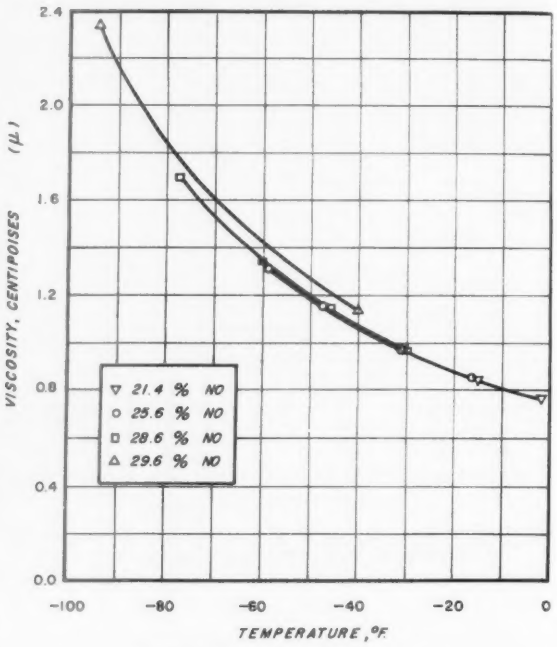

Fig. 7 Viscosity of mixed oxides

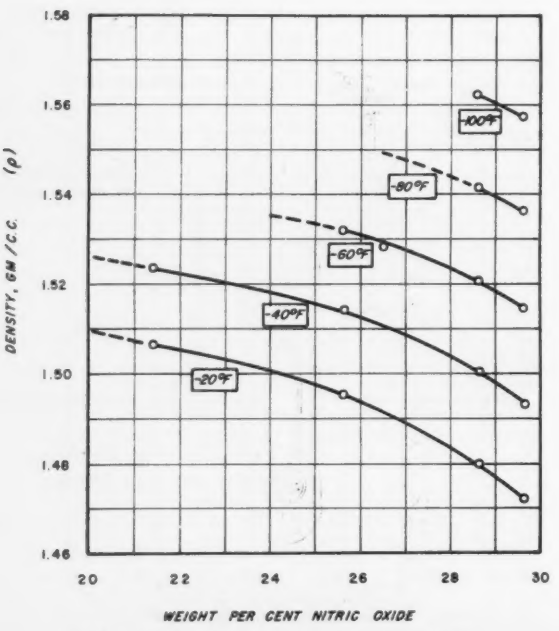

Fig. 6 Isotherms of density for mixed oxides

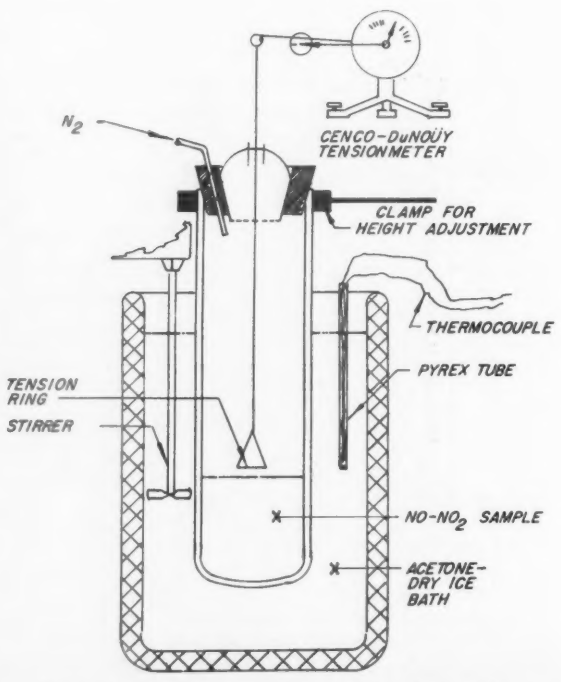

Fig. 8 Apparatus for measurement of surface tension

stability of N_2O_3 decreases, and nitric oxide is released to the status of a solute and can exert increased pressure.

Density

The density of mixed oxides was determined by weighing a glass hydrometer float of known volume and mass while immersed in the sample. As shown in Fig. 4, an acetone-dry ice bath was used to obtain the desired temperature. The apparent weight of the hydrometer was used to calculate the density of the mixed oxides. Determinations, which were made over a range of temperatures from 0 to −100 F and a range of concentrations from 21.4 to 29.6 weight per cent nitric oxide, are shown in Fig. 5. Fig. 6, a crossplot of the data presented in Fig. 5, shows density isotherms.

Viscosity

The viscosities of the mixed oxides were measured with an Ostwald viscosimeter, an instrument used to compare the viscosities of two liquids. If the coefficient of one is known, the coefficient of the other can be determined. This method eliminates the tedious experimental work involved in the direct measurement of viscosity, which requires the determination of the rate of flow of a liquid through a capillary tube of known dimensions. Comparison was made with diethyl ether measured over the same temperature range using viscosity data from the International Critical Tables (4). Fig. 7 shows the viscosity of mixed oxides in centipoises plotted against temperature. It can be seen from these data that the viscosities of mixed oxides vary only slightly with composition between 20 and 30 weight per cent nitric oxide.

Surface Tension

The surface tension determinations were made using a Du Noüy ring tensiometer (Fig. 8) and thermostatting the sample for each measurement at each temperature. The ring was suspended by a platinum wire through a small opening in the cap of the sample flask. Results of the measurements for the four compositions of mixed oxides studied are presented in Fig. 9.

Difficulties in handling contributed to the inconsistency of the surface tension data. No means were provided for mixing of the sample to insure constant surface composition. Also despite precautions taken, atmospheric moisture condensed on the inside wall of the sample flask making visibility poor and causing further uncertainties in the surface composition.

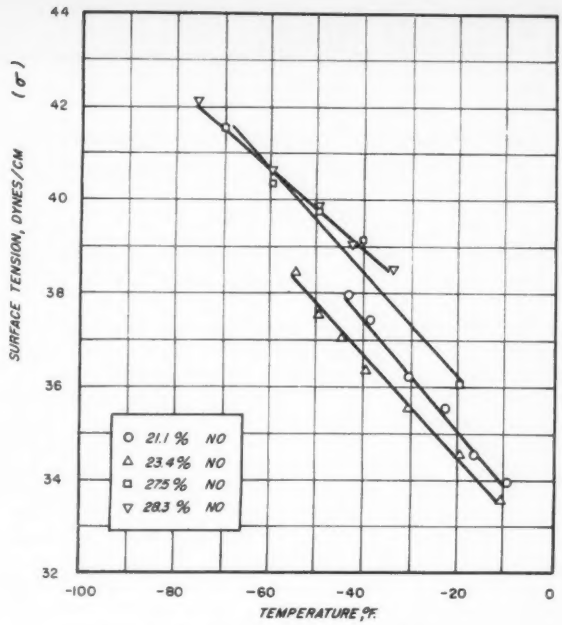

Fig. 9 Surface tension of mixed oxides

References

1 Whittaker, A. G., Sprague, R. W., Skolnik, S. and Smith, G. B. L., "Vapor Pressure and Freezing Points of the System Nitrogen Tetroxide-Nitric Oxide," *J. Amer. Chem. Soc.*, vol. 74, Oct. 1952, pp. 4794–4797.

2 Selleck, F. T., Reamer, H. H. and Sage, B. H., "Volumetric and Phase Behavior of Mixtures of Nitric Oxide and Nitrogen Dioxide," *Ind. and Eng. Chem.*, vol. 45, March 1953, pp. 814–819.

3 Reamer, H. H., Richter, G. N. and Sage, B. H., "Viscosity of Nitric Oxide-Nitrogen Dioxide System in Liquid Phase," *Ind. and Eng. Chem.*, vol. 46, July 1954, pp. 1471–1473

4 "International Critical Tables," vol. V, McGraw-Hill, New York, 1933, p. 11.

ARS PROPELLANT THERMODYNAMICS AND HANDLING CONFERENCE

July 20–21, 1959, Ohio State University, Columbus, Ohio

ROCKET PERFORMANCE CALCULATION TECHNIQUES

HANDLING OF HIGH ENERGY FUELS

PERFORMANCE CALCULATION RESULTS

HANDLING OF FLUORINE

THERMODYNAMIC PROPERTIES OF PROPELLANTS

TRANSPORT PROPERTIES OF PROPELLANTS

Technical Notes

Thermostatic Temperature Control of Satellites and Space Vehicles

R. A. HANEL[1]

U. S. Army Signal Research and Development Laboratory, Fort Monmouth, N. J.

The temperature of satellites and space vehicles varies considerably with orbital conditions. To achieve greater reliability and efficiency in long-life instruments, an automatic temperature control is highly desirable; a radiation thermostat performing this function is discussed. The suggested method regulates temperature by adjusting the effective absorptivity and emissivity. Bimetallic strips automatically move a light shield which exposes surfaces with high and low absorptivitiy-emissivity ratios. No internal power source is needed. Calculations demonstrate the effectiveness of the radiation thermostat. The temperature of the satellite's instruments can be kept constant within a few degrees of the design value, regardless of orbital conditions, internally dissipated power and some erosion of skin coatings.

THE TEMPERATURE of satellites and space vehicles, or of any astronomical body, is determined by the thermal radiation properties of the surface and the amount of internally dissipated power. Absorptivity and emissivity in the visible and infrared region of the spectrum balance the incoming and outgoing radiation; the dissipated power causes a temperature rise until a new equilibrium is reached.

Incoming radiation consists of direct and, when near the Earth or another body, reflected solar radiation; thermal radiation from the Earth, or the moon in case of a moon satellite; and radiation from the stellar background. The amount of outgoing radiation is determined by the emissivity and temperature of the vehicle's surface.

The incoming energy flux is a function of time; it may vary considerably with orbital conditions. Thermal emissivity of the Earth or moon, albedo and the orbit are known or can be predicted with limited accuracy only. These and other uncertainties, such as the aspect ratio for nonspherical bodies, limit the accuracy of thermal calculations. The temperature of an orbiting body can be predicted within a certain range only, and all instruments and circuits have to function properly in this range. For example, Project Vanguard's instrumentation must operate between 0 and 60 C (1).[2]

Satellites with a longer instrument life will have to contend with seasonal changes. An Earth satellite in a near-polar orbit might face the sun 60 per cent of each orbit after launching. Within 2 or 3 months, it will drift into a 100 per cent sun-illuminated orbit. Since even the temperature limits of 0 and 60 C create difficulties for batteries and power transistors, long-life satellites without a temperature control face difficult design problems. Design, construction and test time would be reduced considerably if temperature requirements could be relaxed. Reliability of long-life instruments would certainly improve if the temperature could be adjusted and kept at a predetermined level.

Received July 14, 1958.

[1] Project Scientist.

[2] Numbers in parentheses indicate References at end of paper.

Changing the internally dissipated power is an inefficient way of controlling the temperature; a better method is adjusting absorptivity or emissivity according to the requirements. Coatings which change radiation properties within a rather narrow temperature range centered around 25 C would be ideal, but such coatings are not available. Heat-sensitive paints that change color at certain temperatures have been known for some time and may serve as a starting point for research in this field.

Principle of Radiation Thermostat

The solution presented here uses two coatings with opposite radiation properties. The first one has a high a/e ratio; the Tabor (2) surface with an absorptivity for solar radiation of 0.9 and an emissivity of 0.1 at room temperature is suited for this purpose. The second coating has an extremely low a/e; lead carbonate white paint would be a good choice, since a is about 0.05 and e is 0.95. The Tabor surface would give a high and the white paint a low equilibrium temperature (3). In the recommended configuration, the shell is painted with the two different coatings in a zebra-like fashion.

A perforated hood of highly reflective material can be adjusted so that at times the Tabor surface is completely covered and the white paint determines the heat balance, and at other times the perforated hood covers the white paint and exposes the Tabor surface. The adjustment of the hood is accomplished automatically by a bimetallic strip attached to the instrumentation can or to the shell. If the satellite enters a cooler orbit, the temperature of the can will drop. The bimetallic strips, in good thermal contact with the can, will rotate the perforated hood exposing more of the "black" surface, which in turn leads to more absorption. If it enters a hotter orbit, absorption is reduced. This is an example of negative feedback in a thermomechanical system.

Feasibility of Thermostat

The feasibility of such a thermostat will be demonstrated here by calculating the temperature of an Earth satellite instrumentation similar to the cloud cover experiment of USASRDL (4, 5).[3] However, all calculations and conclusions are applicable to larger, heavier and more sophisticated instruments as well.

In these considerations, a spherical or short cylindrical shell is assumed to be in good thermal contact with the specially coated surfaces, adjustable hood, light baffles for the optic, spin stabilizer, solar batteries, antennas and other devices. The shell encloses the instrumentation can which contains all electronic circuitry, instruments and batteries. In good thermal contact with the can are bimetallic strips and the optics. Shell and can are thermally isolated from each other as much as practicably possible, and they can be treated thermally as two bodies as shown in the energy flow pattern (Fig. 1).

Radiation into the optic and low temperature radiation from the stellar background are small, and in the following considerations are neglected.

Calculation of Energy Flow

The difference between incoming and outgoing energy flux will cause the temperature to rise or fall, depending on which

[3] The cloud cover experiment, scheduled in the IGY Program as Group II on the Vanguard vehicle, will detect and track cloud formations including tropical storms, such as hurricanes and typhoons.

EDITOR'S NOTE: The Technical Notes and Technical Comments sections of ARS JOURNAL are open to short manuscripts describing new developments or offering comments on papers previously published. Such manuscripts are published without editorial review, usually within two months of the date of receipt. Requirements as to style are the same as for regular contributions (see masthead page).

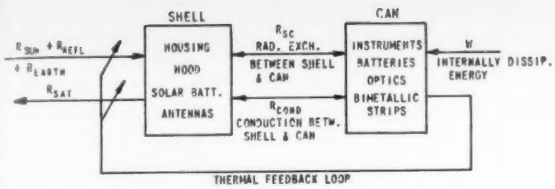

Fig. 1 Energy flow pattern

term preponderates. This is expressed by two equations, one for the shell and one for the can

$$R_{sun} + R_{refl} + R_{Earth} + R_{sc} + R_{cond} - R_{sat} = m_s c_s \frac{dT_s}{dt}$$

$$W - R_{sc} - R_{cond} = m_c c_c \frac{dT_c}{dt} \quad \ldots\ldots [1]$$

If the optic is treated separately, a third equation is required. Each term is analyzed separately

$$R_{sun} = f_1(t) S \frac{1}{4} [a_{s1} A_1 k + a_{s2} A_2 (1 - k) + a_{s3} A_3 + a_{s4} A_4] \quad [2]$$

where $f_1(t)$ is essentially a step function which indicates the amount of time the satellite is in the sun ($f_1 = 1$) and in the shadow ($f_1 = 0$). S is the solar constant: 2cal/min cm^2 = 0.14 watt/cm^2. a_{s1}, a_{s2}, a_{s3} and a_{s4} are the absorption coefficients for solar radiation for 1) the Tabor surface, 2) the white paint, 3) the hood, 4) the rest of the body. A indicates the corresponding areas and k the position of the hood in relation to the black and white strips; k will be made a function of can temperature T_c by the bimetallic strips. The factor $\frac{1}{4}$ expresses the ratio between the cross section of a sphere and its total area.

$$R_{refl} = \frac{\Omega}{4\pi} f_2(t)\, S \mathrm{Alb} [a_{s1} A_1 k + a_{s2} A_2 (1 - k) + a_{s3} A_3 + a_{s4} A_4] \quad [3]$$

Ω is the solid angle under which the Earth appears. It varies with altitude. The function $f_2(t)$ can be approximated by a halfwave rectified cosine function. Its exact value depends on altitude and orbital conditions. Alb is the average albedo of our planet. It can vary between 0.2 and 0.5 depending on cloud cover and geographical latitude. A good average value is 0.35.

$$R_{Earth} = \frac{\Omega}{4\pi} \sigma T_e^4 [a_{l1} A_1 k + a_{l2} A_2 (1 - k) + a_{l3} A_3 + a_{l4} A_4] \quad [4]$$

Thermal radiation of the Earth is on the average equivalent to the radiation of a black body of 250 to 260 K; σ is the Stefan-Boltzmann radiation constant: 5.67×10^{-12} watts per cm^2 deg^4. a_l indicates the long wave absorptivity and emissivity values which correspond to a_s as explained under Equation [2].

$$R_{sc} = a_{sc} A_c \sigma (T_c^4 - T_s^4) \quad [5]$$

Radiation between shell and can be determined by the area of the can, thermal emissivity and absorptivity of the inside of the shell and the outside of the can, and the difference of the fourth powers of the corresponding temperatures.

$$R_{cond} = \rho (T_c - T_s) \quad [6]$$

Energy flux due to conductivity in construction elements between can and shell is proportional to the temperature difference. The factor ρ expresses specific conductivity of support materials and geometric factors. In general this term can be kept smaller than R_{sc}, the previous term.

$$R_{sat} = \sigma T_s^4 [a_{l1} A_1 k + a_{l2} A_2 (1 - k) + a_{l2} A_3 + a_{l4} A_4] \quad [7]$$

Reradiation of the satellite is determined by shell temperature T_s and long wave emissivity. The terms $m_s c_s (dT_s/dt)$, $m_c c_c (dT_c/dt)$ represent the thermal energy which is used to heat the shell and can. m_s, m_c represent mass of shell and can, respectively; c_s, c_c are the specific heats, and (dT_s/dt), (dT_c/dt) are temperature changes per time unit. W is the internally dissipated electrical power. In general, W is also a function of time. However, for this calculation a constant average value is assumed. Introducing these values, two equations are obtained:

Shell

$$\left(\frac{1}{4} f_1 + f_2 \frac{\Omega}{4\pi} \mathrm{Alb}\right) S [a_{s1} A_1 k + a_{s2} A_2 (1 - k) + a_{s3} A_3 + a_{s4} A_4] + \sigma \left(\frac{\Omega}{4\pi} T_e^4 - T_s^4\right) [a_{l1} A_1 k + a_{l2} A_2 (1 - k) + a_{l3} A_3 + a_{l4} A_4] + \sigma a_{sc} A_c (T_c^4 - T_s^4) + \rho (T_c - T_s) = m_s c_s \frac{dT_s}{dt} \quad [8]$$

Can

$$-\sigma a_{sc} A_c (T_c^4 - T_s^4) - \rho (T_c - T_s) + W = m_c c_c \frac{dT_c}{dt}$$

This set of nonlinear nonhomogeneous simultaneous differential equations for T_s and T_c is not solvable in closed form.

However it can be expected that the can temperature will fluctuate around an equilibrium value. Exponentially decreasing terms will satisfy initial conditions. If we assume that the initial temperature at launching T_0 is the desired equilibrium temperature, the exponential terms will become zero, and the can temperature is completely described by equilibrium temperature T_0 and a periodic time-dependent function $T_1(t)$

$$T_c = T_0 + T_1(t) \quad [9]$$

Similarly the shell temperature is

$$T_s = T_0 - \Delta T + T_2(t)$$

where ΔT represents the average temperature difference between can and shell. The fourth-power terms of T_c and T_s will be expanded in a Taylor series and only the linear term taken into account. This is justified, since ΔT and the fluctuating terms T_1 and T_2 are expected to be small with respect to the absolute temperature level T_0

$$T_0 \gg |\Delta T|; |T_1|; |T_2|$$

$$T_c^4(t) \approx T_0^4 + 4 T_0^3 T_1(t)$$

$$T_s^4(t) \approx T_0^4 + 4 T_0^3 [-\Delta T + T_2(t)] \quad \ldots\ldots [10]$$

Introducing these values, the equations become linear in the time-dependent terms, and separation of fluctuating and nonfluctuating parts is possible. For the can

$$-[\rho + a_{sc} A_c \sigma 4 T_0^3] \Delta T + W = 0$$

$$-[\rho + a_{sc} A_c \sigma 4 T_0^3] [T_1(t) - T_2(t)] = m_s C_s \frac{dT_1}{dt} \quad \ldots\ldots [11]$$

The time-independent equation gives the average temperature difference

$$\Delta T = \frac{W}{\rho + a_{sc} A_c \sigma 4 T_0^3} \quad [12]$$

The ΔT varies between a few degrees and 10 to 15 C, depending on the dissipated power and isolation achievable. A normal value of 5 C may be assumed.

Temperature Fluctuations of Can

Temperature fluctuations of the can T_1 may be calculated as a function of fluctuations in the shell T_2 by expanding each term in a Fourier series. Thus

$$T_2 = \sum_n \alpha_n e^{inwt} \qquad T_1 = \sum_n \beta_n e^{inwt} \qquad [13]$$

Introducing this in Equation [11] yields

$$\beta_n = \alpha_n \frac{1}{1 - (inwm_cc_c/a_{sc}A_c\sigma 4T_0^3 + \rho)}$$

which can be approximated by

$$\beta_n = \alpha_n \frac{a_{sc}A_c\sigma 4T_0^3 + \rho}{inwm_cc_c}$$

Therefore

$$T_1 = -i\frac{a_{sc}A_c\sigma 4T_0^3 + \rho}{wm_cC_c} \sum_n \frac{\alpha_n}{n} e^{inwt} \qquad [14]$$

In practice, temperature fluctuations of the can could be kept below 1 per cent of the shell's fluctuations. The can's fluctuations lag approximately 90 deg behind the shell's.

Calculation of Average Temperature

Following the same procedure, the time-independent equation for the shell is

$$\left(\frac{1}{4}\bar{f}_1 + \bar{f}_2\frac{\Omega}{4\pi}\text{Alb}\right)S[a_{s1}A_1k + a_{s2}A_2(1-k) + a_{s3}A_3 + a_{s4}A_4] +$$
$$\sigma\left(\frac{\Omega}{4\pi}T_e^4 - T_0^4 + 4T_0^3\Delta T\right)$$
$$[a_{l1}A_1k + a_{l2}A_2(1-k) + a_{l3}A_3 + a_{l4}A_4] + W = 0 \qquad [15]$$

The bar on f_1 and f_2 indicates average values.

In order to demonstrate the stabilizing action of the system numerically, let us assume the numerical values: A = total surface area of satellite

$a_{s1} = 0.9$	$a_{l1} = 0.1$	$A_1 = 0.25A$	Tabor surface
$a_{s2} = 0.05$	$a_{l2} = 0.95$	$A_2 = 0.25A$	white paint
$a_{s3} = 0.15$	$a_{l3} = 0.12$	$A_3 = 0.25A$	polished metal hood
$a_{s4} = 0.6$	$a_{l4} = 0.418$	$A_4 = 0.5A$	solar batteries and rest of housing

Absorptivity and emissivity for the rest of the housing (a_{s4} and a_{l4}) are chosen so that, for an average orbit, k becomes approximately 0.5, which is the center of the regulation range. This condition can be achieved easily by proper coating of areas between solar cells. The term

$$\left(\frac{1}{4}\bar{f}_1 + \bar{f}_2\frac{\Omega}{4\pi}\text{Alb}\right)S = \bar{Z}$$

which is mainly responsible for the incoming radiation is the most uncertain one. The $\bar{Z}$ may vary from 0.021 for a "cold" orbit (60 per cent sun, low albedo), to 0.04 for a "hot" orbit (100 per cent sun, high albedo).

Solving for the average can temperature T_0

$$T_0 = \Delta T + \left\{\frac{\Omega}{4\pi}T_e^4 + \frac{W}{\sigma A[a_{li}A_if_i(k)]} + \frac{\bar{Z}}{\sigma}\frac{[a_{si}A_if_i(k)]}{[a_{li}A_if_i(k)]}\right\}^{1/4} \qquad [16]$$

In Fig. 2, T_0 is plotted as a function of $\bar{Z}$, showing k as a parameter. In the numerical calculation T_e was assumed to be constant and equal to 255 K. ΔT has been taken equal to 5 C, W = 1 watt, and A = 8000 cm², equivalent to the surface of a 20-in. sphere. Coldest and hottest orbits are indicated in the figure.

Design limits, however, have to reach farther in order to cover uncertainties in numerical assumptions, tolerances in the effect of surface coatings, aging, and other possible changes

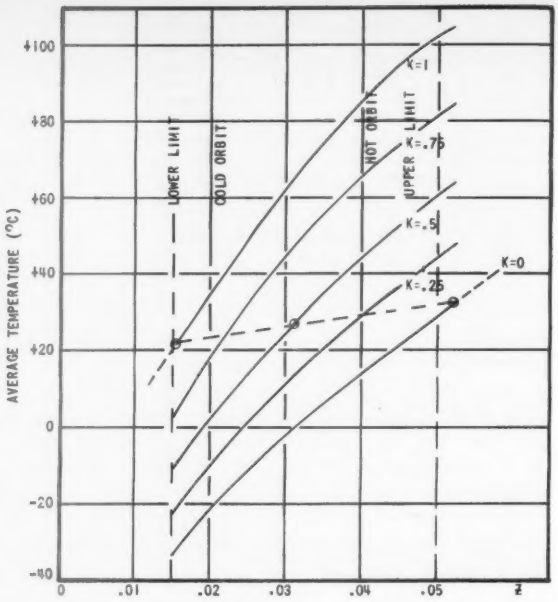

Fig. 2 Temperature as a function of incoming radiation for several values of k. Dashed line shows regulation of thermostat

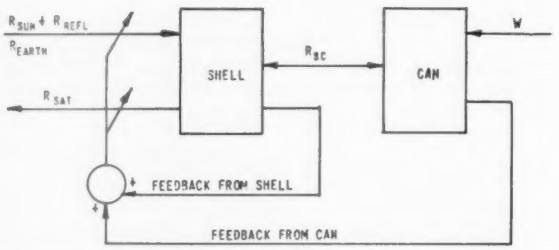

Fig. 3 Energy flow pattern with fast acting feedback loop from shell

of emissivity and absorptivity that may occur due to erosion in orbit. Design limits equivalent to $\bar{Z}$ = 0.015 and 0.05 have been chosen arbitrarily.

Thermal Feedback

In a satellite without a temperature control where k is constant, it can be seen from Fig. 2 that the can temperature can vary 60 C. By making k a function of temperature, this range is reduced. Let k become

$$k = 0.5 + 0.1(300 - T_0) \qquad [17]$$

a condition easily achievable by selecting proper bimetallic strips. The adjustable hood is rotated from one extreme position (k = 0) to the other one (k = 1) within a temperature range of 10 C. This is shown in Fig. 2 by a dashed line which also indicates the can temperature for all orbital conditions.

Regardless of how "cold" or "hot" an orbit may turn out to be, all sensitive instruments will stabilize within ±5 C of the design temperature. If necessary, this range could be

further reduced by increasing the sensitivity of the bimetallic strips.

Temperature Fluctuation of Shell

Temperature fluctuations of the shell can be determined by solving the time-dependent part of Equation [8]

$$\left(\frac{1}{4} f_1 + f_2 \frac{\Omega}{4\pi} \text{Alb}\right) S[a_{si}A_i f_i(k)] - 4\sigma T_0^3 [a_{li}A_i f_i(k)] T_2(t) - (\sigma a_{sc} A_c 4 T_0^3 + \rho) T_2(t) = m_s c_s \frac{dT_s(t)}{dt} \quad [18]$$

or

$$Z[a_{si}A_i f_i(k)] - \left\{4\sigma T_0^3 [a_{li}A_i f_i(k)] + \frac{W}{\Delta T}\right\} T_2 = m_s c_s \frac{dT_2}{dt}$$

In f_1 and f_2, only the fluctuating components will be taken.

The temperature fluctuations of the can T_1 are neglected, since $|T_1| \ll |T_2|$. Expanding Z and T_2 in a Fourier series again

$$Z = \sum_n \gamma_n e^{inwt} \qquad T_2 = \sum_n \alpha_n e^{inwt}$$

$$\alpha_n = \gamma_n \frac{[a_{si}A_i f_i(k)]}{inwm_s c_s + \left[4\sigma T_0^3 a_{li}A_i f_i(k) + \frac{W}{\Delta T}\right]} \quad [19]$$

Assuming reasonable numerical values, calculations show temperature fluctuations of the shell on the order of 20 to 50 C.

These fluctuations are not influenced appreciably by the feedback loop, since fluctuations of the can are only a fraction of the fluctuation of the shell, and therefore k will be practically constant in the time interval of one orbit.

However, shell fluctuations could be reduced if necessary by a fast acting feedback path from the shell to the incoming radiation, as shown in Fig. 3.

Conclusion

The actual construction and geometry of a temperature regulated satellite depends, of course, on the particular purpose and mission of the instruments incorporated in the satellite, but the control of its temperature, as outlined above, should not be too difficult a problem with any satellite shape.

Acknowledgment

The author wishes to thank Dr. H. J. Merrill and W. G. Stroud for their constant encouragement, M. Schach from U. S. Naval Research Laboratory for many helpful discussions, and E. Rich for the construction of a demonstration model.

References

1 Drummeter, L. and Schach, M., "Satellite Temperature Control," presented at IGY Conference Oct. 1957, National Academy of Sciences, Washington, D. C.; *see also* Gast, P. R., "Isolation of the Upper Atmosphere and of a Satellite," in "Scientific Uses of Earth Satellites," J. A. Van Allen, Ed., University of Michigan Press, Ann Arbor, 1956.

2 Tabor, H., "Selective Radiation, Wave Length Discrimination and Wave Front Discrimination," Bulletin Research Council of Israel, A. Met, Phys, and Chem., 5A2, 1956, pp. 119–134.

3 Suomi, V. E., "University of Wisconsin Proposal for Measuring Energy Budget of the Earth from an Earth Satellite," National Science Foundation, U. S. National Committee International Geophysical Year Project 30.11.

4 Stroud, W. G. and Nordberg, W., "Meteorological Measurements from an Earth Satellite Vehicle," chap. 13 in "Scientific Uses of Earth Satellites," J. A. Van Allen, Ed., University of Michigan Press, Ann Arbor, 1956.

5 Hanel, R. and Stampfl, R., "An Earth Satellite Instrumentation for Cloud Measurements," presented at IRE Symposium, New York, March 25, 1958.

6 Wilson, Raymond H., Jr., "Temperature of a Close Earth Satellite Due to Solar and Terrestrial Heating," presented at Infrared Information Symposium, Boston, Sept. 1958.

7 Hass, Georg H. and Drummeter, Louis F., Jr., "Temperature Stabilization of Vanguard Satellites—Theory and Practice," presented at Infrared Information Symposium, Boston, Sept. 1958.

Use of a Catalytic Probe for Detection of Dissociated Nonequilibrium States in Hypersonic Flow

STUART A. HOENIG[1]

University of California, Berkeley, Calif.

It is shown that a wheatstone bridge with one catalytic and one noncatalytic arm can be used as a sensitive detector for dissociation in hypersonic flow.

A NUMBER of authors have discussed the design and operation of hypersonic wind tunnels (1 to 3).[2] These devices may be driven by a shock tube, an electric arc or a plasma jet, but they have one common feature. The working fluid, generally air, is heated to almost 10^4 K and allowed to expand through a diverging nozzle to produce a high Mach number flow.

The question of attainment of thermochemical equilibrium in the downstream test section region of such tunnels has been seriously questioned by Bray (4). Experiments by Wegner and his group (5) have indicated that for a special gas mixture ($N_2 + N_2O_4$), the flow in a supersonic nozzle may have an appreciable frozen component.

It is the purpose of this paper to suggest a new technique for detection of frozen dissociated flow in hypersonic wind tunnels.

The instrument consists of a wheatstone bridge, two opposite arms of which are platinum wires 0.00254 cm in diameter. One wire is rendered almost 100 per cent noncatalytic by an application of silicon monoxide (6), while the other wire remains uncovered.

The use of platinum for wires is convenient for several reasons. The wire is available in many diameters down to 0.00254 cm, from the Sigmund Cohn Corp. of Mount Vernon, N. Y. The temperature-resistance coefficient is effectively constant up to 1000 K; the wire is easily fabricated by soldering, and platinum is an excellent catalyst for most reactions.

When wire of the smallest diameter is used, it is generally possible to operate the detector in the free molecule flow regime. In this case, no shock wave is formed on the probe, and the mass flux may be simply computed in terms of the density, flow velocity and projected area of the probe.

When the two platinum wires are suddenly exposed to a flow containing a component, such as atomic oxygen which recombines on the uncoated wire surface, the resistances of the two arms will change to a different degree due to the difference in the heat inputs.

We can gain some idea of the sensitivity of the instrument by considering the minimum detectable unbalance to be 50×10^{-6} v. Now we draw the usual bridge circuit as shown in Fig. 1, where A and B are the platinum wires, and C represents a fixed resistor.

The voltage drop in arms A and B are

$$V_A = \frac{A}{A + C} V_1 \qquad V_B = \frac{B}{B + C} V_1$$

Their difference is the voltage detected ΔV. Hence

$$\Delta V = V_1 \left[\frac{A}{A + C} - \frac{B}{B + C}\right] \quad [1]$$

To obtain a first order result, take $C = A$ and $B = A + \delta$, then Equation [1] reduces to

$$\Delta V = \frac{1}{2} \left(\frac{\delta}{2A + \delta}\right)$$

Received Dec. 22, 1958.

[1] Graduate Research Engineer, Low Pressures Research.

[2] Numbers in parentheses indicate References at end of paper.

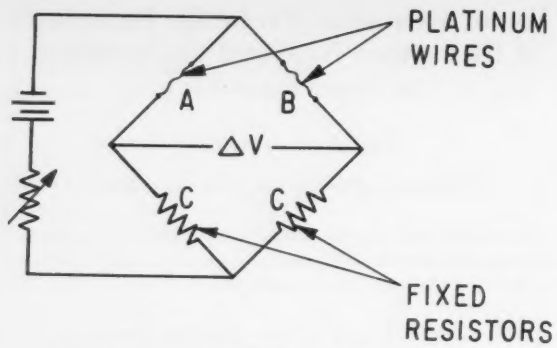

Fig. 1 Wheatstone bridge for catalytic detection probe

An unbalance of $\Delta V = 50 \times 10^{-6}$ v for a value of $A = 10$ ohms, $V_1 = 10$ v gives a difference in resistance between A and B of $\Delta R \sim 2 \times 10^{-4}$ ohms.

The resistance-temperature coefficient of platinum wire is 0.003 ohms per deg C, which indicates that a temperature difference of $\Delta T = 6.66 \times 10^{-2}$ C is the minimum detectable value. We can now calculate how much differential heat input this represents.

We shall write the first law of thermodynamics in the form

$$Q = C_p m \Delta T \qquad [2]$$

where C_p and m refer to the platinum wire, nominally chosen as 1-cm long. Using Equation [2], we see that this temperature difference represents a differential heat input of 2.5×10^{-7} cal. The heat of formation of 1 mole of oxygen is 1.18×10^5 cal, hence, the above heat input represents the formation of 1.27×10^{12} oxygen molecules.

All measurements in hypersonic wind tunnels are of a transient nature, and we can consider an appropriate measurement time to be, say, 100 μsec. This is about 1 per cent of the usual running time, and is a sufficiently short interval so that conduction to the wire supports may be ignored and radial temperature gradients in the wires may be neglected (7).

The detectable number of oxygen molecule formations is therefore 1.27×10^{16} oxygen molecules/sec, which represents a heat input of 2.44×10^{-3} cal/sec.

We shall assume that every oxygen atom that strikes the bare platinum wire recombines, while no recombination occurs on the coated wire. Present experiments indicate that this is a good approximation to the actual situation, and it allows a simple estimate of instrument sensitivity.

Let us consider the use of a device of this type in a more or less typical hypersonic wind tunnel, i.e., that operated by Perry at Tullahoma, Tenn. (8).

The operating fluid is air, which is heated by an arc discharge and then allowed to flow through a diverging nozzle. Typical stagnation conditions are: $T_0 = 6000$ K, $P_0 = 1155$ atm. Under these conditions, the fraction of oxygen dissociated may be obtained from (9), and is found to be approximately 51.4 per cent even after the effect of pressure has been accounted for.

Conditions in the test section at $M = 16$ are: $V = 4.27 \times 10^5$ cm/sec, $T = 180$ K, $P = 1.8 \times 10^{-4}$ atm, as taken from (8). Under these conditions, the mean free path will be approximately 2.75×10^{-2} cm. Hence, a wire 2.54×10^{-3} cm in diameter will satisfy the conditions for free molecule flow, $(\lambda/\alpha) > 10$. In free molecule flow, no shock wave will appear on the wire, and we can calculate the number flux hitting the wire from $N = nVA$, where n is the number of particles per cm^3, V is the flow velocity, and A the projected wire area. The value of n is $n = 8.2 \times 10^{15}$ molecules/cm^3, and therefore N is 140×10^{17} molecules/sec. Of this flux, 80 per cent may be considered inert, leaving a flux of oxygen molecules 2.80×10^{18} sec^{-1}. If the initial dissociation fraction of $\sim$50 per cent is unchanged, as might be expected from the work of Bray (4), we would have roughly 1.4×10^{18} molecules formed per sec on the catalytic wire, or about 100 times the minimum detectable fraction, calculated previously. This indicates that even a dissociated fraction as low as 1 per cent in the free stream might be detected, hence the enormous sensitivity of this simple device.

We have assumed that the heat input from recombination can be separated from that due to convection. This involves essentially the assumption that the heat inputs are at least of similar orders of magnitude.

The data on heat transfer that Perry presented was for models so large that continuum conditions prevailed. In order to estimate free molecule heat transfer at $M = 16$, we shall extrapolate Perry's data (8) down to free molecule flow conditions, and extrapolate the data of Eberly and Wong (10, 11) on free molecular flow upward to $M = 16$ for comparison.

Perry's data yields $(Nu/\sqrt{Re}) = 0.30$, which at a Reynolds number of 3.33 gives $Nu = 0.547$. This represents heat transfer at the stagnation point, and for an average Nusselt number we should divide by about 2, giving $Nu = 0.273$. Eberly presents data for free molecular heat transfer to spheres which, when extrapolated to $M = 16$, $Re = 3.33$, give an average Nusselt number of 0.300. The data of Wong for cylinders at Mach numbers from 3 to 5 yield an average value of $Nu = 0.300$. Under the circumstances, we are justified in taking an average value of $Nu = 0.290$ for the free molecule flow in the hypersonic tunnel.

The heat transfer coefficient is therefore $6.1 \times 10^{-3} \times$ cal/cm^2 sec C, and the heat input from convection may be taken from $q = hA\Delta T$, where ΔT is based on the initial difference between stagnation and wire temperatures. (The increase in equilibrium wire temperature over stagnation temperature can be ignored in this instance since the Knudsen number is only about 7.3, and we seek only order-of-magnitude results.)

Under these assumptions, the convective heat input is $q = 0.296$ cal/sec; now previously we derived the minimum detectable heat input to the catalytic wire from recombination to be 2.44×10^{-3} cal/sec. Hence, under the worst conditions the heat input from recombination is 1 per cent of the convective heat input, and under the most favorable conditions it is of the same order of magnitude.

It is important to note that the use of a wheatstone bridge in this application removes almost all the effect of convective heating. Under these circumstances, even an atomic oxygen content of 1 per cent should be easily detectable.

We have considered only the oxygen atom content of the flow. If the working fluid is air, the products of the discharge will include many more unstable species. Since there is very little information about the recombination of such species on catalytic surfaces, they have been ignored in this analysis. No doubt their presence will result in a somewhat increased sensitivity for the detector discussed above.

Conclusion

A device has been described which can be used for detection of nonequilibrium dissociated flow in hypersonic wind tunnels.

References

1 Hertzberg, A., "The Shock Tunnel and Its Applications to Hypersonic Flight," Cornell Aero. Lab. Rep. AD-1052-A-5, AFOSR TN 57-268, June 1957.

2 Hertzberg, A., "The Application of the Shock Tube to the Study of the Problems of Hypersonic Flight," Jet Propulsion, July 1956, p. 549.

3 Hufton, P. A., "Hypersonic Facilities in the Aerodynamics Department," Royal Aircraft Establishment, AGARD Rep. 146, 1957.

4 Bray, K. N. C., "Departure from Dissociation Equilibrium in a Hypersonic Nozzle," Aero. Research Council Rep. 19-983, March 1958, NACA N-61403.

5 Wegner, P., Marte, J. and Thiele, C., "Study of Supersonic Flows With Chemical Reactions. Measurements of Rate Constants of the Reac-

tion $N_2 + N_2O_4$ & $N_2 + 2NO_2$ at Low Reactant Concentration," JPL Progress Rep. no. 20-249, June 1958.
6 Hertzberg, A., private communication.
7 Hoenig, S. A., "Use of a Constant Current Hot Wire for the Measurement of Extreme Temperatures," *Rev. Sci. Instr.*, vol. 29, no. 8, Aug. 1958, pp. 704–705.
8 Perry, R. W. and MacDermott, W. N., "Development of the Spark-Heated Hypervelocity, Blowdown Tunnel—Hotshot," AEDC-TR-58-6, AD 157 138, June 1958.
9 Huff, V., Gordon, S. and Morrell, V., "General Method and Thermodynamic Tables for Computation of Equilibrium Composition and Temperature of Chemical Reactions," NACA Rep. 1037, 1951.
10 Eberly, D. K., "Forced Convection Heat Transfer from Spheres to a Rarefied Gas," Univ. of Calif. Eng. Proj. Rep. HE-150-140, July 1956.
11 Wong, H., "Design and Development of a Free-Molecule Heat Transfer Probe," Univ. of Calif. Eng. Proj. Rep. HE-150-143, Oct. 1956.

Velocity of Tank Fragments

SAUNDERS B. KRAMER[1]

Lockheed Aircraft Corp., Sunnyvale, Calif.

An investigation was carried out to determine the positions as functions of time of the sections of an exploded tank in the upper atmosphere idealized as a 6-ft diameter sphere, since the geometry involved afforded a desirable distribution of the fragments and permitted immediate derivation of descriptive equations. The sphere was pressurized using helium, and was considered to have primacord over its surface so that upon detonation a spherical scattering of fragments would occur. To simplify calculations it was supposed that 10 such fragments of equal mass and size were generated in a given detonation.

Analysis for Spherical Case

EXAMINATION of the thermodynamics of this problem leads to an equation which relates the rate of change of internal energy in the compartment to the rate of energy flow through the gap formed by the separating bodies. The ideal gas laws are assumed to apply here; thus we have

$$\frac{d}{dt}(U) = -wh \qquad [1]$$

where

U = total internal energy at any instant
w = mass flow rate
h = enthalpy (heat content) per unit mass of the gas in the compartment

Now

$$U = mu \qquad [2]$$

where

u = the internal energy per unit mass of the gas (helium) contained in the compartment
m = mass of gas in the compartment

If the gas flow is assumed to be choked (i.e., a critical pressure ratio is reached or exceeded—and this is true since the pressure outside the compartment is practically zero), we have

$$w = 0.2096\frac{PA}{\sqrt{T}} \qquad [3]$$

where

A = area through which gas flows
P = value of the total pressure at any time in the compartment
T = value of the temperature in the compartment (in deg R) at any time

Substituting Equations [2 and 3] in [1], we have

$$\frac{d}{dt}(mu) = -\frac{0.2096PA\,h}{\sqrt{T}} \qquad [4]$$

Since we have assumed the gas to be ideal

$$u = C_vT$$

$$h = C_pT$$

where C_v, C_p are the specific heats (and are constant).

The gap area through which the originally enclosed gas escapes is formed as the spherical surface separates along the primacord boundaries. If the original surface is $4\pi R_0^2$ and some increase in radius takes place at an incremental time after detonation, then the area through which the enclosed helium escapes is

$$4\pi(R^2 - R_0^2) = A_{(\text{escape})} \qquad [5]$$

This may be written as

$$4\pi(R - R_0)(R + R_0) = A_{(\text{escape})} \qquad [5a]$$

If we call the increase in radius X, the space coordinate, Equation [5a], may be described by

$$4\pi(X)(X + 2R_0) = A_{(\text{escape})} \qquad [5b]$$

Equation [4] then becomes

$$\frac{d}{dt}(mT) = -\gamma(0.2096)\sqrt{T}\,4\pi X(X + 2R_0)P \qquad [6]$$

where

$$\gamma = \frac{C_p}{C_v} = \frac{5}{3} \text{ for helium}$$

Equation [6] relates the rate of change of internal energy within the sphere to the rate of energy flow through the gap formed by the separating bodies.

The equation relating the acceleration of the fragments follows: Suppose we have 10 fragments of equal mass and equal area, then each fragment receives $\frac{1}{10}$ of the pressure-derived force acting. The equation for the acceleration of each fragment is

$$\left(\frac{4\pi R_0^2}{10}\right)P\left(\frac{1}{m_1}\right) = \ddot{X} \qquad [7]$$

where m_1 is the mass of one fragment.

From the equation of state for an ideal gas

$$PV = mRT \text{ (at any time)} \qquad [8]$$

so that, since R is constant, and assuming the volume contained in the spherical boundary is approximately constant during the time the pressure goes to, say, 10 per cent of its initial value, we have

$$\frac{P}{P_0} = \frac{m}{m_0} = \frac{T}{T_0} \qquad [9]$$

where P, T and m are pressure, temperature and mass of the gas at any time, and P_0, T_0 and m_0 are their values at $t = 0$. Substituting in Equation [6] we have

$$\frac{d}{dt}(mT) = -\gamma(0.2096)\sqrt{T}\,\frac{4\pi X(X + 2R_0)}{m_0T_0}P_0mT \qquad [10]$$

If we use Equation [9] and the relationship

$$\frac{m}{m_0} = \left(\frac{P}{P_0}\right)^{1/\gamma} \qquad [11]$$

Received Jan. 13, 1959.
[1] Senior Scientist, Spacecraft Design.

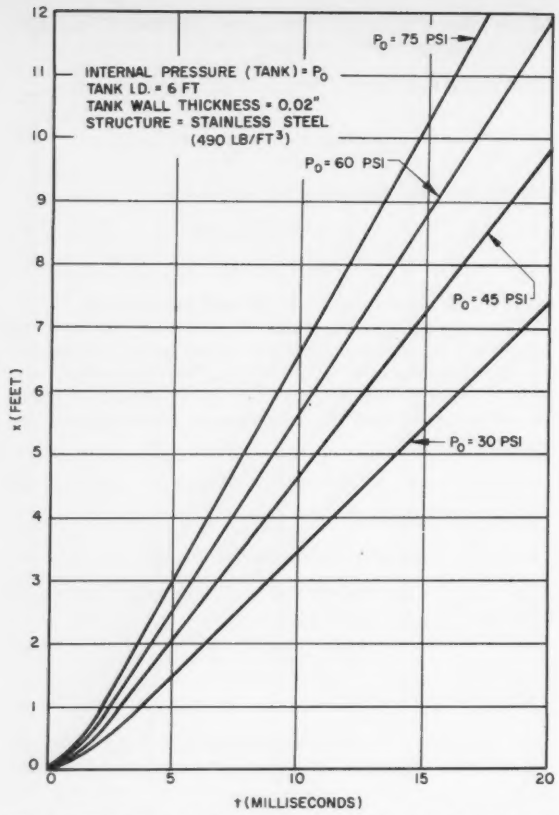

Fig. 1 Movement of fragments of exploded spherical tank vs. time

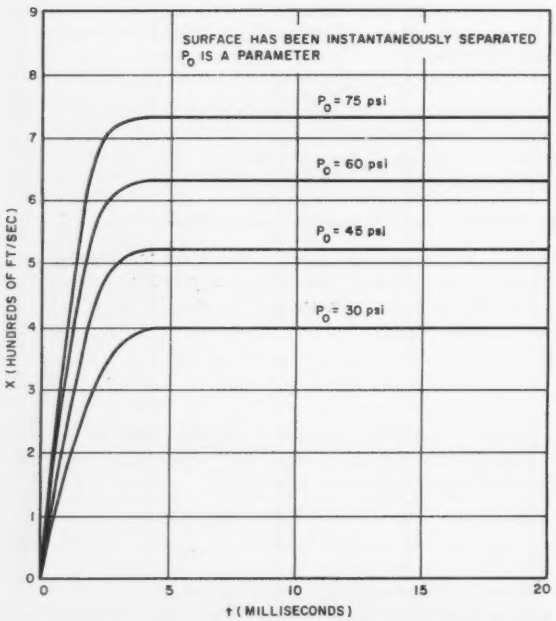

Fig. 2 Velocity attained vs. time for fragments of an initially pressurized spherical tank

the result

$$T = \frac{m^{\gamma-1}}{m_0{}^{\gamma-1}}\, T_0 \qquad [12]$$

is obtained.

Let

$$\frac{T_0}{m_0{}^{\gamma-1}} = K_2{}^{-\gamma} \qquad [13]$$

so that

$$T = \frac{m^{\gamma-1}}{K_2{}^{\gamma}}$$

Substituting Equation [13] into [10], and [9 and 13] into [7], the results are, respectively

$$\frac{d}{dt}\,(m^{\gamma}) = \frac{-K_1 X}{K_3{}^{\gamma/2}}\,(X + 2R_0)m^{(3\gamma-1)/2} \qquad [14]$$

and

$$\ddot{X} = \frac{K_2}{K_3{}^{\gamma}}\, m^{\gamma} \qquad [15]$$

If we now solve Equation [15] for m^{γ}, substitute the result into Equation [14] and differentiate as indicated, we have

$$\frac{K_2{}^{(\gamma-1)/2}\gamma K_3{}^{1/2}}{K_1}\,(\dddot{X}) = -X(X + 2R_0)\ddot{X}^{(3\gamma-1)/2\gamma} \qquad [16]$$

We shall call the lead constant of Equation [16] C_0 and recall that for helium $\gamma = 1.66 \sim 5/3$, so that we now have

$$C_0\dddot{X} = -X(X + 2R_0)\ddot{X}^{6/5} \qquad [17]$$

The initial conditions are

$$X = \dot{X} = 0 \quad \text{at} \quad t = 0$$

$$\ddot{X} = \ddot{X}_{\max} = K \quad \text{at} \quad t = 0 \qquad [18]$$

This problem is solved for a chosen value of m_1, the fragment mass, and for various values of P_0, the initial pressure in the sphere. Changes in P_0 give rise to variations in m_0, the initial weight of gas contained in the sphere.

To obtain Fig. 1, the sphere has been chosen as 0.02-in. thick (the radius is then 3.00167 ft) and of stainless steel; hence the value ascertained for m_1 is 9.225 lb mass.

Equation [17], because of its very nonlinear nature, could not be handled by any standard analytical techniques (other than numerical analysis), and was therefore solved using the 1103A computer.

Discussion and Conclusions

Figs. 1 and 2 describe the results obtained. Here, the positions attained by the fragments and the velocity of the fragments as a function of time are shown for the exploded spherical tank. These results should be examined with at least the following qualifications:

1 Movement and position have been considered for a field-free space, i.e., with no forces acting after final velocity is attained.

2 Velocity values noted are higher than would be the actual case since boundary separation by primacord would leave a gap through which a considerable portion of gas would escape, thus lowering the final velocity of the fragments.

3 Numerical results show that the volume enclosing the gas is not constant during the time the pressure goes to 10 per cent of its initial value; at present, the error thereby introduced is not known.

4 Fragment scattering will not be entirely symmetrical, since a certain amount of tumbling will occur, yielding then a somewhat indeterminate distribution.

Burning Rate of an H-Atom Propellant[1]

HOWARD B. PALMER[2]

College of Mineral Industries, The Pennsylvania State University, University Park, Pa.

THE RECENT success of Windsor (1)[3] in trapping pure H atoms as a solid prompts added interest in the possibility of using H-atom recombination for propulsion. For this reason, an attempt to calculate a priori the one-dimensional burning rate of an H-atom propellant seems worthwhile. The kinetics are about as simple as one could hope to find for a propellant, being those for atom recombination, and the physical properties of the system can be calculated rather well. In treating the flame problem, one has the advantages that there is no need for concern regarding an ignition temperature—it will be the initial temperature of the gas—and that the chemical reaction has zero activation energy. Our physical picture is that the propellant consists of H atoms in a matrix, which we take to be solid H_2. The upper limit of H-atom concentration in the matrix is taken to be about 10 per cent, following the theoretical work of Golden (2).

The propellant is envisioned as being held at 4 K, with vaporization at its boiling point at a rate determined by the heat flux from the reaction zone. It is assumed that no combination of H to form H_2 takes place prior to vaporization, so that we need deal only with a gaseous reaction. Although this assumption cannot be exact, it is thought not to introduce serious error, since for recombination in the liquid phase it is necessary for H atoms to diffuse over a distance of a few molecular diameters, and the time required for this is long (as will be seen) compared to the time necessary for heating to the vaporization temperature. A second assumption that appears justifiable ex post facto is that the extraction of heat from the flame by the vaporizing liquid has no effect upon the temperature gradient in the gas adjacent to the surface. If, in addition, we assume constant pressure reaction conditions and no diffusion, then the gas reaction can be handled as though it were a reaction in a static system at constant pressure, and the temperature can be calculated as a function of time. The temperature gradient at the surface will correspond to the initial rate of change of gas temperature.

For the reaction, $2\ H + M \xrightarrow{k_1} H_2 + M$, the rate constant k_1 is about 10^{16} cc^2/mole^2 sec, almost independent of temperature (3), so that

$$-dC_H/dt \doteq 10^{16} C_H{}^2 C_M \qquad [1]$$

where the assumption is made that any M (H or H_2) has the same efficiency in promoting H-atom combination.

The rate of change of temperature is

$$dT/dt = -(dC_H/dt)(\Delta H_r/2)/(\tilde{C}_p{}^{H_2} C_{H_2} + \tilde{C}_p{}^{H} C_H) \qquad [2]$$

where ΔH_r is the heat of reaction, and $\tilde{C}_p$ is molar heat capacity at constant pressure. The initial value of dT/dt, converted to a spatial gradient by dividing by the initial gas flow velocity S_0 away from the propellant surface, determines the flux of heat conducted to the surface for vaporization. Thus the heat balance is

$$\lambda_0 (dT/dt)_0 / S_0 = S_0 \rho_0 \Delta H_{vap} \qquad [3]$$

where the subscript zero refers to the surface, and ΔH_{vap} includes the heats of fusion and of heating to the boiling point as well as the heat of vaporization of the liquid. For these quantities the approximation is made that the propellant has the physical properties of pure molecular hydrogen.

Although in a practical system the pressure might be expected to be several atm, an initial calculation at 1 atm seems appropriate. For a propellant having one H atom per 10 H_2 molecules

T_0	= 20.7 K
ρ_c	= 1.12×10^{-3} g/cc
ΔH_{vap}	= 129.3 cal/g
λ_0	= 3.8×10^{-5} cal/cm deg sec
$C_0{}^H$	= 5.4×10^{-5} mole/cc
$C_0{}^{H_2}$	= 5.35×10^{-4} mole/cc
ΔH_r	= −103.3 kcal/mole H_2
$C_0{}^M$	= 5.9×10^{-4} mole/cc
$(\tilde{C}_p{}^H)_0$	= 4.96 cal/mole deg
$(\tilde{C}_p{}^{H_2})_0$	= 6.62 cal/mole deg

From Equation [1], $(-dC_H/dt)_0 = 1.72 \times 10^4$ mole/cc sec. Equation [2] then yields $(dT/dt)_0 = 2.33 \times 10^{11}$ deg/sec, and solving [3] for S_0, we get

$$S = 7840 \text{ cm/sec}$$

The rate of change of temperature seems enormous, but we note the temperature gradient at the surface is $(dT/dx)_0 = 2.98 \times 10^7$ deg/cm. At 20 K, the mean free path in a gas is of the order of 10^{-6} cm, so that the temperature gradient is roughly 30 deg per mean free path. This may imply that a normal thermal conductivity coefficient should not be used; however, it may be pointed out that the experimental temperature profiles in typical gaseous flames (4) show gradients of the order of degrees per mean free path, and it is generally assumed that normal thermal conductivity coefficients can be used in theoretical treatments of such flame systems, aside from the anomalies brought about by entropy changes (5). A further point is that the temperature gradient is of the order of that found in weak shock waves, to which theories of shock structure using normal transport coefficients have been applied with fair success (6).

The linear burning rate of the solid will be

$$S_s = S_0 \rho_0 / \rho_s = 125 \text{ cm/sec}$$

where the solid has been assumed to have the density of liquid H_2. The mass consumption rate per unit area of the solid is

$$\dot{m}/A = S_s \rho_s = 8.76 \text{ g/cm}^2 \text{ sec}$$

The effect of pressure upon the burning rate can be estimated if the effect of pressure upon the ΔH_{vap} term can be approximated. Because the variation of the enthalpy of liquid H_2 with pressure is extremely difficult to estimate, we may as a first approximation take ΔH_{vap} to be a constant. Raising the pressure to 2 atm raises the vaporization temperature by 2.3 K, to 23.0 K. The new S_0 is 1.04×10^4 cm/sec, and the new $S_s = 3.02 \times 10^2$ cm/sec. For an empirical fit of the type $S_s = ap^n$, this gives $n = 1.28$.

Some of the initial assumptions can be tested on the basis of the results. Diffusion coefficients in the liquid phase have values around 10^{-5} cm^2/sec at room temperature; if we suppose the activation energy for diffusion to be 5 kcal, D for liquid H_2 at 20.7 K is of the order of 10^{-55} cm^2/sec. Although this figure may be unrealistically small, it would nevertheless appear to guarantee that the effect of diffusion in the liquid will be nil. In the particular propellant chosen for discussion here, there is a mechanism other than diffusion available for atom recombination in the liquid phase. If the matrix had been Ne, for example, diffusion would have offered the only mechanism; however, with a mixture of H and H_2, recombination of H could conceivably occur in the liquid through a sort of chain transfer involving formation of H_3 and its redissociation to H_2 and H. This is just the ortho-para hydrogen conversion reaction, which has an activation energy around 7.5

Received Jan. 30, 1959.

[1] Acknowledgment is made of the financial support of Project SQUID, supported by the Office of Naval Research, Department of the Navy, under contract Nonr 1858(25) NR-098-038. Reproduction in full or in part is permitted for any use of the United States Government.

[2] Associate Professor, Department of Fuel Technology.

[3] Numbers in parentheses indicate References at end of paper.

kcal (7) and which therefore will be negligibly slow at 20 K.

The rate of heat extraction from the flame by the vaporization of the liquid may be compared to the rate of heat release. Per square cm of surface, the vaporization rate requires about 10^3 cal/sec. The material vaporized from this area has an initial heat release rate of about 10^6 cal/sec. Thus the gaseous reaction is virtually unaffected by the vaporization requirement.

In conclusion, it is noted that the expression for the linear burning rate

$$S_g^2 = k(C_0^H)^2 C_0^M \lambda_f \Delta H_r \tilde{M}_0^{av} / [2\,\rho_g^2 \Delta H_{vap}(\tilde{C}_p)_0^{av}]$$

where $\tilde{M}_0^{av}$ is the mean molecular weight (initially), is similar to simple gaseous flame theories such as that of Damköhler (8) except that temperatures do not appear in it. Since the ignition temperature was specified as the initial gas temperature in this case, the term expressing the enthalpy change for heating of reactants to the ignition temperature has become just the ΔH_{vap}. The estimate of the temperature gradient at the ignition point in the Damköhler treatment, which involves the difference between initial and final temperature, a correction factor and an average reaction rate, has been replaced by a more direct calculation using known kinetics, concentrations and thermal quantities.[4]

References

1 "Magnetic Field Separates H Atoms," *Chem. Engng. News*, vol. 37, no. 2, 1959, p. 38.

2 Golden, S., "Free-Radical Stabilization in Condensed Phases," *J. Chem. Phys.*, vol. 29, no. 1, 1958, pp. 61–71.

3 Pease, R. N., in "Combustion Processes," Lewis, B., Pease, R. N. and Taylor, H. S., eds., Princeton University Press, 1956, pp. 196–197.

4 Friedman, R., "Measurement of the Temperature Profile in a Laminar Flame," in "Fourth Symposium (International) on Combustion," Williams and Wilkins, Baltimore, 1953, pp. 259–263.

5 Hirschfelder, J. O., "Heat Conductivity in Polyatomic, Electronically Excited, or Chemically Reacting Mixtures. III," in "Sixth Symposium (International) on Combustion," Reinhold, New York, 1957, pp. 351–366.

6 Thomas, L. H., "Note on Becker's Theory of the Shock Front," *J. Chem. Phys.*, vol. 12, no. 11, 1944, pp. 449–457; discussed by Greene, E. F., Cowan, G. R. and Hornig, D. F., "The Thickness of Shock Fronts in Argon and Nitrogen and Rotational Heat Capacity Lags," *J. Chem. Phys.*, vol. 19, no. 4, 1951, pp. 427–434.

7 Trotman-Dickenson, A. F., "Gas Kinetics," Butterworths, London, 1955, p. 173.

8 Damköhler, G., "Der Einfluss der Turbulenz auf die Flammengeschwindigkeit in Gazgemischen," *Zeitschrift für Elektrochemie*, vol. 46, no. 11, 1940, pp. 601–626; discussed by Gaydon, A. G. and Wolfhard, H. G., "Flames," Chapman & Hall, London, 1953, pp. 88–89.

[4] The adiabatic flame temperature for the 1:10 H-H_2 propellant at 1 atm is only 720 K, almost independent of pressure for pressures of 1 atm or more. The ideal I_{sp} for this system, operating in a vacuum (operation in the atmosphere would, of course, be exceedingly inefficient for p_c = 1 atm) is 472 sec. For a 1:5 H-H_2 propellant, if it could be made, the 1 atm adiabatic flame temperature is 1330 K, and the corresponding I_{sp} is 660 sec.

Generalized Solution for the Problem of Pipe Flow With Friction and Heat Addition

R. W. McJONES[1] and M. L. CAPLAN[2]

Marquardt Aircraft Co., Van Nuys, Calif.

A generalized chart method is presented for the rapid solution of pipe flow problems involving compressible fluids, including the combined effects of friction and heat addition. A typical chart is shown for the case of subsonic air flow through a duct of unspecified but constant wall temperature. Similar charts can be constructed for other problems.

Received Feb. 4, 1959.

[1] Research Consultant. Member ARS.

[2] Research Engineer.

THE CONSTRUCTION of a generalized chart occurred to the authors as an extension of Shapiro's graphical presentation of particular calculations on page 246 of (1).[3] It appeared that if enough particular cases were calculated from low Mach number to choking and if the results were properly plotted, the resulting chart would cover all possible intermediate problems. Just as the calculations were complete and various plotting parameters were being considered, previous unpublished work by Frank Rom of the NACA Lewis Laboratory was discovered. He had done substantially identical work in 1953 and had prepared a completely workable chart. The present calculations are in excellent agreement with Rom's, and the present chart is little more than a refined version of his.

Development of Generalized Solution

Compressible fluid flow with friction and heat transfer involves interrelated changes in Mach number, total pressure and temperature. These changes are clearly described by the influence coefficients of (1) which lead to the following equations for flow in constant area ducts with constant mass flow and no work done by the fluid

$$\frac{\Delta M^2}{M^2} = \frac{[1+\gamma M^2]\{1+[(\gamma-1)/2]M^2\}}{(1-M^2)}\frac{\Delta T_0}{T_0} + \frac{\gamma M^2\{1+[(\gamma-1)/2]M^2\}}{(1-M^2)}\,4f\frac{\Delta L}{D} \quad [1]$$

$$\frac{\Delta P_t}{P_t} = \frac{-\gamma M^2}{2}\left(\frac{\Delta T_0}{T_0} + 4f\frac{\Delta L}{D}\right) \quad [2]$$

Any generalized solutions are clearly dependent upon the existence of a fixed relationship between wall friction and gas temperature change. The possibility that a suitable relationship exists is suggested by Reynold's analogy, and (2) develops the required equations for both the case of constant wall temperature (considered here) and the case of uniform heat flux. With some notation changes, Equation [22] of (2) becomes

$$\frac{\Delta L}{D}\left(\frac{10}{R_e^{0.2}}\right) = \frac{\Delta T/T_w}{0.0092\,(k_w/c_{pw}\mu_w)^{0.6}(T/T_w)^{2/3}(1-T/T_w)} \quad [3]$$

Notation here is consistent with reference (2), except that the present R_e is defined as $\rho VD/\mu_w$, where ρ and V are based on average values from continuity, but μ_w is gas viscosity at the wall temperature. The various test reports mentioned in (2) have since been consolidated and published as (3).

Process lines for the present chart were calculated on a digital computer using an available program based on Equation [1]. A wall temperature of 2000 R was used for the bulk of the calculations; however, check calculations using T_w = 900 R and 3460 R verified the validity of the generalized chart.

Selection of Chart Format

The various quantities which may be of interest in flow problems include total and static pressure, Mach number, velocity, total and static temperature, density, etc., and are too numerous to include on a single chart. When the channel area, wall temperature and mass flow are constant, the continuity equation may be reduced to the following form which suggests the format finally selected

$$\frac{\sqrt{T_t/T_w}}{P_t A^*/A} = \text{constant} \quad [4]$$

The gas-to-wall temperature is placed along the abscissa together with the corrected tube length parameter; this scale is made linear in tube length to give a better physical representation and to facilitate solution of problems where tube length is given and temperature ratios must be found by trial

[3] Numbers in parentheses indicate References at end of paper.

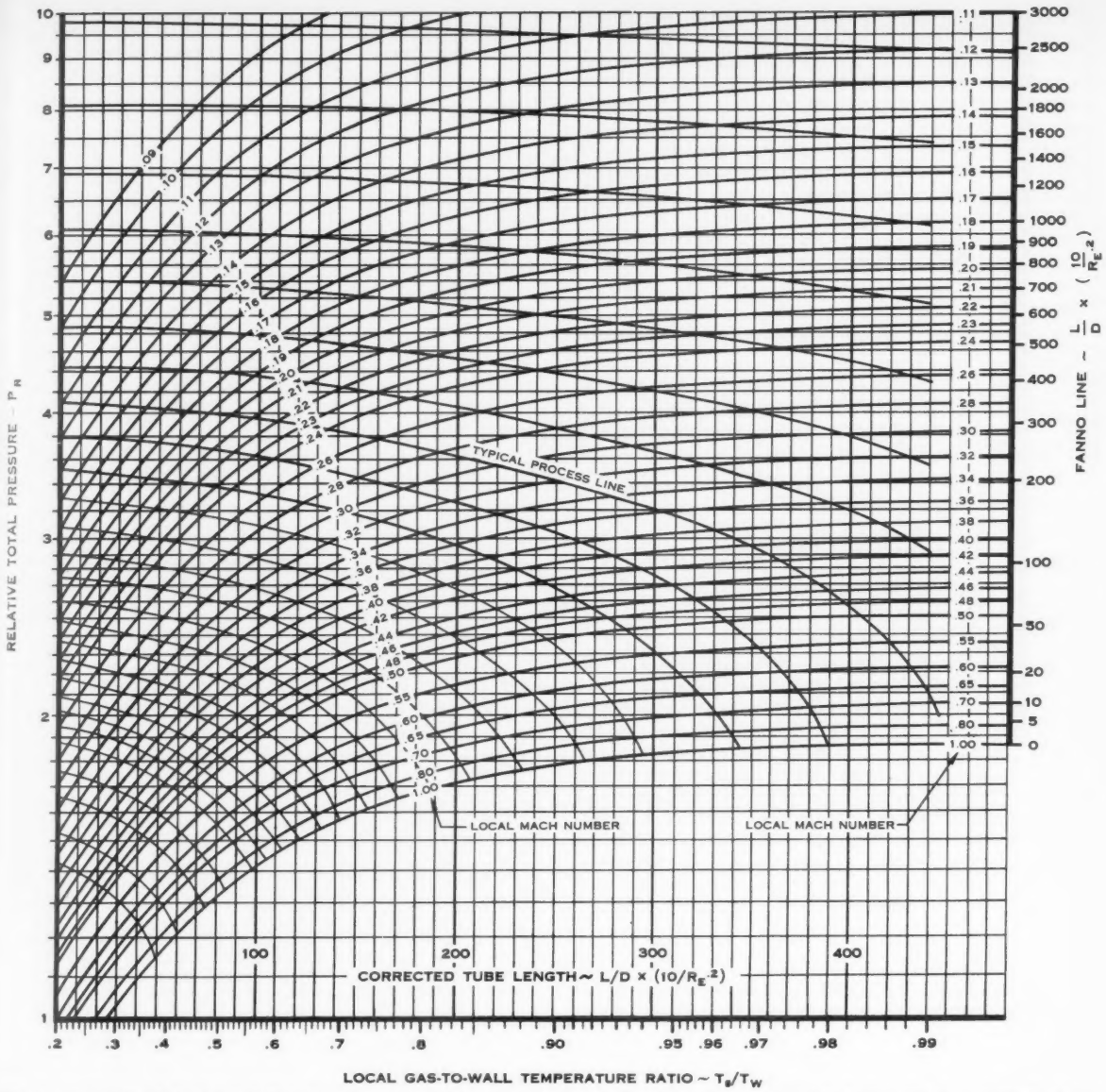
RELATIVE TOTAL PRESSURE ~ P_R
FANNO LINE ~ $\frac{L}{D} \times \left(\frac{10}{R_E^{.2}}\right)$
TYPICAL PROCESS LINE
LOCAL MACH NUMBER
LOCAL MACH NUMBER
CORRECTED TUBE LENGTH ~ L/D × $(10/R_E^{.2})$
LOCAL GAS-TO-WALL TEMPERATURE RATIO ~ T_g/T_W

Fig. 1 Generalized chart for air flow in a pipe with constant wall temperature. Example: Geometric $L/D = 63$, $T_w = 2000$ R, $R_e = 10^4$ (using viscosity at T_w). At inlet, $T_{gi} = 1200$ R, $M_i = 0.34$, $P_{ti} = 200$ psia. Calculate $L/D \times 10/R_e^{0.2} = 63 \times 10/6.3 = 100$. Locate inlet point at $(T_g/T_w)_i = 0.6$ and $M_i = 0.34$; read inlet $P_{Ri} = 2.65$, and inlet corrected tube length parameter = 110. Follow process line to exit corrected tube length = 110 + 100 = 210. Read at exit, $M_e = 0.61$, $(T_g/T_w)_e = 0.85$. $P_{Re} = 2.03$. Calculate exit gas temperature = 0.85 × 2000 = 1700 R, exit total pressure 200(2.03/2.65) = 153 psia.

and error. Relative total pressure is placed along the ordinate, which is made logarithmic for convenience. Lines of constant Mach number are then constructed from Equation [4]. Although $\gamma = 1.4$ is implied in the A^*/A vs. Mach number relationship, check calculations show negligible overall chart error for air temperature approaching $T_w = 3460$ R.

The chart thus defined, Fig. 1, is a plane of constant mass flow, so the typical process lines computed as described above (as well as any other lines which might be drawn) automatically satisfy continuity.

The Fanno line plotted along the right-hand edge of Fig. 1 relates total pressure, Mach number and corrected tube length for the case of zero heat transfer. It is also useful in problems where the final gas-to-wall temperature exceeds the chart cutoff at $T_g/T_w = 0.99$. As a matter of interest, at $T_g/T_w = 0.5$, the temperature term in Equation [2] is only 3 per cent of the friction term, and at $T_g/T_w = 0.99$, it is down to 1 per cent.

Chart Construction for Other Cases

Construction of a chart for the case of heat transfer from the gas to an isothermal wall follows exactly the procedure outlined herein, except that the total pressure change due to heat transfer will be of opposite sign. The case of uniform heat flux is of frequent interest and can be handled by this method if a generalized relationship between gas temperature and tube

length can be obtained. The results given in Fig. 6 of (2) suggest that a single curve of relative gas temperature vs. corrected tube length can be constructed such that it will approximate flow with constant heat flux between any two arbitrarily selected end points. Once this curve is obtained, the generalized chart can be readily constructed. A problem involving any arbitrary wall temperature variation can, of course, be handled with the present chart by assuming an equivalent tube having step changes in wall temperature to approximate the given temperature profile. The overall solution is then obtained by combining the separate solutions for each constant temperature tube increment.

References

1 Shapiro, A. H., "The Dynamics and Thermodynamics of Compressible Fluid Flow," vol. I, Ronald Press, New York, 1953.

2 Pinkel, B., Noyes, R. N. and Valerino, M. F., "Method for Determining Pressure Drop of Air Flowing Through Constant-Area Passages for Arbitrary Heat-Input Distributions," NACA TN 2186, 1950.

3 Humble, L. V., Lowdermilk, W. H. and Desmon, L. G., "Measurements of Average Heat-Transfer and Friction Coefficients for Subsonic Flow of Air in Smooth Tubes at High Surface and Fluid Temperatures," NACA TR 1020, 1951.

On Satellite Librations

G. M. SCHINDLER[1]

University of California, Santa Barbara, Calif.

When a satellite is not perfectly round but oblong, it will oscillate about an attitude of equilibrium somewhat like a pendulum. These oscillations are called "librations." The present paper deals with the librations of a satellite built in the shape of a dumbbell, which consists of two spheres M_1 and M_2 of equal mass m separated by a rigid but weightless rod of length $2e$. The center of gravity of the satellite is supposed to move exactly in a circular orbit. It is shown that the frequency of such oscillations depends very strongly on the angle of excursion and that it ranges from a finite positive value to infinity when the excursion varies between $\pm\pi/2$ and zero.

THE RESULTS to be found in literature on the problem of determining the librations of a satellite built in the shape of a dumbbell differ from each other as far as already rather strong simplifications on the basic equations have been made. In connection with such simplifications, it is not surprising that a frequency of the dumbbell was found to be of the magnitude of the satellite frequency around the Earth. This is true only for a proper choice of the excursion angle, and it shall be shown here that by a suitable choice of the excursion, it is always possible to perform a libration which period is exactly the same as the period of the satellite in the circular orbit.

Discussion

Let ρ be the radius between the center of gravity of the dumbbell system and the center of the Earth (Fig. 1). At time t the rod connecting the two spheres M_1 and M_2 of equal mass m builds the angle φ with the vertical. Now, due to their different distances from the geocenter, the two spheres

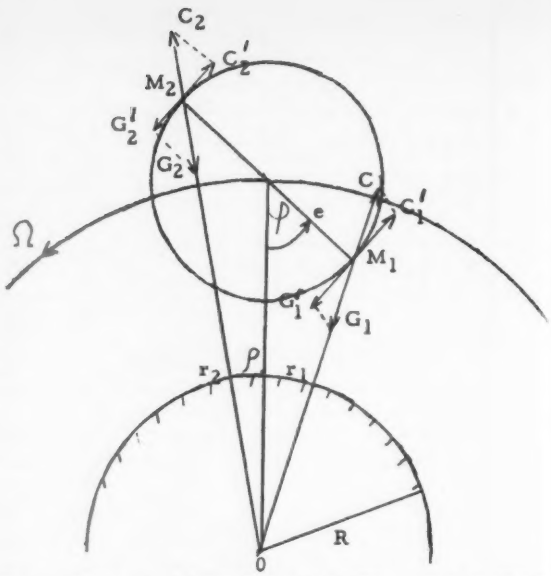

Fig. 1. Geometry of dumbell-shaped satellite around the Earth

suffer different attractions, viz.

$$G_1 = \frac{mgR^2}{r_1^2} = \frac{mgR^2}{(\rho^2 + e^2 - 2\rho e\cos\varphi)}$$
$$G_2 = \frac{mgR^2}{r_1^2} = \frac{mgR^2}{(\rho^2 + e^2 + 2\rho e\cos\varphi)} \quad \ldots\ldots [1]$$

where

R = radius of the Earth surface
g = gravitational acceleration at Earth surface

Similarly, because they are forced to participate in the same orbiting revolution at the common angular velocity Ω around 0, the two masses experience different centrifugal forces

$$C_1 = mr_1\Omega^2 = m\Omega^2(\rho^2 + e^2 - 2\rho e\cos\varphi)^{1/2}$$
$$C_2 = mr_2\Omega^2 = m\Omega^2(\rho^2 + e^2 + 2\rho e\cos\varphi)^{1/2} \quad \ldots\ldots [2]$$

If the angle φ is taken to be positive in the counterclockwise direction, then the restoring force is acting on the first sphere

$$me\ddot{\varphi} = -(G_1' - C_1') = -\frac{m\rho}{r_1}\sin\varphi\left(\frac{gR^2}{r_1^2} - r_1\Omega^2\right) \quad [3]$$

while the second sphere suffers the restoring force

$$me\ddot{\varphi} = G_2' - C_2' = \frac{m\rho}{r^2}\sin\varphi\left(\frac{gR^2}{r_2^2} - r_2\Omega^2\right) \quad [4]$$

The total restoring moment is then given by the sum of both forces in Equations [3 and 4]

$$2me\ddot{\varphi} = mg\rho R^2\sin\varphi\left(\frac{1}{r_2^3} - \frac{1}{r_1^3}\right) \quad [5a]$$

or

$$\ddot{\varphi} = \frac{g\rho R^2}{2e}\sin\varphi\left[\frac{1}{(\rho^2 + e^2 + 2\rho e\cos\varphi)^{3/2}} - \frac{1}{(\rho^2 + e^2 - 2\rho e\cos\varphi)^{3/2}}\right] \quad [5b]$$

From Equation [5a] it follows that the total restoring force $2me\ddot{\varphi}$ is pointing toward the positive direction of φ if $(3\pi/2) < \varphi < 2\pi$ and $(\pi/2) < \varphi < \pi$, and that it points toward the

Received Feb. 2, 1959.

[1] Assoc. in Mathematics, Consultant.

negative direction of φ if $0 < \varphi < (\pi/2)$ and $\pi < \varphi < (3\pi/2)$. This causes an oscillation around the vertical axis $\varphi = 0$, which is the attitude of stable equilibrium. The position $\varphi = \pi/2$, however, can only be considered to be the attitude of non-stable equilibrium, since the dumbbell always tends to the stable position $\varphi = 0$, if it is deflected from the position $\varphi = \pi/2$.

Since in the general equation of motion [5b] the angular velocity Ω does not occur, there is no relation between the periods of the dumbbell and the satellite around the Earth.

Equation [5b] is valid for arbitrary orbit. We now assume the satellite to be in circular orbit, that is, $\rho(t) =$ constant. Then we can integrate Equation [5b] with respect to the time t, and we obtain

$$\dot{\varphi}^2 = g\left(\frac{R}{e}\right)^2\left[\frac{1}{(\rho^2+e^2-2\rho e\cos\varphi)^{1/2}} + \frac{1}{(\rho^2+e^2+2\rho e\cos\varphi)^{1/2}} + K\right] \quad [6]$$

where K is an integration constant, which is determined by the initial condition of $t = t_0$

$$\varphi(t_0) = \varphi_0 \qquad \dot{\varphi}(t_0) = \dot{\varphi}_0 \quad [7]$$

K then turns out to be

$$K = \dot{\varphi}_0^2 \cdot \left(\frac{e}{R}\right)^2 \cdot \frac{1}{g} - \frac{1}{(\rho^2+e^2-2\rho e\cos\varphi_0)^{1/2}} - \frac{1}{(\rho^2+e^2+2\rho e\cos\varphi_0)^{1/2}} \quad [8]$$

Now, the time for one complete cycle swing of the dumbbell is given by

$$T = \frac{e}{R\sqrt{g}}\int_0^{2\pi} \frac{d\varphi}{\sqrt{Z(\varphi)+K}} \quad [9]$$

where

$$Z(\varphi) = \frac{1}{\sqrt{\rho^2+e^2-2\rho e\cos\varphi}} + \frac{1}{\sqrt{\rho^2+e^2+2\rho e\cos\varphi}} = \frac{1}{r_1} + \frac{1}{r_2} \quad [10]$$

$Z(\varphi)$ is limited between the boundaries

$$\frac{2}{\sqrt{\rho^2+e^2}} \leqq Z(\varphi) \leqq \frac{2\rho}{\rho^2-e^2} \quad [11]$$

This implies that for sufficient high initial velocity $\dot{\varphi}_0$, the constant K can be arbitrarily large, so that the time T in Equation [9] can be arbitrarily small. However, we are not very much interested in this obvious result, since the most interesting case is that where we release the dumbbell from the position $\varphi = \varphi_0$ for free oscillation. This would be the case where $\dot{\varphi}_0 = 0$ and $0 < \varphi_0 < (\pi/2)$. We then have

$$K = -\left[\frac{1}{(\rho^2+e^2-2\rho e\cos\varphi_0)^{1/2}} + \frac{1}{(\rho^2+e^2+2\rho e\cos\varphi_0)^{1/2}}\right] \quad [12]$$

For reasons of symmetry we obtain

$$T = \frac{4e}{R\sqrt{g}}\int_0^{\varphi_0} \frac{d\varphi}{\sqrt{(1/\sqrt{\rho^2+e^2-2\rho e\cos\varphi}) + (1/\sqrt{\rho^2+e^2+2\rho e\cos\varphi}) + K}} \quad [13]$$

It is hopeless to try to solve this hyperelliptical integral. For actual purposes, instead of solving Equation [13] one can solve the differential equation for $t(\varphi)$

$$\frac{dt}{d\varphi} = \frac{4e}{R\sqrt{g}} \frac{1}{\sqrt{\frac{1}{r_1}+\frac{1}{r_2}+K}} = f(\varphi) \quad [14a]$$

with the initial condition

$$t(\varphi_0) = t_0 \quad [14b]$$

which may be done by computer application. The time T is then given by

$$T = t(0) - t(\varphi_0) = (t_1 - t_0) \quad [14c]$$

However, the integral in Equation [13] can be investigated for $\varphi_0 \to (\pi/2)$ and for $\varphi_0 \to 0$.

For this purpose it is convenient to use the substitution

$$\cos\varphi = -A\cos 2\lambda \quad [15]$$

where A is given by

$$A = \frac{1}{2}\left(\frac{\rho}{e} + \frac{e}{\rho}\right) \quad [16]$$

We then have

$$\begin{aligned}\sqrt{\rho^2+e^2-2\rho e\cos\varphi} &= r_1 = \sqrt{2(\rho^2+e^2)}\cos\lambda \\ \sqrt{\rho^2+e^2+2\rho e\cos\varphi} &= r_2 = \sqrt{2(\rho^2+e^2)}\sin\lambda\end{aligned} \quad [17]$$

and

$$T = \frac{8eA\sqrt{\sqrt{2(\rho^2+e^2)}}}{R\sqrt{g}}\int_{\lambda_0}^{\lambda_1} \frac{\sin 2\lambda\, d\lambda}{\sqrt{(1-A^2\cos^2 2\lambda)\,[(1/\cos\lambda)+(1/\sin\lambda)-(1/\cos\lambda_0)-(1/\sin\lambda_0)]}} \quad [18]$$

where

$$\begin{aligned}\cos\varphi_0 &= -A\cos 2\lambda_0 \\ 1 &= -A\cos 2\lambda_1\end{aligned} \quad [19]$$

We further use the expansions

$$\begin{aligned}1 - A^2\cos^2 2\lambda &= (1 - A\cos 2\lambda)(1 + A\cos 2\lambda) = (\lambda_1 - \lambda)\,[c_1 + P(\lambda_1 - \lambda)] \\ \frac{1}{\cos\lambda} + \frac{1}{\sin\lambda} - \frac{1}{\cos\lambda_0} - \frac{1}{\sin\lambda_0} &= (\lambda - \lambda_0)\,[d_1 + Q(\lambda - \lambda_0)]\end{aligned} \quad [20]$$

Where $P(\lambda_1 - \lambda)$ and $Q(\lambda - \lambda_0)$ are regular power series in λ for $\lambda_0 \leq \lambda \leq \lambda_1$ which start at least with the first power of $(\lambda_1 - \lambda)$ and $(\lambda - \lambda_0)$, respectively, and

$$c_1 = 2A \sin 2\lambda_1$$

$$d_1 = \frac{\sin \lambda_0}{\cos^2 \lambda_0} - \frac{\cos \lambda_0}{\sin^2 \lambda_0} \qquad \ldots\ldots\ldots\ldots\ldots\ldots\ldots\ldots\ldots\ldots [21]$$

We then have to solve the integral

$$I = \int_{\lambda_0}^{\lambda_1} \frac{\sin 2\lambda \, d\lambda}{\sqrt{(\lambda_1 - \lambda)[c_1 + P(\lambda_1 - \lambda)](\lambda - \lambda_0)[d_1 + Q(\lambda - \lambda_0)]}}$$

$$= \frac{1}{\sqrt{c_1 d_1}} \int_{\lambda_0}^{\lambda_1} \frac{\sin 2\lambda}{\sqrt{(\lambda_1 - \lambda)(\lambda - \lambda_0)}} \left[1 + \sum_{\nu=1}^{\infty} \binom{-\frac{1}{2}}{\nu} \left(\frac{P(\lambda_1 - \lambda)}{c_1}\right)^{\nu}\right]\left[1 + \sum_{\mu=1}^{\infty} \binom{-\frac{1}{2}}{\mu} \left(\frac{Q(\lambda - \lambda_0)}{d_1}\right)^{\mu}\right] d\lambda \quad [22]$$

Now, the integral

$$\int_{\lambda_0}^{\lambda_1} \frac{d\lambda}{\sqrt{(\lambda_1 - \lambda)(\lambda - \lambda_0)}} = B\left(\frac{1}{2}, \frac{1}{2}\right) = \pi \qquad [23]$$

exists, where $B(p, q)$ is the Eulerian Beta-function. Since P and Q are regular power series in the entire integration interval, the integral I in Equation [22] exists for all values of λ_0 and λ_1 where both c_1 and d_1 are unequal to zero. As can be recognized from Equation [19], the range of λ_0 and λ_1 is limited by

$$\frac{\pi}{4} < \lambda_0 < \lambda_1 < \frac{\pi}{2} \qquad [24]$$

if φ_0 varies from zero to $(\pi/2)$. This implies that the magnitudes d_1 and c_1 are unequal to zero, except in the case when λ_0 tends to $\pi/4$, that is, for $\varphi_0 \to (\pi/2)$. In this limit case, d_1 vanishes, and, therefore, the integral in Equation [22] is infinite. This proves the fact that the time T tends to infinity if the excursion φ_0 of the dumbbell tends to $\pi/2$. Now, λ_1 is greater than $\pi/4$. If λ_0 tends to λ_1, the integral I in Equation [22] tends to $(1/\sqrt{c_1 d_1})\pi \sin 2\lambda_1$. The limit period T_0 is then obtained from [18 and 19]

$$\lim_{\lambda_0 \to \lambda_1} T = T_0 = \frac{2\pi}{R\sqrt{g}} \cdot \sqrt{\frac{2e}{\rho}} \cdot \frac{1}{\sqrt{[1/(\rho - e)]^3 - [1/(\rho + e)]^3}} \qquad [25]$$

Using here the expansion

$$\left(\frac{1}{\rho - e}\right)^3 - \left(\frac{1}{\rho + e}\right)^3 = \frac{1}{\rho^3} \sum_{\nu=1}^{\infty} \frac{(2\nu + 1)!}{(2\nu - 1)!} \left(\frac{e}{\rho}\right)^{2\nu - 1} = \frac{1}{\rho^3}\left[6\frac{e}{\rho} + 20\left(\frac{e}{\rho}\right)^3 + \ldots\right] \qquad [26]$$

the limit period T_0 is found in a first approximation (all higher terms of the ratio e/ρ are neglected) to be

$$T_0 \approx \frac{2\pi}{R\sqrt{g}} \cdot \frac{\rho\sqrt{\rho}}{\sqrt{3}} = \frac{1}{\sqrt{3}} \cdot \tau \qquad [26a]$$

where τ is the period of the satellite in the circular orbit. This result has already been found by Klemperer and Baker for small excursions. Since the series in Equation [26] consists of positive terms only, the exact limit period T_0 is even smaller than that given by the approximation in Equation [26a]

$$T_0 < \frac{1}{\sqrt{3}} \tau < 0.6\,\tau \qquad [27]$$

From the fact that the dumbbell period ranges from a finite value, which is even less than $0.6\,\tau$, to infinity, it follows that it is always possible by a proper choice of the excursion to perform a period which equals exactly the satellite period.

In conclusion, we prove the following *Theorem:* If for two different dumbbell systems ρ_1, e_1 and ρ_2, e_2, where ρ_1 and ρ_2 are the radii of the circular orbits, respectively, and e_1 and e_2 are the radii of the dumbbells, respectively, the ratios e_1/ρ_1 and e_2/ρ_2 are the same, then the square of the ratio between both dumbbell periods is equal to the cube of the ratio between the radii of the dumbbells, supposing that the initial conditions are the same.

In order to prove this theorem, we first have

$$\frac{e_1}{\rho_1} = \frac{e_2}{\rho_2} = \alpha \qquad [28]$$

As can be seen in Equation [16], the constant A does not change its value. Since the initial conditions are supposed to be the same, the excursion φ_0 is the same. This implies that the boundaries λ_0 and λ_1 are the same in both cases, as can be recognized in Equation [19]. Then the integral in [18] does not change at all. If we denote by T_1 and T_2 the period time in both cases, respectively, we obtain from Equation [18]

$$\frac{T_1}{T_2} = \frac{\sqrt{\sqrt{2(\rho_1^2 + e_1^2)} \cdot e_1}}{\sqrt{\sqrt{2(\rho_2^2 + e_2^2)} \cdot e_2}} \qquad [29]$$

Using here Equation [28] we have

$$\left(\frac{T_1}{T_2}\right)^2 = \left(\frac{e_1}{e_2}\right)^3 = \left(\frac{\rho_1}{\rho_2}\right)^3 \qquad [30]$$

which proves the theorem. This theorem is an analogue to Kepler's third law

$$\left(\frac{\tau_1}{\tau_2}\right)^2 = \left(\frac{\rho_1}{\rho_2}\right)^3 \qquad [31]$$

where τ_1 and τ_2 are the times of one period of the satellites, respectively. From Equations [30 and 31] one can conclude that there exists a linear relation between T and τ

$$T = C \cdot \tau \qquad [32]$$

However, the proportional factor C depends essentially on the ratio e/ρ and on the initial condition φ_0, as shown previously.

References

1 Klemperer, W. B. and Baker, R. M. L., Jr., "Satellite Librations," Proc. Seventh International Astronautical Congress, Rome, Sept. 17–22, 1956.

2 Wheelon, A. D., "An Introduction to Midcourse and Terminal Guidance," GM-TM-0165-00252, Space Technology Laboratories, June 1958.

Time for Escape Using a Succession of Small Impulses

ROBERT E. ROBERSON[1]

Autonetics Div. of North American Aviation, Inc., Downey, Calif.

J. B. PETERSON[2] has pointed out that an efficient escape from an orbit can be made with low thrust if the thrust is applied in a series of short impulses at perigee. The total impulse required is the same as if it were delivered in one big burst. He observes that the penalty one pays is in time.

It is of some interest to see just how bad this time penalty is. Consider an initial circular orbit of radius R about a body whose mass times the gravitational constant equals K. The velocity increment required for escape is $\Delta V = \sqrt{2K/R} - \sqrt{K/R}$. Suppose, however, that thrust limitations prevent adding more than $\Delta v = \Delta V/N$ in any (essentially impulsive)

Received Feb. 6, 1959.

[1] Chief, Astronautical Sciences. Now with Systems Corporation of America, Los Angeles, Calif. Member ARS.

[2] Peterson, J. B., "Note on 'Take-off from Satellite Orbit,'" JET PROPULSION, vol. 27, Dec. 1957, pp. 1263–1264.

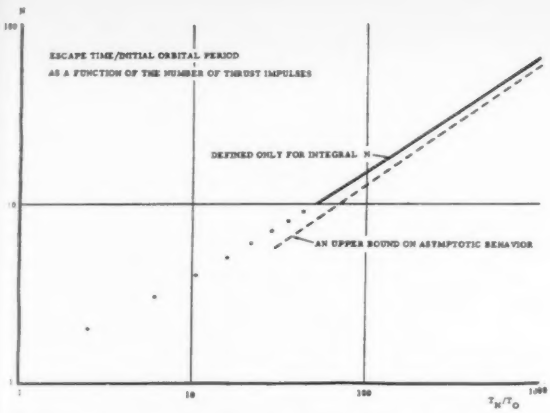

Fig. 1 Time for escape in units of initial orbital period (abscissa)as a function of number of impulses required to produce escape velocity (ordinate)

burst. After each revolution, at perigee, Δv is added. The problem is to find the time required to escape by this process. Let

T_0 = period of circular orbit
T_i = period of the elliptical orbit during the ith revolution (that is, after application of the ith small impulse)
v_i = the perigee velocity at the beginning of the ith revolution after the impulse

It is easy to show that $T_i/T_0 = (2 - Rv_i^2/K)^{-3/2}$. Now $v_i = \sqrt{K/R} + i\Delta v$ $(i = 1, 2, \ldots, N)$. Hence

$$\frac{T_i}{T_0} = \left[1 - 2(\sqrt{2} - 1)\frac{i}{N} - (\sqrt{2} - 1)^2\frac{i^2}{N^2}\right]^{-3/2}$$

It should be apparent that escape will occur after N impulses, whence the time to escape is

$$T_N = \sum_{i=1}^{N-1} T_i$$

(The velocity after N impulses is $v_N = \sqrt{K/R} + N\Delta v = \sqrt{K/N} + \Delta V = \sqrt{2K/N}$, precisely escape velocity.)

The quantity T_N/T_0 is shown as a function of N in Fig. 1 for $N = 1, 2, \ldots, 100$. For larger N, an approximate asymptotic result is useful. The value of the sum for T_N/T_0 is approximated by the integral

$$N\int_{1/2N}^{1-1/2N} \frac{dx}{[1 - 2(\sqrt{2} - 1)x - (\sqrt{2} - 1)^2x^2]^{3/2}}$$

although this integral will give a value a little too high because of the rapidly increasing slope of the integrand as x nears unity. Evaluating the integral and keeping only the most rapidly growing term in N, one obtains

$$\log\left(\frac{T_N}{T_0}\right) \sim \frac{3}{2}\log N + \frac{3}{2}\log\left(1 + \frac{1}{\sqrt{2}}\right)$$

This relation is shown as the straight line of the figure, from which it appears that the approximation indeed gives a value of T_N/T_0 which is slightly too high.

This result is instructive. It strongly bears out one's intuitive feeling that the time delay for an escape of this kind is prohibitive. As an example, consider the case in which a satellite is in a 800 km circular orbit with velocity 7452 m per sec, escape velocity being 10,539 m per sec. Suppose that only 1 m per sec can be added in any one revolution, whence $N = 3{,}087$ and $T_N/T_0 \approx 378{,}500$. Since $T_0 = 6052$ sec, $T_N \approx 26{,}520$ days—hardly an acceptable break-away time. Even if the velocity increment is given in 30 bursts of 102.9 m per sec each, the total break-away time is about 21 days. The latter is an artificial case of course. The only reason for going to this kind of escape maneuver in the first place is in connection with the use of *very* low thrust systems in which the velocity increment in any one burst is very much smaller than the required 3087 m per sec.

Attitude Stabilization by Means of Solar Radiation Pressure

ROBERT L. SOHN[1]

Space Technology Laboratories, Inc., Los Angeles, Calif.

This paper demonstrates the feasibility of stabilizing the attitude of a space vehicle by means of solar radiation pressure. If a suitable weathervane-type tail surface is attached to the vehicle, solar radiation pressure, acting on the weathervane, will stabilize the vehicle against disturbing torques which arise from gravitational eccentricities (dumbbell effect), meteorite impacts and solar radiation pressures.

ONE VERY difficult problem confronting the designer of long duration space flight vehicles is that of controlling and stabilizing the orientation of the vehicle for long periods of time. For example, it might be desirable to orient a communications satellite in a given direction, and maintain that direction to close tolerances. Or during lunar or interplanetary flights, a constant attitude might be required for various reasons. Now, if disturbing torques, such as solar radiation pressures or gravitational torques cause the vehicle to rotate away from the desired orientation, a suitable corrective torque must be applied. At present, a fluid jet of some type is usually assumed to supply the restoring moment.[2] Even though the disturbing torques are small, jets cannot be used over long periods of time without consuming large quantities of propellant.

Solar Radiation Attitude Stabilization System

Several people have proposed the utilization of solar radiation pressure as a thrusting device for space vehicles, "solar sailing" as it has been called (1).[3] They have demonstrated that although solar radiation pressure is low, it nonetheless can be significant for thrusting purposes.

It seems entirely reasonable that solar radiation pressure could also be used to good advantage in an attitude stabilization system. The disturbing torques (solar radiation pressure, gravitational torques and meteorite impact) are very small, and, as will be shown, are of the same order of magnitude as the solar radiation pressure restoring torque. These effects will be examined in turn to compare the disturbing torques with the solar weathervane restoring torques.

Solar Radiation Pressure Disturbing Torque

Consider a vehicle moving broadside to the sun in the absence of any gravitational field. A disturbing torque will exist if the center of pressure is not coincident with the center of mass. It is possible to stabilize the vehicle against this torque by attaching a weathervane tail surface to the vehicle in such

Received Feb. 2, 1959.

[1] Member of the Technical Staff. Member ARS.

[2] Even if flywheels are used in the attitude control system, the imposition of some maximum rotational speed on the flywheel forces the designer to supply fluid jets to work off excess speeds.

[3] Numbers in parentheses indicate References at end of paper.

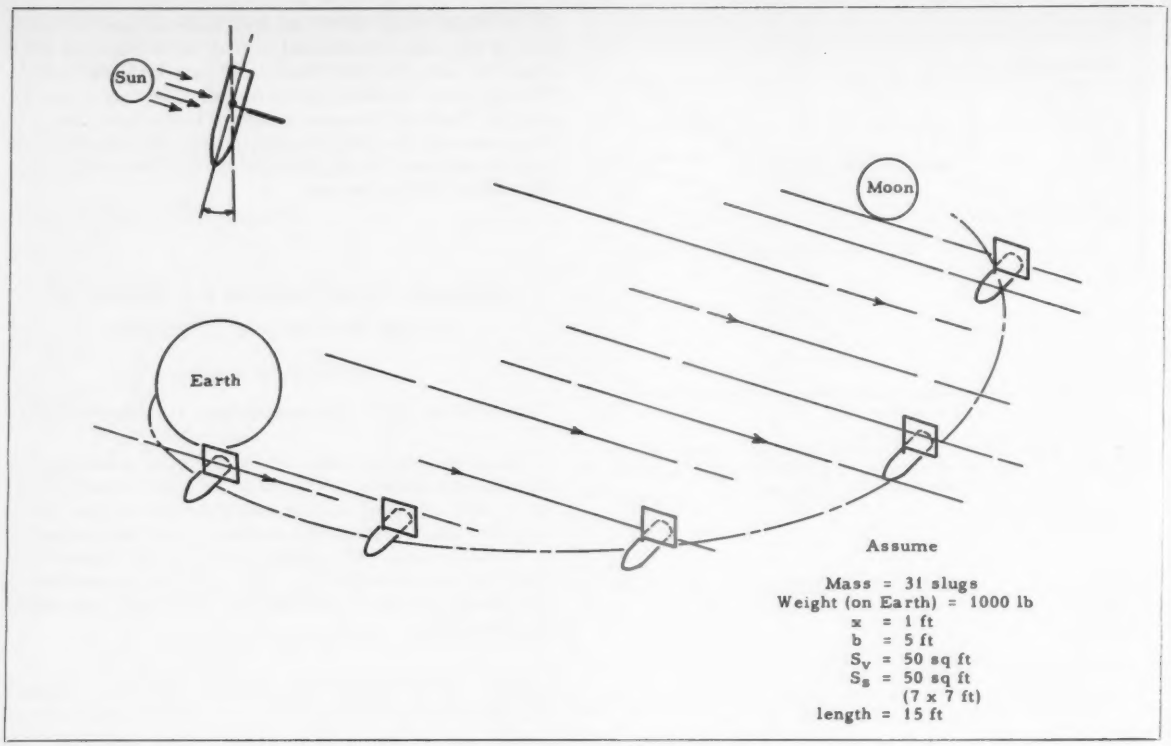

Fig. 1 Use of a solar stabilizer sail during a lunar flight

a way that solar radiation strikes the weathervane and rights the vehicle (see Fig. 1).

The disturbing torque of the vehicle τ_v is

$$\tau_v = PS_v x$$

where

P = solar radiation pressure, lb/ft²
S_v = exposed surface area of vehicle, ft²
x = distance from center of mass to center of pressure, ft

The righting torque of the sail τ_s is

$$\tau_s = PS_s b\psi \qquad \text{(for small } \psi\text{)}$$

where

S_s = surface area of stabilizer, ft²
b = stabilizer moment arm, ft
ψ = yaw angle, radian

Equating the torques gives the equilibrium yaw angle ψ as

$$\psi = \frac{xS_v}{bS_s}$$
$$= 11.5 \text{ deg}$$

where the numerical value is obtained by inserting the design numbers of Fig. 1 into the above equation. If the surface is movable, the yaw angle could be held to zero deg by deflecting the surface through an angle δ

$$\delta = \frac{xS_v}{bS_s}$$
$$= 11.5 \text{ deg}$$

Gravitational Disturbing Torques

The upsetting gravitational torque is

$$\tau_g = I\omega^2\left(1 + 2\,\frac{g}{r\omega^2}\right)\sin\beta\cos\beta \qquad \text{(general)}$$
$$= 3I\omega^2 \sin\beta\cos\beta \qquad \text{(satellite)}$$

where

ω = rate of angular movement about attracting mass, radian per sec
r = radius out from attracting mass, ft
I = moment of inertia, slug-ft²
β = flight path angle measured from local gravitational vector, radian

In order to compare the solar radiation pressure stabilizer capacity with the gravitational torque disturbance, two cases were studied: Vehicle in a 300-nautical mile altitude satellite orbit, and the vehicle in an escape shot to the moon.

In the satellite case, it was found that the vehicle design shown previously (with a stabilizer area of 50 ft²) was capable of trimming out the gravitational torque under the worst conditions, namely when $\beta = 45$ deg.

In the lunar case, a slightly different vehicle was assumed. The stabilizer design was held fixed, but the moment of inertia was increased by a factor of 10, to $I = 300$ slug-ft². The sail area required to hold the vehicle in equilibrium along the flight path as a function of time after launch is shown in Fig. 2. Since the flight to the moon takes approximately 2.5 days (3600 min), the graph represents a small portion of the total flight. After 27 min of flight, the 50-ft² stabilizer can trim out all gravitational eccentricities, even with the large moment of inertia.

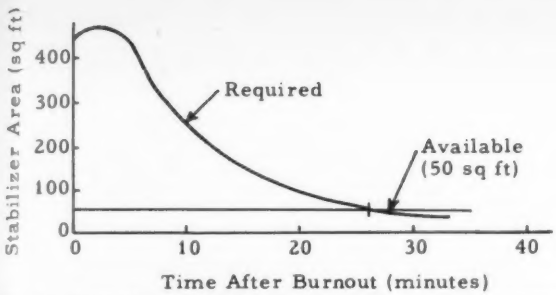

Fig. 2 Comparison of required and available stabilizer capacity during lunar flight

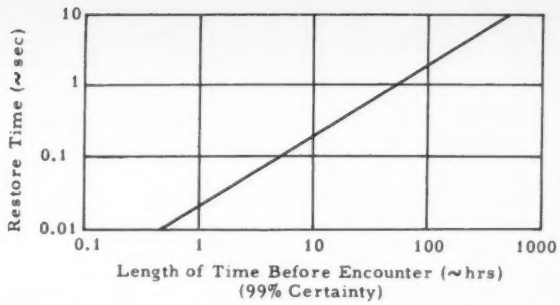

Fig. 3 Time to restore vehicle after meteorite disturbance

By a slight rotation of the vehicle, so as to align its centerline with the local vertical, all of the gravitational torque could be eliminated. Since there is no compelling reason to orient the centerline along the line of flight, at least for the first few hours of flight, there is no reason why the solar stabilizer could not be used during escape shots.

If it were mandatory to hold some arbitrary attitude during escape, jet boosters could be used for the first 30 min, until the solar stabilizer became adequate. These jets would be tiny in size and could be attached to the sail framework. In this way, the basic sail manipulators would also orient the jets. Further, the same servomechanisms used to control the sail could simultaneously control the jets.

Meteorite Disturbances

Finally, it is possible for meteorites to disturb vehicle orientation. These disturbances are extremely small. Fig. 3 has been prepared to show their effect. The distribution frequency of the meteorites is based on data from Carter (2). Fortunately, the large meteorites are encountered so seldom that the vehicle has no difficulty in righting itself before the next meteorite strikes it. The smaller meteorites have so little impulse that, although they are encountered more frequently, they cause little disturbance. The meteorites were assumed to strike 10 ft from the missile's center of mass. Meteorite disturbances should pose no problem.

Dynamic Stability

With the weathervane fixed at some equilibrium angle, the vehicle is statically stable, but dynamically neutrally stable. If disturbed, the vehicle will oscillate indefinitely with an amplitude equal to twice the disturbance angle. This can be demonstrated as follows. The excess torque is

$$-I\ddot{\psi} = \tau_s - \tau_v$$

The solution for ψ can be written as follows, using the subscript 0 to indicate initial conditions. Time t is in sec

$$\psi = \frac{\dot{\psi}_0}{\sqrt{A}} \sin \sqrt{A}\, t + \left(\psi_0 - \frac{xS_v}{bS_s}\right) \cos \sqrt{A}\, t + \frac{xS_v}{bS_s}$$

$$\text{period} = \frac{2\pi}{\sqrt{A}}$$

$$A = \frac{PS_s b}{I} \qquad \text{(square of the natural frequency)}$$

A rate sensor can be placed in the control system to deflect the surface in proportion to the yaw rate ($\delta = k\dot{\psi}$, k being the proportionality constant). The vehicle is then damped and will return to equilibruim. The equation of motion becomes (ignoring the mass of the stabilizer)

$$-I\ddot{\psi} = PS_s b(\psi + \delta) - PS_v x$$

The solution for the above equation is

$$\psi = \left\{\psi_0\left[1 + \frac{1}{(r_2/r_1) - 1}\right] - \frac{\dot{\psi}_0/r_1}{(r_2/r_1) - 1}\right\} e^{r_1 t} + \left[\frac{(\dot{\psi}_0/r_1) - \psi_0}{(r_2/r_1) - 1}\right] e^{r_2}$$

$$\left.\begin{aligned} r_1 &= -\frac{Ak}{2} + \sqrt{\left(\frac{Ak}{2}\right)^2 - A} \\ r_2 &= -\frac{Ak}{2} - \sqrt{\left(\frac{Ak}{2}\right)^2 - A} \end{aligned}\right\} \quad \frac{Ak}{2} > \sqrt{A}$$

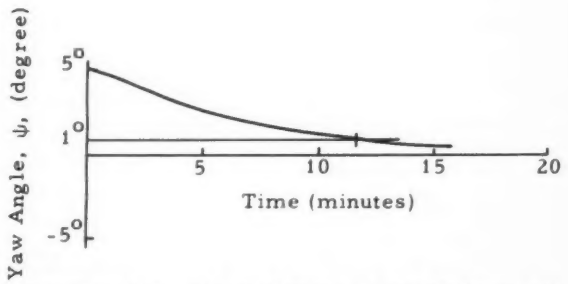

Fig. 4 Time history of yaw following a 5 deg disturbance (with rate damper)

A typical time history of the motion is shown in Fig. 4 for the vehicle described in Fig. 1. It can be seen that the vehicle corrects a 5 deg disturbance to within 1 deg in about 12 min.

Conclusions

The brief calculations presented above serve to indicate that a solar weathervane stabilizer is capable of orienting a vehicle traveling in solar space. Although the corrective torques produced by the stabilizer are small, they are nonetheless compatible with the external disturbing torques.

References

1 Garwin, R. L., "Solar Sailing—A Practical Method of Propulsion Within the Solar System," Jet Propulsion, vol. 28, no. 3, March 1958, pp. 188–190.
2 Carter, L. J., "Realities of Space Travel," Putnam, London, 1957.

Technical Comments

Further Comments on the Powered Flight Trajectory of a Satellite

THEODORE N. EDELBAUM[1]

United Aircraft Corp., East Hartford, Conn.

A NUMBER of authors, e.g., (1, 2),[2] have treated satellite launching mechanics by assuming that if

(a) The distance covered during powered flight is small compared to the Earth's radius, then

(b) The gravitational field may be taken as uniform during powered flight, or, equivalently, the centrifugal acceleration due to motion around the Earth may be neglected.

The assumption is usually made that (b) follows from (a). That this is not necessarily true for speeds on the order of satellite velocity has been demonstrated analytically in (3). In a recent note (4) the author of reference (1) has stated that reference (3) is in error and that assumption (b) does follow from (a). The author uses two arguments to support this thesis. The first argument is essentially a restatement, in vector notation, that it is "clear" that (b) follows from (a). The second argument uses a higher approximation that allows for first order variations in the gravitational field. The result of this approximation reduces to the result of approximation (b) when, and only when

(c) The powered flight time is small compared to $\sqrt{R_e/2g}$ = 9.5 min. (R_e = radius of the Earth.)

If (b) does really follow from (a), then the result of the higher approximation should reduce to the first approximation when (a) is satisfied and not when some new requirement (c) is introduced.

In fact, (c) is very restrictive. This may be shown by using some results for the optimum duration of powered flight. In (2) it is shown that if (b) is satisfied, the optimum duration of powered flight is

$$T = \sqrt{\frac{2y}{g}}$$

where

T = duration of powered flight
y = altitude

For this time to satisfy (c), the square root of the distance covered during powered flight must be small compared to the square root of the Earth's radius, a much more restrictive assumption than (a).

A more important result is the optimum duration of powered flight for a realistic inverse square, central gravitational field (5). For this case the duration of powered flight is equal to approximately half of a satellite's period, the $\sqrt{2}\,\pi$ times the time given in (c)!

In closing, it may be said that (b) is true if both (a) and (c) are satisfied, but that this combination is a very restrictive condition which is usually not even approximately satisfied by real satellites.

References

1 Fried, B. D., "On the Powered Flight Trajectory of an Earth Satellite," Jet Propulsion, vol. 27, June 1957, pp. 641–643.

2 Okhotsimskii, D. E. and Eneev, T. M., "Certain Variational Problems Associated with the Launching of an Artificial Earth Satellite," in "The Russian Literature of Satellites, Part 1," International Physical Index, Inc., New York, 1958, pp. 5–44.

3 Edelbaum, T. N., "Comments on the Powered Flight Trajectory of a Satellite," Jet Propulsion, vol. 27, Dec. 1957, pp. 1260–1261.

4 Fried, B. D., "Corrections to 'Comments on the Powered Flight Trajectory of a Satellite,'" Jet Propulsion, vol. 28, May 1958, p. 342.

5 Summerfield, M., "Problems of Launching an Earth Satellite," Astronautics, vol. 2, Dec. 1957, pp. 34–37.

Received Nov. 10, 1958.

[1] Research Engineer, Research Department. Member ARS.

[2] Numbers in parentheses indicate References at end of paper.

Comment on "Frictional Electricity in Missile Systems"

WILLIAM J. GUMAN[1]

Rensselaer Polytechnic Institute, Troy, N. Y.

ON READING Mr. Molmud's article[2] "Frictional Electricity in Missile Systems," I recalled an unusual occurrence of electrification. While performing a test at a Mach number of 2.5 in a continuous flow supersonic wind tunnel in which the air was highly contaminated with oil mist, it was noticed that a buildup of an electrical charge on the sting support discharged to the sting arm, burning through one of the two plastic pressure leads imbedded in the arm. The discharge occurred at a sharp corner of the sting support and left a pattern of concentric alternately light and dark circles on the arm (apparently the residue of burned plastic). Figs. 1 and 2 show the side view and top view of this pattern (see arrows), as well as the burned pressure lead. The discharge was subsequently eliminated by rounding off the sharp corner.

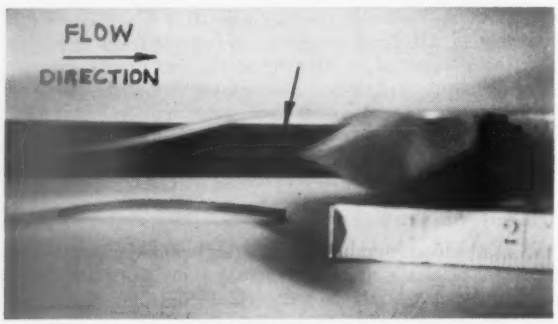

Fig. 1 Side view

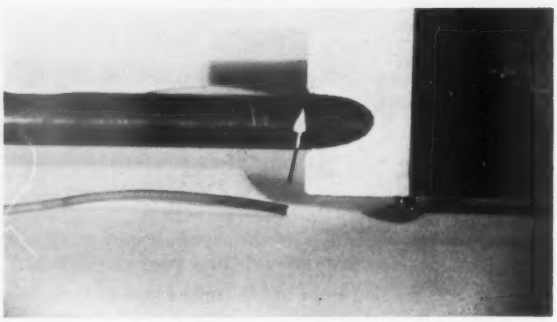

Fig. 2 Top view

Received Feb. 13, 1959.

[1] Assistant Professor of Aeronautical Engineering.

[2] Molmud, P., "Frictional Electricity in Missile Systems," ARS Journal, vol. 29, no. 1, 1959, pp. 73–75.

Comments on "Photochemistry of the Upper Atmosphere as a Source of Propulsive Power"

STERGE T. DEMETRIADES[1]

Aerojet-General Corp., Azusa, Calif.

THE AUTHOR notes with interest the excellent review paper by A. F. Charwat, "Photochemistry of the Upper Atmosphere as a Source of Propulsive Power" which appeared in ARS JOURNAL (1).[2] For the record, it is appropriate to draw attention to some previous work of this author and his co-workers (2, 3, 4) carried out independently at the Astronautics Laboratory of the Aerojet-General Corp. under sponsorship of the Office of Advanced Studies, Air Force Office of Scientific Research, contract no. 49(638)-111, and summarized in a recent note (5). Charwat's independent conclusions are in agreement with the previous conclusions of this author.

It is unfortunate that the article (6) which described the so-called "First Mono-Atomic Oxygen Ramjet" did not clearly differentiate between the work done at Aerojet and the work done elsewhere. However, this author's conclusions were amply documented in reports available to "qualified requestors" (3,4). Therefore the publication of his negative results in the open literature, at the expense of more fruitful projects, was not considered justified. The work of this author indicates that the defects of the fuel-less atomic-oxygen powerplant can be summed up by the following statement: At orbital speeds, its drag is too high; at suborbital speeds, the lift is too low. Although the thrust of a "fuelled" atomic-oxygen orbital powerplant (i.e., a powerplant which uses the energy of recombination of oxygen atoms to heat and expand an expellant or propulsive fluid) can be made greater than its drag, there is no real advantage to be gained by this scheme for extending the lifetime of low altitude satellites. With the same fuel weight one could achieve better results with an ordinary microrocket (firing in pulses if necessary).

The usefulness of the atomic oxygen in the upper atmosphere for auxiliary power generation is doubtful, since at orbital speeds the stagnation energy of 1 cc of air is at least 10 times greater than the recombination energy available in the same volume. At the same time, at altitudes above 110 km solar energy can provide, ideally, more power per unit area of receiver than atomic oxygen. Therefore, it appears that for practical power-generation purposes, the atomic oxygen of the Earth's atmosphere can be safely neglected. However, the measurement of accommodation coefficients, collision cross-sections, etc., of oxygen and other atoms make the study of the chemosphere and of artificial flows containing large fractions of oxygen and nitrogen atoms, a problem of considerable scientific interest.

This author feels that it is now time for the study of powered flight in the upper atmosphere to focus on an entirely different objective. Although it has been recognized for some time that great economies can be effected in space travel by splitting the problem into two distinct phases, the booster phase (concerned mainly with escape from the Earth's gravitational field) and the sustainer phase (concerned with providing low thrust at very high specific impulse for long periods of time), the devices proposed for solving the second phase of the problem (ion rockets, colloid rockets, plasmajets, etc., deriving energy from a nuclear reactor) still suffer from the disadvantage that the greater part of the weight of the space vehicle must be made up of propulsive fluid.[3] Since with present techniques it takes scores of pounds of propellant and powerplant to put 1 lb into orbit, even greater economies can result if the weight of propulsive fluid required for space flight can be eliminated from the total take-off mass.

The essential feature of this scheme is to lift only the energy source into orbit at approximately 100 km, and at that point to collect the propulsive fluid (air) for continuing the journey into space. This can be accomplished by a Propulsive Fluid Accumulator, or PROFAC, and it is a rather simple matter to show the startling reduction in take-off mass made possible by this approach. The PROFAC can maintain a low altitude (100 to 120 km) orbit by making use of a magnetogasdynamic (MGD) ramjet to overcome drag. The energy requirements of the MGD ramjet and PROFAC equipment can be met by relatively low power nuclear generators (1 to 10 mw).

Received March 4, 1959.

[1] Consultant. Member ARS.

[2] Numbers in parentheses indicate References at end of paper.

[3] Propulsive fluid or expellant or working fluid or reaction mass is the mass that must be ejected to provide thrust. These terms are used to signify that this mass does not contain the energy required for its own acceleration. When it contains that energy, the correct term is propellant.

References

1 Charwat, A. F., "Photochemistry of the Upper Atmosphere as a Source of Propulsive Power," ARS JOURNAL, vol. 29, no. 1, 1959, pp. 108–114.

2 Farber, M., Demetriades, S. T., Kretschmer, C. B. et al., Progress Reports to the Directorate of Advanced Studies, AFOSR, ARDC, nos. 0103-01-1 to 0103-01-7, Contract AF-49(638)-111, covering the period from March 14, 1957, to Nov. 14, 1958.

3 Demetriades, S. T. and Farber, M., "A Theoretical Study of the Recombination Kinetics of Atomic Oxygen," Aerojet-General Corp., Technical Note 21, AFOSR TN 58-18, ASTIA no. AD 148 057, Nov. 8, 1957.

4 Demetriades, S. T. and Kretschmer, C. B., "Preliminary Investigation of an Atomic-Oxygen Power Plant," Aerojet-General Corp., Technical Note 23, AFOSR TN 58-325, ASTIA no. AD 154 229, March 4, 1958.

5 Demetriades, S. T., "Upper Atmosphere Atomic-Oxygen Power Plant," *J. Aero/Space Sci.*, vol. 25, Oct. 1958, p. 653.

6 Yaffee, M., "First Mono-Atomic Ramjet Vehicle Designed for 59 Mi. Altitude," *Aviation Week*, April 7, 1958, p. 65.

Comments on "A Ballistic Bomb Method for Determining the Experimental Performance of Rocket Propellants"

R. H. WOODWARD WAESCHE[1]

Rohm & Haas Co., Redstone Arsenal Research Division, Huntsville, Ala.

IN THEIR article (1)[2] Messrs. Griffin, Turner and Angeloff mention that they adapted the gun propellant concept of "force" to give experimental values of specific impulse from small amounts of novel materials. The method yields impulse without need of thrust data or a known configuration. In addition, the authors suggest that tests be conducted with this method to determine its usage in the solid propellant field. In view of this suggestion, it may interest the authors to know that a closed bomb method of determining impulse has been in use at the Rohm & Haas Co., Redstone Arsenal Research Division, since March 1955, and that the Naval Ordnance Test Station and Aerojet-General Corp. have been using the experimental method since 1956.

However, this liquid gun method does present a slightly different approach from the one used at this division, aside from the fact that it is used here for solid propellants. It has been found more convenient and accurate at Rohm & Haas to use this test as a relative one, utilizing a "control" propellant, rather than the direct one used at OMCC. The relative method utilizes the fact that, neglecting changes in γ (the ratio of specific heats), the specific impulse of an unknown propellant can be obtained from the relation

$$\frac{(PV/m)^{1/2}_{\text{unknown}}}{(PV/m)^{1/2}_{\text{control}}} = \frac{(I_{sp})_{\text{unknown}}}{(I_{sp})_{\text{control}}} \qquad [1]$$

Received March 4, 1959.

[1] Physicist.

[2] Numbers in parentheses indicate References at end of paper.

The pressure term is the maximum pressure attained in the closed bomb, corrected for heat loss and igniter pressure. The volume term is corrected only for co-volume of the propellant gases. Correction for γ can be made in the term

$$\left(\frac{2\gamma}{\gamma - 1}\right)^{1/2}\left[1 - \left(\frac{P_a}{P_c}\right)^{\frac{\gamma-1}{\gamma}}\right]^{1/2}$$

appearing (2) in the equation for

$$\frac{I}{(nRT_c)^{1/2}} = f(\gamma, P) \qquad [2]$$

In every case, optimum expansion is assumed, generally to 14.7 psia from 1000 psig. It may be shown by thermodynamic considerations that the closed bomb relative force method yields the maximum impulse obtainable from a given formulation.

The closed bomb relative force method has been used at Rohm & Haas to determine impulses for a wide range of solid propellants, including samples from NOTS, Thiokol Chemical Corp. (both Redstone and Elkton Divisions), Standard Oil Co. (Whiting Lab), Grand Central Rocket Co., Allegany Ballistics Laboratory, Jet Propulsion Laboratory, Army Rocket and Guided Missile Agency, Aerojet-General Corp., and a wide variety of Rohm & Haas propellants. Nearly every existing type of solid propellant was tested in this survey, made in 1956 through the generous cooperation of the participating agencies. Good agreement was found with motor firing data.

Drawings of the bomb and some experimental experience may be obtained from the author, including precision and methods of correcting for heat loss, which can affect results significantly in solid propellants.

References

1 Griffin, D. N., Turner, C. F. and Angeloff, G. T., "A Ballistic Bomb Method for Determining the Experimental Performance of Rocket Propellants," ARS JOURNAL, vol. 29, no. 1, 1959, pp. 15–19.

2 "Rocket Fundamentals," OSRD 3992, p. 24.

Book Reviews

Ali Bulent Cambel, Northwestern University, *Associate Editor*

Elastic Waves in Layered Media, by W. Maurice Ewing, Wenceslas S. Jardetzky and Frank Press, McGraw-Hill Book Co., New York, 1957, 380 + xii pp. $10.

Reviewed by YI-YUAN YU
Polytechnic Institute of Brooklyn

This monograph written by three geophysicists is the outgrowth of a plan to make a uniform presentation of the investigations on earthquake seismology, underwater sound and model seismology carried on by the group connected with Lamont Geological Observatory of Columbia University. Since the book presents a systematic treatment of elastic-wave problems quite general in nature in addition to the specific geophysical applications, it should be found useful also in other fields as the authors hoped. In particular, the verification by experimental data of the theoretical results given here and there throughout the book should be of interest to scientists and engineers whose work is related to elastic-wave propagation and vibration problems.

The treatment is almost exclusively based upon the Theory of Linear Elasticity. Thus, the fundamental equations of small motion in an elastic body (reducible to the special case of an ideal fluid) together with some general solutions are briefly presented in the first chapter (23 pp.). Chapter 2 (50 pp.) is concerned with some classical topics on the homogeneous and isotropic half space, such as the reflection of harmonic plane waves at the free surface, Rayleigh's theory of surface waves and Lamb's integral solutions for an impulsive force applied along a line or at a point. Methods of evaluation of the integrals in Lamb's solutions are described in detail, and experimental verification of these solutions through the use of models is finally mentioned in this chapter. The propagation of plane waves and waves from an impulsive point source are again discussed in chapter 3 (50 pp.) for two semi-infinite media separated by a plane interface. Here the theory and experiment related to the problem of "refraction arrival" in seismology are discussed. A general n-layered half space is then dealt with in chapter 4 (131 pp.), in which the wave propagation due to an impulsive point source is given for a two- or three-layered liquid half space and for a liquid layer on a solid bottom. In the same chapter, the propagation of harmonic plane waves (Rayleigh and Love waves) is investigated for a two-layered solid half space and for the same when covered by an additional liquid layer, and many important geophysical problems are discussed. Chapter 5 (26 pp.) considers the effects of gravity, curvature and viscosity (through the use of the Voigt and Maxwell models for a viscoelastic solid). Chapter 6 (47 pp.) is on plates and cylinders, in which the well-known problem of Rayleigh and Lamb on the vibration of a plate and that of Pochhammer on the vibration of a cylindrical rod are discussed together with other problems. The last chapter (37 pp.) is concerned with wave propagation in heterogeneous isotropic media with variable velocity. Two appendixes (14 pp.) deal with the method of steepest descent and Rayleigh's principle. At the end of each chapter is a very comprehensive list of references on the topics discussed, which was compiled from the world literature, including the Russian, with a total of more than 600 entries.

It is only natural that the selection of topics reflects strongly the interest of the geophysicist. Seven-eighths of the book is devoted to semi-infinite bodies. Although the remaining one-eighth of the book (chapter 6) is on plates and cylinders, these also invariably extend to infinity. The authors did mention finite-size plates and rods, such as on page 281, "The plate can have either finite or infinite dimensions, and we now restrict ourselves to the latter case," and on page 312, "To extend the results mentioned here to vibrations of a finite rod, additional boundary conditions at the ends must be taken into account." These however do not reveal what would happen if such finite-body problems were to be solved on the basis of the exact Theory of Elasticity; to satisfy all the boundary conditions of a problem would be found extremely difficult. Such difficulty to a very large extent may be avoided if the problems are solved by using approximate theories, which are available for plates, rods and cylindrical tubes (such as those given in references 53, 54, 84 and 87 quoted in chapter 6 of the book) and are accurate enough for some practical purposes. In spite of its limited use in the

vibration studies of finite bodies, the exact Theory of Elasticity is nevertheless still important in that the accuracy of an approximate theory may be checked by comparing the results obtained from both theories for certain problems of bodies extending to infinity.

Another comment may be made that plates and cylinders composed of more than one solid layer (such as those used in sandwich construction) are not considered in the book, although the wave propagation and vibration problems of such bodies may readily be formulated by the use of the exact Theory of Elasticity. When such layered plates and cylinders are of finite dimensions, it is again desirable to use approximate theories. Such theories for layered plates, for instance, may be developed by employing the method given in reference 53 of chapter 6.

Needless to say, the comments in the last two paragraphs are from a viewpoint other than that of a geophysicist and are meant to supplement rather than to criticize the book. In fact, the reviewer feels that the book is so admirably written that it is a definite contribution to the literature on elastic-wave propagation.

Fluid Dynamic Drag, by Dr.-Ing. S. F. Hoerner, published by the author, Midland Park, N. J., 1958, xiv + 402 pp. $14.50.

Reviewed by RICHARD F. HOGLUND
Northwestern University

This book is a considerably revised and enlarged successor to "Aerodynamic Drag," published by the author seven years ago. The change in title is occasioned by the addition of two chapters concerning hydrodynamic resistance and the characteristics of waterborne craft. Another new chapter deals with wind forces on structures. The remainder of the book, dealing with aerodynamic drag of aircraft, missiles, landborne vehicles and other objects, is largely unchanged in organization but considerably enlarged by the incorporation of recent data, particularly in the transonic and supersonic speed ranges. The new book is considerably easier to read than the earlier edition, being improved in quality of printing and clarity of presentation, particularly in the figures.

The product of a dedicated effort in collecting, correlating and evaluating data, the book compactly presents a wealth of information on fluid dynamic resistance. The coverage is broad, including treatments of such diverse subjects as drag of aircraft, automobiles, railroad trains, the human body, parachutes, hydrofoils, bluff bodies in hypersonic flow and drag in rarefied atmospheres. Primary reliance is made on experimental data with theory used for extrapolation and correlation. In many instances, the methods of correlating and presenting the data are original. The sources of the author's information are carefully referenced and include virtually all applicable American and German publications through 1957.

In assessing the book, it must be considered that it is the only one of its

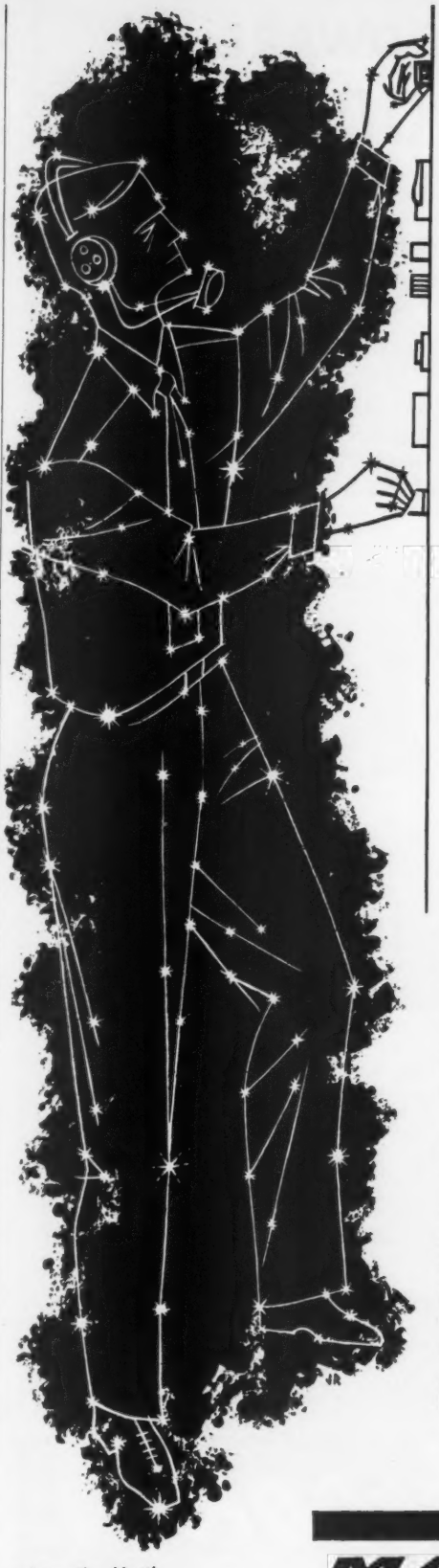

ARE YOU "WAY OUT THERE"?

ELECTRONIC ENGINEERS AND SCIENTISTS—whether their interests are "way out there" or closer home—can count on recognition at Martin. Your readiness for more responsibility will be reviewed constantly, verified by top-flight men eager to further your advancement for the benefit of all.

If your field is Navigation, Ground Support Equipment, Anti-Submarine Warfare, Surveillance or any other branch of electronics, write or phone William Spangler, Professional Employment, Dept. A5, The Martin Company, Baltimore 3, Maryland.

where the North meets the South

MARTIN
BALTIMORE

MISSILE HARDWARE
by NEWBROOK

Specializing in

- **MOTOR CASES**
  Solid and Liquid Propellants
- **JATO CASES**
- **NOZZLES**
- **PLENUM CHAMBERS**
- **BLAST TUBES**
- **FUEL INJECTORS**

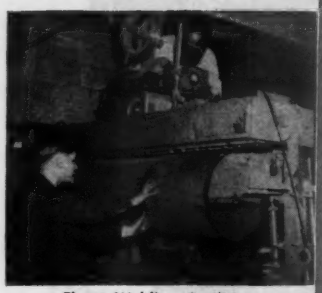

Finest Welding Facilities
Certified Welders

Machining Nozzles

X-Ray Inspection

We have the "KNOW-HOW"

We have developed new techniques, new methods, new processes that effect production economy so necessary to a successful missile program.

Here at Newbrook you will find men with experience gained from doing... a modern plant with up-to-date equipment... precision inspection to meet your most exacting quality control requirements.

And most important, Newbrook specialization results in strict reliability! Let us help you with your Missile Hardware problems.

Below: Machining Motor Cases

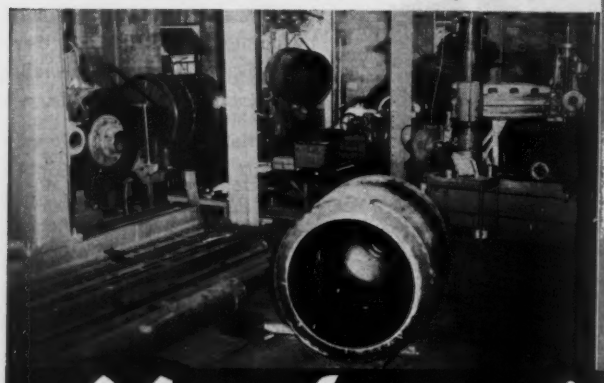

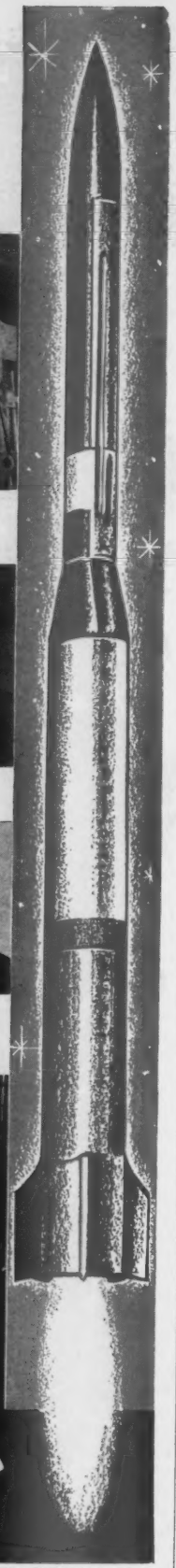

Newbrook
MACHINE CORPORATION

45 MECHANIC ST. PHONE 45 SILVER CREEK, N. Y.

kind available. For a person unfamiliar with the volume, it is not especially easy to use as a handbook. However, according to the author, it is not intended to be. Instead, it is designed to provide sufficient information for guiding the user to a solution of his problem. Perusing the volume, one feels that there is an overemphasis on the aerodynamic characteristics of obsolete configurations, such as the airplanes of the 1930's and early 1940's. In spite of this, the book represents a collection of information valuable to many engineers. For the practicing aerodynamicist, the data compilation and evaluation of this book can save considerable time and effort in making performance or loading computations. Yet it is written simply enough that any engineer concerned with objects moving through fluids can make use of the information. Thus, although not considered suitable as a textbook, "Fluid Dynamic Drag" is an important reference work recommended to the many engineers concerned with drag forces.

Advanced Dynamics, by John E. Younger, The Ronald Press Company, New York, 1958. $8.50.

Reviewed by RALPH BURTON
University of Missouri

Persons who show a real facility with the principles first covered in introductory engineering mechanics courses are rare. Their skill is seldom, if ever, acquired without further study, since it calls for an overall perspective of mechanics along with a proficiency in the several parts of the subject. Younger has written a textbook that will be welcomed by teachers attempting to provide such a course of study.

In rather broad chapters, he deals with kinematical analysis, dynamic specification of a rigid body, dynamics of angular motion, dynamics of plane motion, dynamics of motion in three dimensions, dynamics of beams. He includes discussion of elastic phenomena, Castigliano's theorem, and a pretty thorough introduction to vibration. Problems appear throughout the text. Younger's method of presentation is to break the subject down into parts and deal with these in some detail. In some ways this presentation leaves me unsatisfied. Often he seems to make several cases out of what might more logically be thought of as different aspects of a single case. On the other hand, this leaves little to be supplied by the student and may be the best way to prepare him to *use* his mechanics. Another objection is concerned with the author's reluctance to include discussion of the *meaning* of what is done. For example, there is very little discussion of Newton's laws of motion, and I do not believe it is ever made clear just why laws 1 and 3 are needed. I feel that additional discussion is needed also to clarify the presentation of angular momentum and the variable mass problem.

These objections should not be allowed to detract from the choice of material, the well worked out derivations and the suitability of the book for a one-semester course for engineers.

FROM LAGRANGIAN TO LIFT-OFF

Sometimes forgotten during the thundering ascent of a space probe rocket are months of meticulous analysis, engineering and planning. The staff of Space Technology Laboratories is now engaged in a broad program of space research for the Air Force, the National Aeronautics and Space Administration and the Advanced Research Projects Agency under the direction of the Air Force Ballistic Missile Division. For space probe projects STL provides the total concept approach, including preliminary analysis, sub-system development, design, fabrication, testing, launch operations and data evaluation. The total task requires subtle original analysis in many fields as well as sound technical management.

The STL technical staff brings to this space research the talents which have provided system engineering and technical direction since 1954 to the Air Force Ballistic Missile Program. Major missile systems currently in this program are Atlas, Titan, Thor and Minuteman.

The scope of STL's responsibilities offers creative engineers, physicists and mathematicians unusual opportunities to see their ideas tested in working hardware. Inquiries are invited regarding staff openings in the areas of Advanced Systems Analysis, Rocket Propulsion, Space Flight Mechanics, Dynamics, Structural Analysis, and Aerodynamics.

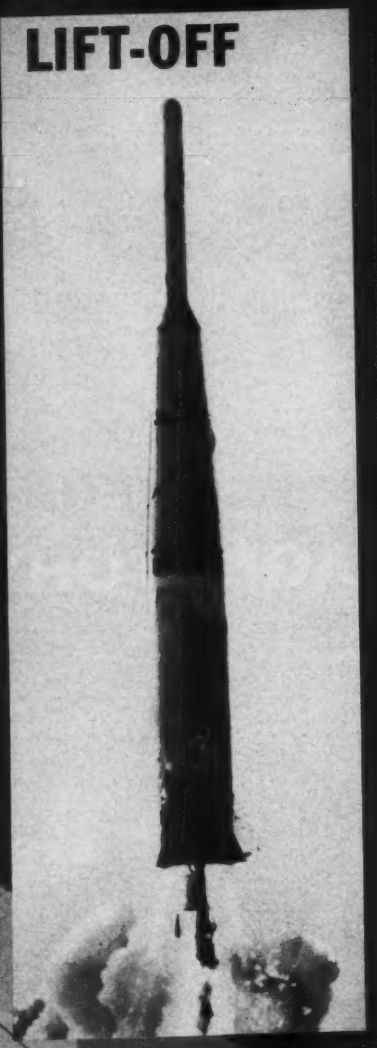

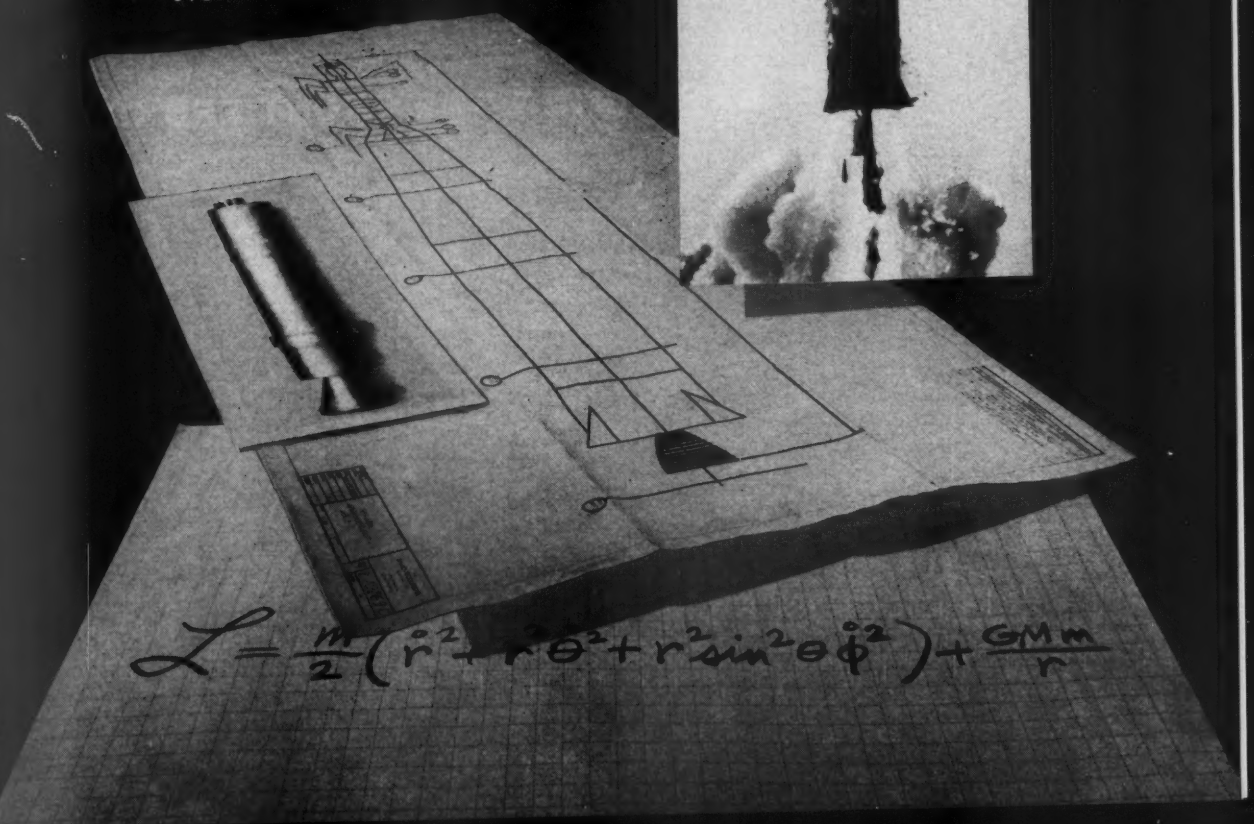

$$\mathcal{L} = \frac{m}{2}\left(\dot{r}^2 + r^2\dot{\theta}^2 + r^2\sin^2\theta\,\dot{\phi}^2\right) + \frac{GMm}{r}$$

Space Technology Laboratories, Inc.
P. O. Box 95004, Los Angeles 45, California

MAGNETOHYDRODYNAMICS

EXPANDING THE FRONTIERS OF SPACE

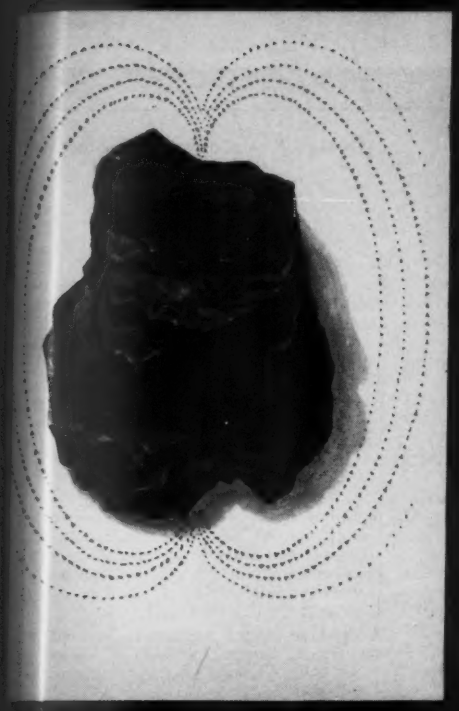

MAGNETOHYDRODYNAMICS Lockheed's 3rd Annual Symposium* on this important new field—which deals with the behavior of conducting fluids in magnetic fields—attracted physicists from all over the world. As portrayed by the artist, man's earliest experiments with magnetic forces involved the use of the ancient lodestone. Solar prominences are a dramatic example of such forces under investigation today.

Lockheed Missiles and Space Division has complete capabilities in more than 40 areas of science and technology—from concept to operation. Headquarters are at Sunnyvale, California, on the San Francisco Peninsula, with research and development facilities located in the Stanford Industrial Park, in nearby Palo Alto and at Van Nuys in the San Fernando Valley, of Los Angeles. A 4,000 acre, company-owned test base, 40 miles from Sunnyvale, conducts all phases of static field testing. In addition, complete flight testing is conducted at Cape Canaveral, Fla., Alamogordo, N.M., and Vandenberg AFB, Calif. as an integral part of every stage of missile and space programs at Lockheed.

The Division's advanced research and development programs now under intensive study provide a fascinating challenge to creative engineering. These programs include: man in space; space communications; electronics; ionic, nuclear and solar propulsion; magnetohydrodynamics; oceanography; computer research and development; operations research and analysis; human engineering; electromagnetic wave propagation and radiation; materials and processes and others.

Lockheed's programs reach far into the future and deal with unknown environments. It is a rewarding future which scientists and engineers of outstanding talent and inquiring mind are invited to share. Write: Research Development Staff, Dept. E-25, 962 W. El Camino Real, Sunnyvale, California. U.S. Citizenship required.

"The organization that contributed most in the past year to the advancement of the art of missiles and astronautics."
NATIONAL MISSILE INDUSTRY CONFERENCE AWARD.

ACHNOLOGY

Lockheed MISSILES AND SPACE DIVISION

Weapons Systems Manager for the Navy POLARIS FBM; DISCOVERER SATELLITE; Army KINGFISHER; Air Force Q-5 and X-7

SUNNYVALE, PALO ALTO, VAN NUYS, SANTA CRUZ, SANTA MARIA, CALIFORNIA
CAPE CANAVERAL, FLORIDA · ALAMOGORDO, NEW MEXICO · HAWAII

*Copies of the proceedings of the first two symposiums were published by the Stanford University Press, Palo Alto, Calif. and are available in book form. Results of this year's symposium will be published shortly by the same house.

New Patents

George F. McLaughlin, *Contributor*

Production of ammonium pentaborate and boric oxide (2,867,502). H. Stange and S. L. Clark, Tonawanda, N. Y., assignor to Olin Mathieson Chemical Corp.

Method consists of thermally decomposing ammonium pentaborate from borax.

Guided missile design (184,208) and Ramjet missile design (184,209). A. J. Bell, C. W. Besserer and E. A. Bonney, W. Hyattsville, Md., assignors to the U. S. Navy.

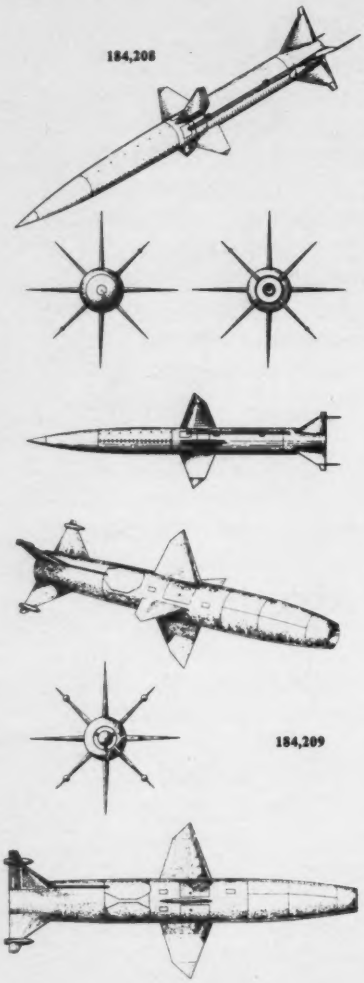

Developed at the Applied Physics Laboratory, Johns Hopkins University, Silver Spring, Md. in 1949. The guided missile, now in service, is the Terrier; the ramjet missile, about to go into service, is the Talos. Both missiles have undergone modifications since the original designs shown in the accompanying illustrations.

EDITOR'S NOTE: Patents listed above were selected from the Official Gazette of the U.S. Patent Office. Printed copies of patents may be obtained from the Commissioner of Patents, Washington 25, D. C., at a cost of 25 cents each; design patents, 10 cents.

Navigation device (2,867,393). R. M. Burley, Syosset, N. Y., assignor to Bendix Aviation Corp.

A member periodically interrupting rays from a celestial body, and cooperating with a sensitive means to produce signals when the energy received varies. Reversible motors operate azimuth and elevation controls in response to the signals and reference voltages to maintain the craft on a fixed course.

Method for the separation of hydrides (2,867,498). J. S. Roscoe and G. W. Schaeffer, St. Louis, Mo., assignors to Olin Mathieson Chemical Corp.

Process consists of contacting a mixture of lithium aluminum hydride and aluminum hydride with a molar amount, based on the moles of the hydrides present, of a lower tertiary alkyl amine while the reactants are in admixture with a lower dialkyl. The precipitate is separated from the reaction mixture.

Conversion of sodium tetrachloroaluminate to sodium aluminum hydride (2,867,499). C. D. Good and H. B. Batha, Grand Island, N. Y., assignors to Olin Mathieson Chemical Corp.

Process consists of reacting the two products with a lower dialkyl ether maintained in liquid phase, to form an addition product of aluminum chloride, and reacting the addition product with sodium hydride.

Self-stabilized burner (2,867,977). R. S. Buck, Glastonbury, Conn., assignor to United Aircraft Corp.

Ramjet power plant having means for automatically adjusting a blocking member in any one of various positions. A mechanism senses pressure of gases approaching the combustion chamber, proportionately blocking their passage.

Auxiliary rotor airfoil (2,868,302). A. C. Peterson, Minneapolis, Minn.

Jet units, at a substantial distance from the axis of a mounting pylon, supplied by fluid under pressure from a chamber controlled by a pressure responsive element.

Apparatus for igniting fuels (2,867,979). J. W. Mullen II, Richmond, Va., assignor to Experiment, Inc.

Ramjet with flameholder comprising an annular shroud with apertures to the manifold formed by the hollow of the shroud.

Aerodynamic wave machine (2,867,981). M. Berchtold, Paoli, Pa., assignor to I-T-E Circuit Breaker Co.

Machine to produce shaft power for a compressor and turbine, operating on a forward cycle of instantionary flow phenomenon. A first stator plate has a hot exhaust port and a cold air pick-up port. A second stator plate has a cold air intake port and a hot intake nozzle. The pick-up port has a higher pressure than the nozzle, causing a reflected compression wave.

Combustion chambers for jet propulsion engines (2,867,982). J. S. Clarke and E. S. Collinson, Wexford, Ontario, Canada, assignors to Joseph Lucos (Industries) Ltd.

Baffle with openings through which air from an annular entrance can flow between burner nozzles. Plates mounted on the approach side of the baffle set up a swirling motion in the air passing through the openings.

Gyroscopic apparatus (2,868,021). H. B. Sedgfield and W. F. Luttrelle, Holyport, England, assignors to The Sperry Gryoscope Co. Ltd.

Electromagnets, fixed to a gimbal frame support, having air gaps across which flux passes radially in the plane of the frame axes displaced at an angle to each frame axis. An energized coil connected to the rotor case is bowed outwardly in opposite positions to thread the gaps in the electromagnets.

Device for transforming rotary movemen to linear movement (2,868,030). H. Forwald, Ludvika, Sweden, assignor to Allmanna Svenska Elektriska Aktiebolaget.

Externally screw-threaded sleeve mounted to rotate with a driven shaft, and having limited axial movement. A nut engaging the threads is attached to a member extending beyond the housing to transmit linear motion from the rotary motion of the driving shaft.

Adjustable mirror support in successive dispersion monochrometer (2,868,063). E. L. Weiss, Philadelphia, Pa., assignor to Leeds and Northrup Co.

System including radiant energy dispersing means and a pair of angularly related plane mirrors for causing the energy to make another pass through the dispersing means. Mirrors are supported so as to provide a fine focus adjustment of the dispersed energy.

Jet propelled vertical take-off aircraft (2,868, 477). H. E. Chaplin, Hayes, England, assignor to The Fairey Aviation Co. Ltd.

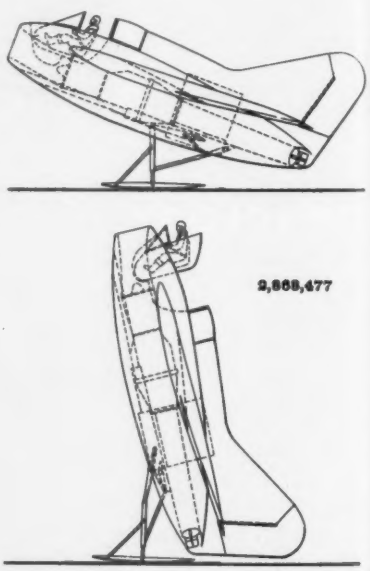

Jet engine capable of giving a total static thrust exceeding the weight of the aircraft. The undercarriage is movable to a position in which it supports the fuselage in a position for vertical takeoff. Power driven means, controllable by the pilot, moves the cockpit so the pilot remains in a horizontal seated position during changes of the angularity of the fuselage relative to the ground.

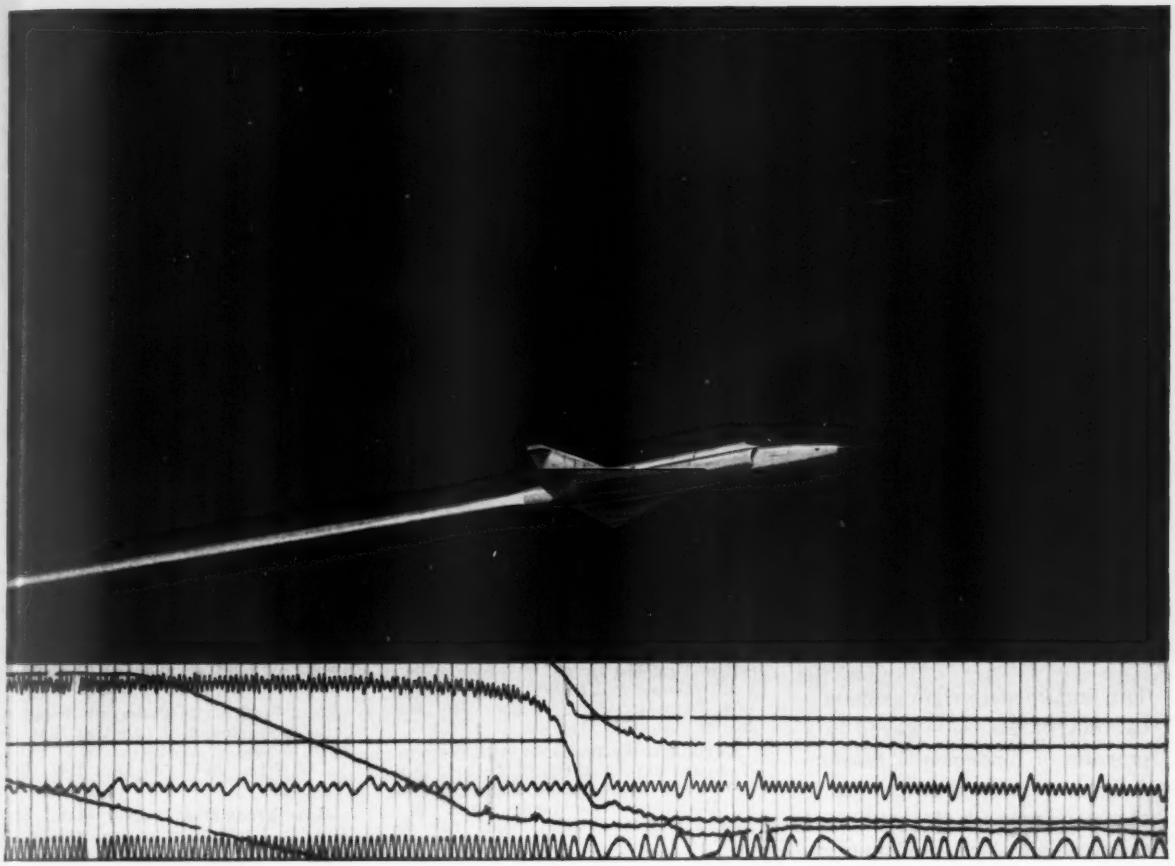

Now from Du Pont:

a complete line of photorecording papers and films

Du Pont now makes photorecording papers *and* films for your various recording needs. Here's what our complete photorecording line includes:

PHOTORECORDING PAPERS

Lino-Writ 1. Orthochromatic paper designed for average test requirements at lower writing speeds.

Lino-Writ 2. Moderately high-speed orthochromatic paper for use in intermediate speed recording requirements.

Lino-Writ 3. For high-frequency oscillographic traces without loss of detail.

These three papers are available in two types: Type B, standard-weight stock when greater opacity is required, and Type W, a thin, 100% all-rag stock.

Lino-Writ 4. It's the toughest, fastest, whitest paper you can use; 20% thinner than Type W, accommodates writing speeds as high as 5000 cps at maximum amplitude. Exceptional exposing and processing latitude. All-rag stock has unusual wet or dry strength.

PHOTORECORDING FILMS

CRONAR* Recording Film (High Speed)—relative speed (tungsten): 30.

Lino-Flex 1 (Regular Speed)—relative speed (tungsten): 10.

Both of these films are on Du Pont's exclusive CRONAR polyester photographic film base, which offers unexcelled strength, exceptional dimensional stability and flexibility. These fast-drying films have a fine matte surface which accepts pencil and ink markings.

PHOTORECORDING CHEMICALS

Lino-Writ Rapid Processing Chemicals Kit. Du Pont's high-speed, low-odor chemicals designed for rapid stabilization processing of papers *and* films.

For more information on our complete photorecording line, write: E. I. du Pont de Nemours & Co. (Inc.), Photo Products Department, Wilmington 98, Delaware. In Canada: Du Pont Company of Canada Limited, Toronto.

*CRONAR is Du Pont's trademark for its polyester photographic films

This advertisement was prepared exclusively by Phototypography

DU PONT
REG. U. S. PAT. OFF.

Better Things for Better Living . . . *through Chemistry*

Senior staff openings in basic research

THE BOEING SCIENTIFIC RESEARCH LABORATORIES are engaged in a program of fundamental research designed to make contributions to the progress of the physical sciences. High-level staff positions are open now in the fields of

Gas Dynamics
Plasma Physics
Mathematics
Solid State Physics
Electronics
Physical Chemistry
Geoastrophysics

Boeing grants scientists the latitude and independence needed to achieve and maintain leadership in their special fields. Scientists interested in carrying on their work in this kind of stimulating research environment are invited to communicate with Mr. G. L. Hollingsworth, Associate Director, Boeing Scientific Research Laboratories.

P. O. Box 3822 - JTA
Boeing Airplane Company
Seattle 24, Washington

BOEING

Technical Literature Digest

M. H. Smith, *Associate Editor,* **and M. H. Fisher,** *Contributor*
The James Forrestal Research Center, Princeton University

Jet Propulsion Engines

Rocket Motor Impulse Measurements by Means of an Inertia Wheel, by Benjamin V. Connor, *Calif. Inst. Tech., Jet Propulsion Lab., Mem.* no. 20-167, Sept. 1958, 12 pp.

The Research Combustor of the Instituto di Macchine, Politecnico di Torino, by F. Filippi, *L'Aerotecnica,* vol. 38, April 1958, pp. 88–95. (In Italian.)

On the Influence of the Form of Rocket Combustion Chambers, by L. Poggi, *L'Aerotecnica,* vol. 38, April 1958, pp. 109–110. (In Italian.)

Flame Stabilization in a Ramjet Combustion Chamber, by G. Salvatore, *L'Aerotecnica,* vol. 38, April 1958, pp. 111–116. (In Italian.)

Upper Atmosphere Atomic-oxygen Power Plant, by Sterge T. Demetriades, *J. Aero/Space Sci.,* vol. 25, Oct. 1958, p. 653.

Results of Theoretical Rocket Motor Performance Calculations for Liquid Propellant Systems, by G. W. Elverum Jr., J. S. Martinez and R. W. Gillespie, *Calif. Inst. Tech. Jet Propulsion Lab. Mem.* no. 20-159, Nov. 1957, 34 pp.

Combustor Performance with Various Hydrogen-oxygen Injection Methods in a 200-Pound-thrust Rocket Engine, by M. F. Heidmann and Louis Baker Jr., *NACA RM* no. E58E21, Sept. 1958, 45 pp.

Aerodynamics of Jet Propelled Missiles

General Formulation of Powered Flight Trajectory Optimization Problems, by Burton D. Fried, *J. Appl. Phys.,* vol. 29, Aug. 1958, pp. 1203–1209.

Effect of Favorable Pressure Gradients on Transition for Several Bodies of Revolution at Mach 3.12, by John R. Jack, *NACA TN* 4313, July 1958, 28 pp. diagrs., photo.

Correlation by the Hypersonic Similarity Rule of Pressure Distributions and Wave Drags for Minimum-drag Nose Shapes at Zero Angle of Attack, by Leland H. Jorgenson, *NACA Res. Mem.* A53F12, Aug. 1953, 23 pp., diagrs. (Declassified from Confidential by authority of *NACA Res. Abstr.* 128, 7/28/58.)

Angle of Attack Convergence of a Spinning Missile Descending through the Atmosphere, by Herman L. Leon, *J. Aero/Space Sci.,* vol. 25, Aug. 1958, pp. 480–484.

The Supersonic Blunt-body Problem—Review and Extension, by Milton D. Van-Dyke, *J. Aero/Space Sci.,* vol. 25, Aug. 1958, pp. 485–496.

The Flow of a Supersonic Jet in a Supersonic Stream at an Angle of Attack, by F. Edward Ehlers and Torstein Strand, *J. Aero/Space Sci.,* vol. 25, Aug. 1958, pp. 497–503.

EDITOR'S NOTE: Contributions from Professors E. R. G. Eckert, J. P. Hartnett, T. F. Irvine Jr. and P. J. Schneider of the Heat Transfer Laboratory, University of Minnesota, are gratefully acknowledged.

Heat Transfer and Fluid Flow

Flow Visualization Techniques Applied to Combustion Problems, by E. F. Winter, *J. Roy. Aeron. Soc.,* vol. 62, no. 568, April 1958, pp. 268–276.

Variable Fluid-property Problems in Free Convection, by E. M. Sparrow and J. L. Gregg, *ASME Paper* 57–A–46, Dec. 1–6, 1957, 8 pp.

The Thermal Conductivity of Nitrogen and Argon in the Liquid and Gaseous States, by H. Ziebland and J. T. A. Burton, *Brit. J. Appl. Phys.,* vol. 9, Feb. 1958, pp. 52–59.

Thermal Resistance of Eddy, by L. G. Clark and W. W. Hagerty, *J. AIChE,* vol. 3, no. 4, Dec. 1957, pp. 523–527.

On the Decay of Homogeneous Turbulence before the Final Period, by R. Deissler, *Phys. Fluids,* vol. 1, March-April 1958, pp. 111–121.

Combined Effects of Turbulence and Roughness on Transition, by H. Dryden, *ZAMP,* vol. 9B, 1958, pp. 249–258.

Heat Transfer to Turbulent Boundary Layer Downstream of Injection Slot, by R. A. Seban, H. W. Chan and S. Scesa, *ASME Paper* 57–A–36, Dec. 1–6, 1957, 11 pp.

Mass Transfer in Liquid Metal Systems, I: Thermal Gradient Transfer, by J. W. Taylor, *Nuclear Power,* vol. 3, Feb. 1958, pp. 53–57.

Some Effects of Kinetic Heating on the Stiffness of Thin Wings—Analysis of Flexural and Torsional Stiffnesses for Large Deformation of Thin Solid Wings, by S. L. Kochanski and J. H. Argyris, *Aircr. Engng.,* vol. 30, March 1958, pp. 82–85.

Numerical Determination of Transitory Temperatures in Wings, by G. Lehr, *Rev. Document. de la Tech. Aeron. Mondiale,* no. 48, Jan. 1958, pp. 3–14.

The Effects of Kinetic Heating on Aircraft Structures, by A. W. Kitchenside, *J. Roy. Aeron. Soc.,* vol. 62, Feb. 1958, pp. 105–117.

An Experimental Study of the Effect of Mass Injection at the Stagnation Point of a Blunt Body, by Howard M. McMahon, *Calif. Inst. Tech., Guggenheim Aeron. Lab., Hypersonic Res. Proj., Mem.* 42, May 1958, 132 pp.

The Thermodynamics of Steady Conduction-diffusion-reaction States of Multicomponent Fluid Systems, by W. Byers Brown, *Trans. Faraday Soc.,* vol. 54, June 1958, pp. 772–784.

Thermal Diffusion in Liquids, by Stephen Whitaker and R. L. Pigford, *Ind. & Engng. Chem.,* vol. 50, July 1958, pp. 1026–1032.

Calculation of Reaction Profiles behind Steady-state Shock Waves, I: Application to Detonation Waves, by Russell E. Duff, *J. Chem. Phys.,* vol. 28, June 1958, pp. 1193–1197.

High-temperature Gas Viscosities, I: Nitrous Oxide and Oxygen, by C. J. G. Raw and C. P. Ellis, *J. Chem. Phys.,* vol. 28, June 1958, pp. 1198–1200.

Ettingshausen Effect and Thermomag-

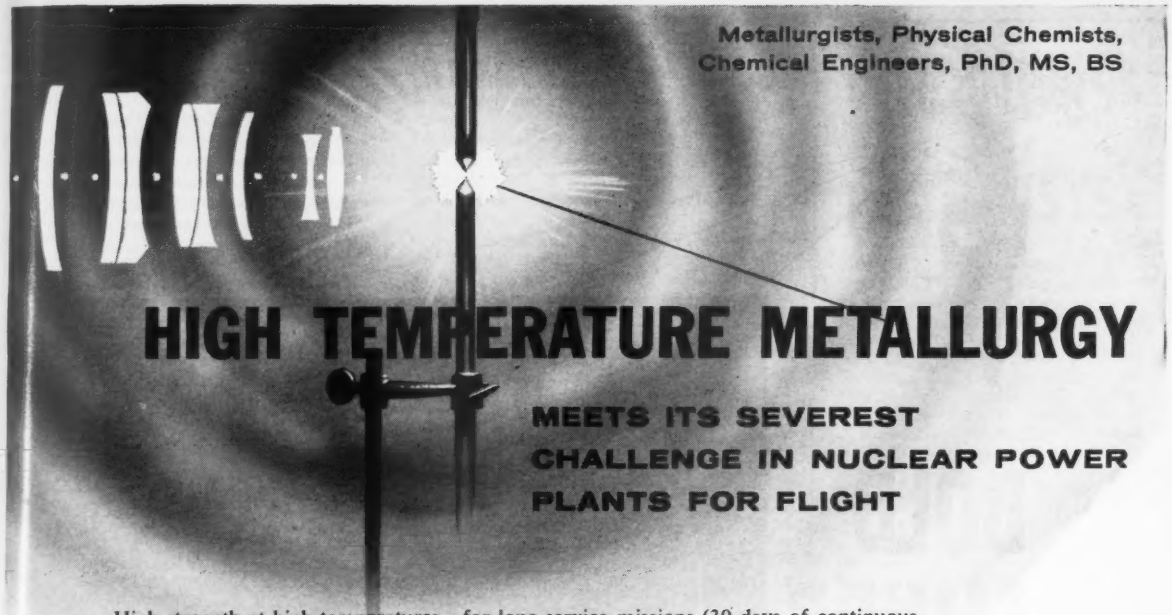

Metallurgists, Physical Chemists,
Chemical Engineers, PhD, MS, BS

HIGH TEMPERATURE METALLURGY

MEETS ITS SEVEREST CHALLENGE IN NUCLEAR POWER PLANTS FOR FLIGHT

High strength at high temperatures – for long service missions (30 days of continuous flight and more are envisaged) is a primary consideration in the selection and development of materials for structures and components of General Electric's 2nd and 3rd generation nuclear propulsion systems for flight application.

A complex of additional parameters, however, must be taken into consideration by G-E engineers and scientists... radiation effects, nuclear properties for specific application, stringent weight limitations, etc.

Engineers and Scientists who value the opportunity to do original work with a company that fosters free inquiry and initiative, are invited to inquire about positions now open in both APPLIED RESEARCH *and* MATERIALS DEVELOPMENT:

DIRECT processing and procurement of basic alloys for elevated temperature applications. PhD, MS, 3-7 years experience.

CONDUCT liaison with technical production and project personnel on problems related to quality in fuel element production. PhD, MS, 3-7 years experience.

ADVISE Materials Testing Lab on materials problems and techniques. Direct experimental, physical, mechanical and electrical tests. PhD, MS, 3-7 years experience.

CARRY ON investigations of reactions in the solid state for Materials Testing Laboratories. PhD, Physical Chemistry.

PARTICIPATE in research on advanced moderator materials. Investigations in field of ionic, covalent and metallic bonding; hydrogen stability in metals at elevated temperatures; kinetics of advanced moderator systems. MS.

PERFORM laboratory investigations in metallurgical melting, casting, fabricating and forming processes. Also phase studies; solid solution alloy studies. MS preferred.

DIRECT studies on materials used in moderator materials development. PhD.

PROGRAM and evaluate specific tests on fuel element materials and assemblies. Compile and publish data. MS, BS, 5-7 years R&D experience.

CONDUCT project technical liaison on materials selection and processing. Develop design data on materials. BS, 5-7 years experience with high temperature alloys.

CARRY OUT liaison with materials subcontractors. BS with 7-9 years experience in development or sales engineering.

ASSIST in development of instrumentation for measuring high temperatures and other instrumentation. MS, BS, 1-3 years experience.

If you qualify, please write in confidence,
including salary requirements, to: Mr. P. W. Christos, Div. 35-ME.

AIRCRAFT NUCLEAR PROPULSION DEPARTMENT

GENERAL ELECTRIC

P.O. Box 132 • Cincinnati 15, Ohio

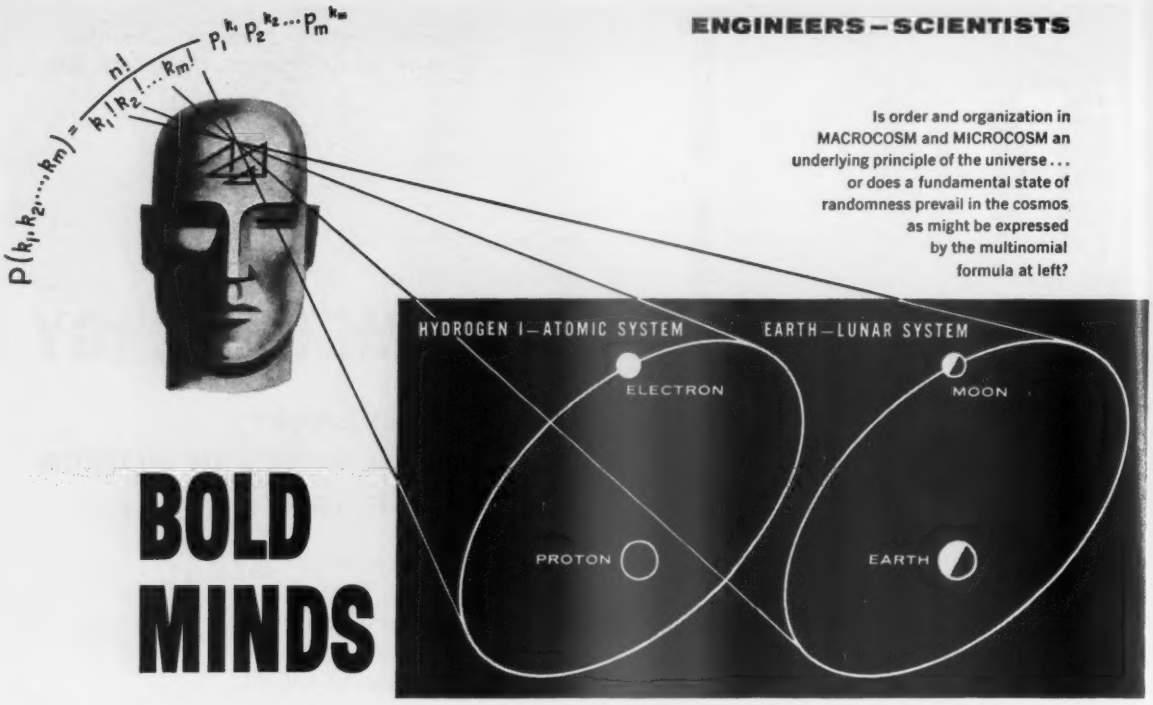

ENGINEERS—SCIENTISTS

Is order and organization in MACROCOSM and MICROCOSM an underlying principle of the universe... or does a fundamental state of randomness prevail in the cosmos as might be expressed by the multinomial formula at left?

BOLD MINDS

THROUGHOUT HISTORY..... BOLD MINDS have sought to understand the forces at work in the universe, and as they developed working hypotheses, endeavored to turn all knowledge to their own purposes, devising philosophical and mechanical systems of their own.

As old hypotheses become inadequate or untenable, thinking men devise new ones. So the concept of a "flat" world has changed to an oblate orbiting spheroid—mere speck in a vast and expanding universe; so "empty" formless space is regarded as a curved continuum occupied by random knots of turbulence (creating the new branch of mechanics—hydromagnetics).

Today new horizons of discovery and surmise arise before the speculative mind.

ENGINEERS AND SCIENTISTS AT REPUBLIC FEEL KINSHIP WITH ALL BOLD MINDS OF PAST AND PRESENT, AS THEY FACE THE EXHILARATING CHALLENGES OF CREATING VEHICLES TO FLY IN ENVIRONMENTS WHERE NEW APPROACHES IN THERMO/AERODYNAMICS MUST BE MADE...AS WELL AS APPROPRIATE PROPULSION AND ELECTRONIC SYSTEMS TO POWER AND GUIDE TRANSIT IN SPACE

Groups of Research, Development and Experimental Engineers and Scientists at Republic Aviation are now working on projects over the whole range of aeronautics and astronautics—from supersonic and hypersonic weapons systems, both manned and unmanned, to plasma propulsion and space electronics.

Imaginative professional men at many levels of experience are invited to inquire about opportunities indicated below:

ELECTRONICS
- Inertial Guidance & Navigation
- Digital Computer Development
- Systems Engineering
- Information Theory
- Telemetry-SSB Technique
- Doppler Radar
- Countermeasures
- Radome & Antenna Design
- Microwave Circuitry & Components
- Receiver & Transmitter Design
- Airborne Navigational Systems
- Jamming & Anti-Jamming
- Miniaturization-Transistorization
- Ranging Systems
- Propagation Studies
- Ground Support Equipment

THERMO, AERODYNAMICS
- Theoretical Gasdynamics
- Hyper-Velocity Studies
- Astronautics Precision Trajectories
- Airplane/Missile Performance
- Air Load and Aeroelasticity
- Stability and Controls
- Flutter & Vibration
- Vehicle Dynamics & System Designs
- High Altitude Atmosphere Physics
- Re-entry Heat Transfer
- Hydromagnetics
- Ground Support Equipment

PLASMA PROPULSION
- Plasma Physics
- Gaseous Electronics
- Hypersonics and Shock Phenomena
- Hydromagnetics
- Physical Chemistry
- Combustion and Detonation
- Instrumentation
- High Power Pulse Electronics

NUCLEAR PROPULSION & RADIATION PHENOMENA
- Nuclear Weapons Effects
- Radiation Environment in Space
- Nuclear Power & Propulsion Applications
- Nuclear Radiation Laboratories

A new $14,000,000 Research Center—to be completed this year—is part of Republic's far-ranging R&D programs aimed at major state-of-the-art breakthroughs in every flight regime & environment.

Send resume in complete confidence to:
Mr. George R. Hickman, ENGINEERING EMPLOYMENT MANAGER—DEPT. 10E

REPUBLIC AVIATION
FARMINGDALE, LONG ISLAND, NEW YORK

netic Cooling, by B. J. O'Brien and C. S. Wallace, *J. Appl. Phys.*, vol. 29, July 1958, pp. 1010–1012.

Electrically Driven Shock Tube, by D. E. Bloxsom Jr., *J. Appl. Phys.*, vol. 29, July 1958, pp. 1128–1129.

Flows in Partly Dissociated Gases, by Manfred Heil, *J. Aero/Space Sci.*, vol. 25, July 1958, pp. 459–460.

The Injection of Air into the Dissociated Hypersonic Laminar Boundary Layer, by Sinclaire M. Scala, *J. Aero/Space Sci.*, vol. 25, July 1958, pp. 461–462.

On the Aerodynamic Heating of Blunt Bodies, by E. R. van Driest, *ZAMP*, vol. 9B, March 25, 1958 (Jakob Ackeret anniv. vol.), pp. 233–248.

Combustion, Fuels and Propellants

Calculated Heats of Formation and Combustion of Boron Compounds (Boron, Hydrogen, Carbon, Silicon), by Aubrey P. Altshuller, *NACA Res. Mem.* E55G26, Oct. 1955, 28 pp.

Aluminum Borohydride as an Ignition Source for Turbojet Combustors, by David M. Straight, Edward A. Fletcher and Hampton H. Foster, *NACA Res. Mem.* E53G15, Sept. 1953, 19 pp. (Declassified from Confidential by authority of *NACA Res. Abstr.* 129, 7/17/58.)

The Heat of Combustion of Tetraethyldiborane, by Stanley Tannenbaum, *NACA Res. Mem.* E53E11, Jan. 1957, 5 pp. (Declassified from Confidential by authority of *NACA Res. Abstr.* 129, 7/17/58.)

Fundamental Flame Velocity, Heat of Combustion, and Spontaneous Ignition Temperature of Dimethylaminodiborane, by Robert R. Hibbard and Gordon L. Dugger, *NACA Res. Mem.* E52L23, Dec. 1956, 6 pp. (Declassified from Confidential by authority of *NACA Res. Abstr.* 129, 7/17/58.)

Continuous Combustion Problems in Aero Engines, by A. Capetti, *L'Aerotecnica*, vol. 38, Feb. 1958, pp. 3–7. (In Italian.)

Flame Stabilization in Air-breathing Jet Engines, by F. Filippi, *L'Aerotecnica*, vol. 38, Feb. 1958, pp. 19–38. (In Italian.)

Liquid Propellants for Rocket Engines, by E. Macioce, *L'Aerotecnica*, vol. 38, Feb. 1958, pp. 44–47. (In Italian.)

On Turbulence in Flames, by A. G. Prudnikov, *Akad. Nauk SSSR, Izvestia, Otdel. Tekh. Nauk*, no. 7, July 1958, pp. 130–133.

Preparation and Thermal Stability of Lithium Titanium Fluoride, by George J. Janz, Max R. Lorenz and Charles T. Brown, *J. Amer. Chem. Soc.*, vol. 80, Aug. 20, 1958, pp. 4126–4128.

Detonation Velocity of Gaseous Ozone, by A. G. Streng, C. S. Stokes, and L. A. Streng, *J. Chem. Phys.*, vol. 29, Aug. 1958, pp. 458–459.

The Ignition of Primary Explosives by Electric Discharges, by R. M. H. Wyatt, P. W. J. Moore, G. K. Adams and J. F. Sumner, *Proc. Roy. Soc., London*, vol. A 246, July 29, 1958, pp. 189–196.

The Explosion of Silver Azide in an Electric Field, by F. P. Bowden and A. C. Mclaren, *Proc. Roy. Soc., London*, vol. A 246, July 29, 1958, pp. 197–198.

Structure and Stability of Inorganic Azides, by B. L. Evans, *Proc. Roy. Soc., London*, vol. A 246, July 29, 1958, pp. 199–202.

Thermal Decomposition, Inflammation, and Detonation, by W. E. Garner, *Proc. Roy. Soc., London*, vol. A 246, July 29, 1958, pp. 203–215.

The Initiation of Explosion by Neutrons, A-particles and Fission Products, by F. P. Bowden, *Proc. Roy. Soc., London*, vol. A 246, July 29, 1958, pp. 216–218.

The Effect of Nuclear Radiation on Explosives, by J. V. R. Kaufman, *Proc. Roy. Soc., London*, vol. A 246, July 29, 1958, pp. 219–232.

Preparation and Properties of Crystals of KN_3 and NaN_3, by R. W. Dreyfus and P. W. Levy, *Proc. Roy. Soc., London*, vol. A 246, July 29, 1958, pp. 233–239.

The Initiation of Explosion by Light, by J. Eggert, *Proc. Roy. Soc., London*, vol. A 246, July 29, 1958, pp. 240–247.

Ignition of Explosives by Light, by J. H. L. McAuslan, *Proc. Roy. Soc., London*, vol. A 246, July 29, 1958, pp. 248–253.

The Growth of Explosion in Solids, by A. D. Yoffe, *Proc. Roy. Soc., London*, vol. A 246, July 29, 1958, pp. 254–256.

Some Considerations on the Mechanism of Initiation of Detonation Explosives, by K. K. Andreev, *Proc. Roy. Soc., London*, vol. A 246, July 29, 1958, pp. 257–267.

The Initiation of Explosives by Shock, by G. P. Chachia and E. G. Whitbread, *Proc. Roy. Soc., London*, vol. A 246, July 29, 1958, pp. 268–273.

Sympathetic Detonation and Initiation by Impact, by R. J. Eichelberger and M. Sultanoff, *Proc. Roy. Soc., London*, vol. A 246, July 29, 1958, pp. 274–280.

Deflagration to Detonation Transition in Solid and Liquid Explosives, by M. A. Cook, D. H. Pack and W. A. Gey, *Proc. Roy. Soc., London*, vol. A 246, July 29, 1958, pp. 281–283.

The Initiation of Condensed Explosives by Shock Waves from Metals, by W. R. Marlow and I. C. Skidmore, *Proc. Roy. Soc., London*, vol. A 246, July 29, 1958, pp. 284–287.

Materials of Construction

Fatigue of Structural Materials at High Temperatures, by B. J. Lazan, *NATO, AGARD, Rep.* 156, Nov. 1957, 27 pp.

Influence of Hot-working Conditions on High-temperature Properties of a Heat-resistant Alloy, by John F. Ewing and J. W. Freeman, *NACA Rep.* 1341, 1957, 52 pp. (supersedes TN 3727).

Limit Design for Economical Missile Structures, by L. A. Reidinger, *Aviation Age*, vol. 30, Oct. 1958, pp. 32–39.

301 Stainless Modified for 800 Deg F and Up, by D. B. Roach, A. M. Hall, R. Sergesen and A. R. Stargardter, *Aviation Age*, vol. 30, Oct. 1958, pp. 58–63.

Friction and Wear with Reactive Gases at Temperatures up to 1200° C, by Gordon P. Allen, Donald H. Buckley and Robert L. Johnson, *NACA TN* 4316, Sept. 1958, 26 pp.

A Phenomenological Relation between Stress, Strain Rate, and Temperature for Metals at Elevated Temperatures, by Elbridge Z. Stowell, *NACA Rep.* 1343, 1958, 6 pp. (supersedes TN 4000).

Structures and Heat at Supersonic and Hypersonic Speeds, by B. Dorleac, *NATO, AGARD, Rep.* 149, Nov. 1957, 78 pp. (In French.)

On Ceramic-metallic Materials, Ceramic Materials and High Temperature Protecting Lines for Jet Engines, by R. M.

ENGINEERS AND SCIENTISTS

Here is your opportunity to grow with a young, expanding subsidiary of the Ford Motor Company. Outstanding career opportunities are open in Aeronutronic's new RESEARCH CENTER, overlooking the Pacific at Newport Beach, and the facility in Glendale, California. You will have all the advantages of a stimulating mental environment, working with advanced equipment in a new facility, located where you can enjoy California living at its finest.

PhD and MS RESEARCH SPECIALISTS with 5 to 7 years' experience in heat transfer, fluid mechanics, thermodynamics, combustion and chemical kinetics, and thermoelasticity. To work on theoretical and experimental programs related to re-entry technology and advanced rocket propulsion. Specific assignments are open in re-entry body design, high temperature materials studies, boundary layer heat transfer with chemical reaction, thermal stress analysis, and high temperature thermodynamics.

PROPULSION ENGINEERS with 5 years' experience in liquid and solid rocket design and test. Familiarity with heat transfer problems in engines desirable. To work on program of wide scope in R & D of advanced concepts in rocket engine components, and for missile project work.

APPLIED MATHEMATICIANS, 3–5 years' recent experience required and A.B. or M.A. degree. Experience in numerical analysis and computer work in connection with rockets and rocket propellants.

STRESS HIGH TEMPERATURE MATERIALS. Mechanical or Metallurgical Engineer, must be familiar with thermal stress and shock as well as elasticity and plasticity. Application to nose cones and thrust chambers.

FLIGHT TEST & INSTRUMENTATION ENGINEERS with 5 to 10 years' experience in laboratory and flight test instrumentation techniques. Will develop techniques utilizing advanced instrumentation associated with space vehicles.

THEORETICAL AERODYNAMICIST. Advanced degree and at least 5 years' experience in high-speed aerodynamics. Knowledge of viscid and gas flows required. To work on program leading to advanced missile configurations. Work involves analysis of the re-entry of hypersonic missiles and space craft for determining optimum configuration.

CERAMICIST. M.S. or Ph.D. required and 3–5 years' recent experience with high temperature materials, structures and cermets.

ENGINEER or PHYSICIST. With experience in the use of scientific instruments for making physical measurement. Work related to flight test and facility instrumentation. Advanced degree desired with minimum of 3 years of related experience.

Qualified applicants are invited to send résumés and inquiries to Mr. R. W. Speich, Aeronutronic Systems, Inc.

AERONUTRONIC

a subsidiary of Ford Motor Company

2234 Air Way Bldg. 19, Glendale, Calif.
CHapman 5-6651

Newport Beach, Glendale, Santa Ana, and Maywood, California

You can explore new areas at IBM in

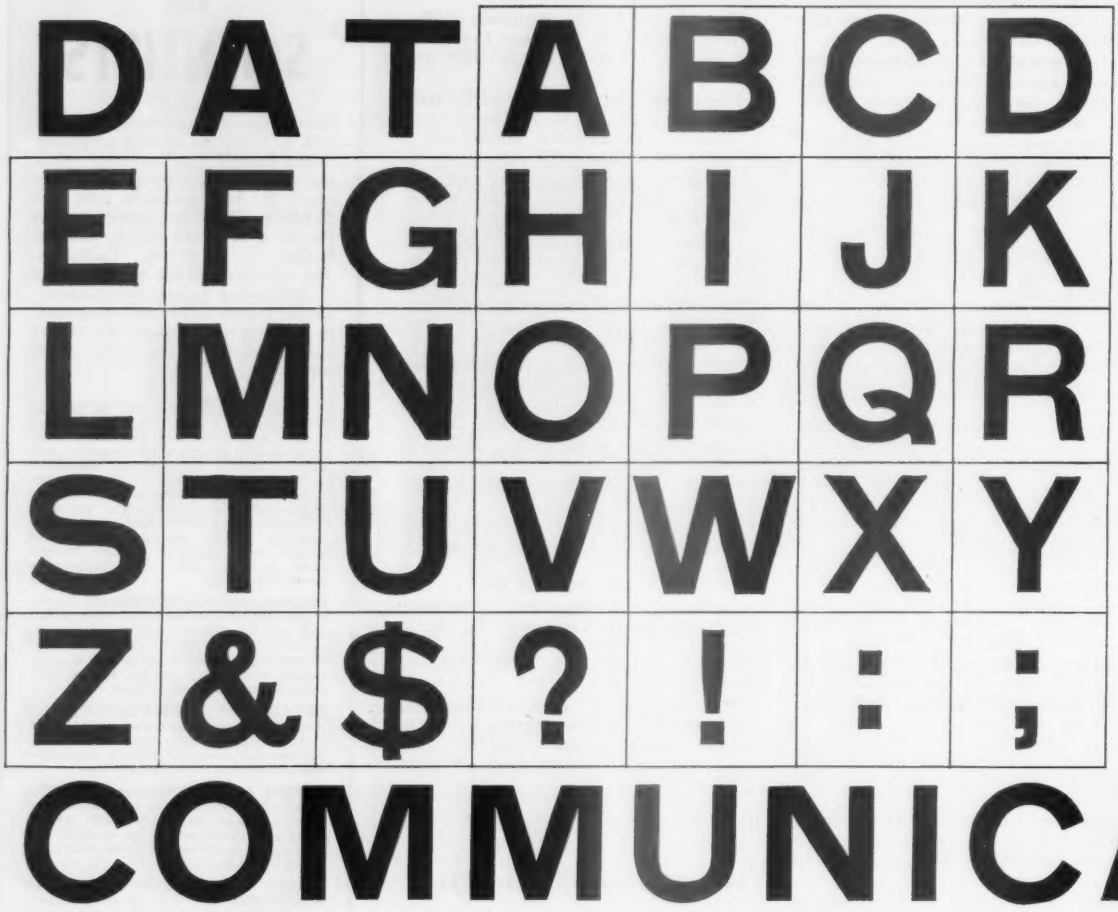

Creative people at IBM are hard at work on a problem that has vexed man since the dawn of history—communication with his fellow beings. The rapid transmission of precise data is vital in this fast-moving age. One group of engineers and scientists at IBM is working on multiplexing techniques to channel data. This data has to be made available at maximum speed at desired times and places. Another group is developing computer systems that will control complete warehousing or industrial operations. For the military, IBM is designing a computer that will make available in real time, data concerning troop strength and dispositions. This important work needs imaginative people. If you want to be a part of this world of discovery and development, there are many opportunities at IBM.

A NEW WORLD OF OPPORTUNITY. Both technical and administrative engineering careers offer parallel advancement opportunities and rewards at IBM. You will enjoy unusual professional freedom, comprehensive education programs, the assistance of specialists of diverse disciplines, and IBM's wealth of systems know-how. Working independently or as a member of a small team, your individual contributions are quickly recognized and rewarded. This is a unique opportunity for a career with a company that has an outstanding growth record.

IBM®

For details, write, outlining background and interests, to:
Mr. R. E. Rodgers, Dept. 572E
IBM Corporation
590 Madison Avenue
New York 22, N. Y.

INTERNATIONAL BUSINESS MACHINES CORPORATION

CAREERS AVAILABLE IN THESE AREAS...

CIRCUIT DESIGN & RESEARCH
COMMUNICATIONS
COMPONENT ENGINEERING
COMPUTER ANALYSIS & DESIGN
CRYOGENICS
ENGINEERING PHYSICS
INERTIAL GUIDANCE
INDUSTRIAL CONTROL
INFORMATION THEORY
LOGICAL DESIGN
MATHEMATICS
OPTICS
PROGRAMMING
RADAR
REAL TIME STUDIES
SEMICONDUCTOR DESIGN
SOLID STATE DEVELOPMENT
SYSTEMS DEVELOPMENT

Qualifications: B.S., M.S., or Ph.D. in Electrical or Mechanical Engineering, Physics, or Mathematics — and proven ability to assume a high degree of technical responsibility in your sphere of interest.

GENERAL DESCRIPTIONS OF SOME ASSIGNMENTS:

SYSTEMS ENGINEERS to analyze and design computer systems. Backgrounds required include analog to digital conversion; analyses and preparation of diagnostic programs; development of complex devices in servo-mechanisms or radar for advanced systems.

LOGICAL DESIGNERS with two to four years' experience outlining logical blocks. Previous computer experience desirable. Some experience in transistorized equipment specification helpful. Must have strong interest in the theoretical and practical aspects of checking means and various codes, redundancy, error detection and correction, information flow, and other factors.

SOLID STATE ENGINEERS AND SCIENTISTS to do applied research on precision linear circuitry employing solid state devices using analog to digital conversion techniques and sample data. Experience in feed-back amplifier design desirable. Also opening for engineers with experience in precision, low-level linear circuits employing solid state, to work on analog to digital conversion techniques.

AT 1 O NS:

2	9
3	8
4	7
5	6

INDUSTRIAL CONTROL ENGINEERS to perform precision AC and DC electric measurements. Assignments in amplifier design, relay circuit logic, test equipment development, analog to digital conversion, and noise reduction.

CIRCUIT DESIGNERS to design transistor amplifiers, relay lines, transistor tube conversion circuits. Develop systems circuit specifications, perform circuit evaluation experiments and reliability criteria. Other openings in circuit design for magnetic devices.

MATHEMATICIANS to do digital computer programming, handle analysis-of-variance and multiple-regression type problems. Design experiments for wide variation of engineering applications. Knowledge of application of probability or game theory desirable.

Carelli, *L'Aerotecnica*, vol. 38, no. 2, April 1958, pp. 71–87. (In Italian.)

Instrumentation, Data Recording, Telemetering

Kinematic Drift of Single-Axis Gyroscopes, by R. H. Cannon Jr., *J. Appl. Mech.*, vol. 25, no. 3, Sept. 1958, pp. 357–360.

Telemetry Standards for Guided Missiles, *Electronics*, vol. 31, Oct. 24, 1958, pp. 96–98.

Five Hole Spherical Pitot Tube, by P C. Pien, *David Taylor Model Basin, Rep.*, 1229, May 1958, 17 pp.

High-pressure Gas-to-liquid Transducer, by Don O. Coffin, *Rev. Sci. Instr.*, vol. 29, Oct. 1958, p. 896.

Microwave Manometer, by Arnold G. Kramer and Philip M. Platzman, *Rev. Sci. Instr.*, vol 29, Oct. 1958, p. 897.

Guidance Components and Systems

How to Beat Instrument Blindness, by George A. LeHew and James R. Andres, *Aviation Age*, vol. 30, Oct. 1958, pp. 64–69.

Microelectronics: Small Circuits Set for Big Role in Future Systems, by James Holahan, *Aviation Age*, vol. 30, Oct. 1958, pp. 20–21, 166–170.

Guidance for the Space Age, by C. J. Mundo and E. W. Tooher, *Aero/Space Engng.*, vol. 17, no. 9, Sept. 1958, pp. 30–33.

Some Effects of Wind and Temperature Gradients on the Design of Missile Flight Control Systems, by Melvin W. Lifson, *Aero/Space Engng.*, vol 17, no. 9, Sept. 1958, pp. 49–52.

Effects of Gyrosconic Cross Coupling on Missile Automatic Flight Control Systems, by J. G. McCracken, *Aero/Space Engng.*, vol. 17, Nov. 1958, pp. 70–73.

Flight Vehicle Design and Testing

On the Optimum Trajectory of a Rocket, by Robert R. Newton, *J. Franklin Inst.*, vol. 266, Sept. 1958, pp. 155–187.

Topics in Dynamic Programming for Rockets, by Angelo Miele and James O. Cappellari Jr., *Purdue Univ., School of Aeron. Engng., Rep.* A-58-5 (*AFOSR-TN-58-685; ASTIA AD* 162218), July 1958, 58 pp., 7 figs.

Missile Noise as a Factor in Reliability, by Paul S. Veneklasen, *Aero/Space Engng.*, vol. 17, no. 9, Sept. 1958, pp. 44–48.

Problems in the Development of a Guided Weapon, by J. Clemow, *J. Roy. Aeron. Soc.*, vol. 62, no. 575, Sept., 1958, pp. 663–673.

On Flight Trajectories in the Neighborhood of a Known Trajectory, by R. M. Rosenberg, *J. Franklin Inst.*, vol. 266, no. 2, Aug. 1958, pp. 109–128.

Space Flight

Rocket Propulsion Requirements for Satellites and Moon Missions, by John L Sloop, *Aero/Space Engng.*, vol. 17, Nov. 1958, pp. 36–44, 50.

An Application of Solar Radiation to Space Navigation, by S. James Press, *Aero/Space Engng.*, vol. 17, Nov. 1958, pp. 51–54.

Y.C. Lee

His full name is Yuan Chu'en Lee, but to most of us at Aerojet, he's known as "Y.C." As Director of Corporate Research, Y.C. is in charge of our astronautical, other-planetary endeavors.

Y.C. and his associates are grappling with the knottier questions of space technology and advanced propulsion. They're studying advanced magnetohydrodynamics, extraterrestrial physics, and relativistic problems. They're looking for new fuels based on ions, gaseous free radicals, and nuclear plasmas.

Fundamental research has kept Aerojet at the forefront of the rocket field. Thanks to people like Y.C. and his team, we'll stay there.

That team, by the way, is hand-picked. It's one of several such groups at Aerojet that offer opportunities of unusual scope to the scientific and engineering imagination. Let us see a resume if this is your kind of challenge. The address: AEROJET-GENERAL CORPORATION, P.O. Box 296, Azusa, California or P.O. Box 1947, Sacramento, California. Attn: Director of Scientific and Engineering Personnel.

AEROJET-GENERAL CORP.

THE GENERAL TIRE

AZUSA AND SACRAMENTO, CALIFORNIA • A SUBSIDIARY OF THE GENERAL TIRE & RUBBER COMPANY

Air-breathing Power Plants in the Space Era, by Peter G. Kappus, *Aero/Space Engng.*, vol. 17, Nov. 1958, pp. 62–65, 69.

On the Mechanisms of Meteoric Ablation, by Sin-I. Cheng, *Princeton Univ., Dept. Aeron. Engng., Rep.* 427 (*AFOSR-TN*-58-649; *ASTIA AD* 162181), April 1958, 21 pp., 8 figs.

Bibliography of Space Medicine, *Public Health Service, Publication* 617 (Bibliography series 21), 1958, 49 pp.

Satellite Orbits in Theory and Practice, by D. G. King-Hele and R. H. Merson, *J. Brit. Interplanet. Soc.*, vol. 16, no. 8, July-Aug. 1958, pp. 446–453.

Russian Technical Articles*

About Noise Stability of Pulse Frequency Telemetering, by N. V. Pozin, *Automatika i Telemekhanika*, vol. 19, no. 10, Oct. 1958, pp. 968–979. (In Russian.)

Pulse Servosystems Including Two Pulse Elements with Unequal Repetition Periods, by Fan Chun-wui, *Automatika i Telemekhanika*, vol. 19, no. 10, Oct. 1958, pp. 917–930. (In Russian.)

Determination of Periodic Behavior of Automatic Control Systems Having a Nonlinear Part with Piece-linear Characteristic, by L. A. Gusev, *Automatika i Telemekhanika*, vol 19, no. 10, Oct. 1958, pp. 931–944. (In Russian.)

About Equivalency of Discontinuous and Continuous Control Systems, by V. A. Rubtsov, *Automatika i Telemekhanika*, vol. 19, no. 10, Oct. 1958, pp. 945–957. (In Russian.)

On the Theory of Gas Jets, by L. N. Stretensky, *Doklady Akad. Nauk SSSR*, vol. 119, April 21, 1958, pp. 1113–1114. (In Russian.)

A Spectrographic Investigation of the Condition of a Gas Behind a Shock Wave, by N. N. Sobolev and others, *Izvestiia Akad. Nauk SSSR, Ser. Fiz.*, vol. 22, June 1958, pp. 730–736. (In Russian.)

On Certain Exact Solutions of the Gas Dynamics Equations, by S. S. Grigorian, (translated from *Doklady Akad. Nauk SSSR*, vol. 121, Aug. 1, 1958, pp. 606–609). Morris D. Friedman, Inc., Needham Heights 94, Mass., Translation no. G-156.

One-Dimensional Self-Similar Motions of a Conducting Gas in a Magnetic Field, by V. P. Korobeinikov (translated from *Doklady Akad. Nauk SSSR*, vol. 121, Aug. 1, 1958, pp. 613–615). Morris D. Friedman, Inc., Needham Heights 92, Mass., Translation no. K-187.

Mass Transfer During Absorption with Bubbling, by A. A. Ravdel (translated from *Zhur. Priklad. Khim.*, vol. 31, no. 7, 1958). Associated Tech. Services, P. O. Box 271, East Orange, N. J., Translation no. RJ-1500.

The Solution of Gas Bubbles in a Liquid, by A. A. Ravdel (translated from *Zhur. Priklad. Khim.*, vol. 26, no. 7, 1953, pp. 752–756). Associated Tech. Services, P. O. Box 271, East Orange, N. J., Translation no. RJ-1501.

The Use of Frontal Analysis in Gaseous-Liquid Chromatography of Radioactive and Non-radioactive Gases, by M. I. Ianovsky and G. A. Gaziev, *Doklady Akad. Nauk SSSR*, vol. 120, June 1, 1958, pp. 812–814. (In Russian.)

Chemical Actions of Atoms Having Energies Comparable with the Activation Energy, by B. N. Provotorov, *Doklady Akad. Nauk SSSR*, vol. 120, June 1, 1958, pp. 838–840. (In Russian.)

Quasi-stationary Thermal Regime of Explosive Reaction Processes, by A. G. Merzhanov and F. I. Dubovitsky, *Doklady Akad. Nauk SSSR*, vol. 120, June 11, 1958, pp. 1068–1071. (In Russian.)

A Boundary Problem in the Thermal Explosion Theory, by V. V. Barzykin and A. G. Merzhanov, *Doklady Akad. Nauk SSSR*, vol. 120, July 21, 1958, pp. 1271–1273. (In Russian.)

On the Theory of Thermal Chain Flame Propagation, by L. A. Lovachev, *Doklady Akad. Nauk SSSR*, vol. 120, July 21, 1958, pp. 1291–1293. (In Russian.)

Relaxation Reaction Between Shock Waves and the Burning Zone, by S. M. Kogarko and V. I. Skobelkin, *Doklady Akad. Nauk SSSR*, vol. 120, July 21, 1958, pp. 1280–1283. (In Russian).

On the Stability of Flame Propagation, by G. I. Barenblatt and Ia. B. Zeldovich (translated from *Priklad. Matemat. i Mekhan.*, vol. 21, no. 6, 1957, pp. 856–859). Morris D. Friedman Inc., Needham Heights 92, Mass., Translation no. B-135.

Exact Solution of the Nonlinear Problem of an Explosion in a Gas with Variable Initial Density, by V. P. Korobeinikov (translated from *Doklady Akad. Nauk SSSR*, vol. 117, no. 6, 1957, pp. 947–948). Morris D. Friedman, Inc., Needham Heights 92, Mass., Translation no. K-170.

On Spin Near the Gas Detonation Limits, by Ia. K. Troshin and K. I. Shchelkin (translated from *Izvestiia Akad. Nauk SSSR, Otdel. Tekh. Nauk*, no. 8, 1957, pp. 142–143). Morris D. Friedman, Inc., Needham Heights 92, Mass. Translation no. T-129.

On Spin Detonation, by B. V. Voitsekhovskii (translated from *Doklady Akad. Nauk SSSR*, vol. 114, no. 4, 1957, pp. 717–720). Morris D. Friedman, Inc., Needham Heights 92, Mass., Translation no. V-125.

Errors in the Measurement of Flame Temperature in a Stream with Thermocouples, by K. P. Vlasov and N. V. Kokushkin (translated from *Izvestiia Akad. Nauk SSSR, Otdel. Tekh. Nauk*, no. 8, 1957, pp. 137–141). Morris D. Friedman, Inc., Needham Heights 92, Mass., Translation no. V-128.

Investigation of Certain Singularities in the Combustion of Motor Fuel Sprays, by D. I. Raibov and Iu. B. Sviridov, *Akad. Nauk SSSR, Izvestiia, Otdel. Tekh. Nauk*, 4, April 1958, pp. 133–137. (In Russian.)

Some Instances of Motions of a Viscous Gas in Narrow Spaces of Variable Thickness, by Ya. M. Kotlyar, *Akademii Nauk, SSSR, Izvestiia, Otdel. Tekh. Nauk*, 5, May 1958, pp. 35–39. (In Russian.)

Effect of a Slightly Blunt Leading Edge upon its Streamlined Flow at Hypersonic Speeds, by G. G. Chernyi, *Akademii Nauk SSSR, Izvestiia, Otdel. Tekh. Nauk*, no. 4, April 1958, p. 54–66. (In Russian.)

* The editors of Technical Literature Digest are making a systematic search for pertinent Russian articles, both in the original Russian and in translated form. For the balance of 1959, these will appear in a separate section with this heading, mainly to draw the readers' attention to the new listing. After that, they will appear item by item under the proper subject headings.

Environment for Dynamic Career Growth

for Engineers and Scientists

Ability is important in getting ahead in engineering and science. But of almost equal importance is the environment in which you work. A dynamic environment that provides challenge and scope, unexcelled facilities, and plenty of room at the top, can accelerate your advance to higher levels of responsibility and income.

This is the kind of environment you'll find at Boeing...pictured and described in Boeing's new 24-page booklet, "Environment for Dynamic Career Growth."

The booklet, in addition, reports on engineering and science assignments in connection with current Boeing projects—from advanced military and commercial jet aircraft to space vehicles, guided missiles and intercontinental ballistic missiles. It also outlines Boeing research and development activities, and documents the dynamic Boeing environment that fosters career growth of engineers and scientists.

There are openings at Boeing, now, for engineers and scientists of all categories, all experience and educational levels. A Boeing assignment in Research, Design, Production or Service could be the answer to your future.

Write *today* for your free copy of the 24-page book "Environment for Dynamic Career Growth." Indicate your degree(s) and field of interest. Address: Mr. Stanley M. Little, Boeing Airplane Co., P.O. Box 3822 - JPB Seattle 24, Washington.

BOEING

SOUTHWEST
"Monoball"
SELF-ALIGNING BEARINGS

CHARACTERISTICS

	ANALYSIS	RECOMMENDED USE
1	Stainless Steel Ball and Race	For types operating under high temperature (800-1200 degrees F.).
2	Chrome Alloy Steel Ball and Race	For types operating under high radial ultimate loads (3000-893,000 lbs.).
3	Bronze Race and Chrome Steel Ball	For types operating under normal loads with minimum friction requirements.

Thousands in use. Backed by years of service life. Wide variety of Plain Types in bore sizes 3/16" to 6" Dia. Rod end types in similar size range with externally or internally threaded shanks. Our Engineers welcome an opportunity of studying individual requirements and prescribing a type or types which will serve under your demanding conditions. Southwest can design special types to fit individual specifications. As a result of thorough study of different operating conditions, various steel alloys have been used to meet specific needs. Write for Engineering Manual No. 551. Address Dept. JP-59.

SOUTHWEST PRODUCTS CO.
1705 SO. MOUNTAIN AVE., MONROVIA, CALIFORNIA

CHEMISTS

- ANALYTICAL PhD or equivalent to perform research on new analytical methods and techniques.
- INORGANIC ORGANIC PhD or equivalent for synthetic chemistry. Industrial experience required—preferably in fuels, oxidizers and propellant technology.
- PHYSICAL—PhD or M.S. Supervisory experience and background in experimental and theoretical thermodynamics and cybernetics required. To supervise research programs in evaluation of physical and ballistic properties of liquid and solid propellants.
- PHYSICAL—B.S. with education or experience emphasis on experimental thermodynamics, particularly heat capacity measurements.

CHEMICAL ENGINEERS

- DEVELOPMENT ENGINEERS with experience in design analysis, and operation of bench scale units and pilot plants.
- SENIOR PROCESS ENGINEER with broad rather than specialized pilot plant and production experience including design and economic studies. Technical supervisory experience required.

OTHER

- APPLICATIONS RESEARCH CHEMIST or ENGINEER with industrial experience and interest in several technological fields. To explore new industrial products or applications of existing products.
- PROPELLANT TESTING SPECIALIST—Chemist, Physicist or Engineer, B.S., M.S., or PhD with a minimum of 3 years' experience in small scale testing and evaluation of liquid and solid propellants. To organize and coordinate programs for broadened utilization of high energy fuels.

Permanent positions with producer of Boron chemicals and high energy fuels located 25 miles north of Pittsburgh's Golden Triangle.
Please send resume including salary requirements in confidence to:

PERSONNEL MANAGER
CALLERY CHEMICAL COMPANY
Callery
Pennsylvania

Index to Advertisers

AEROJET-GENERAL CORP. ..... Back cover, 390
D'Arcy Advertising Co., Los Angeles, Calif.

AERONUTRONIC SYSTEMS, INC. 387
Honig-Cooper, Harrington & Miner, Los Angeles, Calif.

ALLIED CHEMICAL CORP., NITROGEN DIV. ..... 2nd cover
G. M. Basford Co., New York, N.Y.

BOEING AIRPLANE CO. 384, 391
Calkins & Holden, Seattle, Wash.

CALLERY CHEMICAL CO. 392
Commerce Advertising Agency, New York, N.Y.

CONSOLIDATED CONTROLS CORP. 321
DeGarmo Advertising Agency, New York, N.Y.

E. I. DU PONT DE NEMOURS & CO., INC. 383
N. W. Ayer & Son, Inc., Philadelphia, Pa.

GENERAL ELECTRIC CO., AIRCRAFT NUCLEAR PROPULSION DEPT. 385
Deutsch & Shea, Inc., New York, N.Y.

GENERAL MOTORS CORP., OLDSMOBILE DIV. 323
D. P. Brother & Co., Detroit, Mich.

GROVE VALVE & REGULATOR CO. ..... 3rd cover
L. C. Cole & Co., Inc., San Francisco, Calif.

INTERNATIONAL BUSINESS MACHINES CORP. 388, 389
Benton & Bowles, Inc., New York, N.Y.

LOCKHEED MISSILES & SPACE DIV. 380, 381
Hal Stebbins, Inc., Los Angeles, Calif.

THE MARTIN CO. 377
VanSant Dugdale & Co., Inc., Baltimore, Md.

NEWBROOK MACHINE CORP. 378
Melvin F. Hall Agency, Inc., Buffalo, N.Y.

RAMO-WOOLDRIDGE, A DIV. OF THOMPSON RAMO-WOOLDRIDGE INC. 324
The McCarty Co., Los Angeles, Calif.

REPUBLIC AVIATION CORP. 386
Deutsch & Shea, Inc., New York, N.Y.

SOUTHWEST PRODUCTS CO. 392
O. K. Fagan Adv. Agency, Los Angeles, Calif.

SPACE TECHNOLOGY LABORATORIES, INC. 379
Gaynor & Ducas, Inc., Beverly Hills, Calif.